620.5
458
AUG 5 1930
B93

U. S. DEPARTMENT OF COMMERCE

BUREAU OF STANDARDS JOURNAL OF RESEARCH

Vol. 5 JULY, 1930 No. 1

CONTENTS

RP. No.	TITLE AND AUTHOR	Page
183.	A comparison of resolving power and sensitivity of photographic plates with varying development. Burt H. Carroll and Donald Hubbard	1
184.	Resonance and quenching of the third principal series line of caesium. C. Boeckner	13
185.	Relationships between Rockwell and Brinell numbers. S. N. Petrenko	19
186.	Photo-ionization of caesium by line absorption. F. L. Mohler and C. Boeckner	51
187.	Regularities in the spectra of lutecium. William F. Meggers and Bourdon F. Scribner	73
188.	A new consistometer and its application to greases and to oils at low temperatures. Ronald Bulkley and F. G. Bitner	83
189.	Method of measuring strains between glazes and ceramic bodies. H. G. Schurecht and G. R. Pole	97
190.	The preparation of fiber test sheets. Merle B. Shaw, George W. Bicking, and Leo W. Snyder	105
191.	The Geiger tube electron counter. L. F. Curtiss	115
192.	Flow characteristics of special Fe-Ni-Cr alloys and some steels at elevated temperatures. H. J. French, William Kahlbaum, and A. A. Peterson	125
193.	The characteristics of two-blade propeller fans. H. L. Dryden and P. S. Ballif	185

Bureau of Standards Journal of Research

CONTENTS OF RECENT NUMBERS

February, 1930 (Vol. 4, No. 2)

RP140. Standards for testing magnetic permeameters. Raymond Sanford. Price 5 cents.

RP141. Ultra-violet reflecting power of aluminum and several other metals. W. W. Coblentz and R. Stair. Price 5 cents.

RP142. The ring and ball method of test for softening point of bituminous materials, resins, and similar substances. Percy H. Walker. Price 5 cents.

RP143. Rayon as a paper-making material. Merle B. Shaw and George W. Bicking. Price 5 cents.

RP144. A precision method of calibrating a tuning fork by comparison with a pendulum. Charles Moon. Price 5 cents.

RP145. The principles of measurement and of calculation in their application to the determination of diophantine quantities. Edward W. Washburn. Price 10 cents.

RP146. Durability tests of spar varnish. C. L. Came. Price 5 cents.

RP147. A new dead-weight testing machine of 100,000 pounds capacity. L. B. Tuckerman, Herbert L. Whittemore, and Serge N. Petrenko. Price 5 cents.

RP148. Applying a visual double-modulation type radio range to the airways. H. Diamond. Price 10 cents.

RP149. The absorption of sound at oblique angles of incidence. P. R. Heyl, V. L. Chrisler, and W. F. Snyder. Price 5 cents.

RP150. Sensitivity of a galvanometer as a function of its resistance. H. B. Brooks. Price 5 cents.

RP151. Heat capacities in some aqueous solutions. Frederick D. Rossini. Price 5 cents.

March, 1930 (Vol. 4, No. 3)

RP152. Preliminary investigations upon two cellulosic wastes as sources for Xylose. W. L. Hall, C. S. Slater, and S. F. Acree. Price 5 cents.

RP153. Design of a portable temperature-controlled piezo oscillator. V. E. Heaton and W. H. Brattain. Price 5 cents.

RP154. A 12-course radio range for guiding aircraft with tuned reed visual indication. H. Diamond and F. G. Kear.

RP155. Applying the radio range to the airways. F. G. Kear and W. E. Jackson. Price 5 cents.

RP156. New piezo oscillations with quartz cylinders cut along the optical axis. August Hund and R. B. Wright. Price 20 cents.

RP157. Transverse tests of H-section column splices. James H. Edwards, H. L. Whittemore, and A. H. Stang. Price 10 cents.

RP158. Engine-ignition shielding for radio reception in aircraft. H. Diamond and F. G. Gardner. Price 15 cents.

RP159. Development of the visual type radiobeacon system. J. H. Dellinger, H. Diamond, and F. W. Dunmore. Price 20 cents.

Research papers are available as separates for purchase from the Superintendent of Documents United States Government Printing Office, Washington, D. C.

U. S. DEPARTMENT OF COMMERCE
R. P. LAMONT, Secretary
BUREAU OF STANDARDS
GEORGE K. BURGESS, Director

BUREAU OF STANDARDS JOURNAL OF RESEARCH

July, 1930
Vol. 5, No. 1

UNITED STATES
GOVERNMENT PRINTING OFFICE
WASHINGTON : 1930

For sale by the Superintendent of Documents, Washington, D.C. - Price 40 cents; $2.75 Per Year on Subscription

For a partial list of previous research papers appearing in BUREAU OF STANDARDS JOURNAL OF RESEARCH, see pages 2 and 3 of the cover.

A COMPARISON OF RESOLVING POWER AND SENSITIVITY OF PHOTOGRAPHIC PLATES WITH VARYING DEVELOPMENT

By Burt H. Carroll and Donald Hubbard

ABSTRACT

Special developers recommended for reducing the graininess of photographic images are all based on increasing the solvent action of the solution on silver bromide, and decreasing the reduction potential. Five of these formulas were compared with ordinary pyrogallol and metol-hydroquinone by testing sensitivity and resolving power of three emulsions, each developed with each of the developers. These results were supplemented by practical spectrographic tests, and experiments with two other developers. Little useful improvement over the standard developers was obtained in any case, as increased resolution was, in general, accompanied by decreased sensitivity. These results do not apply to the pictorial use of special development to reduce graininess.

CONTENTS

	Page
I. Introduction	1
II. Experimental procedure	3
1. Choice of plates	3
2. Sensitometry	3
3. Measurement of resolving power	3
4. Spectrographic tests	4
5. Developers	4
(*a*) Material	4
(*b*) Formulas	5
III. Discussion of results	6
1. Sensitivity	6
2. Resolving power	10
3. Utility of the developers	11
IV. Summary	11
V. Acknowledgments	11

I. INTRODUCTION

Both scientific and practical applications of photography tend to demand a better combination of sensitivity and resolving power than is now available. While recent investigations have shown that, other conditions being the same, sensitivity increases with the size of the silver halide grains in an emulsion so that there is a fundamental connection between the two, the resolving power of the developed image is always far less than the limit imposed by the silver halide grain size. Part of this is caused by clumps of grains in the emulsion, and part by the substitution of irregular and much larger grains of silver in the developed image for the original grains of silver halide. The latter at least is obviously susceptible to some control by the conditions of development. In the extreme case of development after fixation, where the silver halide grain has been removed and the silver

of the developed image is deposited from the developing solution, Seyewetz[1] has shown that the metal may be deposited in compact hexagonal crystals quite different from the spongy grains produced by any developing agent[2] under the conditions of "chemical" development.

"Chemical" development may, however, be modified so as to produce smaller silver grains, with a probable decrease in the frequency of clumps, by decrease in the reduction potential, and increase in the solubility of the silver halide in the developing solution. The result is that a considerable proportion of the silver halide is reduced in solution, and the silver deposited on the development nucleus as in "physical" development. This type of developer was first used and explained by the Lumières and Seyewetz,[3] and the same principles are involved in the "borax" developers now in wide use by the motion-picture industry. A high concentration of sodium sulphite is used to increase the solubility of the silver halide, and carbonate is entirely omitted, so that the alkalinity is relatively low (pH approximately 9) and the reduction potential is correspondingly decreased. The alkalinity of sulphite solutions is somewhat too low and borax is generally added to raise it to the desired value; being a good buffer, it may be added in sufficient quantity to maintain the pH reasonably constant during development. The use of borax has given its name to this class of developer, although the high concentration of sulphite is really the more important feature. Practical studies of the variables in this class of developer are given by Carlton and Crabtree[4] and by Moyse and White.[5]

This comparison of a number of developer formulas by their effect on the characteristics of three emulsions was intended primarily for choice of developers for use in difficult spectography, such as stellar spectra, Zeeman patterns, or band spectra. The requirements may be summarized as (1) the minimum error in determination of the distance between closely separated lines, combined with (2) the minimum exposure for recording the lines. The first is not determined solely by the grain size of the image, since resolving power is dependent to a very large extent on fog, and contrast; the factors involved are summarized by Sandvik,[6] who emphasizes the necessity of measuring resolving power by tests related to the intended application. The second requirement makes it necessary to consider the effect of development on the effective sensitivity of the plate, since the differences in resolving power characteristic of emulsions differing by 50 per cent in speed are, in general, as great as any which can be produced by special development. There is obviously no advantage in the use of a high-speed emulsion and special developer if both sensitivity and resolving power can be equaled by a moderate speed emulsion with standard development, and we are unable to understand how the Lumières and Seyewetz[7] are able to pass so lightly over this point.

---

[1] Seyewetz, Chimie et Ind., Special No.; p. 418; September, 1925.
[2] Ross, The Physics of the Developed Silver Image, chap. 1.
[3] A. and L. Lumière and A. Seyewetz, Brit. J. Phot., **51**, pp. 630, 866; 1904.
[4] Carlton and Crabtree, Trans. Soc. Motion Picture Engrs., **13**, pp. 406–444; 1929.
[5] Moyse and White, Trans. Soc. Motion Picture Engrs., **13**, pp. 445–452; 1929.
[6] Sandvik, Proc. 7th Int. Cong. Phot., p. 243; 1928.
[7] A. and L. Lumière and A. Seyewetz, Sci. et. Ind. Phot., **12**, p. 128; 1928; "On compensera facilement l'inconvénient de la legère surexposition exigée par ce révélateur en s'addressant à une émulsion très sensible comme celle de la plaque Lumière 'Étiquette Violette'."

II. EXPERIMENTAL PROCEDURE

1. CHOICE OF PLATES

All tests were made with plates, as the precision measurements of spectrography and astronomy are still impossible on film base.

The Seed's 23 was chosen as a moderate-speed emulsion of the general type most useful in spectrography. The Speedway and Press plates are the fastest emulsions available on glass from their respective makers. The resolving power most frequently becomes a serious consideration when it is necessary to use this type of plate, and the advantages of special developers may be expected to be most evident with those emulsions.

2. SENSITOMETRY

Sensitometric measurements were made by the standard methods of this bureau. Exposure was by nonintermittent sector wheel at an intensity of 1 m candle of the quality of noon sunlight.

The Seed's 23 and Speedway plates were tested with a light source consisting of a gas filled incandescent light operated at a color temperature of 2,810° K. and a filter of Corning "Daylite" glass. The Press plates were exposed to the source adopted by the Seventh International Congress of Photography, an incandescent light operated at 2,360° and the corresponding Davis-Gibson filter. The difference in speed numbers with these sources appears to be within the limits of error of sensitometry. Development was carried out at 20° using the brush method for the developers where the maximum time did not exceed 12 minutes. The slow developers, requiring 30 to 120 minutes, were necessarily used without agitation; the plates were left emulsion up in the solution and did not develop the streaks which are liable to occur in a vertical tank. Densities were measured in diffuse light, the fog density being automatically subtracted; using backed plates, the fog strip was uniform throughout. Speed numbers are $10/i$. Where a single number is given, the curves crossed on the exposure axis within the limits of error; a noticeable shift with time of development is indicated by the use of three speed numbers. Some indication of the changes in the underexposure region is given by the density at an exposure of 0.0294 candle meter second; the exponent (as $D^{1.0}_{0.029}$) indicates the contrast to which the plate was developed.

3. MEASUREMENT OF RESOLVING POWER

Resolving power was measured with the same parallel-line test object and lens used for this purpose by Davis and Walters,[8] their procedure being in complete agreement with the later recommendations of Sandvik.[9] The test object consists of groups of six parallel lines separated by spaces of equal width, in which the density exceeds that of the lines by approximately 4. This was photographed on the backed test strips at such scale that the distances between centers of lines in the image varied from 8.3 μ to 25 μ. Each test strip was given a series of exposures increasing by a factor of about one-third. The performance of the lens at $f/11$ was found to be slightly superior to that at $f/16$ because of the distinct appearance of diffraction at the smaller stop.

---

[8] Davis and Walters, B. S. Sci. Paper No. 439.

[9] See footnote 6, p. 2.

Plates were developed to a contrast within their normal workin range. On completing the sensitometer tests, γ was plotted again the time of development, and also against the corresponding values fog, and the required time read off the curve. As a check on the inte polation, sensitometer exposures were developed with each set resolution tests strips. Except where excessive fog would be pr duced, the Seed's 23 plates were developed to a γ of approximate 1.5 and the Speedway to approximately 1.0. The Press plates we developed to what was judged, from inspection of the curve of against fog, to be the optimum contrast; we consider the result with this emulsion the most satisfactory.

The greatest uncertainty in determination of resolving power lie in assigning a number to any given test image. The strips wer observed with a binocular microscope with 25 mm objectives an 10× eyepieces under lighting conditions found to impose very littl eyestrain. A considerable number of readings were also made b projection at 800 diameters, the image being observed from 1 or 2 m distance; the light intensity was too low for comfort, and the result while in reasonable agreement with those by the other method, are considered less satisfactory. The criterion for resolution which wa applied, was that all six lines of a group should appear suitable fo definite settings of a cross hair. The resolution number assigned t a test strip was the minimum separation resolved at any one of the series of exposures. All tests were made in quadruplicate; the num ber given in the tables for a given emulsion, developer, and observe is the average of four strips.

Three or four observers were used in all cases. The identity o the test strips could not be entirely concealed from the observers, but there is little evidence of prejudice. The errors of observation will be discussed with the results.

4. SPECTROGRAPHIC TESTS

Some of the developers were compared under conditions of actual spectrographic work. The carbon arc band at 3,883 A was photo graphed with the large grating spectrograph of the spectroscopic section of this bureau, using a concave grating of 21-foot radius, 15,000 lines per inch and a 5 μ slit width. After careful focusing on backed lantern-slide plates, Speedway plates (emulsion 2469) were given a series of eight exposures each to the same source. Figure 1 is a reproduction at 163 diameters of the band head on the lantern slide focus plate and on Speedway plates developed with five formulas, the best exposure in each case being selected for enlargement.

5. DEVELOPERS

(a) MATERIAL

The developing agents were commercial materials passing the United States Government specifications with the exception of para phenylenediamine (base). This is very unstable in air. The avail able material was twice sublimed under reduced pressure at the start of the investigation, the product being white and giving a nearly colorless solution, but it was distinctly darkened in a few weeks. Sodium carbonate was assayed by acid titration, and sodium sul-

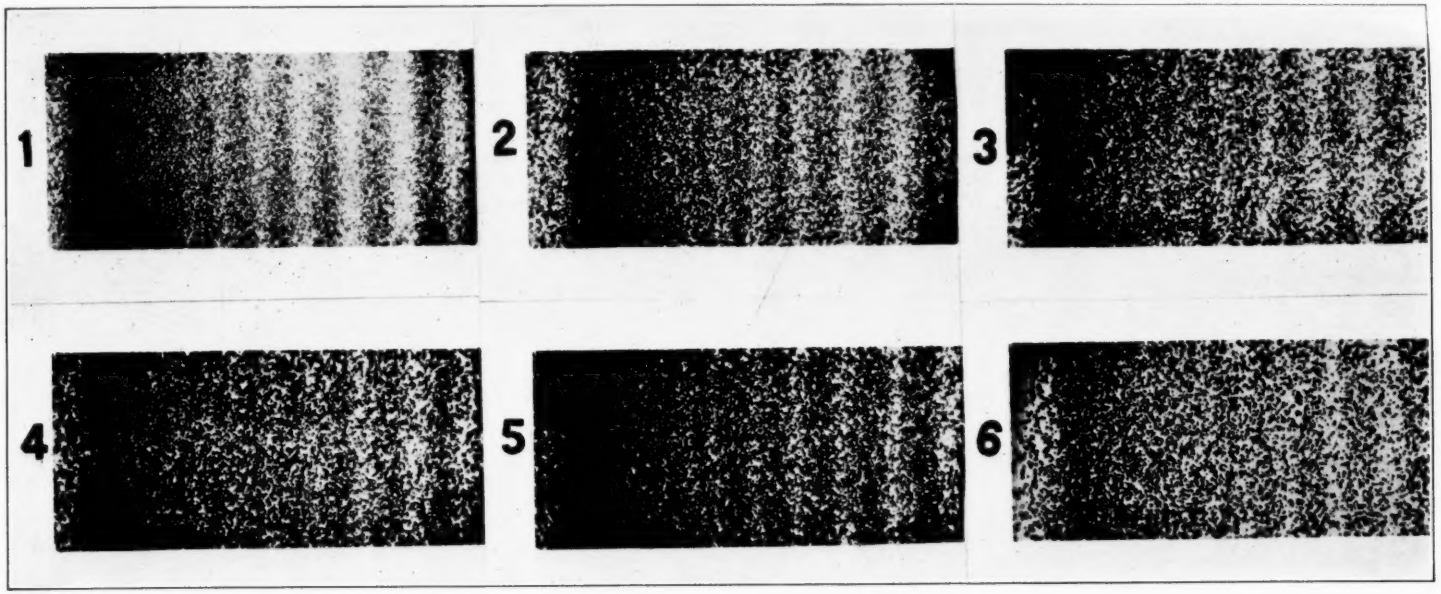

FIGURE 1.—*Spectrograms of carbon arc band at 3,883 A*

Taken on—
1. Lantern slide plate.
2. Speedway plate developed with *p*-phenylenediamine-borax formula.
3. Speedway plate developed with metol-hydroquinone-borax formula.
4. Speedway plate developed with metol-borax formula.
5. Speedway plate developed with metol-borax formula +0.5g *KBr*/liter.
6. Speedway plate developed with concentrated metol-hydroquinone formula.

phite by iodine titration. The amounts given represent actual Na_2CO_3 and Na_2SO_3; U. S. P. borax was twice recrystallized for use.

(b) FORMULAS

Pyrogallol.—This is the developer normally used for sensitometry at the Bureau of Standards:

Stock solutions:			
A	Water	ml	1,000
	Pyrogallol	g	60.0
	Potassium metabisulphite	g	12.0
B	Water	ml	1,000
	Sodium sulphite	g	95
C	Water	ml	1,000
	Sodium carbonate	g	70

For use, 1 volume each of A, B, and C plus 7 volumes of water.

Concentrated metol-hydroquinone.—A developer of the universal type much used for practical work at this bureau:

Water	ml	1,000
Metol	g	1.6
Hydroquinone	g	5.6
Sodium sulphite	g	21.3
Sodium carbonate	g	30.0
Potassium bromide	g	.75

Dilute metol-hydroquinone.—Recommended by Lumières and Seyewetz [10] as giving a slight reduction in grain size, equivalent to the Metol-hydroquinone-borax formula:

Metol	g	0.16
Hydroquinone	g	.30
Sodium sulphite	g	3.0
Sodium carbonate	g	1.6
Potassium bromide	g	.2
Water to make	liter	1.0

Metol-hydroquinone-borax.—Recommended for reduction of graininess in motion-picture negatives: [11]

Metol	g	2.0
Sodium sulphite	g	100
Hydroquinone	g	5.0
Borax	g	2.0
Water to make	liter	1.0

Carlton and Crabtree [12] state that graininess can be further decreased by reducing the concentration of developing agents in this formula to one-half, other concentrations being unchanged.

Metol-borax.—Recommended by Moyse and White for use with motion-picture negatives.[13]

Metol	g	2.5
Sodium sulphite	g	75
Borax	g	5.0
Water to make	liter	1.0

p-Phenylenediamine-borax.—Recommended by the Lumières and Seyewetz [14] as "giving the best results."

---

[10] Lumières and Seyewetz, Sci. et. Ind. Phot., **8A**, p. 126; 1928.
[11] Crabtree, Trans. Soc. Motion Picture Eng., p. 77; 1927.
[12] See footnote 4, p. 2.
[13] Moyse and White, Trans. Soc. Motion Picture Eng., **13**, p. 445; 1929.
[14] Lumières and Seyewetz, Sci. et. Ind. Phot., **7A**, p. 108; 1927.

p-Phenylenediamine (base)	g	10
Sodium sulphite	g	60
Borax	g	50
Water to make	liter	1.0

p-Phenylenediamine-carbonate.—The Lumières and Seyewetz [15] state that this formula gives more rapid development and better density than the diamine-borax, but the grain is noticeably coarser.

p-Phenylenediamine (base)	g	10
Sodium sulphite	g	60
Sodium carbonate	g	3.0
Water to make	liter	1.0

Hydroquinone-borax:

Hydroquinone	g	5.0
Sodium sulphite	g	75.0
Borax	g	5.0
Water to make	liter	1.0

Physical developer:[16]

Metol	g	25.0
Citric acid	g	50.0
20 per cent gum arabic solution	ml	50.0
Water to make	liter	1.0

For use add 2 ml of 10 per cent silver nitrate to 50 ml of the above.

Of these developers, the pyrogallol and concentrated metol-hydroquinone are common practical formulas. The metol-hydroquinone-borax and metol-borax formulas, which can now be classed as practical, are based on the use of high sulphite concentration and greatly reduced alkalinity with a developing agent of high reduction potential; the rate of development indicates that only a small proportion of the silver in the developed image can be derived from the slow process of solution of silver halide and reduction in solution. In the *p*-phenylenediamine developers the "chemical" development is greatly decreased by the use of a developing agent of low reduction potential,[17] and reduction takes place at a low rate which probably corresponds to "physical" development. The hydroquinone-borax formula is comparable to the *p*-phenylenediamine-borax, in reduction potential and solvent action; it was introduced only to see if a specific effect of the developing agent on the resolution was detectable, as we did not expect it to be of practical value. Physical development is known to have a favorable influence on resolution both by its effect on grain size and because it gives a surface image free from the effects of irradiation. It might be of value in spite of the known depression of speed in case it made possible a resolution which could not be obtained with any emulsion by normal development.

III. DISCUSSION OF RESULTS

1. SENSITIVITY

The sensitometer tests of the three emulsions listed in Tables 1, 3, and 5 show a wide variation in effective sensitivity of a given emulsion developed with the different formulas. This variation increases with

[15] Lumières and Seyewetz, Sci. et. Ind. Phot. **8A**, p. 126; 1928.
[16] Lüppo-Cramer, Phot. Ind., **13**, p. 660; 1915.
[17] Nietz, Theory of Development, rates *p*-phenylenediamine hydrochloride at 0.4 and metol at 20, hydroquinone being taken as 1.0; *p*-phenylenediamine base probably has a slightly higher potential than its salt.

the speed of the plate, but the order in which the developers fall is practically the same for all three emulsions.

The special developers with high solvent action and low reduction potential (*p*-phenylenediamine-borax, *p*-phenylenediamine-carbonate, hydroquinone-borax) caused a very considerable depression in speed; in the extreme case of purely physical development, the loss was 80 to 90 per cent. The dilute metol-hydroquinone developer, which would be closely reproduced merely by diluting the concentrated formula to ten times its volume and doubling the bromide, gave normal speed numbers, but, by far, the worst fog for a given contrast.

The metol-hydroquinone-borax and metol-borax developers somewhat unexpectedly gave higher speeds than the standard formulas, and better densities in the underexposure region at moderate values of γ.

TABLE 1.—*Sensitometric characteristic of Seed's 23 plate (emulsion No. 7855) with the different developers*

[Figures in parentheses indicate time of development in minutes]

Developer	Speed	D $\frac{1.5}{0.029}$	γ			Fog		
Standard pyrogallol	230	0.12	(3) 1.05	(6) 1.50	(12) 2.03	(3) 0.07	(6) .19	(12) 0.42
Concentrated metol-hydroquinone	200	.09	(1.5) 1.44	(3) 2.03	(6) 2.17	(1.5) .08	(3) .14	(6) .41
Dilute metol-hydroquinone	245	-------	(30) .65	(60) .96	(120) 1.30	(30) .31	(60) .65	(120) 1.12
Metol-hydroquinone-borax	320	.13	(3) .73	(6) 1.13	(12) 1.50	(3) .05	(6) .15	(12) .29
Metol-borax	330	.15	(3) .77	(6) 1.20	(12) 1.69	(3) .07	(6) .18	(12) .33
p-Phenylenediamine-borax	165	.10	(30) .84	(60) 1.17	(120) 1.60	(30) .13	(60) .19	(120) .24
p-Phenylenediamine-carbonate	165	.08	(15) .86	(30) 1.07	(60) 1.31	(15) .18	(30) .21	(60) 0.26
Physical developer 10°	(10) 19 (20) 27 (40) 37	.00	(10) .77	(20) 1.30	(40) 1.64	(10) .05	(20) .10	(40) .18

TABLE 2.—*Resolution of Seed's 23 plate (emulsion 7855)*

[The resolution is expressed in microns spacing of the closest set of lines resolved, and values are rounded to 0.5 μ]

Developer	γ	Fog	Resolution as determined by observer			
			C	D	H	S
Standard pyrogallol	1.50	0.24	15.0	15.0	15.0	15.0
Concentrated metol-hydroquinone	1.45	.06	14.0	15.0	16.0	14.5
Dilute metol-hydroquinone	.56	.17	14.5	15.0	17.5	15.0
Metol-hydroquinone-borax	1.57	.36	14.0	15.5	16.0	16.0
Metol-borax	1.33	.24	13.0	15.5	16.5	16.0
p-Phenylenediamine-borax	1.35	.19	12.0	13.5	14.5	14.0
p-Phenylenediamine-carbonate	1.37	.27	13.5	13.5	16.5	15.0
Physical	.90	.08	13.0	14.0	14.5	15.5

TABLE 3.—*Sensitometric characteristics of Eastman Speedway plate (emulsion Nos. 2357 and 2469) with the different developers*

[Figures in parentheses indicate time of development in minutes]

Developer	Emulsion No.	Speed	$D^{1.0}_{0.029}$	γ			Fog		
Standard pyrogallol	(2357)	400	0.15	(3) 0.70	(6) 1.10	(12) 1.30	(3) 0.10	(6) 0.18	(12) 0.35
	(2469)	490	.12	(3) .55	(6) .86	(12) 1.33	(3) .05	(6) .20	(12) .37
Concentrated metol-hydroquinone.	(2357)	300	.12	(1.5) 1.31	(3) 1.33	(6) 1.52	(1.5) .18	(3) .20	(6) .35
Dilute metol-hydroquinone	(2357)	530	.17	(30) .45	(60) .61	(120) .95	(30) .18	(60) .32	(120) .53
Metol-hydroquinone-borax	(2357)	510	.22	(3) .54	(6) .77	(12) .97	(3) .10	(6) .20	(12) .32
Metol-borax	(2469)	525	.20	(3) .45	(6) .80	(12) 1.10	(3) .05	(6) .16	(12) .27
	(2357)	430	.18	(3) .66	(6) .88	(12) 1.20	(3) .12	(6) .20	(12) .30
Metol-borax+0.5 g *KBr/liter*	(2357)	(3) 300 (6) 440 (12) 510	.25	(3) .51	(6) .77	(12) 1.00	(3) .04	(6) .09	(12) .15
p-Phenylenediamine-borax	(2357)	210	.11	(30) .72	(60) .87	(120) 1.05	(30) .15	(60) .26	(120) .39
p-Phenylenediamine-carbonate	(2357)	(30) 220 (60) 220 (120) 420	-------	(30) .67	(60) .95	(120) .90	(30) .23	(60) .30	(120) .41
Physical developer 20°	(2357)	(2) 31 (4) 34 (8) 52	.00	(2) .20	(4) .60	(8) 1.06	(2) .10	(4) .13	(8) .23

TABLE 4.—*Resolution of Eastman Speedway plate (emulsion 2357)*

[The resolution is expressed as microns spacing of the closest set of lines resolved, and values are rounded to 0.5+ μ]

Developer	γ	Fog	Resolution as determined by observer			
			C	D	H	S
Standard pyrogallol	0.84	0.15	15.0	16.5	17.5	16.0
Concentrated metol-hydroquinone	.87	.06	15.5	17.5	17.5	17.0
Dilute metol-hydroquinone	.47	.24	16.0	19.0	19.0	16.0
Metol-hydroquinone-borax	1.09	.36	14.5	18.5	18.5	17.5
Metol-borax	.84	.20	14.0	18.5	18.5	16.5
p-Phenylenediamine-borax	.97	.36	14.0	15.0	15.5	15.0
p-Phenylenediamine-carbonate	.72	.30	15.0	17.5	16.0	15.0

TABLE 5.—*Sensitometric characteristics of Hammer Press plate (emulsion 4063) with the different developers*

[Figures in parentheses indicate time of development in minutes]

Developer	Speed	$D^{1.0}_{0.029}$	γ			Fog		
Standard pyrogallol	680	0.32	(3) 0.64	(6) 1.05	(12) 1.33	(3) 0.08	(6) 0.13	(12) 0.27
Concentrated metol-hydroquinone	495	.26	(1.5) 1.00	(3) 1.45	(6) 1.57	(1.5) .06	(3) .12	(6) .24
Dilute metol-hydroquinone	730	------	(15) .36	(30) .61	(60) .77	(15) .09	(30) .17	(60) .33
Metol-hydroquinone-borax	715	.33	(3) .40	(6) .75	(12) 1.20	(3) .06	(6) .13	(12) .26
Metol-borax	725	.36	(3) .51	(6) .82	(12) 1.13	(3) .07	(6) .14	(12) .23
p-Phenylenediamine-borax	215	.12	(30) .68	(60) .88	(120) 1.13	(30) .14	(60) .19	(120) .27
p-Phenylenediamine-carbonate	300	.22	(15) .54	(30) .73	(60) .92	(15) .14	(30) .18	(60) .24
Hydroquinone-borax	(30) 155 (60) 290 (120) 400	.17	(30) .28	(60) .70	(120) 1.00	(30) .03	(60) .14	(120) .40

TABLE 6.—*Resolution of Hammer Press plates (emulsion 4063)*

[The resolution is expressed in microns spacing of the closest set of lines resolved, and values are rounded to 0.5 μ]

Developer	γ	Fog	Resolution as determined by observer		
			D	H	C
Standard pyrogallol	1.14	0.15	15.0	15.0	19.0
Concentrated metol-hydroquinone	1.35	.11	15.5	15.5	18.0
Dilute metol-hydroquinone	.50	.11	17.0	17.0	18.0
Metol-hydroquinone-borax	1.03	.22	16.5	15.5	18.0
Metol-borax	.92	.16	16.0	15.0	18.5
p-Phenylenediamine-borax	.75	.19	16.0	14.5	15.5
p-Phenylenediamine-carbonate	.75	.16	14.0	14.0	16.5
Hydroquinone-borax	.57	.08	16.0	14.0	16.0

TABLE 7.—*Rating of developers, on resolving power only, by the different observers*

[Two or three numbers are assigned where the resolution numbers for the corresponding developers were identical]

Developer	Numerical order of the developers on scale of decreasing resolution										
	Observer D			Observer C			Observer H			Observer S	
	Seed's 23	Speedway	Press	Seed's 23	Speedway	Press	Seed's 23	Speedway	Press	Seed's 27	Speedway
Standard pyrogallol	3–4–5	2	2	7	5	7	2	3–4	3–4	3–4–5	3–4
Concentrated metol-hydroquinone	3–4–5	3–4	3	4	6	3	3	3–4	5–6	2	6
Dilute metol-hydroquinone	3–4–5	7	7	6	7	6	7	7	7	3–4–5	3–4
Metol-hydroquinone-borax	6–7	5	6	5	3	4	4	5	5–6	6–7	7
Metol-borax	6–7	6	4–5	2	2	5	5–6	6	3–4	6–7	5
p-Phenylenediamine-borax	2	1	4–5	1	1	1	1	1	2	1	1–2
p-Phenylenediamine-carbonate	1	3–4	1	3	4	2	5–6	2	1	3–4–5	1–2

2. RESOLVING POWER

The discrepancies between the observers are of the same order as the differences produced by the developers, so that the only unqualified statement possible is that the development has little effect on resolution. This is disappointing, since both our own photomicrographs and those of the Lumières and Seyewetz [18] show distinctly smaller silver grains in the images developed by the special formulas, while the increasing use of the metol-hydroquinone-borax developer for reducing graininess in motion-picture negatives indicates that this type can decrease the number of clumps of grains. It seems necessary to conclude that resolution as measured by the standard test is not directly dependent on grain size, or on the factors controlling graininess. Preliminary experiments on the accuracy of setting a cross hair on fine lines developed by standard and special formulas gave no indication of any marked improvement; refinements on the technique employed will be necessary, but we believe that a study of the factors influencing accuracy of such distance measurements on plates might be of greater utility than the usual determination of resolving power.

Table 7 shows that the individual observers were more likely to agree on the order in which they placed the developers than on the absolute magnitude of the resolution numbers; there was, however, also a tendency to individual preferences for or against one or two developers, which were maintained on all emulsions and which can not be ascribed to previous bias. The data indicate:

1. Both *p*-phenylenediamine formulas, the hydroquinone-borax, and the physical developers, improved resolution over the standard formulas. The physical developer was no better than those first mentioned.

2. The metol-hydroquinone-borax and metol-borax developers were no better than the standard pyrogallol or metol-hydroquinone in their effect on resolution.

3. The dilute metol-hydroquinone formula gives probably the worst resolution. It is interesting to compare this with the concentrated formula, which gives a much coarser grain, but is so far superior as to contrast and fog that resolution is distinctly better; on a test object of lower contrast ratio, or in actual spectrographic work with faint lines, the superiority would be more marked.

Such improvement as was obtained was as distinct with the Seed's 23 as with the faster plates. The Lumières and Seyewetz [18] report that in the case of a process plate the grain is practically independent of the developer.

In spite of the negative results of the resolution test, there has been general agreement that the spectrum plates developed with the metol-hydroquinone-borax and metol-borax formulas show more detail than the plate developed with the concentrated metol-hydroquinone; this is unquestionably true with the *p*-phenylenediamine-borax. Viterbi [19] has already illustrated good results obtained with the metol-hydroquinone-borax formula, but unfortunately gives nothing for comparison.

---

[18] See footnote 14, p. 5.
[19] Viterbi, Proc. 7th Int. Cong. Phot., pp. 365-367.

The resolution number and silver grain obtained with the hydroquinone-borax and *p*-phenylenediamine-borax developers are very similar. We doubt that the latter reducing agent has a specific influence independent of its reduction potential.

3. UTILITY OF THE DEVELOPERS

Judging the developers by their effects both on resolution and sensitivity, it appears that none of those tried offer a marked improvement over the standard formulas. The *p*-phenylenediamine developers are unfortunately eliminated by their effect on sensitivity. By way of illustration, the Press plate, developed with *p*-phenylenediamine-borax to a γ of 0.75 and fog of 0.19, has a speed of 215 and resolution number of 15; the Seed's 23, developed with concentrated metol-hydroquinone to a γ of 1.45 and fog of 0.06, has a speed of 200 and resolution number of 14. In practice, the use of the latter combination is very obviously preferable. The metol-hydroquinone-borax and metol-borax developers increase the effective sensitivity and may appreciably improve the detail of the image in some cases. They are thoroughly practical developers if it is remembered that they are quite sensitive to the soluble bromide which accumulates in use. A small amount can be compensated by increasing the development time (see Table 3) and may be an advantage; but it is well to remember that in most scientific applications of photography the overhead expense on a given exposure normally makes it very false economy to endanger results by saving developer.

IV. SUMMARY

1. Six developers characterized by increased solvent action on silver bromide and decreased reduction potential have been compared with standard pyrogallol and metol-hydroquinone formulas. The comparison is based on (*a*) sensitometric tests, using three emulsions; (*b*) tests of resolving power by the parallel-line test object, using the same emulsions; and (*c*) spectrographic exposures with one of the emulsions.

2. Only the developers with lowest reduction potential effected an appreciable improvement in resolving power. These developers are of no practical use because they greatly decrease the effective sensitivity.

3. The "borax" developers used in motion-picture laboratories are satisfactory for spectrographic work, but improvement over the standard formulas can not be expected to be large.

V. ACKNOWLEDGMENTS

The resolution test object was prepared by Raymond Davis, photographic technologist. We are also indebted to him and to B. F. Scribner for assistance in examination of the test strips.

WASHINGTON, January 6, 1930.

RESONANCE AND QUENCHING OF THE THIRD PRINCIPAL SERIES LINE OF CAESIUM

By C. Boeckner

ABSTRACT

A helium discharge is used as a source for the study of the resonance radiation from the third principal series line of caesium. This is possible, due to the coincidence of a strong helium line with the caesium line. A number of caesium arc lines are also observed in the fluorescent radiation; they have their origin in lower levels populated by radiation transitions from the initial level ($4P_{1/2}$). The effect of helium on the fluorescent radiation is studied. It is found that collisions between helium and caesium atoms in the $4P_{1/2}$ state transfer the latter only to states differing by less than several hundredths of a volt from the initial state. Transfers to states differing by as much as 0.18 volt are improbable.

CONTENTS

	Page
I. Introduction	13
II. Experimental	14
III. Results	14
IV. Discussion	15

I. INTRODUCTION

In another paper[1] from this laboratory it was noted that the strong 3888 helium line coincided with the third principal series line of caesium and that it was markedly absorbed by caesium vapor. This suggested that a helium tube would serve as an excellent source for the study of caesium resonance radiation; the obvious reasons being the simplicity and intensity of the source and absence of self-reversal. The experiment of illuminating caesium vapor with a helium discharge tube was then carried out and it was found that the expected fluorescence could, indeed, be detected. Fifteen-minute exposures with a Hilger E_2 quartz spectrograph were usually sufficient to photograph the strong lines.

Little work has been done on the excitation of resonance of the higher alkali series lines. Lord Rayleigh[2] illuminated sodium vapor with the second principal series line of sodium and obtained the D lines in emission; Cario and Franck[3] later repeated the experiments. Recently C. J. Christensen and G. K. Rollefson[4] in a similar experiment observed the second line itself and obtained a value for the ratio of the second line to the D lines.

The present paper deals with the fluorescence appearing when caesium atoms are raised to the $4P_{1/2}$ state (the initial state of one component of the third principal series doublet) and the effect of helium in altering the fluorescence.

[1] B. S. Jour. Research (in press).
[2] R. J. Strutt, Proc. Roy. Soc., London (A), **96**, p. 272; 1919.
[3] Cario and Franck, Zs. f. Phys., **11**, p. 87; 1925.
[4] C. J. Christensen and G. K. Rollefson, Phys. Rev., **34**, p. 1157; 1929.

II. EXPERIMENTAL

A simple capillary cold electrode discharge tube containing helium at about 1 cm pressure was used as a source. The tube was operated at 10,000 volts from a transformer; the primary current being about 8 amperes.

The resonance tube was of the type commonly used in the study of resonance and scattering. It was about 30 cm long and was drawn out at one end into a light trap. On the other end was sealed a flat glass window. To reduce scattering, a platinum diaphragm with a narrow slit was placed inside of the tube about a centimeter in back of the window, thus shielding it from the direct light of the discharge. The slit was focused on the spectrograph slit. The resonance tube was illuminated by placing the discharge tube near it, but several centimeters away to reduce scattering from the window and light traps. It was not necessary to use great precautions against scattering except for observations on the resonance line itself, since the lines in the source were in no other case near caesium lines.

To maintain the required caesium vapor pressure the discharge tubes and resonance tubes were placed in a furnace and maintained at a temperature of about 200° C. A small appendix to the resonance tube projected from the furnace and was kept at a somewhat lower temperature. This arrangement insured that the condensed caesium be in the cooler appendix and permitted a definite control of the vapor pressure. The appendix was usually kept at a temperature of 120° C. (corresponding to a vapor pressure of 0.001 mm). This pressure of caesium was found to give the most intense fluorescence. In some of the work the resonance tube was kept on the pumps to insure a good vacuum.

The helium for the quenching experiments was obtained from tanks supplied by the Navy Department and was purified by passage through a charcoal trap immersed in liquid air.

A Hilger E_2 quartz spectrograph was used for photographing the fluorescence. For photographing lines in the near infra-red, neocyanin stained plates were used. These were kindly prepared by B. H. Carroll, of the photographic emulsions laboratory.

III. RESULTS

A list of the lines appearing in the fluorescent spectrum is given below. Rough estimates of the intensities are also given. These were obtained by calibrating the plate with light from a tungsten filament at 2,900° and estimating photographic densities visually. Comparisons at different helium pressures were made by using the helium lines in the scattered light as standards:

No foreign gas	Wave lengths	4 mm helium
$1S$–$4P_{1/2}$ (10)	3, 888. 6	$1S$–$4P_{1/2}$ (2)
	3, 876. 4	$1S$–$4P_{3/2}$ (4)
$1S$–$2P_{3/2}$ (10)	8, 521. 1	$1S$–$2P_{3/2}$ (10)
$2P_{1/2}$–$3S$ faint	7, 609. 7	
$2P_{3/2}$–$3S$ faint	7, 944. 1	
$2P_{1/2}$–$4D_{3/2}$ faint	8, 761. 4	
	6, 973. 1	$2P_{3/2}$–$5D_{3/2, 5/2}$ (10)
	6, 723. 2	$2P_{1/2}$–$5D_{3/2}$ (10)
	4, 593. 2	$1S$–$3P_{1/2}$ (.5)
	4, 555. 3	$1S$–$3P_{3/2}$ (.5)

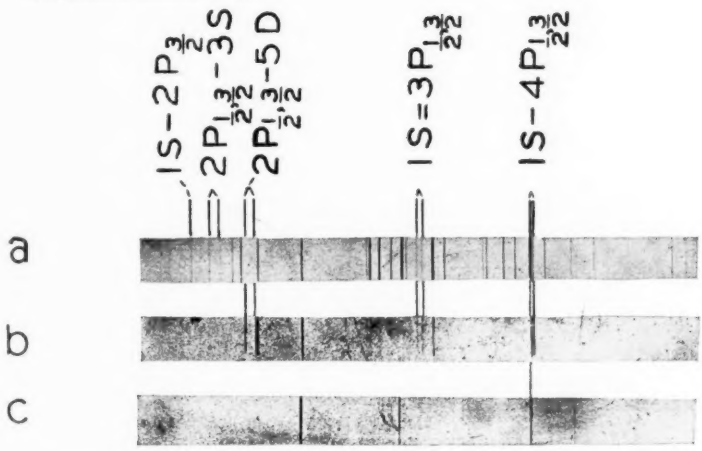

FIGURE 1.—*Caesium fluorescence excited by a helium discharge*

(*a*) Photograph showing infra-red lines, some foreign gas.
(*b*) Fluorescence obtained with 4 mm helium.
(*c*) Fluorescence obtained with no foreign gas.

The most striking effect of the addition of helium is the appearance with great intensity of the doublet $2P_{1/2}$–$5D_{3/2}$, $2P_{3/2}$–$5D_{3/2,\ 5/2}$. The disappearance of the doublet ($2P_{1/2}$–$3S$), ($2P_{3/2}$–$3S$) is also interesting.

The principal series doublet $1S$–$4P_{1/2,\ 3/2}$ seems to attain its normal intensity ratio at 4 mm of helium. At zero pressure the intensity of $1S$–$4P_{1/2}$ is 10; of $1S$–$4P_{3/2}$ is 0; at 0.6 mm of helium $1S$–$4P_{1/2}$ is 4, and $1S$–$4P_{3/2}$ is 2; at 4 mm $1S$–$4P_{1/2}$ is 2 and $1S$–$4P_{3/2}$ is 4.

The intensity of the first principal series line $1S$–$2P_{3/2}$ is not noticeably changed by the addition of helium. The actual magnitude of intensity of this line may be greater than that observed, due to the absorption of the fluorescent radiation in the tube.

The intensity of the fluorescent radiation varies with the caesium pressure and passes through a maximum at about 0.001 mm. Whether the decrease at higher pressures is due to absorption of the exciting light before it reached the field of view, absorption of the fluorescent radiation in the tube, or to actual quenching by caesium, is uncertain.

IV. DISCUSSION

The reasons for the appearance of the lines observed in fluorescence is best seen by the aid of the level diagram in Figure 2. With no foreign gas in the resonance tube the $4P_{1/2}$ level is strongly populated. The radiation transition to the $1S$ from this level gives rise to the observed line $1S$–$4P_{1/2}$. The transitions from $4P_{1/2}$ to all the lower S and D levels undoubtedly occur, but their wave lengths lie too far in the red to be detected by the photographic method. These lower S and D levels, populated by transitions from the $4P_{1/2}$ level, give rise to some lines that can be detected by the use of a neocyanin stained plate; $2P_{1/2,\ 3/2}$–$3S$ $\lambda = 7{,}944$, $7{,}609$ are observed as well as $2P_{1/2}$–$4D_{3/2}$ $\lambda = 8{,}761$. These transitions, as well as the unobserved ones $2P$–$2S$ and $2P$–$3D$, populate the $2P$ levels and give rise to the strong-line $1S$–$2P_{3/2}$. The other component of this doublet, $1S$–$2P_{1/2}$ lies too far in the red to be detected by the photographic plate. It is conceivable that the $3P$ levels could be populated by transitions from $3S$ and $4D$, but the second principal series doublet originating from them ($1S$–$3P_{1/2,\ 3/2}$) could not be observed when a good vacuum existed in the tube. The fact that $1S$–$4P_{1/2}$ and $1S$–$2P_{3/2}$ have the same order of intensity indicates that the return to $1S$ from $4P_{1/2}$ directly has the same order of probability as the return by the indirect route by way of $2P$. This is in agreement with the work of Christensen and Rollefson,[5] who found that the ratio of intensities of the first principal series line to the second was 1.7 when the second was excited optically.

The results obtained upon the addition of helium are best explained by the assumption that collisions of the second kind in which more than several hundredths of a volt are dissipated as kinetic energy are relatively improbable.

The appearance of the strong $1S$–$4P_{3/2}$ and $2P$–$5D$, lines is brought about by the displacement of the atoms from the initial $4P_{1/2}$ level to the neighboring levels $4P_{3/2}$ and $5D$. The $4P_{3/2}$ level is 0.01 volts and the $5D$ levels 0.043 volts higher than the initial $4P_{1/2}$ level. The difference in energy must, of course, come from the thermal energy of the colliding atoms.

[5] See footnote 4, p. 13.

The fact that the lines $2P$–$3S$ do not increase but decrease in intensity when helium is added indicates that the transfer of atoms by collision from the $4P_{1/2}$ state to the $3S$ state, 0.18 volts lower, is improbable. Thus the probability of transfer of energy between states 0.18 volts apart is much less than that between states 0.043 volts apart ($2P_{1/2}$ to $5D$). A rough estimate based on the intensity of the strong $2P_{1/2}$–$5D$ and the intensity at $2P_{3/2}$–$3S$ that could just be detected puts the ratio of these probabilities as less than 1 : 20.

The disappearance of the $2P$–$3S$ lines can be explained by the decrease in population of the $4P$ levels by transfer of atoms to the D levels. Since the $3S$ state is populated by radiation transfers from the P states but not from the D states the population of the $3S$ state must decrease.

Upon the above idea the faint appearance of the lines $1S$–$3P_{1/2, 3/2}$ upon the addition of helium must be explained by radiation transfer to the $3P$ levels. It does not seem reasonable to ascribe these lines to collision transfer from the $4P$ state, since the difference in energy is about 0.5 volt.

These observations seem to be incompatible with the related work of Cario and Franck [6] upon sodium vapor. They illuminated sodium vapor with the second principal series line and observed that the D lines were greatly increased by the presence of a few millimeters of argon. They also observed that the D light emitted in this case was little absorbed as compared to "oridinary" D light.

These facts were explained by saying that atoms were brought down from the $3P$ to the $2P$ state by collisions of the second kind. The difference in energy of 1.6 volts appeared as kinetic energy of translation which meant that the D lines emitted were broadened by the Doppler effect and, hence, were little absorbed.

The work of Christensen and Rollefson [7] would make any increase in the D light of more than 60 per cent impossible. They state that 63 per cent of the atoms in the $3P$ state return to $1S$ by way of the $2P$ state; the most any collision process could do would be to bring about the return of the other 37 per cent (that ordinarily returns directly to $1S$ by radiation) by the same process.

The small probability of collisions of the second kind with dissipation of 0.2 volt as kinetic energy is not surprising. The quenching of the 2,537 resonance radiation of mercury vapor by helium consists in the transfer of the mercury from the $2P_1$ to the metastable $2P_0$ state, 0.22 volts lower. It is found that 1 cm of helium quenches to the extent of 5 per cent, indicating a small probability for the process.

In the experiments of Beutler and Jospehi [8] it is also found that interchanges of energy between excited mercury and sodium, involving an appearance of more than 0.15 volts as kinetic energy, are relatively improbable.

Some figures for the efficiency of several quenching reactions are as follows: Transfer of the sodium atom from $2P_{1/2}$ to the $2P_{3/2}$ state [9] by a helium neon mixture and argon ($\Delta V = 0.002$ volts), here every kinetic theory collision is effective; quenching of Hg resonance [10] by argon and helium ($\Delta V = 0.22$ volts), for argon 0.05 and for helium

[6] See footnote 3, p. 13.
[7] See footnote 4, p. 13.
[8] H. Kallman u. F., London, Zeit. f. Phys. Chem., **B 2,** p. 207; 1929.
[9] W. Lochte Holtgreven, Zeit. f. Phys., **47,** p. 369; 1928.
[10] E. Gaviola, Phys. Rev., **34,** p. 1049; 1929.

0.005 of the kinetic theory collisions are effective; quenching of the D light resonance of sodium [11] by a helium neon mixture ($\Delta V = 2.1$ volts); here 0.017 of the kinetic theory collisions are effective.

It is not possible to give a precise figure for the collision radius for the transfer of caesium atoms in the $4P_{1/2}$ to the $4P_{3/2}$ and $5D$ states, since the life time of the $4P_{1/2}$ state is unknown. The half life of the

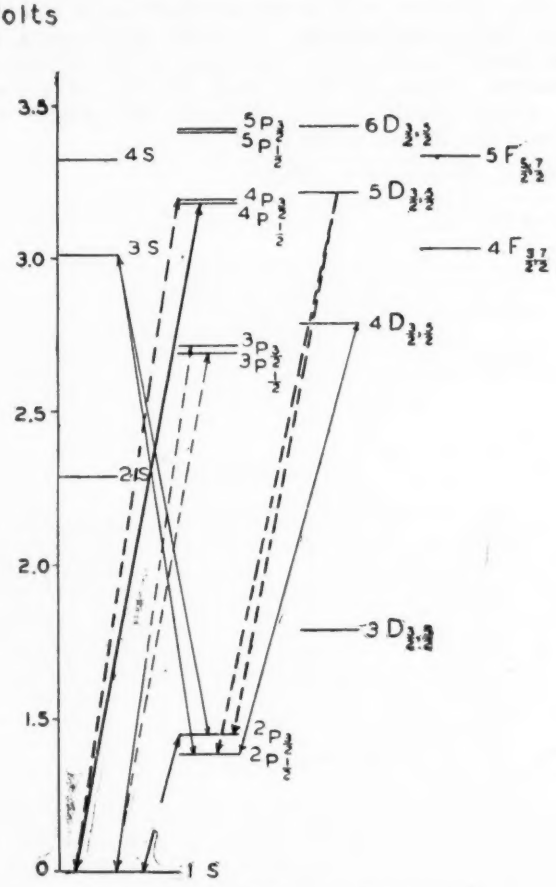

FIGURE 2.—*Level diagram of caesium*

Full lines represent transitions observed with no foreign gas, dotted lines transitions observed with helium present.

caesium $2P$ states is probably the same as that of sodium,[12] 3.7×10^{-8} seconds.

Canal ray experiments show that the higher states of a series have a longer life than the first state, but rarely longer than 10^{-7} seconds.[13] Taking 10^{-7} as a fair value for the life of the $4P_{1/2}$ state and 1 mm of helium as the pressure at which a collision or a radiation transfer is

[11] Mannkopf, Zeit. f. Physik., **36**, p. 315; 1926.
[12] Kirschbaum, Ann. d. Phys., **79**, p. 465; 1926.
[13] Hirsch and Döpel, Ann. d. Phys., **17**, p. 963; 1929.

equally probable, one obtains 3.1×10^{-8} cm for the sum of the helium and caesium radii. The kinetic theory value for helium and normal caesium is 2.9×10^{-8} cm. Thus approximately every kinetic theory collision is effective.

It is interesting to note that Mohler and Boeckner[14] obtain very great radii for the quenching of the higher excited caesium states by caesium itself. For example, normal caesium apparently reacts with caesium in the $4P$ state with a radius which is 10 times the kinetic theory value for normal atoms. At 0.001 m pressure, 0.1 per cent of atoms in the $4P$ state and 20 per cent in the $6P$ state react with neutral caesium atoms to form ions instead of radiating. This quenching action would render difficult the study of resonance radiation from the higher series lines.

WASHINGTON, February 8, 1930.

[14] See footnote 1, p. 13.

RELATIONSHIPS BETWEEN ROCKWELL AND BRINELL NUMBERS [1]

By S. N. Petrenko

ABSTRACT

Comparative Rockwell and Brinell tests were made on a great variety of ferrous and nonferrous metals.

Relationships between Brinell and Rockwell numbers, based on certain simplifying assumptions, are:

$$\text{Brinell number} = \frac{\text{constant}}{130 - \text{Rockwell ball number}}$$

and

$$\text{Brinell number} = \frac{\text{constant}}{(100 - \text{Rockwell cone number})^2}$$

These equations were used as guides in finding empirical formulas which fitted most closely the values determined experimentally. Of all the experimental values obtained in this investigation very few differed by more than 10 per cent from values obtained from these empirical equations.

Empirical equations were also found giving the tensile strengths of steels in terms of their Rockwell numbers. Experimental values checked these equations within an error of plus or minus 15 per cent.

CONTENTS

		Page
I.	Introduction	19
II.	Purpose of investigation	20
III.	Acknowledgments	20
IV.	Apparatus and procedure	20
V.	Theoretical considerations	22
VI.	Experimental data	28
VII.	Correlation of approximate theory and experiment	38
VIII.	Accuracy of empirical conversion formulas	42
IX.	Relationship of Rockwell numbers to tensile strength	44
X.	Results of earlier investigators	47
XI.	Summary	48

I. INTRODUCTION

Indentation hardness tests are growing in importance as a means of checking the uniformity of the mechanical properties of metals used in engineering structures and machines.

If a metal is of uniform composition and the process of its manufacture is reasonably well controlled, uniform indentation numbers are nearly always a sufficient guarantee of its uniform quality. It is also found that the tensile strength of steel can be estimated from its Brinell number with sufficient accuracy for many commercial purposes.

The indentation test is preferred to a tensile test for control purposes because it is nondestructive and relatively inexpensive and because

[1] This paper supersedes a paper (B. S. Tech. Paper No. 334) with the same title and by the same author, published in 1927. The present paper includes the data (Tables 2 and 3) of the earlier paper, and, in addition, the results of many more tests on various heat-treated steels (Table 2 (a)).

it can be applied to pieces of the regular factory output. Since an indentation very seldom impairs the usefulness of a tested piece, it is in many cases not only possible but also practicable to test every piece produced.

Brinell and Rockwell hardness tests are two of the various indentation tests which are being widely used for control purposes, and situations often arise in which a Brinell (or Rockwell) number is needed when only a Rockwell (or Brinell) number can be obtained. In such cases a reliable chart or formula expressing a definite relationship between Rockwell and Brinell numbers is of great practical value.

II. PURPOSE OF INVESTIGATION

The purpose of this investigation was:

1. To make tests on a great number of the metals used in engineering construction and thus obtain data sufficient for determining the relation between Rockwell and Brinell numbers and also the relation between Rockwell numbers and tensile strength.
2. To determine the limits of error within which one of these numbers may be used to estimate the other number and the tensile strength of the material.

III. ACKNOWLEDGMENTS

The materials used in this investigation were contributed by the following manufacturers: Aluminum Co. of America, American Magnesium Corporation, Raritan Copper Works, Chase Metal Works, American Brass Co., Riverside Metal Works, International Nickel Co., Union Drawn Steel Co., Colonial Steel Co., American Rolling Mills Co., Central Alloy Steel Co., Halcomb Steel Co., Firth Sterling Steel Co., Carpenter Steel Co., and Wilson-Maeulen Co.

The metallurgical division of this bureau contributed data on Rockwell and Brinell numbers and tensile strengths for a great variety of steels.[2] (See Table 5.) These data made it possible to get a more conclusive check on the errors involved in the use of the conversion formulas.

Credit is due Dr. L. B. Tuckerman[3] for his many valuable suggestions. Prof. G. F. Rouse made the study of the diamond tool and edited the manuscript.

IV. APPARATUS AND PROCEDURE

The Brinell machine used in this investigation (see fig. 1) is provided with a dead-weight relief valve for maintaining the desired load on the indenting tool. This consists of a spherical piston accurately fitted, without packing, to a cylinder connected with the pressure chamber. This piston carries a crossbar, *A*, and weights, *B*. The maximum pressure is determined by the weights which are lifted by

[2] See Report in Trans. of A. S. M. E., 48, p. 533; 1926; entitled "Rough Turning With Particular Reference to the Steel Cut," by H. J. French and T. G. Digges. The Rockwell and Brinell numbers for hard steels were obtained on samples (Table 5, samples I-9D to I-16B) used by Dr. Gillett, chief, metallurgical division, Bureau of Standards, in his work on molybdenum and cerium steels. The composition, heat treatment, and other data for these steels will be found in the book, Molybdenum, Cerium, and Related Alloy Steels, by H. W. Gillett and E. L. Mack; 1925.

[3] Principal scientist, mechanics and sound division, Bureau of Standards.

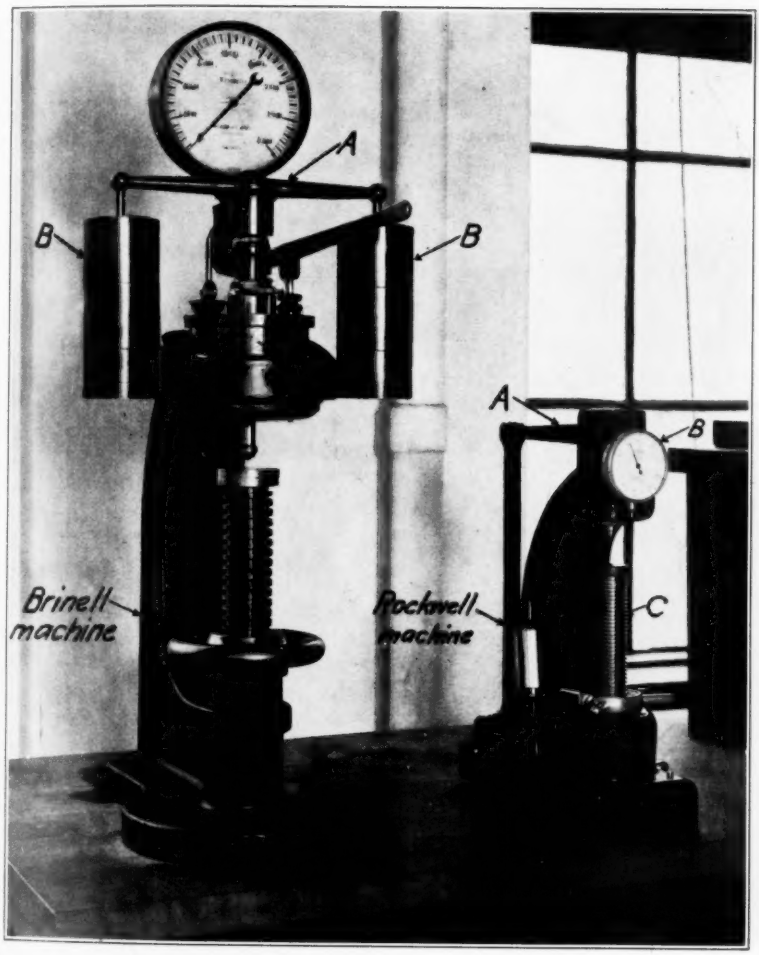

FIGURE 1.—*Brinell and Rockwell machines*

the piston as soon as this pressure is reached. The load remains constant as long as the piston floats.

A standard load of 3,000 kg was used in this investigation on metals having a Brinell number equal to or greater than 70, and a load of 500 kg was used on metals with a Brinell number less than 70. In every case the load was applied for 30 seconds. A Hultgren work-hardened steel ball, 10 mm in diameter, was used as the indenting tool.

The diameter of each indentation was measured with a Brinell microscope having 0.1 mm graduations. Readings were estimated to 0.01 mm.

The Brinell number was obtained directly from a table[4] which gives Brinell numbers corresponding to diameters of indentation.

The Rockwell machine shown in Figure 1 has a dead-weight loading device consisting of a double lever, *A*, having a total multiplication ratio of about 119. Materials listed in Table 2 were tested in this machine. A newer model having only one lever was used for testing the steels listed in Table 3. This machine was checked on the standard blocks used for the older model and all readings fell within limits of plus or minus 5 per cent of depth of indentation.

The specimen was placed on the table of the elevating screw, *C* (fig. 1), and was pressed against the indenting tool until a so-called minor load of 10 kg was acting. Next, the pointer on the indicating dial *B* was set at zero, after which the load was gradually increased to a maximum value, designated the major load. The load was then reduced to 10 kg and the Rockwell number was read from the dial.

The manufacturer recommends the following tools and loads for the Rockwell machine: A steel ball $\frac{1}{16}$ inch (1.588 mm) in diameter with a 100 kg major load, on soft and medium materials; a steel ball $\frac{1}{8}$ inch (3.176 mm) in diameter with a 100 kg major load, on very soft materials; and a diamond tool with a 150 kg major load on hard materials. This diamond tool, commonly called a cone, has an included angle of 120° and an apex lapped to a spherical surface. The tool is patented by the manufacturer, and has the trade name "brale." Other major loads of 100 kg and 60 kg were used with the brale and 60 kg with the $\frac{1}{16}$-inch ball in order to obtain more complete data on the change of Rockwell numbers with change of load or indenting tool.

The direct reading dial *B* is provided with so-called "B" and "C" scales. The Rockwell ball number, designated in this paper by R_B, is read directly from the "B" scale. The cone number, designated in this paper by R_C, is read directly from the "C" scale. The calibration of the scales is such that the depth of indentation in mm, in excess of that produced by the minor load, is $(130-R_B)\times 0.002$ for the ball and $(100-R_C)\times 0.002$ for the cone.

There is no recognized standard for time under load in Rockwell testing. In this investigation the major load was removed approximately three-fourths second after it reached its maximum value.

Tests were made on six specimens to determine the change occurring in a Rockwell number due to a variation of time under load. The results are shown graphically in Figure 2. The greatest variation in average Rockwell number over a 10-second period, a decrease of 0.8

[4] Miscellaneous Publication of the Bureau of Standards, No. 62.

point, was found in the case of steel block C 24–25. The average decrease in Rockwell number, 0.3 of a point, is less than the difference usually found between individual readings on the same specimen.

V. THEORETICAL CONSIDERATIONS

Some symbols used in this discussion are:

Symbol	Meaning
Bn	Brinell number.
${}_nR_{Bm}$	Rockwell ball number, obtained using a major load of n kg and a ball with a diameter of m inches.
${}_kRc$	Rockwell cone number, obtained using a major load of k kg and the brale.

Dr. J. A. Brinell, a Swedish engineer,[5] defined the indentation number which now bears his name as the ratio $\frac{P}{A}$, P being the load on

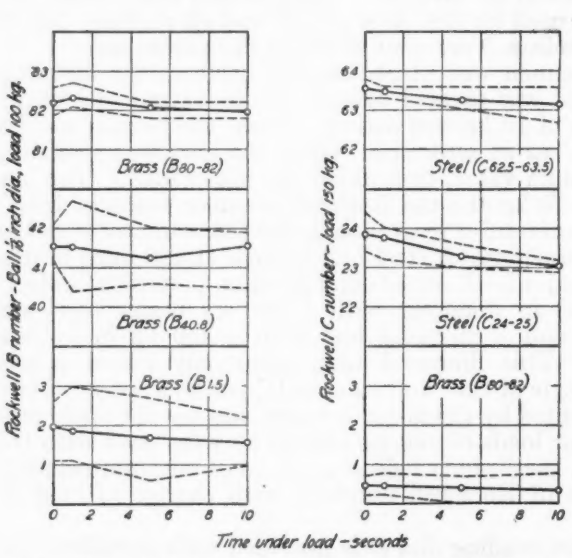

FIGURE 2.—*Effect of time under load upon Rockwell number*

Circles represent average values obtained from five indentations. Dash lines show extreme variations. Values for zero time were obtained within one-half second of the instant the major load reached its maximum value. Identification marks on the standard blocks are given in parentheses.

the indenting tool in kilograms and A the surface area of the indentation in square millimeters.

The Rockwell indentation number is defined as a constant minus the depth of indentation. The constant and the depth are expressed in arbitrarily selected units.

Investigation has shown that the Brinell number, as defined above, is not a constant of the test material; that is, that the area of an indentation is not directly proportional to the load. Many of the

[5] Congrès International des Méthodes d'Essai des Materiaux de Construction, **2**, p. 83; 1901.

causes for this lack of proportionality can be given in a general way, but an exact theoretical discussion which involves the ratio $\frac{P}{A}$ and which takes into account all disturbing factors can not be given.

When it is impossible to carry out an exact deduction of a formula relating to quantities, one may resort to experiment and establish a purely empirical formula. Unfortunately, unless there is a great mass of well-distributed data, the purely empirical formula is, at best, often unsatisfactory. Whenever it is possible to make assumptions which are approximately true and which simplify the problem so that an approximate formula can be derived, there is an obvious advantage in carrying out the derivation because the resulting approximate formula is a valuable guide in finding the most satisfactory empirical formula.

In the present problem the simplifying assumption is Brinell's original assumption that the area of an indentation is always directly proportional to the load. Using this, it is possible to derive approximate formulas for converting Rockwell numbers into Brinell numbers or vice versa.

Applying the definition of the Brinell number to the Rockwell ball test:

$$Bn=\frac{\text{major load}}{\text{surface area of indentation}}=\frac{P}{2\pi rH} \tag{1}$$

where P is the major load, r the radius of the indenting ball, and H the total depth of indentation. Let the depth of indentation due to the minor load only be denoted by h_0 and let $h=(H-h_0)$. Then, assuming that the area of indentation is directly proportional to the load,

$$\frac{H}{h_0}=\frac{P}{10} \text{ or } H=h_0\cdot\frac{P}{10}$$

$$\therefore \quad H=(H-h)\cdot\frac{P}{10}$$

$$H=h\cdot\frac{P}{P-10}$$

But $h=(130-R_B)\times 0.002$

$$\therefore \quad H=(130-R_B)\times 0.002\times\frac{P}{P-10}$$

Substituting in equation (1)

$$Bn=\frac{P-10}{2\pi r(130-R_B)\times 0.002} \tag{2}$$

Equation (2) can be written:

$$Bn=\frac{C}{(130-R_B)} \tag{3}$$

where

$$C=\frac{P-10}{2\pi r\cdot(0.002)} \tag{4}$$

The value of C corresponding to any particular Rockwell ball test is easily found. For instance, considering the ${}_{100}R_{B1/16}$ case, in which a ball $\frac{1}{16}$ inch in diameter is used with a major load of 100 kg

$$C=\frac{90}{2\pi\cdot(0.794)\cdot 0.002}=9{,}020$$

$$\therefore \quad Bn=\frac{9{,}020}{130-{}_{100}R_{B1/16}}$$

Values of C corresponding to the other Rockwell ball tests have been calculated, and all equations are shown in Table 1.

Assuming that the brale is a true cone and applying the definition of the Brinell number to it:

$$Bn=\frac{\text{major load}}{\text{surface area of indentation}}=\frac{P}{\pi\tan\theta\sec\theta H^2}$$

where P is major load, H the total depth of indentation, and θ one-half the angle of the cone.

TABLE 1.—*Approximate relationships between Brinell and Rockwell numbers based on the assumption that area of indentation is directly proportional to load*

Rockwell		Theoretical relationship
Tool	Load	
	kg	
Ball, 1/16 inch (1.588 mm) diameter	100	$Bn=\frac{9{,}020}{130-{}_{100}R_{B1/16}}$.
Ball, 1/8 inch (3.176 mm) diameter	100	$Bn=\frac{4{,}510}{130-{}_{100}R_{B1/8}}$.
Ball, 1/16 inch (1.588 mm) diameter	60	$Bn=\frac{5{,}010}{130-{}_{60}R_{B1/16}}$.
Brale, diamond, true cone having a 120° angle.	150	$Bn=\frac{1{,}896{,}000}{(100-{}_{150}R)^2C}$.
Do	100	$Bn=\frac{1{,}074{,}000}{(100-{}_{100}R_C)^2}$.
Do	60	$Bn=\frac{483{,}000}{(100-{}_{60}R_C)^2}$.
Brale, diamond, the apex being a spherical segment of altitude S, angle of conical portion 120°. (See fig. 3.)	150	Case I · · · For ${}_{150}R_C$ greater than $(100-466.7\,S)$. $Bn=\frac{1{,}492.9}{S(100-{}_{150}R_C)}$. Case II · · · For ${}_{150}R_C$ greater than $(100-2{,}953\,S)$ and less than $(100-466.7\,S)$. $Bn=\frac{150}{46.89S^2+10.882\,(L^2+4.308SL)}$. L is obtained in terms of ${}_{150}R_C$ and S from: $L^3+(4.308S)L+4.308S\,(S-15h_0)=0$ and $(100-{}_{150}R_C)\times 0.002=L+S-h_0$. Case III · · · For ${}_{150}R_C$ less than $(100-2{,}953\,S)$. $Bn=\frac{150}{46.89\,S^2+10.882(L^2+4.308SL)}$. L is obtained in terms of ${}_{150}R_C$ and S from $L^3+(4.308S)L-[60.325S^2+15(d^2+4.308Sd)]=0$ and $(100-{}_{150}R_C)\times 0.002=L-d$.

${}_{100}R_{B1/16}=2\times{}_{100}R_{B1/8}-130$

${}_{100}R_{B1/16}=1.800\times{}_{60}R_{B1/16}-104$

${}_{100}R_C=1.491\times{}_{60}R_C-49.1$

For a 120° cone,

$$Bn = \frac{P}{\pi \cdot \tan 60° \cdot \sec 60° \cdot H^2} = \frac{P}{10.882H^2} \tag{5}$$

If we assume that, in this case also, the area of indentation is proportional to the load,

$$\frac{\text{Major area}}{\text{Minor area}} = \frac{H^2}{h_o^2} = \frac{(h+h_o)^2}{h_o^2} = \frac{P}{10} \tag{6}$$

$$\frac{h+h_o}{h_o} = \sqrt{\frac{P}{10}}$$

$$h_o = \frac{h}{\sqrt{\frac{P}{10}} - 1}$$

and

$$H^2 = \frac{h^2}{\left\{\sqrt{\frac{P}{10}} - 1\right\}^2} \times \frac{P}{10}$$

Using this value of H^2 in equation (5)

$$Bn = \frac{P}{10.882 \times \frac{h^2}{\left\{\sqrt{\frac{P}{10}} - 1\right\}^2} \times \frac{P}{10}}$$

$$= \frac{10\left\{\sqrt{\frac{P}{10}} - 1\right\}^2}{10.882h^2}$$

$$= \frac{(\sqrt{P} - \sqrt{10})^2}{10.882h^2}$$

Now

$$h = (100 - R_C) \times 0.002$$

$\therefore$

$$Bn = \frac{(\sqrt{P} - \sqrt{10})^2}{10.882\,(100 - R_C)^2 \cdot (0.002)^2}$$

This equation can be written:

$$Bn = \frac{C_1}{(100 - R_C)^2} \tag{7}$$

where

$$C_1 = \frac{(\sqrt{P} - \sqrt{10})^2 \cdot}{10.882 \times (0.002)^2} \tag{8}$$

Considering the ${}_{150}R_C$ case, in which the major load is 150 kg,

$$C_1=\frac{(\sqrt{150}-\sqrt{10})^2}{10.882\times(0.002)^2}$$

$$=1{,}896{,}000$$

and

$$Bn=\frac{1{,}896{,}000}{(100-{}_{150}R_C)^2}$$

A list of equations for all of the cone tests is given in Table 1.

The diamond indenting tool furnished with the Rockwell machine by the manufacturer is not a true cone, as assumed in the discussion just given, because it has a rounded apex approximating in form a spherical segment. A theoretical discussion for this form of tool when used with a 150 kg major load will now be given. (Refer to fig. 3.)

Assume that the rounded portion of the brale is a segment of a sphere of radius r. Let h_0 represent the depth of indentation pro-

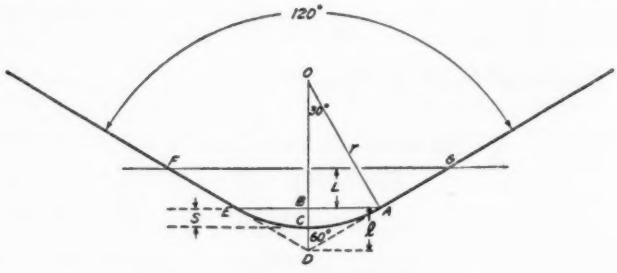

Notation: r, radius of spherical end, distance OA
S, distance BC; S = 0.134 r
ℓ, distance BD; ℓ = 0.2887 r = 2.154 S

FIGURE 3.—*Form of Rockwell brale*

duced by the minor load of 10 kg and h_1 that due to the major load of 150 kg.

Three cases must be considered:

1. The major indentation is spherical; h_1 is less than S.

2. The minor indentation is spherical, while the major indentation is partly spherical and partly conical in form; h_0 is less than S, while h_1 is greater than S.

3. The minor, as well as the major indentation, is partly spherical and partly conical in form. Both h_0 and h_1 are greater than S.

It is assumed that the surface area of an indentation is directly proportional to the load producing it.

The area of a spherical segment having sagitta S and radius r is $2\pi rS$.

For a 120° cone the lateral area of a zone having a section $ABEFGA$ is 10.882 (L^2+2lL), L being the vertical height of the zone.

Case I.—Since both the minor and major indentations are spherical an equation of the form $Bn=\frac{C}{100-{}_{150}R_C}$ expresses the relation between Bn and ${}_{150}R_C$. (See equation (3), p. 23.)

For this particular case $C=\frac{140\times 0.134}{2\pi S\times 0.002}=\frac{1492.9}{S}$, and the relation is

$$Bn=\frac{1492.9}{S(100-{}_{150}R_C)} \tag{9}$$

This equation holds for values of ${}_{150}R_C$ greater than $(100-466.7S)$. This value of ${}_{150}R_C$ is obtained by combining the equations:

$$\frac{\text{depth of minor indentation}}{\text{depth of major indentation}}=\frac{h_0}{S}=\frac{10}{150}$$

and

$$(100-{}_{150}R_C)\times 0.002=S-h_0.$$

Case II.—By definition

$$Bn=\frac{150}{2\pi rS+10.882(L^2+2lL)} \tag{10}$$

where $L=h_1-S$.

Substituting values for r and l in terms of S, equation (10) becomes

$$Bn=\frac{150}{46.89S^2+10.882(L^2+4.308SL)} \tag{11}$$

In order to find a value for the variable L in terms of ${}_{150}R_C$ two other equations must be written. These are:

$$\frac{\text{Major area}}{\text{Minor area}}=\frac{2\pi rS+10.882(L^2+2lL)}{2\pi rh_0}=\frac{150}{10}$$

which reduces to:

$$L^2+(4.308S)L+4.308S(S-15h_0)=0 \tag{12}$$

and

$$(100-{}_{150}R_C)\times 0.002=L+S-h_0 \tag{13}$$

By eliminating h_0 from equations (12) and (13) a value of L is obtained which can in turn be substituted in equation (11) to get an expression containing Bn, ${}_{150}R_C$, and S. This expression would be complicated, and it seems simpler to use equations (11), (12), and (13) as they stand.

These equations hold for values of h_0 greater than 0.0666 S and less than S. The first limit is determined by the fact that the depth of the major indentation just equals S when the depth of the minor indentation, or $h_0=\frac{S}{15}$. The second limit is fixed by the definition of this case.

Case III.—

$$Bn=\frac{150}{2\pi rS+10.882(L^2+2lL)}$$

$$=\frac{150}{46.89S^2+10.882(L^2+4.308SL)} \tag{14}$$

The equations needed to solve for L are:

$$\frac{\text{Major area}}{\text{Minor area}}=\frac{2\pi rS+10.882(L^2+2lL)}{2\pi rS+10.882(d^2+2ld)}=\frac{150}{10}\ (\text{where } d=h_0-S)$$

which reduce to:

$$L^2+(4.308S)L-\{60.325S^2+15(d^2+4.308Sd)\}=0 \tag{15}$$

and

$$(100-{}_{150}R_C)\times 0.002=L-d \tag{16}$$

Equations (14), (15), and (16) can be solved simultaneously to obtain an expression in Bn, ${}_{150}R_C$, and S. In this case it also seems much simpler to use the equations as they are given.

These equations hold for all positive values of d.

Values for ${}_{150}R_C$ and Bn in terms of S given in columns 4 and 5 of Table 6 were calculated by means of equations (9) to (16).

By equating values of Bn given in Table 1, relationships between the Rockwell numbers are obtained. For instance, using the first two values for Bn:

$$\frac{9{,}020}{(130-{}_{100}R_{B1/16})}=\frac{4{,}510}{(130-{}_{100}R_{B1/8})}$$

or

$${}_{100}R_{B1/16}=2\times {}_{100}R_{B1/8}-130$$

The more important equations obtainable in this way are given in Table 1.

Attention is again called to the fact that the formulas discussed above and listed in Table 1 are only approximately true. As will be shown later, empirical formulas, like these in general form, fit experimental data quite satisfactorily.

VI. EXPERIMENTAL DATA

The specimens used in this investigation are listed and described in Tables 2 and 3. Experimental Rockwell and Brinell numbers for specimens listed in Table 2 are found in Table 4. The Brinell and Rockwell numbers for the heat-treated steels are found in the right-hand columns of Table 3.

TABLE 2.—*Materials used for Brinell and Rockwell tests*

TABLE 2.—*Materials used for Brinell and Rockwell tests*

FERROUS MATERIALS

[Condition: As received from mill]

Sample No.	Material	C	Mn	Si	P	S	Ni	Cr	V	W	Yield [a] point	Tensile strength	Elongation in 2 inches
		Per cent	*Per cent*	*Per cent*	*Per cent*	*Per cent*	*Per cent*	*Per cent*	*Per cent*	*Per cent*	*Lbs./in.²*	*Lbs./in.²*	*Per cent*
1	Low-carbon steel	0.16	0.33	0.12	0.007	0.023					57,650	63,500	21.5
53	do	.09									37,550	51,400	41.3
54	Medium-carbon steel	.28									44,700	69,350	31.3
2	do	.31	.52	.26	.014	.033					79,350	91,350	16.5
55	High-carbon steel	.68									62,800	118,500	18.5
4	do	.85	.33	.16	.020	.010					81,900	96,200	23.3
28	Carbon-tool steel	.90											
5	Nickel steel	.35	.74	.12	.014	.022	3.42				96,950	117,450	15.5
27	3½ per cent nickel steel										120,650	198,750	11.5
6	Chromium steel	.91	.30	.36	.016	.014		1.43			88,600	96,300	26.5
57	do	1.01						1.33			108,600	191,250	5.8
7	Nickel-chromium steel	.32	.54	.10	.017	.018	2.88	1.27			79,000	95,550	21.3
56	do	.30					2.14	.82			85,800	131,600	19.0
58	Chromium-vanadium steel	.30						1.11	0.25		92,850	133,350	23.0
9	do	.35	.57	.20	.013	.016		.90	.17		81,950	94,400	24.0
8	Silicon steel	.59	.71	1.88							75,200	104,950	23.8
59	Tungsten steel	.60						3.50		14.00	57,050	115,400	18.5
SS	Stainless steel	.30	.30					13.00			69,600	108,000	25.5
BC	High-speed steel	.65						4.50	1.50	13.50	54,300	110,600	20.5
A	Cast iron	3.83	.72	1.51	.400	.072							
C	do	3.60	.42	1.76	.820	.052							
H	do	3.18	.46	2.66	1.85	.078							

[a] Determined as stress at which the deformation is 0.01 inch in 2 inches.

TABLE 2.—*Materials used for Brinell and Rockwell tests*—Continued

NONFERROUS MATERIALS

Sample No.	Material	C	Mn	Si	Ni	Al	Cu	Mg	Sn	Zn	Pb	Fe	Condition[1]	Yield point[2]	Tensile strength	Elongation in 2 inches
		Per cent	*Per cent*	*Per cent*	*Per cent*	*Per cent*	*Per cent*	*Per cent*	*Per cent*	*Per cent*	*Per cent*	*Per cent*		*Lbs. in.*^{2}	*Lbs. in.*^{2}	*Per cent*
10	SAE-Al-alloy No. 30		0.08	0.58		90.8	7.95			Nil.		0.59	Cast	12,700	16,400	1.5
11	Al-alloy, 2 S		.01	.35		99.0	.19					.44	Rolled	5,650	14,950	37.0
12	Duralumin		.60	.35		94.36	3.71	0.49				.49	do	38,150	58,300	16.0
13	Magnesium (2039)							99.9					Extruded, 300° C	19,000	28,650	11.3
14	Mg-alloy (2038)		.3			4.0		Balance.					Cast, sand, 685° C		8,900	2.5
15	Mg-alloy (2016-HT)		.3			4.0		Balance.					Rolled, h. t. at 450° C.; quenched in water.	21,550	35,400	16.8
16	Mg-alloy (2016-R)		.3			4.0		Balance.					Extruded, 290° C.; rolled 450° C.	28,200	37,850	16.1
17	Mg-alloy (2016-E)		.3			4.0		Balance.					Extruded, 290° C	29,700	40,000	17.5
20	Phosphor bronze (soft)		.05				89.35		10.23	Nil.	0.01	.04	Cold-rolled, annealed	26,500	61,550	77.3
21	Phosphor bronze (hard).		.05				89.35		10.23	Nil.	.01	.04	Cold-rolled	86,600	101,000	22.0
22	Nickel silver (soft)		.21		17.92		63.70			18.0	Nil.	.17	Cold-rolled, annealed	27,850	61,400	44.0
23	Nickel silver (hard)		.19		18.13		63.73			17.77	.015	.16	Cold-rolled	85,000	86,700	8.5
24	Brass (soft)						65.12			34.79	.08	.01	Cold-rolled, annealed	14,770	43,200	80.5
25	Brass (hard)						65.12			34.79	.08	.01	Cold-rolled	54,250	60,550	27.5
33	Monel metal	0.2	1.75	.1	66.0		30.0					2.0	Hot-rolled	34,800	86,650	48.8
34	Nickel	.1	.25	.1	99.0		.2					.5	do	33,950	84,850	48.0
35	Aluminum bronze (soft).					7.92	91.90			.18			Cold-rolled, annealed	14,200	61,800	74.3
36	Aluminum bronze (hard).					7.55	92.16			.29			Cold-rolled	33,000	63,900	66.0
37	Copper (soft)						99.97						Cold-rolled, annealed	8,550	30,600	54.0
38	Copper (hard)						99.97						Cold-rolled	34,000	35,650	31.5

[1] As reported by the manufacturer.

[2] Determined as stress at which the deformation is 0.015 inch in 2 inches.

TABLE 3.—*Heat-treated materials used for Brinell and Rockwell tests*

FERROUS MATERIALS

TABLE 3.—*Heat-treated materials used for Brinell and Rockwell tests*

FERROUS MATERIALS

Sample No.	Material	Heat treatment			Chemical composition										Bn	150Rc
		Quenching medium	Quenching temperature	Drawn	C	Mn	Si	P	S	Cr	Ni	V	W	Co		
			° F.		*Per cent*	*Per cent*	*Per cent*	*Per cent*	*Per cent*	*Per cent*	*Per cent*	*Per cent*	*Per cent*	*Per cent*		
D–15	Carbon steel	Brine	1,420	Not drawn	0.80	0.20	0.25	0.001	0.015						724	67.5
D–5	do	do	1,420	340° F., 30 min	.80	.20	.25	.001	.015						678	64.5
D–6	do	do	1,420	450° F., 30 min	.80	.20	.25	.001	.015						627	60.8
D–2	do	do	1,420	505° F., 30 min	.80	.20	.25	.001	.015						599	58.1
D–12	do	do	1,420	610° F., 30 min	.80	.20	.25	.001	.015						557	55.3
D–7	do	do	1,420	665° F., 30 min	.80	.20	.25	.001	.015						514	52.3
D–8	do	do	1,420	755° F., 30 min	.80	.20	.25	.001	.015						476	49.3
D–9	do	do	1,420	855° F., 30 min	.80	.20	.25	.001	.015						427	45.3
D–10	do	do	1,420	915° F., 30 min	.80	.20	.25	.001	.015						389	42.2
D–11	do	do	1,420	1,000° F., 30 min	.80	.20	.25	.001	.015						333	36.7
D–4	do	do	1,420	1,050° F., 30 min	.80	.20	.25	.001	.015						310	33.9
D–13	do	do	1,420	1,110° F., 60 min	.80	.20	.25	.001	.015						277	29.3
D–14	do	do	1,420	1,175° F., 30 min	.80	.20	.25	.001	.015						250	25.0
D–3	do	do	1,420	1,215° F., 30 min	.80	.20	.25	.001	.015						240	23.4
D–1	do	do	1,420	1,250° F., 60 min	.80	.20	.25	.001	.015						221	19.1
E–4	do	do	1,420	Not drawn	1.20	.20	.25	.001	.015						755	68.4
E–2	do	do	1,420	310° F., 30 min	1.20	.20	.25	.001	.015						686	67.1
E–7	do	do	1,420	450° F., 30 min	1.20	.20	.25	.001	.015						631	62.7
E–3	do	do	1,420	550° F., 30 min	1.20	.20	.25	.001	.015						587	58.6
E–8	do	do	1,420	665° F., 30 min	1.20	.20	.25	.001	.015						529	54.3
E–9	do	do	1,420	755° F., 30 min	1.20	.20	.25	.001	.015						491	51.9
E–12	do	do	1,420	850° F., 30 min	1.20	.20	.25	.001	.015						439	47.7
E–13	do	do	1,420	915° F., 30 min	1.20	.20	.25	.001	.015						403	44.2
E–14	do	do	1,420	980° F., 30 min	1.20	.20	.25	.001	.015						352	40.5
E–5	do	do	1,420	1,050° F., 30 min	1.20	.20	.25	.001	.015						313	34.7
E–1	do	do	1,420	1,110° F., 30 min	1.20	.20	.25	.001	.015						295	32.5
E–15	do	do	1,420	1,130° F., 30 min	1.20	.20	.25	.001	.015						279	29.4
E–10	do	do	1,420	1,175° F., 30 min	1.20	.20	.25	.001	.015						259	26.5
E–11	do	do	1,420	1,235° F., 30 min	1.20	.20	.25	.001	.015						246	23.8
E–6	do	do	1,420	1,300° F., 30 min	1.20	.20	.25	.001	.015						224	19.9

115233°—30—3

TABLE 3.—*Heat-treated materials used for Brinell and Rockwell tests*—Continued

FERROUS MATERIALS—Continued

Sample No.	Material	Heat treatment			Chemical composition										Bn	150Rc
		Quenching medium	Quenching temperature	Drawn	C	Mn	Si	P	S	Cr	Ni	V	W	Co		
			° F.		Per cent	Per cent	Per cent	Per cent	Per cent	Per cent	Per cent	Per cent	Per cent	Per cent		
2B-1	3½ per cent nickel steel	Water	1,600	Not drawn	0.15	0.49		0.029	0.020		3.46				394	41.9
2B-4	do	do	1,600	950° F., 60 min	.15	.49		.029	.020		3.46				224	20.8
2B-5	do	do	1,600	1,250° F., 60 min	.15	.49		.029	.020		3.46				183	10.9
4B-1	do	do	1,500	Not drawn	.35	.76		.010	.020		3.44				516	53.0
4B-2	do	do	1,500	350° F., 60 min	.35	.76		.010	.020		3.44				488	47.9
4B-3	do	do	1,500	650° F., 60 min	.35	.76		.010	.020		3.44				387	39.9
4B-4	do	do	1,500	950° F., 60 min	.35	.76		.010	.020		3.44				285	30.4
4B-5	do	do	1,500	1,250° F., 60 min	.35	.76		.010	.020		3.44				212	17.5
1D-4	Chromium steel	Oil	1,500	950° F., 60 min	1.01	.22		.026	.024	1.33					345	37.3
1D-5	do	do	1,500	1,250° F., 60 min	1.01	.22		.026	.024	1.33					284	30.1
C-1	High chromium steel	do	1,750	Not drawn	2.20	.20	.30	.001	.015	12.0		0.80		0.50	748	68.0
C-3	do	do	1,750	310° F., 30 min	2.20	.20	.30	.001	.015	12.0		.80		.50	703	65.2
C-5	do	do	1,750	550° F., 30 min	2.20	.20	.30	.001	.015	12.0		.80		.50	628	60.9
C-9	do	do	1,750	{915° F., 30 min {850° F., 30 min	2.20	.20	.30	.001	.015	12.0		.80		.50	574	56.3
C-10	do	do	1,750	{1,000° F., 30 min {980° F., 30 min	2.20	.20	.30	.001	.015	12.0		.80		.50	538	54.3
C-6	do	do	1,750	1,050° F., 30 min	2.20	.20	.30	.001	.015	12.0		.80		.50	506	51.9
C-11	do	do	1,750	Twice 1,130° F., 30 min. each	2.20	.20	.30	.001	.015	12.0		.80		.50	456	48.1
C-12	do	do	1,750	1,175° F., 30 min	2.20	.20	.30	.001	.015	12.0		.80		.50	433	45.4
C-14	do	do	1,750	1,235° F., 30 min	2.20	.20	.30	.001	.015	12.0		.80		.50	401	42.8
C-13	do	do	1,750	1,265° F., 30 min	2.20	.20	.30	.001	.015	12.0		.80		.50	377	40.7
C-8	do	do	1,750	1,300° F., 30 min	2.20	.20	.30	.001	.015	12.0		.80		.50	342	36.8
C-4	do	do	1,750	1,330° F., 30 min	2.20	.20	.30	.001	.015	12.0		.80		.50	330	35.1
C-15	do	do	1,750	1,380° F., 30 min	2.20	.20	.30	.001	.015	12.0		.80		.50	301	32.1
C-2	do	do	1,750	1,440° F., 60 min	2.20	.20	.30	.001	.015	12.0		.80		.50	269	26.9
C-7	do	do	1,750	1,440° F., 3 hr., 15 min	2.20	.20	.30	.001	.015	12.0		.80		.50	247	24.1
6C-1	Chromium-nickel steel	do	1,550	Not drawn	.30	.70		.035	.027	.82	2.14				469	47.5
6C-2	do	do	1,550	350° F., 60 min	.30	.70		.035	.027	.82	2.14				472	48.0
6C-3	do	do	1,550	650° F., 60 min	.30	.70		.035	.027	.82	2.14				423	42.8
6C-4	do	do	1,550	950° F., 60 min	.30	.70		.035	.027	.82	2.14				321	34.2
6C-5	do	do	1,550	1,250° F., 60 min	[illegible]	[illegible]		[illegible]	[illegible]	[illegible]	[illegible]				[illegible]	[illegible]

B-2	Chromium-vanadium steel.	Brine	1,475	Not drawn	.90	.20	.25	.001	.015	.80		.20			702	65.1
B-1	do	do	1,475	310° F., 30 min	.90	.20	.25	.001	.015	.80		.20			671	63.4
B-7	do	do	1,475	450° F., 30 min	.90	.20	.25	.001	.015	.80		.20			627	59.3
B-3	do	do	1,475	550° F., 30 min	.90	.20	.25	.001	.015	.80		.20			578	56.6
B-8	do	do	1,475	665° F., 30 min	.90	.20	.25	.001	.015	.80		.20			538	53.6
B-12	do	do	1,475	755° F., 30 min	.90	.20	.25	.001	.015	.80		.20			502	51.0
B-9	do	do	1,475	850° F., 30 min	.90	.20	.25	.001	.015	.80		.20			456	47.1
B-10	do	do	1,475	915° F., 30 min	.90	.20	.25	.001	.015	.80		.20			420	44.6
B-11	do	do	1,476	980° F., 30 min	.90	.20	.25	.001	.015	.80		.20			401	42.9
B-4	do	do	1,475	1,050° F., 30 min	.90	.20	.25	.001	.015	.80		.20			354	38.2
B-14	do	do	1,475	Twice, 1,110° F., 30 min. each	.90	.20	.25	.001	.015	.80		.20			325	34.7
B-13	do	do	1,475	1,175° F., 30 min	.90	.20	.25	.001	.015	.80		.20			290	31.0
B-15	do	do	1,475	1,215° F., 60 min	.90	.20	.25	.001	.015	.80		.20			259	26.2
B-6	do	do	1,475	1,300° F., 30 min	.90	.20	.25	.001	.015	.80		.20			236	22.3
B-5	do	do	1,475	Twice, 1,330° F., 30 min. each	.90	.20	.25	.001	.015	.80		.20			224	20.4
A-5	High-speed steel	Oil	2,330	Not drawn	.68	.20	.32	.001	.015	4.00		1.00	18.00		709	66.2
A-1	do	do	2,330	1,100° F., 30 min	.68	.20	.32	.001	.015	4.00		1.00	18.00		698	63.3
A-2	do	do	2,330	1,200° F., 30 min	.68	.20	.32	.001	.015	4.00		1.00	18.00		657	60.7
A-4	do	do	2,330	1,235° F., 30 min	.68	.20	.32	.001	.015	4.00		1.00	18.00		611	57.3
A-6	do	do	2,330	1,265° F., 30 min	.68	.20	.32	.001	.015	4.00		1.00	18.00		547	53.0
A-7	do	do	2,330	1,300° F., 30 min	.68	.20	.32	.001	.015	4.00		1.00	18.00		500	49.9
A-8	do	do	2,330	1,330° F., 30 min	.68	.20	.32	.001	.015	4.00		1.00	18.00		444	45.5
A-10	do	do	2,330	1,360° F., 30 min	.68	.20	.32	.001	.015	4.00		1.00	18.00		403	42.7
A-3	do	do	2,330	1,420° F., 30 min	.68	.20	.32	.001	.015	4.00		1.00	18.00		368	39.0
A-12	do	do	2,330	1,440° F., 1 hr., 15 min	.68	.20	.32	.001	.015	4.00		1.00	18.00		340	35.7
A-9	do	do	2,330	1,480° F., 1 hr., 30 min	.68	.20	.32	.001	.015	4.00		1.00	18.00		313	33.8
A-11	do	do	2,330	1,525° F., 30 min.; 6 hr., 20 min., cooling from 1,525° F. to 1,370° F.	.68	.20	.32	.001	.015	4.00		1.00	18.00		304	32.0
A-13	do	do	2,330	1,600° F., 30 min.; 7 hr., cooling from 1,600° to 1,370° F.; 14 hr. at 1,370° F.; showed slight carbon absorption so 1/32 in. was machined off. Sample was then reheated to 1,460° and oil quenched.	.68	.20	.32	.001	.015	4.00		1.00	18.00		256	23.7
A-14	do	do	1,650	1,410° F., 14 hr	.68	.20	.32	.001	.015	4.00		1.00	18.00		284	29.4

TABLE 4.—*Rockwell and Brinell indentation numbers for materials described in Table 2*

I. FERROUS MATERIALS

Sample No.	*Bn*	$_{100}R_{B1/16}$ [1]	$_{100}R_{B1/8}$ [2]	$_{60}R_{B1/16}$	$_{150}R_C$ [3]	$_{100}R_C$	$_{60}R_C$
53	98	55.2	91.8	90.1	−24.0	8.0	
54	125	68.2	99.1	96.8	−6.7	20.0	
1	129	74.0	102.5	99.0	−5.0	23.5	
A	156	79.0					
28	178	85.3	106.2	105.0	7.5	33.3	
C	192	91.0					
9	204	92.6	112.0	109.5	16.5	39.0	
2	204	94.9	112.8	111.4	18.4	40.7	
7	212	93.8	112.5	110.2	18.6	40.2	
H	216	94.0					
6	224	96.4	113.1	111.7	20.0	40.1	
55	225	98.4	113.2	112.0	19.7	42.4	
SS	225	98.0	114.0	112.3	21.6	42.2	
8	226	96.8	112.8	111.1	22.2	42.0	
59	230	96.8	112.1	111.7	19.1	41.2	
4	232	97.2	114.2	112.2	22.0	42.5	
BC	239	98.0	112.6	111.9	21.2	42.0	
5	248	97.6	113.5	112.5	22.5	42.1	
56	256	102.3	116.2	114.6	27.7	46.0	
58	268	104.6	117.1	116.2	28.4	48.1	
57	339	108.0	118.8	117.4	36.8	52.1	
27	367	111.6	121.4	120.2	41.9	56.8	

II. NONFERROUS MATERIALS

11	28.0	(4)	−3.0	−25.0	(4)	(4)	
37	42.0	−39.0	35.6	35.0	(4)	(4)	
14	43.4	−40.0	42.0	39.0	(4)	(4)	(4)
13	43.5	(4)	46.0	34.0	(4)	(4)	
15	50.3	−15.0	59.6	53.5	(4)	(4)	
24	[5] 51.4	9.5	66.1	64.9	(4)	(4)	
16	56.8	4.1	70.1	62.7	(4)	(4)	
17	61.3	20.0	75.0	70.4	(4)	−12.0	
10	67.7	25.0	81.0	77.0	[6] −35.0	0	
35	72	36.5	76.7	76.0	(4)	−6.5	
38	75	33.9	86.5	79.2	−35.0	0	
20	95	51.1	86.8	85.0	−29.0	6.0	
22	103	58.4	90.7	90.2	−21.0	12.3	
36	111	65.2	93.9	93.1	−15.0	14.9	
12	123	69.9	98.1	97.2	−8.8	19.3	
25	126	72.8	102.1	99.0	−3.0	22.8	
34	132	74.3	99.0	98.6	−6.1	21.8	
33	147	78.5	101.9	100.5	1.0	27.1	
23	174	88.8	110.7	108.1	13.1	36.3	
21	218	98.3	114.3	112.4	21.8	42.0	

[1] Standard Rockwell B number.
[2] Standard Rockwell E number.
[3] Standard Rockwell C number.
[4] Too soft.
[5] For 3,000 kg load *Bn*=65.
[6] About.

Table 5 contains data obtained in the metallurgical division of this bureau.

All tensile-strength data were obtained on A. S. T. M. standard specimens (0.500 inch diameter, 2-inch gage length).

All steel specimens were machined before an indentation was made. Certain tests made on nonferrous materials showed that results obtained on the rolled surfaces differed a negligible amount from those obtained on machined surfaces. Therefore in many of the tests on nonferrous materials indentations were made on the rolled surfaces of the specimens as received from the manufacturer.

The Rockwell indentations on each specimen were located between and near the Brinell indentations. Each experimental indentation number listed in the tables is the average obtained from at least four indentations.

The following study was made on each of five Rockwell brales. By means of a contour measuring projector giving a magnification of 234, a shadow of the brale was formed on a screen, the shadow being a projection of a cross section of the tool through its axis. The outline of the shadow was carefully traced. A second and a third tracing were obtained after the brale had been rotated 60° and 120°, respectively, about its axis.

TABLE 5.—*Data on steels furnished by metallurgical division, Bureau of Standards*

Sample No.	Brinell No.	$_{100}R_{B1/16}$	$_{150}R_C$	Experimental tensile strength
				*Lbs./in.*²
16-3	125	71.4		68,500
16-4	128	70.1		69,200
20-2	131	77.7		70,000
20-1	134	75.7		69,500
4-R	156	83.1		82,500
4-F	157	83.4		84,500
4-CA	161	86.0		84,500
4-C	165	85.5		85,000
15-7	167	85.8		91,000
17-1	168	83.9		87,300
4-Q	169	86.9		86,500
14-1	169	87.4		77,500
7-2	170	84.5		87,300
4-FA	170	86.5		83,000
4-RA	170	87.2		86,000
15-1	170	87.5		92,500
15-8	173	85.0		91,000
4-F	173	86.7		84,500
4-FA	174	87.0		92,000
14-2	174	86.6		77,500
3-FA	175	89.7		91,000
4-F	180	89.7		91,500
4-FA	181	89.6		93,000
4-F	181	89.3		92,500
4-RA	184	88.9		92,500
4-F	187	89.2		92,000
3-FA	189	90.3		93,000
3-F	191	90.0		93,500
3-RA	192	91.7		96,000
3-RA	193	91.3		92,000
3-R	194	91.8		98,000
4-R	195	92.4		97,000
3-A	197	95.3	12.6	103,000
35-1	197	93.5		92,000
36-2	197	91.3		99,500
35-2	198	94.6		93,500
36-1	199	91.4		99,000
3-FA	204	92.6		102,000
3-F	207	92.9		103,500
3-RA	209	95.5		101,500
3-R	209	94.5		101,500
4-R	215	98.7	16.8	102,500
3-A-1	223	97.1		100,000
3-FA	226	100.0	20.2	113,500
4-RA	229	98.4	21.3	114,500
4-R	229	97.5		116,000
3-A-2	229	96.8		115,000
10-1	229	99.5	21.1	115,500
10-2	229	95.0		107,600
	229	95.0		107,000

TABLE 5.—*Data on steels furnished by metallurgical division, Bureau of Standards*—Continued

Sample No.	Brinell No.	$100R_{B1/16}$	$100R_C$	Experimental tensile strength
				Lbs./in.²
14-RA	247	99.0	23.8	126,000
14-F	248	100.3	24.9	124,000
13-O-A	250	101.6	25.9	128,000
11-F	252	101.1	25.3	123,700
13-O	254	101.5	25.9	128,000
13-CA	255	100.4	26.0	126,000
13-C	255	101.1	25.8	127,500
32-1	255	101.3	23.3	123,000
12-FA	256	101.4	26.5	124,000
12-C	257	103.9	25.5	122,500
12-CA	257	102.9	25.7	122,500
12-F	260	101.5	27.0	125,000
32-2	262	101.2	23.3	123,000
33-1	262	101.9	24.8	126,500
33-2	262	102.4	26.2	126,000
11-R	265	103.0	26.8	128,500
10-A-2	265	100.4	27.2	119,000
11-RA	267	103.1	27.6	125,500
10-F	267	102.3	26.6	127,000
10-FA	269	102.8	27.6	128,500
7-RA	270	103.0	28.8	131,000
7-R	273	103.0	29.4	132,500
11-FA	273	102.8	27.7	130,500
10-R	285	104.7	30.0	134,000
11-A-4	288	101.9	27.7	134,000
10-RA	293	105.2	32.2	138,500
12-RA	297	105.9	31.0	136,000
28-4	300	107.1	31.1	142,500
12-R	300	105.9	32.8	138,000
26-1-A	302	106.4	33.5	145,700
14-A-2	304	106.1	34.5	150,000
11-A-1	305	104.3	29.3	134,000
14-A-1	306	105.9	34.4	150,500
15-A-2	311	104.6	32.0	149,700
12-A-2	317	105.9	33.6	148,000
12-A-1	321	106.3	33.5	149,500
15-A-1	321	105.2	32.5	147,000
30-A-8	330	110.1	32.9	149,000
10-A-1	334	110.8	34.4	147,500
20-2	341	113.4	33.2	167,500
20-1	363	112.8	36.4	180,400
20-4	363	113.9	35.0	170,000
25-2	363	112.7	36.4	167,000
20-3	375	114.4	36.2	181,300
25-1	388	115.0	41.2	186,700
27-A-6	388	114.5	39.8	190,000
27-A-3	395	115.0	40.5	200,500
I-9D	407	----------	41.9	192,500
I-32D	408	----------	42.4	192,500
I-28B	434	----------	43.6	205,000
I-8B	450	----------	45.9	214,700
I-32C	512	----------	50.5	246,500
I-9C	518	----------	50.0	250,000
I-28A	525	----------	51.0	256,500
I-30D	527	----------	51.1	273,700
I-10D	536	----------	52.2	265,700
I-16B	542	----------	51.7	283,000

TABLE 6.—*Table of values for diamond brale*

	h_0	d	L	Rockwell C number load 150 kg	Brinell number	For S=0.0224 mm			For S=0.0291 mm		
						Bn	$_{150}Rc$	$\frac{1}{\sqrt{Bn}}$	Bn	$_{150}Rc$	$\frac{1}{\sqrt{Bn}}$
Case I	h_0 varies from 0 to $0.0666S$			Rockwell C number varies from (100–466.7 S) to 100	Brinell number varies from $\frac{3.199}{S^2}$ to ∞	∞	100	0	∞	100	0
						33,324	98	0.0055	25,651	98	0.0062
						16,662	96	.0077	12,826	96	.0088
						11,108	94	.0095	8,550	94	.0108
						8,331	92	.0110	6,413	92	.0125
						6,665	90	.0123	5,130	90	.0140
						6,378	89.5	.0125	3,778	86.4	.0163
Case II	$0.07S$	-------	$0.049S$	100– 489.5 S	$3.048/S^2$	6,075	89.0	.0128	3,599	85.8	.0167
	$.10S$	-------	$.453S$	100– 676.0 S	$2.133/S^2$	4,251	84.9	.0153	2,519	80.3	.0199
	$.15S$	-------	$1.012S$	100– 931.0 S	$1.422/S^2$	2,834	79.1	.0188	1,679	72.9	.0244
	$.20S$	-------	$1.487S$	100–1,143 S	$1.066/S^2$	2,125	74.4	.0217	1,259	66.7	.0282
	$.30S$	-------	$2.286S$	100–1,493 S	$.711/S^2$	1,417	66.6	.0266	840	56.6	.0345
	$.40S$	-------	$2.963S$	100–1,781 S	$.533/S^2$	1,062	60.1	.0307	629	48.2	.0399
	$.50S$	-------	$3.559S$	100–2,030 S	$.427/S^2$	851	54.5	.0343	504	40.9	.0445
	$.60S$	-------	$4.100S$	100–2,250 S	$.355/S^2$	708	49.6	.0376	419	34.5	.0488
	$.70S$	-------	$4.596S$	100–2,448 S	$.305/S^2$	608	45.2	.0406	360	28.8	.0527
	$.80S$	-------	$5.059S$	100–2,630 S	$.267/S^2$	532	41.1	.0434	315	23.5	.0563
	$.90S$	-------	$5.494S$	100–2,797 S	$.237/S^2$	472	37.4	.0460	280	18.6	.0597
	$1.00S$	-------	$5.905S$	100–2,953 S	$.213/S^2$	425	33.9	.0485	251	14.1	.0631
Case III	$1.10S$	$0.10S$	$6.306S$	100–3,103 S	$.193/S^2$	385	30.5	.0510	228	9.7	.0662
	$1.20S$	$.20S$	$6.705S$	100–3,253 S	$.176/S^2$	351	27.2	.0534	208	5.3	.0694
	$1.30S$	$.30S$	$7.103S$	100–3,402 S	$.161/S^2$	321	23.8	.0558	190	1.0	.0725
	$1.40S$	$.60S$	$8.293S$	100–3,846 S	$.127/S^2$	253	13.8	.0629	150	−12.0	.0817

For Case I corresponding values of Bn and $_{150}Rc$ are calculated by use of the formula $Bn=\frac{1,492.9}{S(100-{}_{150}Rc)}$.

A circle was then drawn for each tracing, fitting as closely as possible the curved portion. The lines bounding the conical portion were extended to determine the point D. (See fig. 3.) Values of CD and r could then be determined. These data are found in Table 7.

The extent to which the experimental Brinell and Rockwell numbers obtained in this investigation may have been influenced by peculiar characteristics of the particular machines used is not known. No attempt was made to find and interpret any systematic differences in the experimental values for steels which might result from different treatments. A. Heller [6] has shown that depth of hardening is a very important factor to be considered in deriving conversion formulas for steels.

[6] American Machinist, Apr. 4, 1929.

TABLE 7.—*Data on Rockwell diamond brales*

Manufacturer's No.	Position [1]	Angle of cone	r [2]	CD	S calculated from r	S calculated from CD
		° ′	mm	mm	mm	mm
26-1886	1	120 0	0.200	0.0336	0.0268	0.0
	2	120 6	.180	.0293	.0241	.0
	3	120 18	.192	.0315	.0257	.0
26-1832	1	119 55	.182	.0271	.0244	.0
	2	119 51	.167	.0271	.0224	.0
	3	120 3	.199	.0326	.0267	.0
26-15	1	120 1	.202	.0315	.0271	.0
	2	120 1	.191	.0315	.0256	.0
	3	120 18	.201	.0326	.0269	.0
29-1893	1	119 41	.212	.0336	.0284	.0
	2	119 32	.200	.0326	.0268	.0
	3	119 53	.197	.0315	.0264	.0
26-224	1	120 25	.205	.0326	.0275	.0
	2	120 4	.198	.0315	.0265	.0
	3	119 48	.197	.0315	.0264	.0

[1] The brale was turned into position 2 from position 1 by rotating it 60° about its axis. An additional 60° rotation brought it into position 3.
[2] The meaning of the notation used in this table is given in fig. 3.

VII. CORRELATION OF APPROXIMATE THEORY AND EXPERIMENT

When one plots the first three equations of Table 1 using values of R_B and $\frac{1}{Bn}$ as coordinates, straight lines are obtained. Likewise, the second three equations give straight lines if values of R_c and $\frac{1}{\sqrt{Bn}}$ are used as coordinates. Graphs of the first, second, and fourth of these equations are shown by dash lines in Figures 4 and 5.

The curve forming the upper boundary of the shaded area in Figure 5 was plotted from data found in columns 7 and 8, Table 6, and the curve forming the lower boundary was plotted from values found in columns 10 and 11.

The upper curve gives the theoretical relationship between Bn and ${}_{150}R_C$ for a brale in which $S=0.0224$ mm, and the lower curve does the same for a brale in which $S=0.0291$ mm. These particular values of S were chosen merely because they were the minimum and maximum values found in the study of the five tools and may represent an extreme variation in S. Average values would show less variation.

Certain facts are made evident by an inspection of the theoretical straight line curve (for a true cone) and the theoretical curves bounding the shaded areas.

The effect of the spherical portion of the brale upon the theoretical relationship between Bn and ${}_{150}R_C$ is quite small for ${}_{150}R_C=10$, but gradually increases and becomes quite large at ${}_{150}R_C=70$.

If two brales are used having different values of S, the effect of this difference in S is quite small for ${}_{150}R_C=10$, but becomes considerably larger at ${}_{150}R_C=70$.

Thus the theoretical value of Bn corresponding to ${}_{150}R_C=70$ is 1,678 for $S=0.0224$ mm and only 1,460 for $S=0.0291$ mm.

Experimental values taken from Tables 3 and 4 are plotted in Figures 4 and 5. Considering Figure 4, we see that the points do not fall along the theoretical straight lines, but that their mean

positions are determined fairly well by the two full lines. Since these are straight lines, equations of the form $Bn = \frac{C}{(130 - R_n)}$ can be used as conversion formulas. The numerical values to be substituted for C are the reciprocal slopes of the experimental curves. Thus, the

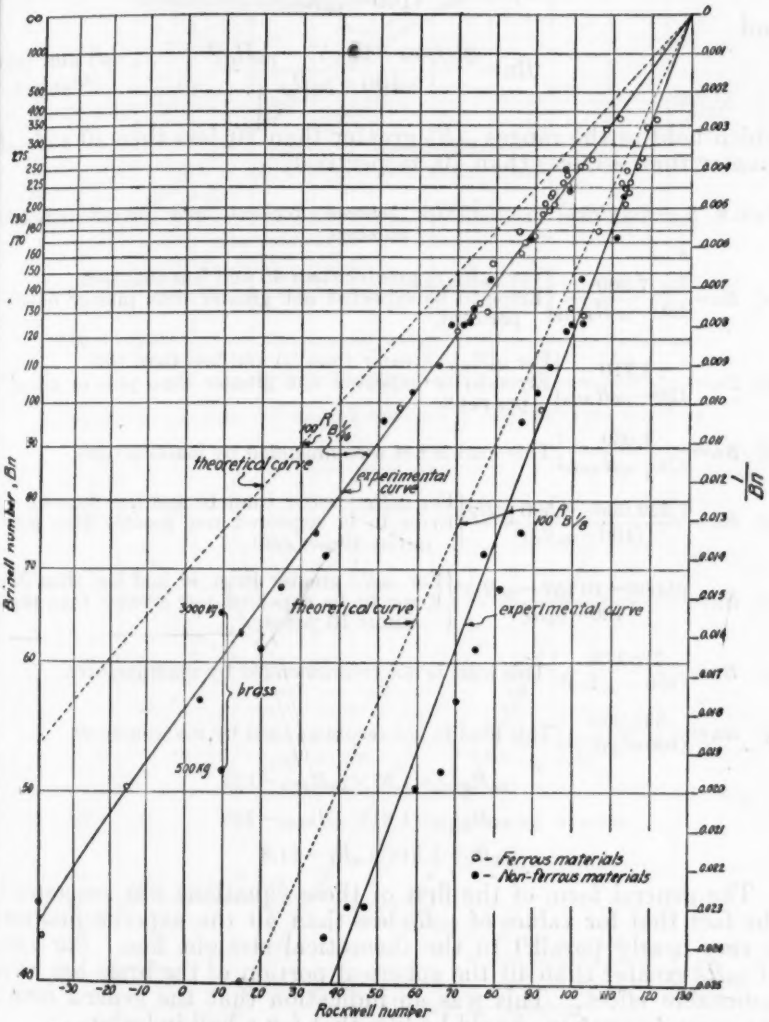

FIGURE 4.—*Relation of Brinell numbers to Rockwell ball numbers*

reciprocal slope of the ${}_{100}R_{B1/16}$ line is $\frac{146}{0.020} = 7{,}300$, and the equation is:

$$Bn = \frac{7{,}300}{(130 - {}_{100}R_{B1/16})}$$

Equations (*a*), (*b*), and (*c*) of Table 8 were obtained in this way.

The experimental points plotted in Figure 5 determine a curve which is displaced from the theoretical curves. As would be expected,

its general form is like that of the theoretical curves for a brale with a spherical apex.

This curve was used to determine the empirical equations:

$$Bn=\frac{1{,}520{,}000-4{,}500\,{}_{150}R_C}{(100-{}_{150}R_C)^2}$$

and

$$Bn=\frac{25{,}000-10\,(57-{}_{150}R_C)^2}{100-{}_{150}R_C}$$ (*d*) and (*e*) of Table 8

which hold in the ranges ${}_{150}R_C$ greater than 10, less than 40 and ${}_{150}R_C$ greater than 40, less than 70, respectively.

TABLE 8.—*Empirical relationships between Rockwell and Brinell indentation numbers*

(*a*) $Bn=\frac{7{,}300}{130-{}_{100}R_{B1/16}}$ { For ${}_{100}R_{B1/16}$ greater than 40 and less than 100. Error to be expected not greater than plus or minus 1 per cent.

(*b*) $Bn=\frac{3{,}710}{130-{}_{100}R_{B1/8}}$ { For ${}_{100}R_{B1/8}$ greater than 30 and less than 100. Error to be expected not greater than plus or minus 1 per cent.

(*c*) $Bn=\frac{4{,}030}{130-{}_{60}R_{B1/16}}$ } This load is not recommended by manufacturer.

(*d*) $Bn=\frac{1{,}520{,}000-4{,}500\,{}_{150}R_C}{(100-{}_{150}R_C)^2}$ { For ${}_{150}R_C$ greater than 10 and less than 40. Error to be expected not greater than plus or minus 10 per cent.

(*e*) $Bn=\frac{25{,}000-10\,(57-{}_{150}R_C)^2}{100-{}_{150}R_C}$ { For ${}_{150}R_C$ greater than 40 and less than 70. Error to be expected not greater than plus or minus 10 per cent.

(*f*) $Bn=\frac{768{,}000}{(100-{}_{100}R_C)^2}$ } This load is not recommended by manufacturer.

(*g*) $Bn=\frac{333{,}000}{(100-{}_{60}R_C)^2}$ } This load is not recommended by manufacturer.

$${}_{100}R_{B1/16}=1.97\times{}_{100}R_{B1/8}-126$$

$${}_{100}R_{B1/16}=1.81\times{}_{60}R_{B1/16}-105$$

$${}_{100}R_C=1.518\times{}_{60}R_C-51.8$$

The general form of the first of these equations was suggested by the fact that for values of ${}_{150}R_C$ less than 40 the experimental curve is very nearly parallel to the theoretical straight line. For values of ${}_{150}R_C$ greater than 40 the spherical portion of the brale has a very noticeable effect. This was an indication that the general form of the second equation should be like that for a ball indenter.

Equations (*f*) and (*g*) of Table 8 were obtained by following the procedure used in getting equations (*a*), (*b*), and (*c*). In place of each of these equations we should very likely have two equations similar in form to (*d*) and (*e*). There was not sufficient data available for checking this point.

The last three equations of Table 8 were obtained by equating values of *Bn* taken from this same table. These equations differ very little from the corresponding theoretical equations of Table 1. A graphical comparison of two cases is made in Figure 6.

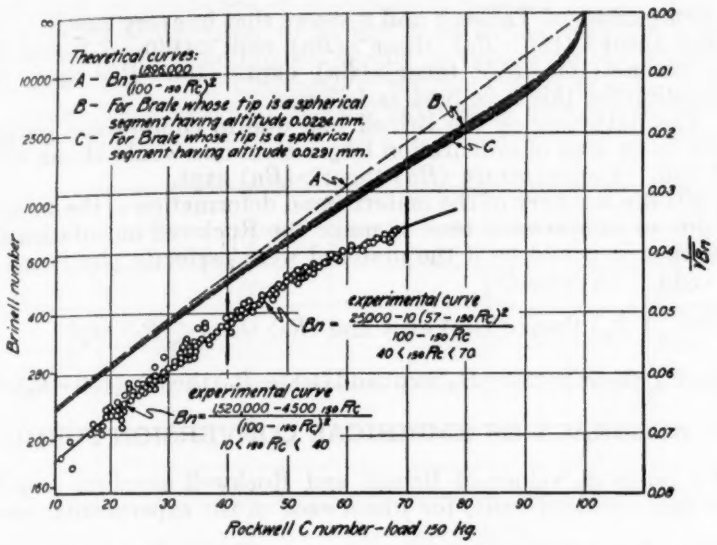
Theoretical curves:
A - Bn = 1895.000 / (100 - 150 Rc)²
B - For Brale whose tip is a spherical segment having altitude 0.0226 mm.
C - For Brale whose tip is a spherical segment having altitude 0.0291 mm.
experimental curve
Bn = 25000 - 10 (57 - 150 Rc)² / 100 - 150 Rc
40 < 150 Rc < 70
experimental curve
Bn = 1520.000 - 4500 150 Rc / (100 - 150 Rc)²
10 < 150 Rc < 40
Brinell number
Rockwell C number - load 150 kg.
1/√Bn

FIGURE 5.—*Relation of Brinell numbers to Rockwell cone numbers*

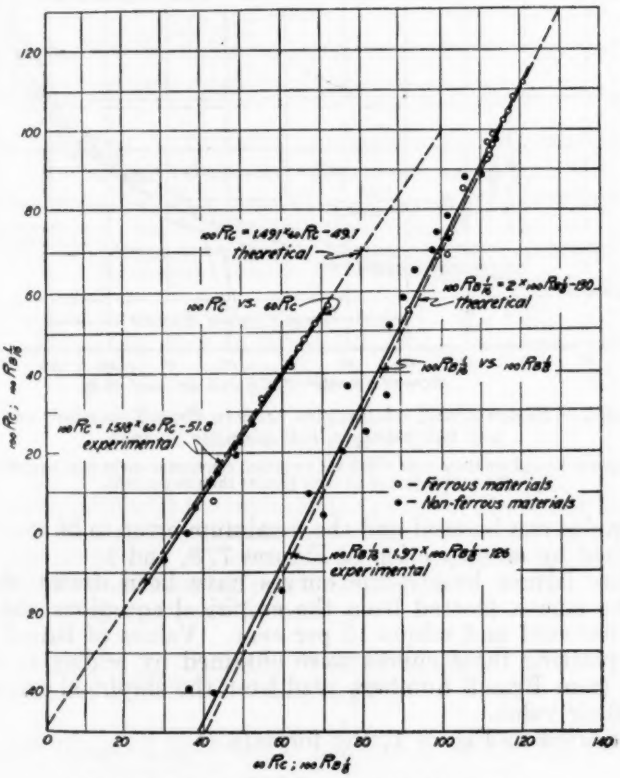
100 Rc = 1.491 * 60 Rc - 49.1
theoretical
100 Rc vs. 60 Rc
100 Rc = 1.518 * 60 Rc - 51.8
experimental
100 Rb 1/16 = 2 * 100 Rb 1/8 - 130
theoretical
100 Rb 1/16 vs. 100 Rb 1/8
100 Rb 1/16 = 1.97 * 100 Rb 1/8 - 126
experimental
○ - Ferrous materials
● - Non-ferrous materials
100 Rc ; 100 Rb 1/8
60 Rc ; 100 Rb 1/8

FIGURE 6.—*Comparison of Rockwell numbers*

A comparison of Tables 1 and 8 shows that in every case:
(Bn) theor$\times(130-R_B)$ theor$>(Bn)$ expt$\times(130-R_B)$ expt and (Bn) theor$\times(100-R_C)^2$ theor$>(Bn)$ expt$\times(100-R_C)^2$ expt. The explanation for this is in part as follows:

1. The flattening of the Brinell ball due to compression probably results in an area of indentation larger than one would obtain with a rigid ball. Consequently (Bn) theor$>(Bn)$ expt.

2. Elastic recovery of the material and deformation of the indenting tool due to compression tend to make the Rockwell indentation shallower than it would be if the material were perfectly plastic and the tool rigid. As a result:

$$(R_B)\ \text{theor}<(R_B)\ \text{expt and}\ (R_C)\ \text{theor}<(R_C)\ \text{expt}$$

or

$$(130-R_B)\,\text{theor}>(130-R_B)\,\text{expt and}\,(100-R_C)\,\text{theor}>(100-R_C)\,\text{expt.}$$

VIII. ACCURACY OF EMPIRICAL CONVERSION FORMULAS

The range of values of Brinell and Rockwell numbers (standard loads and standard tools) for which each of the experimental conver-

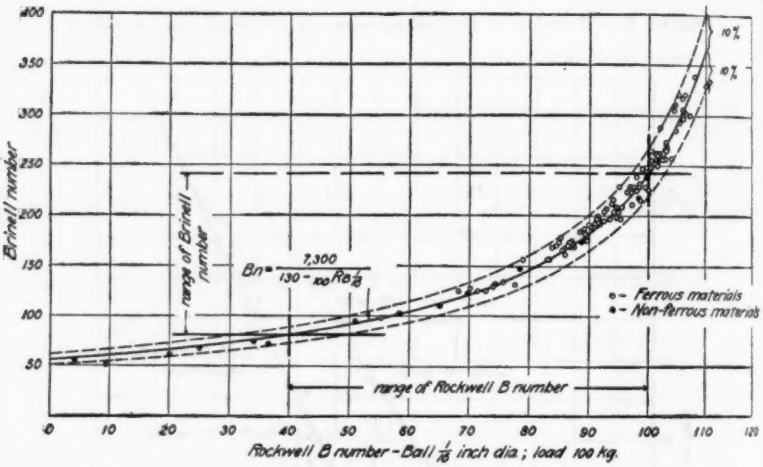

FIGURE 7.—*Experimental relationship between Brinell numbers and Rockwell ball numbers, ball diameter 1/16 inch*

The ranges indicated are those over which the empirical conversion curve may be applied with the expectation of no error greater than 10 per cent.

sion formulas can be used and the maximum error to be expected can be obtained by an inspection of Figures 7, 8, and 9.

In these figures broken-line curves have been drawn above and below the curves plotted from the empirical equations and marked plus 10 per cent and minus 10 per cent. Values of Brinell number used in plotting these curves were obtained by adding to and subtracting from Brinell numbers read from the empirical curves 10 per cent of their value.

As indicated in Figure 7, the formula

$$Bn=\frac{7{,}300}{(130-{}_{100}R_{B1/16})}$$

can be used for the range of Rockwell B number (ball 1/16 inch diameter; load 100 kg) from 40 to 100 or of Brinell number from 80 to 240. All of the experimental points in this range fall within the 10 per cent limits. The upper end of the range is set at ${}_{100}R_{B1/16}=100$, even though there seems to be good agreement between theory and experiment for larger values of ${}_{100}R_{B1/16}$. This is done because the

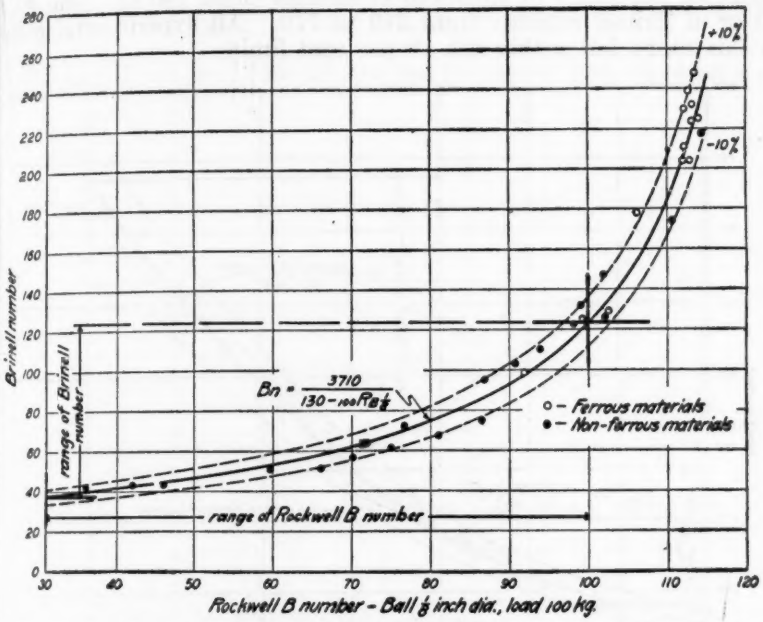
Brinell number
range of Brinell number
Bn = 3710 / 130 − 100RB1/8
+10%
−10%
o – Ferrous materials
• – Non-ferrous materials
range of Rockwell B number
Rockwell B number - Ball 1/8 inch dia., load 100 kg.

FIGURE 8.—*Experimental relationship between Brinell numbers and Rockwell ball numbers, ball diameter 1/8 inch*

The ranges indicated are those over which the empirical conversion curve may be applied with the expectation of no error greater than 10 per cent.

relative effect of an error in ${}_{100}R_{B1/16}$—that is, the ratio of the error to $(130-{}_{100}R_{B1/16})$—is very large when ${}_{100}R_{B1/16}$ is greater than 100. As shown in Figure 8 the formula

$$Bn=\frac{3{,}710}{130-{}_{100}R_{B1/8}}$$

holds about equally well throughout the range of Rockwell B number (ball 1/8 inch diameter; load 100 kg) from 30 to 100 or of Brinell number from 40 to 125. The check on the accuracy of this formula is not conclusive because of insufficient data.

As shown in Figure 9, the formula

$$Bn=\frac{1{,}520{,}000-4{,}500\times{}_{150}R_C}{(100-{}_{150}R_C)^2}$$

holds for the range of Rockwell C number (load 150 kg) from 10 to

40 or of Brinell number from 180 to 370. Ninety-five per cent of the experimental points fall within the 10 per cent limits.

Likewise, the formula

$$Bn = \frac{25{,}000 - 10\ (57 - {}_{150}R_C)^2}{100 - {}_{150}R_C}$$

holds for the range of Rockwell C number (load 150 kg) from 40 to 70 or of Brinell number from 370 to 770. All experimental points in this range fall within the 10 per cent limits.

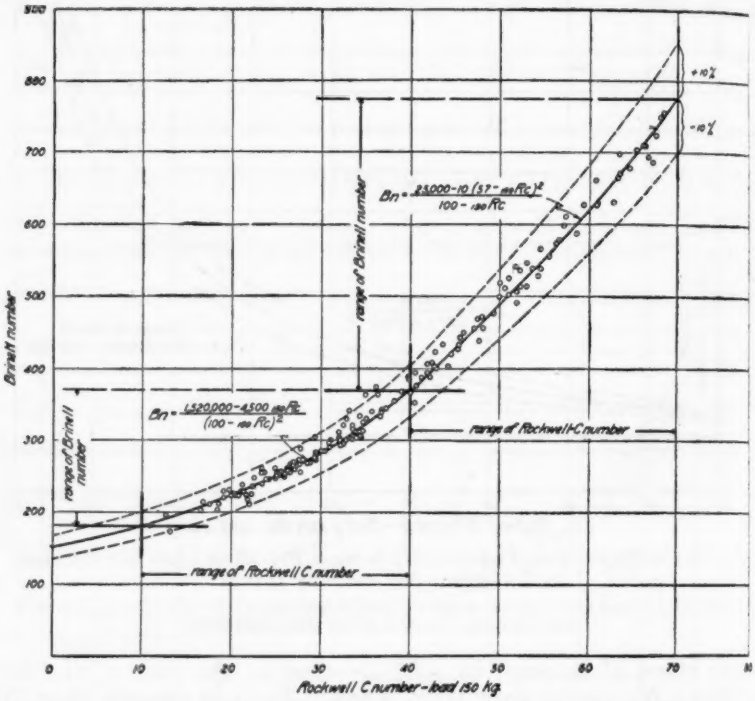

FIGURE 9.—*Experimental relationship between Brinell numbers and Rockwell cone numbers*

The ranges indicated are those over which the empirical conversion curve may be applied with the expectation of no error greater than 10 per cent.

IX. RELATIONSHIP OF ROCKWELL NUMBERS TO TENSILE STRENGTH

Earlier investigators [7] have established the fact that a rough proportionality exists between the tensile strength of steel and its Brinell number.

The equations sometimes used in calculating the tensile strength of steel [8] are:

Tensile strength (lbs./in.^{2}) = 515 Bn for Brinell numbers less than 175.

Tensile strength (lbs./in.^{2}) = 490 Bn for Brinell numbers greater than 175.

[7] Die Brinellsche Kugeldruckprobe, P. W. Döhmer, Berlin; 1925.
[8] See Die Brinellsche Kugeldruckprobe, P. W. Döhmer, Berlin, p. 48; 1925.

Since an empirical relationship between Bn and ${}_{100}R_{B1/16}$ has been found (see Table 8) the above equations can be transformed to read:

$$\text{Tensile strength (lbs./in.}^2) = \frac{3,760,000}{130 - {}_{100}R_{B1/16}} \text{ for } {}_{100}R_{B1/16} \text{ less than 88.}$$

$$\text{Tensile strength (lbs./in.}^2) = \frac{3,580,000}{130 - {}_{100}R_{B1/16}} \text{ for } {}_{100}R_{B1/16} \text{ greater than 88.}$$

The dash lines in Figure 10 are the graphs of these equations.

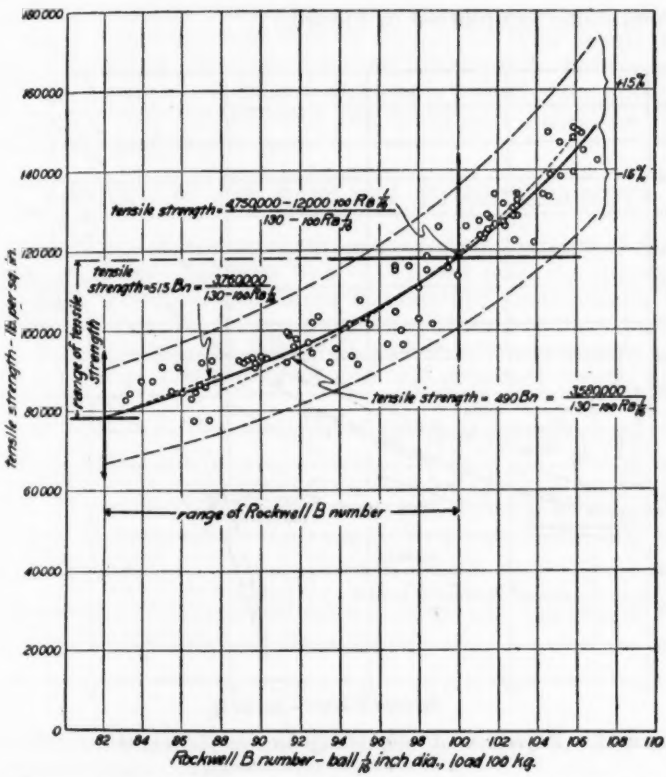

FIGURE 10.—*Experimental relationship between the tensile strength of steel and Rockwell ball number, ball diameter 1/16 inch*

The ranges indicated are those over which the empirical conversion curve may be applied with the expectation of no error greater than 15 per cent.

The full line curve in Figure 10 is the graph of the empirical equation:

$$\text{Tensile strength (lbs./in.}^2) = \frac{4,750,000 - 12,000 \times {}_{100}R_{B1/16}}{130 - {}_{100}R_{B1/16}}$$

the general form of which was suggested by the last two equations given above. None of the experimental tensile strengths differ from corresponding values obtained from this curve by more than 15 per cent. It is suggested that this equation be used over the range of

Rockwell B number (ball 1/16 inch diameter; load 100 kg) from 82 to 100 or of tensile strength from 80,000 to 120,000 lbs./in.^{2}.

If values of Bn in terms of ${}_{150}R_C$ (see equations (d) and (e), Table 8 be multiplied by 490 the following expressions are obtained:

$$\text{Tensile strength (lbs./in.}^2) = \frac{10^5(7{,}450 - 22 \times {}_{150}R_C)}{(100 - {}_{150}R_C)^2} \text{ for } {}_{150}R_C \text{ less than 40}$$

$$\text{Tensile strength (lbs./in.}^2) = \frac{490(25{,}000 - 10(57 - {}_{150}R_C)^2)}{100 - {}_{150}R_C} \text{ for } {}_{150}R_C$$

greater than 40.

These equations are plotted in Figure 11.

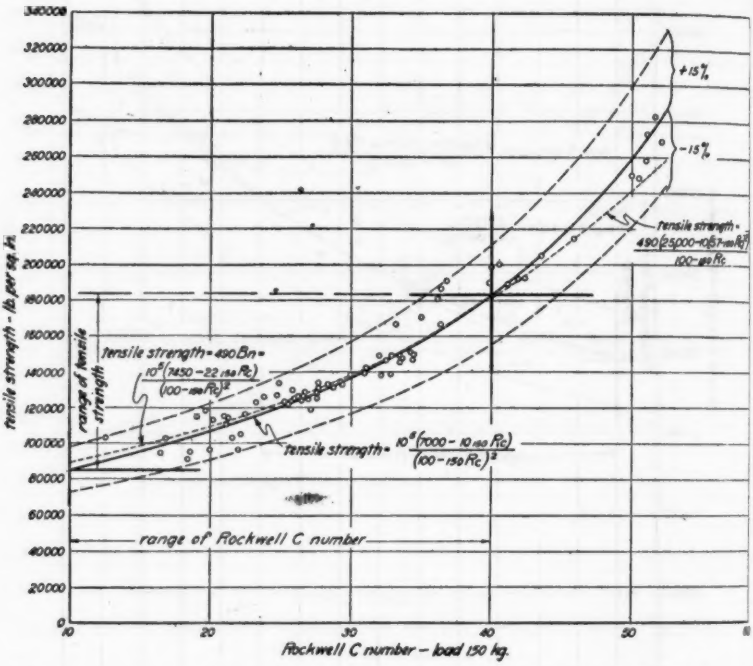
tensile strength - lbs. per sq. in.
Rockwell C number - load 150 kg.
range of Rockwell C number
range of tensile strength
+15%
-15%
tensile strength = 490 Bn =
tensile strength =
tensile strength =

FIGURE 11.—*Experimental relationship between the tensile strength of steel and Rockwell cone number*

The ranges indicated are those over which the empirical conversion curve may be applied with the expectation of no error greater than 15 per cent.

The full line curve in this Figure 11, which seems to satisfy the experimental data better than the dash line curves, especially in the range above ${}_{150}R_C = 40$, is a graph of the empirical equation:

$$\text{Tensile strength (lbs./in.}^2) = \frac{10^5(7{,}000 - 10 \times {}_{150}R_C)}{(100 - {}_{150}R_C)^2}.$$

None of the experimental values differ by more than 15 per cent from corresponding values read from the full line conversion curve. This

accuracy is about the same as that holding in a conversion from Brinell number to tensile strength.[9]

It is suggested that this curve be used only over the range of Rockwell C number (load 150 kg) from 10 to 40 or of tensile strength from 90,000 to 190,000 lbs./in.^{2}. The experimental check on the curve in the range above ${}_{150}R_C=40$ is not sufficient to warrant using it as a conversion curve. With the exception of the two aluminum alloys (Nos. 11 and 12), which fall in line with the ferrous alloys, the nonferrous alloys showed no definite relationships between tensile strengths and Rockwell numbers. This was to be expected in view of the failure of previous investigators to find definite relationships for nonferrous metals (with the exception of aluminum alloys) between tensile strengths and Brinell numbers. The recent work of Schwarz [10] indicates that no general relationship between tensile strength and a single indentation number is possible, the approximate proportionality existing for steel and duralumin being the result of their relatively high elastic ratio.

X. RESULTS OF EARLIER INVESTIGATORS

The desirability of having some means for comparison of the Rockwell and the Brinell numbers was recognized with the increased use of the Rockwell machine. During the last few years several investigations have been made for the purpose of obtaining the experimental relationships between the Rockwell and the Brinell numbers. The summary of these investigations and the principal results obtained are found below:

1. S. C. Spalding, Transactions of the American Society for Steel Treating, October, 1924.

The experiments were made on steels having a tungsten content of about 17 per cent and drawn at different temperatures. The results showed that within the range *Bn* greater than 300 and less than 650 the Brinell number is linearly related to the Rockwell cone number. No conversion formula was recommended, but the relationship between the Rockwell cone number and the Brinell number may be roughly expressed by the equation

$$Bn=12.5{}_{150}R_C-137$$

2. I. H. Cowdrey, Transactions of the American Society for Steel Treating, February, 1925.

Many ferrous and nonferrous materials were tested, including overstrained, cold-worked, and heat-treated material. The following equations were derived:

$$Bn=\frac{{}_{100}R_{B1/16}+273}{6.49-0.048\times{}_{100}R_{B1/16}}$$

and

$$Bn=\left\{\frac{{}_{150}R_C+192}{88.3}\right\}^{6.21}$$

[9] See Relation Between Maximum Strength, Brinell Hardness, and Scleroscope Hardness in Treated and Untreated Alloy and Plain Steels, by R. A. Abbot, Proc. Am. Soc. Test. Mat., 15; 1915.

[10] Otto Schwarz, Zugfestigkeit und Härte bei Metallen, Forschungsarbeiten auf dem gebiete des Ingenieurwesens, Heft 313; 1929.

3. R. C. Brumfield, Transactions of the American Society for Steel Treating, June, 1926.

These tests also included nonferrous materials and steels treated in various ways. The following equations were derived:

$$Bn = \frac{6{,}600}{127 - {}_{100}R_{B1/16}}$$

and

$$Bn = \frac{1{,}880{,}000}{(112 - {}_{150}R_C)^2}$$

The results obtained in these investigations are plotted in Figures 12 and 13. In Figure 12 the Brinell and the Rockwell numbers are

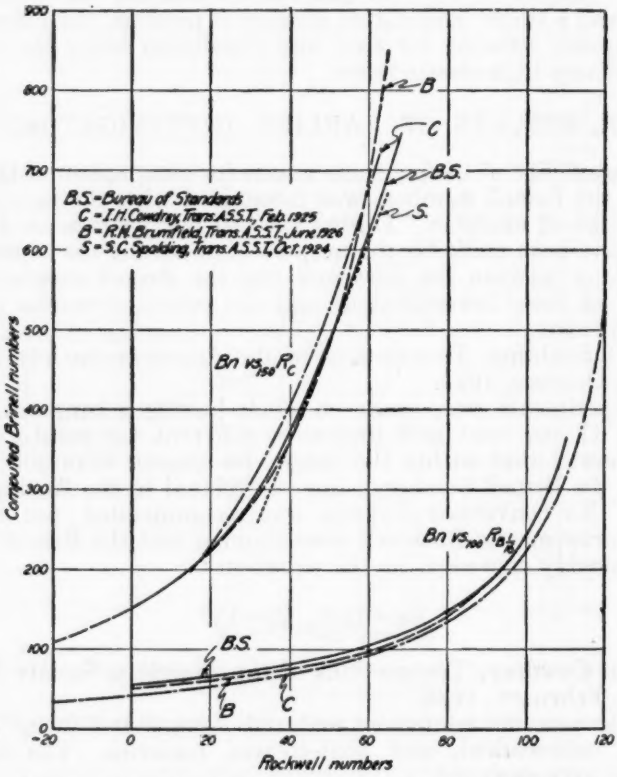

FIGURE 12.—*Relationships between Brinell and Rockwell numbers given by different investigators*

plotted using uniform scales, so that a ready comparison of the Brinell numbers computed from the Rockwell numbers can be made. In Figure 13 the Rockwell numbers are plotted: ${}_{100}R_{B1/16}$ against $\frac{1}{Bn}$ and ${}_{150}R_C$ against $\frac{1}{\sqrt{Bn}}$, as was done in Figures 4 and 5. In this way the differences between the various equations are brought out more clearly.

It will be noted that Brumfield's equations are of the same type as the equations given in this paper. The agreement between the two groups of equations is fairly good, except for the upper range of the Rockwell cone number.

XI. SUMMARY

The tensile strengths and the Brinell and Rockwell indentation numbers were obtained for a variety of ferrous and nonferrous metals.

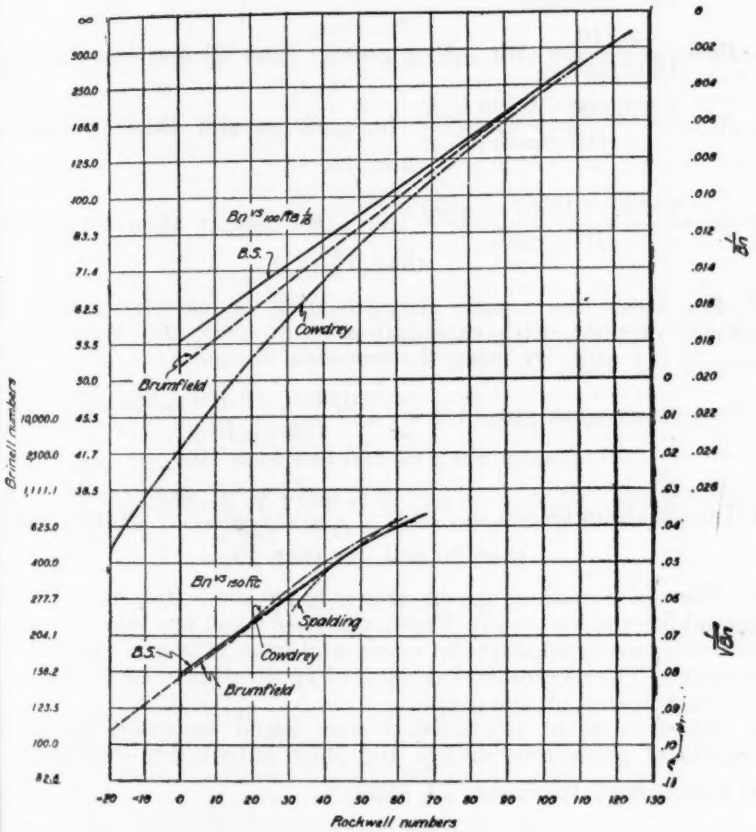

FIGURE 13.—*Relationships between Brinell and Rockwell numbers obtained by different investigators*

Rockwell number vs. $\frac{1}{\sqrt{Bn}}$ and $\frac{1}{Bn}$

1. The experimental indentation numbers made it possible to obtain semiempirical formulas for calculating Brinell numbers from Rockwell numbers, or vice versa. When used over the range specified each of these formulas gives values in which the error to be expected is not greater than plus or minus 10 per cent.

Using the following notation:

$_{100}R_{B1/16}$; Rockwell B number, ball 1/16 inch diameter, load 100 kg.

$_{100}R_{B1/8}$; Rockwell B number, ball 1/8 inch diameter, load 100 kg.

$_{150}R_C$; Rockwell C number, brale, load 150 kg.

these equations are:

(*a*) $Bn=\frac{7,300}{130-{}_{100}R_{B1/16}}$ for $_{100}R_{B1/16}$ greater than 40 and less than 100.

(*b*) $Bn=\frac{3,710}{130-{}_{100}R_{B1/8}}$ for $_{100}R_{B1/8}$ greater than 30 and less than 100.

(*c*) $Bn=\frac{1,520,000-4,500\ {}_{150}R_C}{(100-{}_{150}R_C)^2}$ for $_{150}R_C$ greater than 10 and less than 40.

(*d*) $Bn=\frac{25,000-10(57-{}_{150}R_C)^2}{100-{}_{150}R_C}$ for $_{150}R_C$ greater than 40 and less than 70.

2. For steels the tensile strength may be calculated from the Rockwell number, with expectation of an error less than plus or minus 15 per cent, by using the empirical formulas:

(*a*) Tensile strength (lbs./in.^{2}) $=\frac{4,750,000-12,000\ {}_{100}R_{B1/16}}{130-{}_{100}R_{B1/16}}$ for $_{100}R_{B1/1}$ greater than 82 and less than 100.

(*b*) Tensile strength (lbs./in.^{2}) $=\frac{10^5(7,000-10\times{}_{150}R_C)}{(100-{}_{150}R_C)^2}$ for $_{150}R_C$ greater than 10 and less than 40.

3. The six equations given above have been plotted. On each graph additional curves are drawn, one above and one below the given conversion curve, showing the maximum error to be expected in using the curve. The recommended range of application of each conversion curve is indicated on the graph.

4. No discernible relationship was found between the tensile strengths of nonferrous metals and their indentation numbers.

WASHINGTON, December 29, 1929.

PHOTO-IONIZATION OF CÆSIUM BY LINE ABSORPTION

By F. L. Mohler and C. Boeckner

ABSTRACT

Method.—The ionization of cæsium by line absorption has been investigated by means of the space-charge method. Light resolved by a monochromator is used and the relative sensitivity in the region of line absorption, as compared to the region of continuous absorption beyond the limit, is measured.

Ionization by a continuous spectrum.—The effect is directly proportional to the light intensity. Relative sensitivity is independent of electrical conditions and temperature of the vapor. The reduction of the effect by an absorbing column of cæsium vapor in the light path indicates that the effective absorption line width is about 0.007 A at 0.003 mm pressure. This width increases with pressure. Relative sensitivity rises rapidly with vapor pressure between 0.0002 and 0.004 mm and drops slowly above 0.01 mm.

Ionization by monochromatic light.—A helium line at 3888 A is coincident with one of the cæsium lines and measurements of the absorption of this line by cæsium and of the photo-ionization produced give the probablity of ionization of an excited atom in the 4 P_1 state as a function of the vapor pressure.

Discussion.—Measurements of relative sensitivity to continuous spectrum excitation are corrected for absorption and slit width to give the probability of ionization of excited atoms in states 4 to 8 P and higher states near 9 P, 12 P, 16 P, and 25 P. This probability is shown to be proportional to the chance that an excited atom collides with another cæsium atom during the life of the excited state. The probability of ionization at a collision varies from nearly one for higher states to 0.003 for the 4 P state. Results are consistent with a theory of Franck's that ionization results from the combination of excited and normal atoms to form molecule ions.

CONTENTS

	Page
I. Introduction	52
1. The problem	52
2. Cæsium absorption	52
II. Experimental procedure	54
1. Method	54
2. Radiation flux	55
3. Properties of the space charge tube	55
III. Ionization by a continuous spectrum	56
1. Intensity relation	56
2. Effect of electron current and voltage	56
3. Temperature effect	56
4. Absorption effect	57
5. Pressure effect	59
6. Quenching by foreign gases	60
IV. Ionization by helium lines	61
1. The helium line at 3,888 A	61
2. Ionization by 3,188 A of helium	62
3. Ionization by other line sources	62
V. Discussion	63
1. Restriction of the problem	63
2. Correction for absorption	63
3. The pressure variation of efficiency	66
4. The hypothesis of molecule ion formation	69
VI. Summary	71

I. INTRODUCTION

1. THE PROBLEM

Experiments on the photo-ionization of cæsium vapor by Mohler Foote, and Chenault[1] have shown that in addition to the predicted ionization beyond the absorption series limit resulting from continuous absorption there was some ionization by line absorption. Illumination with light from an incandescent lamp analyzed by a monochromator showed separate sharp peaks in the ionization at the fourth, fifth, sixth, and seventh lines of the principal series, while the partially or completely unresolved higher lines gave an effect which increased to a maximum at the limit (3,184 A). The third line gave a barely measurable effect and the second line no effect. Recent results by Lawrence and Edlefsen[2] show a similar phenomenon in rubidium vapor with peaks at the fourth, fifth, and sixth lines, though one other peak at 3,490 A does not coincide with an absorption line. These measurements have been made by observing the neutralizing effect of the ions on a thermionic current limited by electron space charge. The method is extremely sensitive and unaffected by surface photo-electric emission though it does not give an absolute measure of the ion current.

Mohler, Foote, and Chenault proposed the theory that the excited atoms produced by line absorption were ionized by atomic collisions in which the ionization energy (maximum 0.7 volt) came from thermal agitation. It has been pointed out in criticism[3,4] that the probability of such thermal ionization is too small to account for the observed effect, and Franck and Jordan have suggested that electron collisions with excited atoms might explain the ionization, since measurements were made in the presence of an electron current. Another suggestion of Franck's is that the excited atoms on collision with normal atoms form molecule ions.

The criticism that the ionization by line absorption is too great to be explained by thermal agitation is borne out by the following experiments, but a quantitative estimate of the probability of ionization involves a knowledge of the ratio of the number of ions produced to the number of quanta absorbed in a fine line of unknown width. For this reason Mohler, Foote, and Chenault limited their discussion to the relative heights of the peaks at the separate lines. Recent investigations of the absorption spectrum of cæsium and of the absolute value of the photo-ionization beyond the series limit offer a basis for further investigation of the ionization by line absorption.

2. CÆSIUM ABSORPTION

A recent paper by Waibel[5] gives quantitative measurements of the absorption by the higher series lines of cæsium. The significant datum in line absorption is the integral of the absorption coefficient across the line and to make the magnitudes measurable he used thin layers of vapor at high pressure so that lines were much broadened. The third column of Table 1 gives Waibel's observed values of $\int k d\nu$ in terms of atomic absorption coefficient and cm^{-1} for the doublet

[1] Mohler, Foote, and Chenault, Phys. Rev., **27**, p. 37; 1926.
[2] Lawrence and Edlefsen, Phys. Rev., **34**, p. 233; 1929.
[3] Franck and Jordan, Anregnung von Quanten Sprüngen durch Stosse, p. 126, Julius Springer, Berlin.
[4] Gudden, Lichtelektrische Erscheinungen, p. 224, Julius Springer, Berlin.
[5] Waibel, Zeits. f. Phys., **53**, p. 459; 1929.

$1S-mP_{1,2}$. The fourth column gives this integral divided by the mean frequency interval between lines $\Delta\nu=(\nu_{m+1}-\nu_{m-1})/2$. This constant ratio should equal the atomic absorption coefficient at the series limit, k_o. The authors [6] have published absolute measurements of the ionization produced by continuous absorption in cæsium vapor from which they compute a value of $k_o=2.3\times10^{-19}$. This is not in satisfactory agreement with the value from Waibel's data, and other measurements give still higher values. For present purposes it has seemed best to use our value of k_o, together with values of $\int k d\nu$ obtained by multiplying Waibel's values by 2.3/0.48 as given in column 5 of Table 1. It will be shown later that the lower value of Waibel would lead to serious inconsistencies in the present results.

TABLE 1.—*Line absorption in cæsium*

m	$1S-mP_1$ in A	$\int k d\nu$ observed	$\frac{\int k d\nu}{\Delta\nu}$	$\frac{\int k d\nu}{k_o=2.3\times10^{-19}}$	Transmission of 4 cm at 0.01 mm
4	3877			(550×10⁻¹⁹)	0.012
5	3612			(288)	.100
6	3477	35×10⁻¹⁹	0.40×10⁻¹⁹	170	.26
7	3398	20.6	.37	100	.45
8	3349	16.2	.43	79	.53
9	3313	12.7	.48	62	.61
10	3288	9.2	.47	45	.70
11	3270	7.3	.49	35	.76
12	3257	5.6	.49	27	.80
13	3246	4.3	.47	21	.84
14	3247	3.4	.47	16	.88
15	3231	2.7	.45	13	.90
16	3225			(11)	.91

Waibel's paper includes values for the width of the lines at various pressures. Results are expressed in terms of the "half width" here denoted by $\delta\lambda$ or $\delta\nu$ which is the interval between points where k has half the maximum value. The different lines of the series have nearly the same half width which varies as the square root of the pressure. For $1S-mP_2$ $\delta\lambda$ varied from 0.55 A at 12.3 mm pressure to 0.30 A at 4.4 mm. From this rate of variation one computes values of 0.05 A at 0.1 mm, 0.015 A at 0.01 mm, and 0.005 A at 0.001 mm. (Pressures reduced to 0° C.) But the Doppler width for cæsium atoms at 500° K. is 0.0055 A so that below 0.001 mm the Doppler broadening will be predominant. Since the lines are doublets in which each component has a hyperfine structure it becomes very complicated to compute the line shapes or widths to be expected at low pressure.

If lines have the shape theoretically predicted for collision broadening [7] then

$$\int k d\nu = k(\text{max.})\ \delta\nu \qquad (1)$$

The transmission of a layer of vapor of length L containing N atoms per cm³ for light coincident with an absorption line is then

$$\text{trans.} = e^{-NL\int k d\nu/\delta\nu} \qquad (2)$$

[6] Mohler and Boeckner, B. S. Jour. Research, **3**, p. 303; 1929.
[7] Handbuch der Physik., **20**, p. 496.

II. EXPERIMENTAL PROCEDURE

1. METHOD

Figure 1 illustrates the type of space-charge tube used in most of this work. This is a quartz tube containing a platinum cylinder anode 4 cm long and 3 cm in diameter. In the ends of the anode are slits about 8 mm wide to admit light and for the cathode leads. The cathode is a hairpin platinum wire coated with oxides. The tube was usually sealed off from the pumps and heated by two independent heating units, one around the body of the tube and one around the appendix so that effects of vapor pressure and temperature could be studied independently. The ionization chamber was kept at about 500° K. for most work.

Vapor pressure was computed from an equation based on data by Kroner.[8]

$$\log p \text{ (mm)} = -3966/T + 7.1650$$

The tube was commonly operated with the filament at a barely visible red heat and with an applied voltage between zero and 1 volt which gives a dark current of the order of 2×10^{-5} amperes. This was balanced by a bridge circuit so that current changes of 10^{-8} amperes

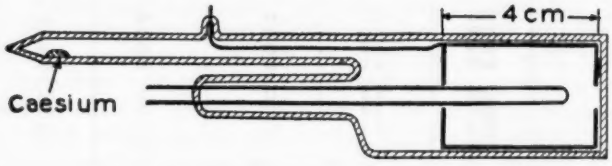

FIGURE 1.—*The type of space charge tube used in this work*

could be measured. The electron current change is of the order of 10^5 or 10^4 times the ion current, the ratio being greatest at low pressure.

Since the sensitivity varies with nearly all operating conditions all the observations consisted of measurements of relative sensitivity for light of frequency ν compared to light of a standard frequency in the region of continuous absorption. For experimental purposes the standard 3,150 A was chosen, though in interpreting results it is more convenient to take the series limit 3,184 A and we have reduced all results to the latter. In the following the relative sensitivity is

$$R(\nu) = \frac{i(\nu)}{i(3{,}184)} \frac{J(3{,}184)}{J(\nu)\,\Delta\nu} \Delta\nu\,(3{,}184) \qquad (3)$$

where i's are the observed current change proportional to the ionization, while the J's are radiation flux in quanta per second and $\Delta\nu$ is the width of the band transmitted by the monochromator. We can safely assume that beyond the series limit the number of ions produced is equal to the number of quanta absorbed.

$$i(3{,}184) = cNLk_o J(3{,}184)\,\Delta\nu\,(3{,}184)$$

[8] Rowe, Phil. Mag., 3, p. 534; 1927.

where N is the number of atoms per cm^3 (2×10^{16} at 1 mm), L is the path length, and k_o is the atomic absorption coefficient. The proportionality factor c between ions and current change is always eliminated by taking ratios.

2. RADIATION FLUX

The source of continous radiation was the light from a 400-watt Mazda projection lamp analyzed by a Bausch & Lomb monochromator. The relative radiation flux in quanta per second is shown in Figure 2. This is based on direct measurements of energy flux

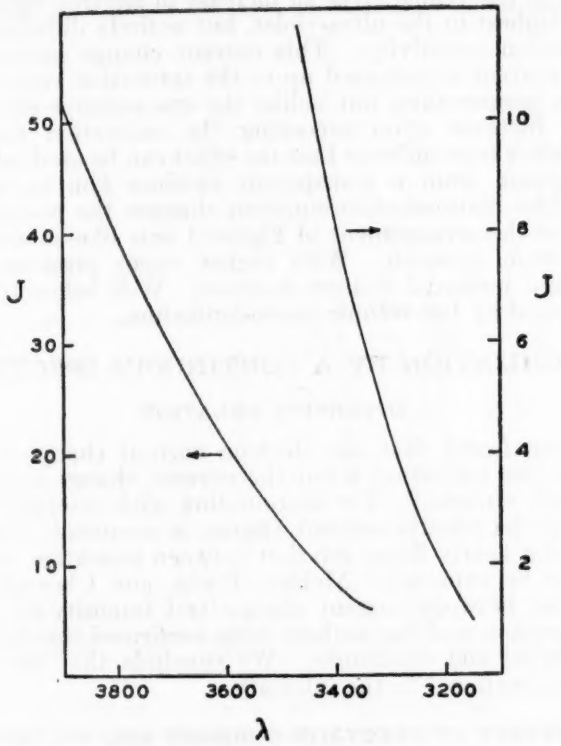

FIGURE 2.—*Relative values of radiation flux in quanta per second of light from a Mazda lamp resolved by a quartz monochromator*

made with a thermopile supplemented by computed values based on radiation laws, the dispersion of quartz and the transmission of glass from a similar lamp. The computed values were only used in the range 3,250 to 3,150.

3. PROPERTIES OF THE SPACE CHARGE TUBE

In a comparison of radiation, strongly absorbed in the front of the ionization chamber with radiation weakly absorbed throughout the length, it is important to know the sensitivity in different parts of the chamber. In a tube such as is shown in Figure 1 a small beam

of light was moved diametrically across the tube and no change in ionization greater than 10 per cent was found until the light beam struck the walls. Again in a tube of similar dimensions with a slit along the length of the cylinder no important change was found as the light was moved from one end of the cylinder to the other. The experiments do not exclude the existence of a thin layer of vapor (1 or 2 mm) at the window which is ineffective. Apart from this possibility we are justified in assuming that all ions produced in the chamber are equally effective.

There is a small surface effect which is greatest with the cæsium at room temperature. Then light of all wave lengths from the ultra-violet to the visible gives an increase in electron current with a sensitivity highest in the ultra-violet, but entirely different from the photo-ionization sensitivity. This current change increases as the thermionic current is increased up to the saturation value by raising the cathode temperature, but unlike the space-charge effect there is no further increase upon exceeding the saturation temperature. These and other tests indicate that the effect can be ascribed to photo-electric emission from a transparent caesium film on the quartz window.[9] The photo-electric emission changes the potential of the film which in the arrangement of Figure 1 acts like an external grid on the electron emission. With higher vapor pressures the film resistance and potential change decrease. Well below 100° C. the effect is masked by the volume photo-ionization.

III. IONIZATION BY A CONTINUOUS SPECTRUM

1. INTENSITY RELATION

It has been found that the electron current change is not proportional to the ionization when the current change is comparable with the dark current.[10] For illumination with resolved light of a Mazda lamp the relative current change is commonly less than 10 per cent and a nearly linear relation between ionization and current change is to be expected. Mohler, Foote, and Chenault found a linear relation between current change and intensity for ionization by line absorption and the authors have confirmed this for a variety of wave lengths and conditions. We conclude that the ionization is directly proportional to the intensity.

2. EFFECT OF ELECTRON CURRENT AND VOLTAGE

Variation of the electron current by changing the filament temperature has no effect on the form of the sensitivity curve. Variation of the applied potential has the effect that strongly absorbed light, notably the 3,612 line, is slightly more effective at high voltage. This can be ascribed to the ability of higher electric fields to draw more ions from the layer of vapor close to the window. There remains no evidence that the ionization process depends on the electron current.

3. TEMPERATURE EFFECT

Careful tests were made to detect a change in the relative sensitivity when the cæsium pressure was kept constant and the tem-

[9] Ives, Astrophys. J., **62**, p. 309; 1925.
[10] Whitman, B. S. Jour. Research, **4** (RP 138), pp. 157–167; January, 1930.

perature of the body of the tube was changed. Figure 3 illustrates the results at a cæsium pressure of 0.0038 mm and temperatures of 162° and 260° C. All results indicate that the relative height of the line peaks is independent of the temperature. Under the conditions of the experiment the pressure remained constant and the density changed. Following results indicate that maintaining a constant vapor density would probably not make a perceptible difference.

4. ABSORPTION EFFECT

It is evident from computations, such as those given in Table 1, that the absorption of a layer of vapor of several centimeters in

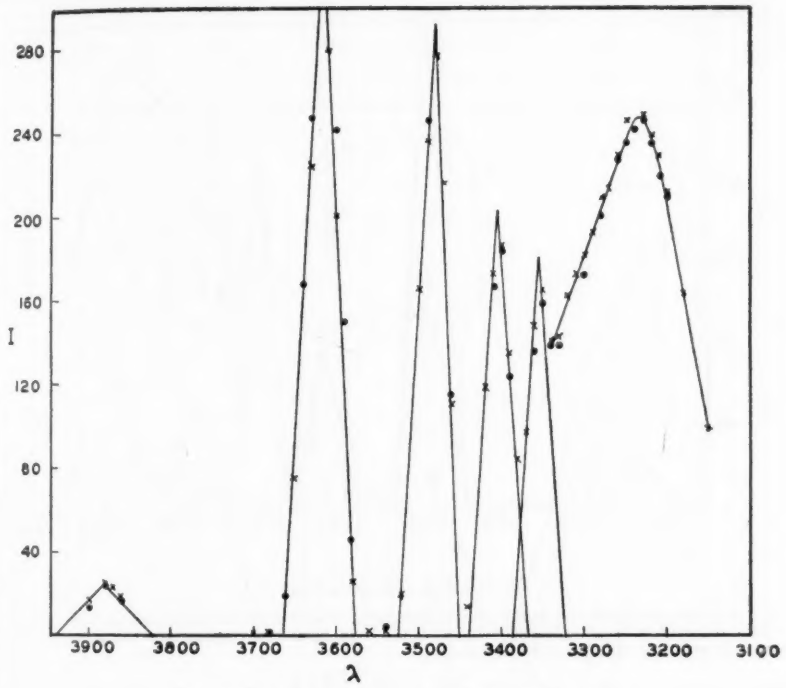

FIGURE 3.—*Ion current v.* λ *at 0.0038 mm*
Circles at 162° C. and crosses at 260° C.

front of the ionization chamber will appreciably reduce the light intensity at the center of the absorption lines even at pressures of 10^{-3} mm or less. Preliminary experiments made with a tube having the ionization chamber 8 cm from the window gave about one-fourth of the relative sensitivity at 3,612 A at a pressure of 0.001 mm which was obtained with the tube shown in Figure 1. The tubes used in previous investigations have had several centimeters of vapor in front of the ionization chamber so that the line absorption sensitivity was reduced.

Quantitative measurements of the absorption were made by placing a cell containing cæsium in front of the space-charge tube and making observations of the change in the ionization when the

cæsium in the absorption cell was heated. Figure 4 illustrates some curves obtained under extreme conditions with an absorption tube 30 cm long. Curves I and II show the observed curves with cæsium at a pressure of 0.14 mm in the space charge tube and at zero and 0.14 mm in the absorption cell. Curve III was obtained with the same pressure in the absorption cell but a much lower pressure, 0.0063 mm, in the space-charge tube. This indicates that there is complete absorption near the center of the lines at this pressure and that by lowering the pressure in the ionization chamber the lines become so narrow that no effective radiation is transmitted. It is interesting that the measurements for Curve II show no diminution in the small

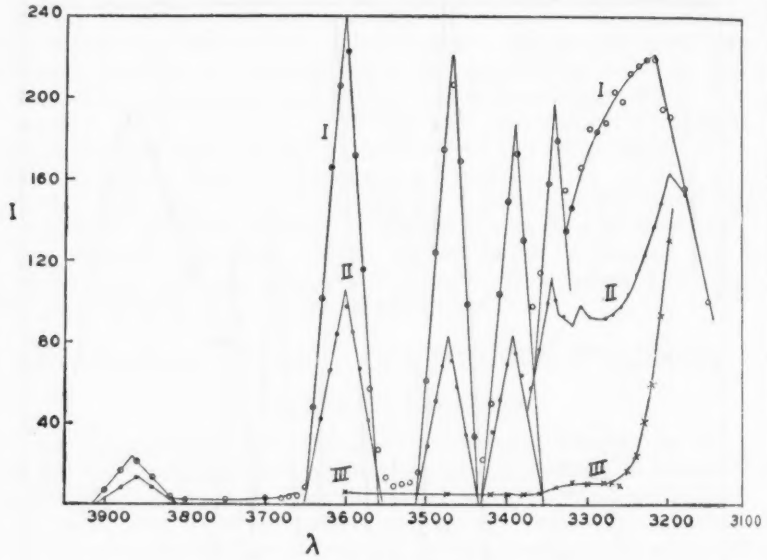

FIGURE 4.—*Ion current v.* λ

I with 0.14 mm of cæsium in the space charge tube; II with a 30 cm column of cæsium vapor at 0.15 mm pressure in the light path; III with the same absorbing column, but the pressure in the space charge tube reduced to 0.0063 mm.

effect between lines though this could not be shown on the scale of the drawing. This effect between the lines becomes much less at lower pressure.

More useful results were obtained at much lower pressures with an absorption cell 4 cm long. Table 2 summarizes the results and includes both the observed transmission e^{-NLk} and NLk. A plot of NLk versus wave length gives a nearly straight line and the values in the table are based on the best straight lines to smooth out accidental errors where NLk is small. It is evident that k is not a constant, but varies with the pressures in both the absorption cell and the space-charge tube. These variations are evidently a consequence of the shape of the absorption lines and the variation of their width with pressure.

TABLE 2.—*Absorption of radiation effective in producing ions by a 4 cm column of vapor*

Wave length	Ionization chamber 0.0031 mm				Ionization chamber 0.0059 mm	
	Absorption, 0.0011 mm		Absorption, 0.0031 mm		Absorption, 0.0031 mm	
	Transmission	*NLk*	Transmission	*NLk*	Transmission	*NLk*
3,612	0.56	0.58	0.40	0.92	0.57	0.57
3,477	.67	.395	.50	.69	.63	.46
3,398	.77	.265	.63	.465	.73	.31
3,347	.83	.185	.72	.33	.80	.22
3,300	.90	.105	.83	.19	.88	.125
3,250	.978	.022	.955	.045	.965	.035
3,200	1.0	0	1.0	0	1.0	0

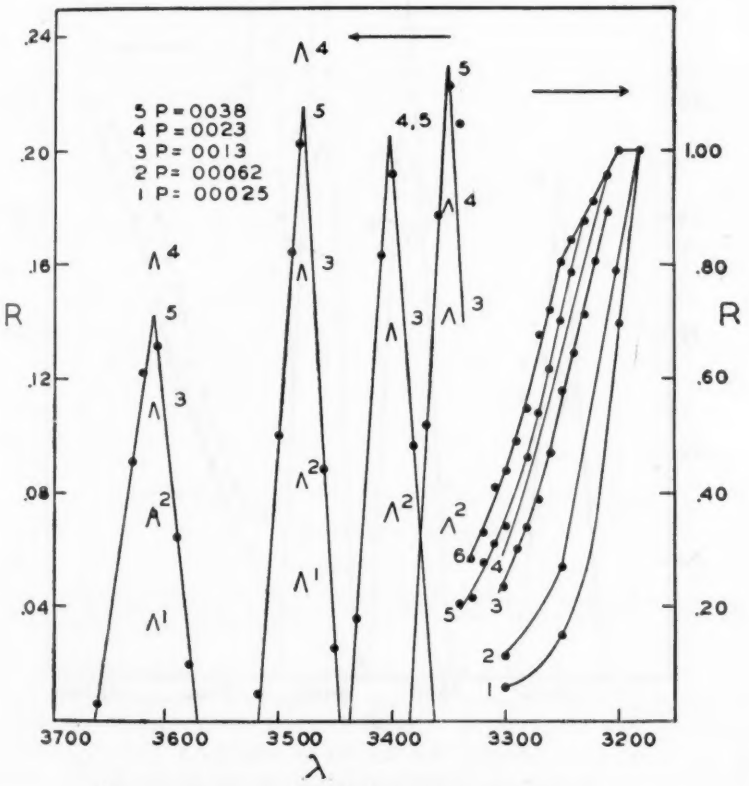

FIGURE 5.—*Relative sensitivity v.* λ

1 at 0.00025 mm, 2 at 0.00062 mm, 3 at 0.0013 mm, 4 at 0.0023 mm, 5 at 0.0038 mm, 6 at 0.0073 mm. Two scales of R left for 3,700 to 3,340, right 3,340 to limit.

5. PRESSURE EFFECT

It is feasible to investigate an extreme range of pressures, and Figures 5 and 6 show the relative sensitivity, R, as defined in equation (3) for pressures ranging between 2.5×10^{-4} and 0.15 mm. At each wave length R rises and then falls with increasing pressure in a

manner which suggests that there are two or more effects which nearly counterbalance each other above 0.002 mm pressure. Ordinates give the effect relative to the limit and since the ionization at the limit is proportional to the pressure the ionization at all wave lengths is always increasing with pressure throughout the range studied.

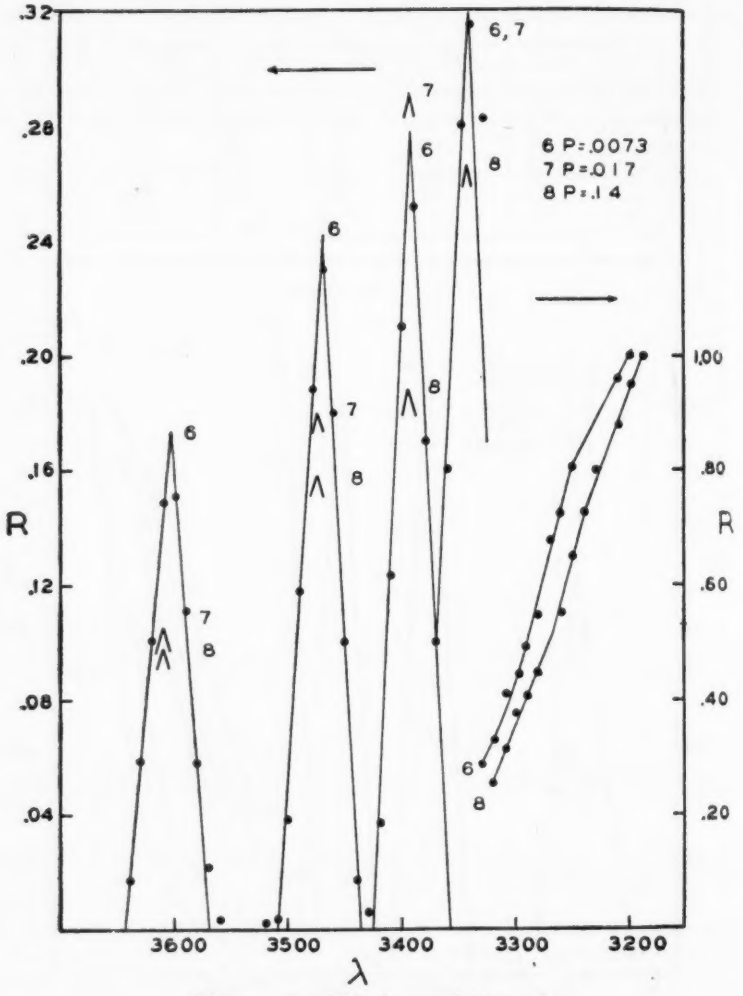

FIGURE 6.—*Relative sensitivity v.* λ

6 at 0.0073 mm, 7 at 0.017 mm, 8 at 0.14 mm. Two scales of *R*.

6. QUENCHING BY FOREIGN GASES

It is difficult to maintain a good vacuum in a sealed-off tube containing an alkali metal, so a preliminary experiment was made with the tube connected to the pumps through a capillary which could be closed with a needle valve. The relative sensitivity to line absorption gradually increased with prolonged pumping to a value appreciably higher than previously obtained in sealed tubes. The experi-

ments furnished a standard for estimating the vacuum in sealed-off tubes, and in the results quoted in this paper the quenching by foreign gas is probably negligible. Quantitative measurements of the effect of adding foreign gases will be presented in another paper.

IV. IONIZATION BY HELIUM LINES

1. THE HELIUM LINE AT 3,888 A

The helium spectrum contains an isolated strong line at 3,888.649 A while the red component of the third doublet of cæsium is at 3,888.622 A. This is very nearly exact coincidence and it was expected that this line would be strongly absorbed by cæsium and give a large photo-electric effect. Experiments bore out this expectation and it

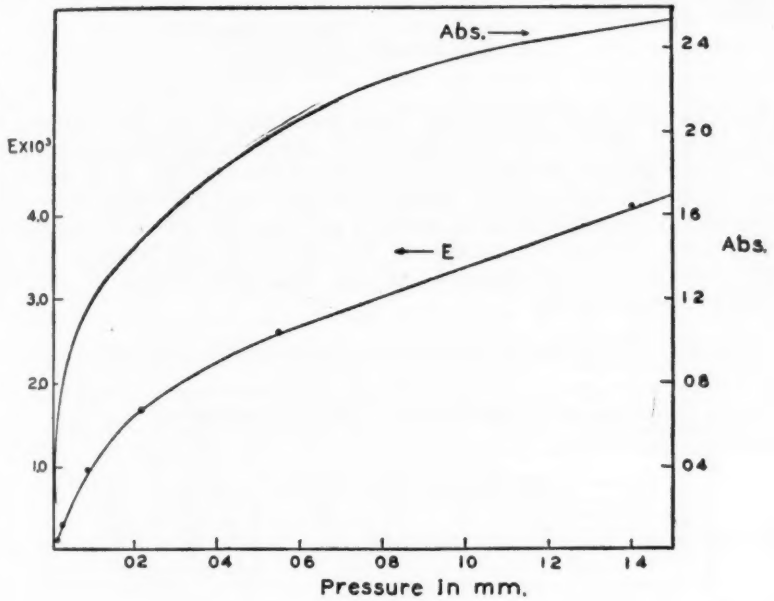

FIGURE 7

Upper curve, right scale, the absorption of the 3,888 helium line by a 4 cm column of cæsium vapor as a function of cæsium pressure. Lower curve, left scale, the quantum efficiency of ionization of cæsium by 3,888 as a function of pressure.

was possible to make direct measurements of the radiation flux, the fraction of this radiation absorbed, and the number of ions produced. Such measurements in contrast to studies with continuous radiation yield directly the probability of ionization of an excited atom (or the quantum efficiency of ion production) without assumptions as to line width and shape.

A small capillary Geisler tube served as a source and the radiation flux for 3,888 and for the 3,130 line of mercury were measured directly by a thermopile under operating conditions. The former was barely measurable so that the absolute value of the final result is much less certain than the relative values.

Absorption of the 3,888 line was measured with a 4 cm absorption cell and a photo-electric cell, and Figure 7, upper curve, shows the absorption as a function of the pressure.

Photo-ionization was measured by a direct comparison of the ionization produced by 3,888 and the 3,130 line of the mercury arc. The effect of both lines was so large that the current change was not proportional to the ionization and it was necessary to determine the current intensity relation at each pressure by reducing the light in known ratios by a series of wire gauze screens. The relative sensitivity R is then

$$R=\frac{I\,(3{,}888)}{I\,(3{,}130)}\times\frac{J\,(3{,}130)}{J\,(3{,}888)}$$

where the I's are the corrected ratio of ionization and the J's are the radiation flux in quanta per second. Assuming that the quantum efficiency of the 3,130 radiation is one, we have for the efficiency of 3,888;

$$E\,(3{,}888)=R\times\frac{Abs\,(3{,}130)}{Abs\,(3{,}888)}$$

The absorption of 3,130 has been determined by the authors as $NL\times 1.85\times 10^{-19}$. Table 3 summarizes the data for the determination of E and Figure 7, lower curve, is a plot of the results. It is seen from the table that the relative sensitivity rises and falls with increasing pressure in the same general manner as R for the effect of continuous radiation. The ratio remains of the order of one because the low efficiency is counterbalanced by the high absorption of 3,888 as compared with 3,130.

TABLE 3.—*The absorption and ionization of cæsium by the 3,888 helium line*

Cæsium temperature (°C.)	Cæsium pressure	R (3,888)	Absorption of 3,130	Absorption of 3,888	E (3,888)
110	0.64×10^{-3}	0.42	0.096×10^{-4}	0.036	0.11×10^{-3}
128	1.9	.77	.285	.078	.28
156	8.5	.89	1.28	.118	.96
173	22	.75	3.3	.150	1.65
193	55	.63	8.3	.20	2.6
214	140	.49	21	.25	4.1

2. IONIZATION BY 3,188 A OF HELIUM

Another helium line which gives measurable photo-ionization is at 3,187.743 *A*. This is within 4 Angstroms of the cæsium series limit. We compute from the series formula given by Miss Mathews [11] that the forty-eighth line lies at 3,187.73, the forty-ninth at 3,187.55. Experiments were limited to a direct comparison of the effect of this line and 3,130 of mercury. For pressures ranging from 0.001 to 0.07 mm there was no change in the relative sensitivity.

3. IONIZATION BY OTHER LINE SOURCES

Strong emission lines, such as 3,650 and 3,340 of mercury which are many Angstroms from cæsium absorption lines, give measurable photo-ionization. This is evidently related to the small effect between lines observed with a continuous spectrum at the higher pressures. Results of experiments on this effect will be published later.

[11] Mathews, Proc. Roy. Soc., **120**, p. 650; 1928.

V. DISCUSSION

1. RESTRICTION OF THE PROBLEM

Ionization by line absorption involves initially the production of an excited atom in an $m\,P$ state. The energy of this state is appreciably below the ionization potential, 0.7 volt below in the extreme case of ionization by the 3,888 line. What is the source of the additional energy required for ionization? The experiments definitely eliminate most of the possibilities. The linear relation between intensity and ionization rules out the hypothesis of a transfer of energy between two excited states. The evidence that sensitivity is independent of electron current shows that ionization is not produced by electron collisions. The absence of temperature effect eliminates the theory that ionization results either directly or indirectly from thermal agitation or from black body radiation. There remains the possibility suggested by Franck that an excited atom in collision with a normal atom forms a molecule which spontaneously becomes ionized. This theory seems to be strongly supported by the experiments though it involves too many unknowns to be definitely established. The probability of ionization would depend on the pressure in a complicated manner. The chance of absorption of a quantum of radiation and the chance that the exicted atom collides to form a molecule before radiation takes place will vary with pressure and possibly the chance of subsequent ionization may depend on pressure as well. The measurements on the ionization by the 3,888 helium line give directly the efficiency of ionization per quantum absorbed. In the following section we attempt to derive this quantum efficiency for ionization at the other lines and thus eliminate the first cause of pressure variation. It remains then to see if the variation in quantum efficiency with pressure can be accounted for by the second pressure effect.

2. CORRECTION FOR ABSORPTION

If $I(\nu)$ is the number of ions produced per second by a flux of $J(\nu)\,\Delta\nu$ quanta per second in a band of width $\Delta\nu$, then

$$I(\nu)=\int_{\Delta\nu} E(\nu)\,J(\nu)\,(1-e^{-NLk})\,d\nu \tag{5}$$

where $E(\nu)$ is the quantum efficiency. Assuming that absorption in a line can be expressed as a constant absorption k_m over a width $\delta\nu$, then

$$I(\nu)=E(\nu)\,J(\nu)\,(1-e^{-NLk_m})\,\delta\nu \tag{6}$$

At the series limit $E=1$ and since NLk_o is very small $1-e^{-NLk_o}=NLk_o$ and

$$I_o=J_oNLk_o\Delta\nu \tag{7}$$

$$E(\nu)=\frac{I(\nu)}{I_o}\,\frac{J_oNLk_o\,\Delta\nu}{J(\nu)\,(1-e^{-NLk_m})\,\delta\nu}$$

$$E(\nu)=R(\nu)\,\frac{NLk_o}{1-e^{-NLk_m}}\,\frac{\Delta\nu}{\delta\nu} \tag{8}$$

where $R(\nu)$ is the quantity plotted in Figures 5 and 6. Where lines are unresolved (3,300 to 3,200) we can make use of the law of absorption near the limit

$$\int_{\Delta\nu} NLk d\nu = NLk_o \Delta\nu$$

If Nlk_m is sufficiently small (less than 0.2) so that $1-e^{-NLk}=NLk$ we have the simple relation that $E(\nu)=R(\nu)$. When NLk_m is larger then E is greater than R and we can use the approximation

$$E(\nu)=\frac{R(\nu)\,NLk_m}{1-e^{-NLk_m}} \tag{9}$$

where k_m applies to one of the unresolved lines near the center of the slit.

In column 5 of Table 2 we have given the measured value of NLk for 4 cm of cæsium vapor at 0.0031 mm for radiation effective in producing ionization at the same pressure. From column 5 of Table 1 we can compute $\int NLk d\nu = NLk_m \delta\nu$ for the same condition, and the quotient gives a value of $\delta\nu$ that can be used in equation (8) for the effective width of our assumed rectangular line at this pressure. Table 4 gives the results and we will use the mean value $\delta\nu=0.065$ cm^{-1} or $\delta\lambda=0.0076$ A. This value is if anything too small, for the Doppler width is 0.0055 A and taking into account the fine structure we would expect an effective width of about 0.01 A. It is important to note that Waibel's values of $\int k d\nu$ would give $\delta\lambda$ only a fifth as large as this, which is clearly impossible.

TABLE 4.—*The effective line width for absorption at 0.0031 mm*

Wave length	$NLk\,\delta\nu$ from Table 1	NLk from Table 2	$\delta\nu$	$\delta\lambda$
3,250	0.6×10^{-3}	0.045	0.13	0.0140
3,300	1.34	.190	.071	.0077
3,349	1.97	.33	.060	.0067
3,398	2.50	.46	.054	.0062
3,477	4.2	.69	.061	.0074
3,612	7.2	.92	.078	.010

TABLE 5.—*Quantum efficiency at 0.0038 mm*

Wave length	$NLk\,\delta\nu$ from Table 1	NLk for $\delta\nu=0.065$	R from Figure 5	Correction equations (8) and (9)	E
3,200			1.00	1.0	1.00
3,225			.90	1.0	.95
3,250	7.3×10^{-3}	0.11	.72	1.05	.76
3,300	19	.29	.34	1.15	.39
3,349	24	.37	.23	1.05	.24
3,398	30	.47	.20	.87	.18
3,477	51	.79	.214	.59	.126
3,612	87	1.35	.14	.44	.062
3,888	168	2.6	.0043	.35	.0015

TABLE 6.—*Quantum efficiency as a function of pressure*

Wave length	Pressure							
	0.00025	0.00062	0.0013	0.0023	0.0038	0.0073	0.017	0.14
	$\delta\nu$							
	0.065	0.065	0.065	0.065	0.065	0.09	0.137	0.395
3200	0.75	0.80	1.00	1.00	1.00	1.00	1.00	1.00
3225	.47	.55	.76	.84	.90	.93	.90	.93
3250	.15	.28	.57	.67	.76	.86	.80	.89
3300	.06	.12	.25	.32	.39	.52	.58	.74	
3347	----------	.066	.14	.18	.24	.35	.39	.57
3398	----------	.056	.10	.166	.18	.26	.31	.39
3477	.02	.038	.074	.124	.126	.16	.15	.31
3612	.009	.020	.033	.059	.062	.092	.075	.19
3877	----------	.0005	.001	.0011	.0015	.002	.0023	.0067

To compute the quantum efficiency E from R by equations (8) and (9) we will make the arbitrary assumption that $\delta\nu = 0.065$ for

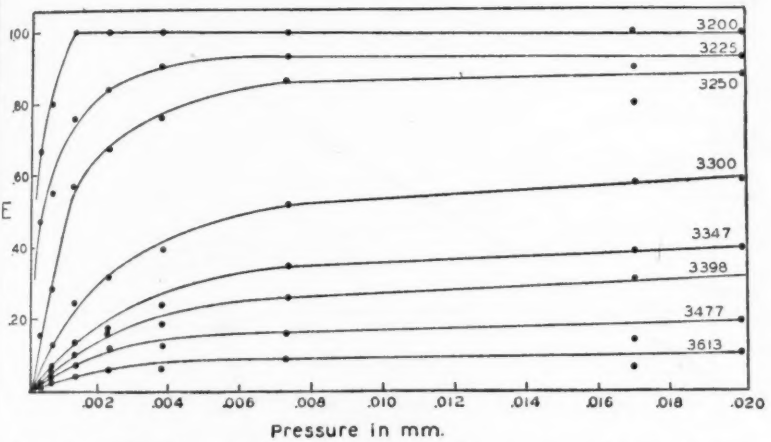

FIGURE 8.—*Quantum efficiency of radiation of various wave lengths for producing ionization as a function of cæsium pressure from data of Figures 5 and 6*

all pressures less than 0.0038 mm and that for higher pressures $\delta\nu = 0.065\sqrt{\frac{p}{0.0038}}$. This relation is consistent with Waibel's width measurements at high pressures. Fortunately corrections are relatively small for the lower pressures, but with increasing pressure the results become increasingly uncertain. Table 5 shows the data for the computation of the quantum efficiency E for one pressure; while Table 6 and Figure 8 summarize results at eight pressures. The correction term for resolved lines based on equation (8) involves the ratio of the integral of the continuous absorption across the slit to the integral of the line absorption across the line and this important part of the correction is independent of the arbitrary assumption as to line width. A mean value of the width $\Delta\nu = 303\ \text{cm}^{-1}$ has been used. The tables include values of E for 3,877 and 3,888 based on the same series

of measurements, but not included in Figures 5 and 6. The value are about twice as great as obtained for 3,888 ionized by the helium line but the difference can be accounted for both in the large error in the absolute value of the latter and in the failure of the above approximations where absorption is high. Figure 8 shows a regular progression of E with the series term and with the pressure that was not apparent in the original data on relative sensitivity. The constant value of E for a setting at 3,200 A for pressures above 0.001 mm is confirmed by the constant relative sensitivity to the 3,188 line of helium and in the latter case there is no question of insufficient resolution masking a change. Other wave lengths except 3,877 and 3,888 seem also to approach a constant but lower efficiency at higher pressures.

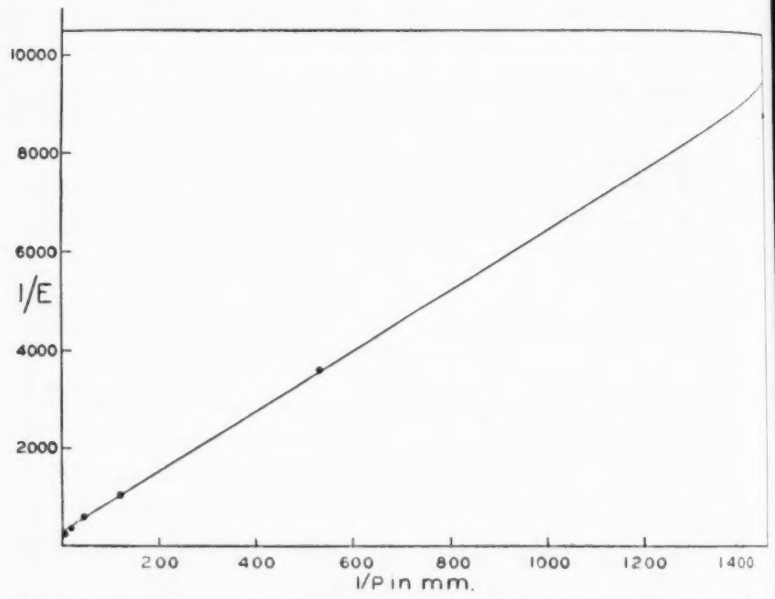

FIGURE 9.—*Plot of reciprocals of quantum efficiency and of pressure for 3,888 from data of Figure 7*

3. THE PRESSURE VARIATION OF EFFICIENCY

Franck's theory of ionization by molecule formation requires that the excited atoms collide during the life of the excited states. The probability P of this will depend on the pressure according to the equation [12]

$$P=\frac{\tau}{T+\tau}=\frac{1}{1+1/A\sigma^2\tau p} \tag{10}$$

where τ is the mean life of the excited state and T is the average time between collisions between excited atoms and normal atoms. $T=1/p\sigma^2A$ where σ is the distance between atom centers at collision, p is the pressure in mm and $A=2.45\times10^{21}$ for cæsium atoms at 500° K.

[12] Turner, Phys. Rev., 23, p. 464; 1924

We will assume that the probability of ionization after a collision, E_c is independent of pressure and see if the relation $E = P\,E_c$ accounts for the pressure variation of E. From equation (10)

$$E = E_c \frac{1}{1 + 1/A\sigma^2\tau p}$$

$$\frac{1}{E} = \frac{1}{E_c}\left(1 + \frac{1}{A\sigma^2\tau p}\right) \tag{11}$$

A plot of the reciprocals of E and p should give a straight line with the intercept on the $1/p$ axis equal to $1/E_c$ and the slope equal to this

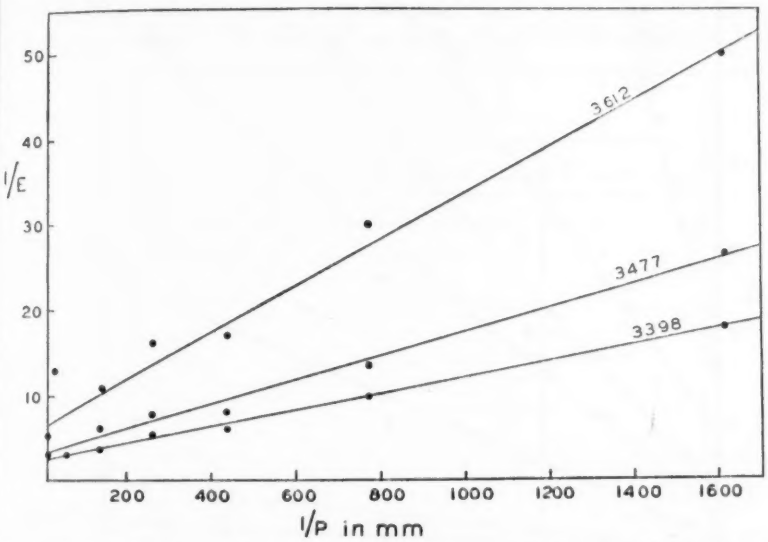

FIGURE 10.—*Reciprocal plots of quantum efficiency and pressure from data of Figure 8*

times $1/A\sigma^2\tau$. Figure 9 shows such a plot for the data on quantum efficiency of ionization by the 3,888 helium line. Here the small deviation near the origin on the reciprocal scale represents a rather large departure from the linear relation at high pressure where experimental error is small. Figures 10 and 11 give reciprocal plots of the quantum efficiency computed from the data on ionization by a continuous spectrum. Here the accidental error is much greater and the straight lines give as close an approximation as could be desired. There are many factors which could give a deviation such as observed in the curve of Figure 9, notably imprisonment of resonance radiation or any other feeding back of energy following the first collision. We conclude that the pressure variation of quantum efficiency is largely accounted for by the variation in the chance of a collision during the life of an excited state and that the probability of ionization at a collision is apparently independent of pressure as well as temperature.

Table 7 gives the numerical values of E_c and $\sigma^2\tau$ computed from the reciprocal plots. Unfortunately there is no safe basis for estimat-

ing either σ^2 or τ independently. The values of the products are surprisingly large. From $\int k d\nu$ one computes a life which measures the average time between absorption and emission of the absorbed line and this is certainly longer than the actual life until any line is emitted. For 3,612 it is 1.2×10^{-5} seconds. There are nine other permitted transmissions from 5 P_2 to mS and mD_{23} and with the crude approximation that all are equally possible the life would be about 10^{-6} seconds. Thus it is seen that the distance of approach for an effective collision with an atom in the 5 P state is probably between

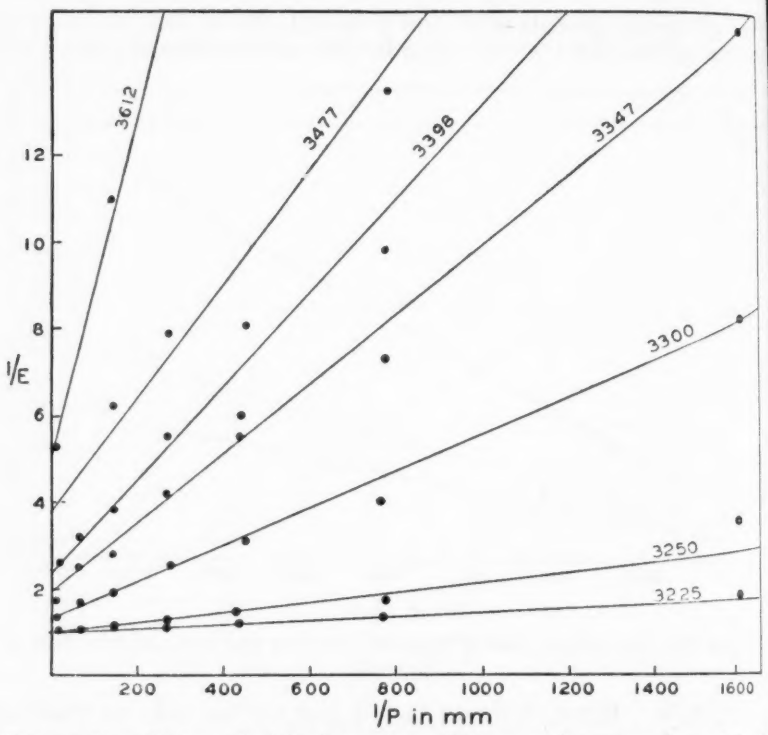

FIGURE 11.—*Reciprocal plots of quantum efficiency and pressure from data of Figure 8*

10^{-7} and 3×10^{-7} cm which is very large even for the greatest possible life. For states 6 P to 10 P the life would progressively increase on the above viewpoint so that σ^2 must decrease to keep the quantity $\sigma^2\tau$ nearly constant. Apparently the large effective radius is not related in a simple manner to the radius of distribution of charge in the mP state which is continuously increasing with m. These details are highly speculative, but the general conclusion as to the magnitude of the product rests directly on the observations of relatively large effects at very low pressure regardless of assumptions as to absorption corrections or the exact nature of the pressure variation of E.

TABLE 7.—*Constants derived from Figures 9, 10, and 11*

m	$1S$–mP	E_e	$\sigma^2\tau$
4	3,888	0.003	0.22×10^{-19}
5	3,612	.154	1.0×10^{-19}
6	3,477	.26	1.1×10^{-19}
7	3,398	.40	1.1×10^{-19}
8	3,347	.50	1.0×10^{-19}
9, 10	3,300	.77	1.2×10^{-19}
12, 13	3,250	.89	3.3×10^{-19}
16	3,225	.93	16×10^{-19}
25	3,200	1.00	48×10^{-19}

4. THE HYPOTHESIS OF MOLECULE ION FORMATION

The results are consistent with Franck's theory that excited atoms when they collide with normal cæsium atoms form molecule ions.

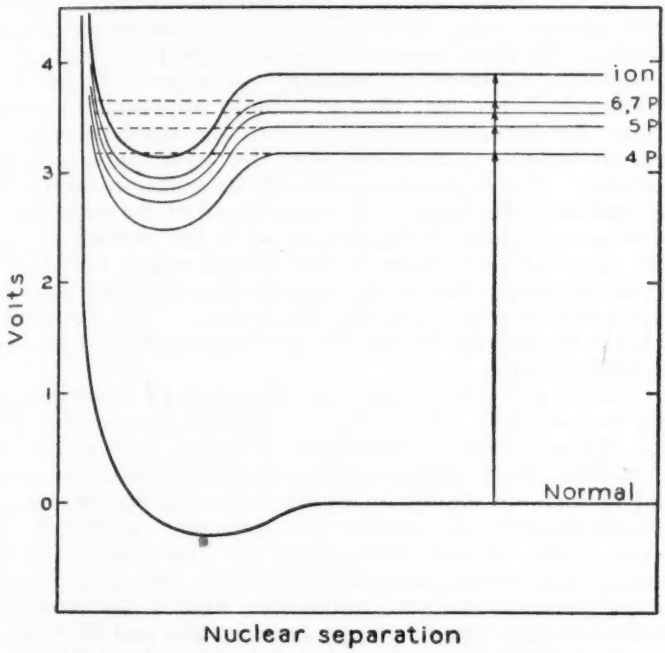

FIGURE 12.—*A Franck Condon diagram of potential energy v. nuclear separation to illustrate the process of molecular ion formation by atomic line absorption*

The ionization potential of the atom is 3.87 volts and the longest wave length which produces ions is 3,888 corresponding to 3.17 volts. We conclude that the potential energy of the molecule ion is at least 0.70 volt less than that of an atom and an atom ion; that is, the work of dissociation of the molecule ion is greater than 0.70 volt. As the probability of ionization by 3,888 is very low, probably this value is close to the threshold and D^+ is nearly 0.7 volt. The energy relations are represented in Figure 12 in the form of a Franck Condon diagram. We have used the convention that the origin of ordinates is the energy of 2 normal atoms; hence, the energy of a normal molecule is

negative. With this convention the ordinates for large values of the atomic separation give the atomic energy levels. The only importa detail is that the minimum for the normal ion is at least as low shown. The process of molecule formation is then, first, the excita tion process raising the atomic energy along a vertical line at th right; second, the collision process is a motion to the left near coincident with one of the horizontal lines (kinetic energy of therm agitation is barely perceptible on this scale); third, the recombinatio process involves a slight dissipation of energy along this horizon path so that the broken line portion of the path is a quantized sta of the excited molecule. Then the atom will oscillate back and fort along this portion of the line until a transition occurs; fourth, th transition will occur either to the ion state or to some lower molecul state.

The chance that it goes to the ion state will depend on the area between the horizontal line and the potential energy curve for the ion in an unknown way, but will clearly increase as we go to highe series terms. We thus have a reason why the probability of ioniza tion at collision, E_c, increases regularly as we go to higher P states The experimental fact that this probability approaches certainty fo high states shows that the probability of the third process—that o combination—is also almost certainty for high states and possibly for all states. The large magnitude of the collision radius can als be visualized from this figure. If we assume that the potential minima have abscissae of about 2 Angstroms, as is the case for a potassium molecule, then the least value of the collision radius would fall at the edge of the drawing; that is, an excited atom reaching any point on the figure would be drawn into the other atom. The potential energy curves must be slightly sloping and not horizontal as drawn over the entire length shown.

The value of 0.7 volt or more for the work of dissociation of the molecule ion indicates that it has a stability comparable with Na_2 and K_2. There is some supporting evidence that alkali molecule ions are stable. Ives [13] gives evidence that the positive ions produced by a hot filament in alkali vapors are molecular aggregates at a low vapor temperature. In cæsium the molecular weight is 1,000 at 0° C., but nearly atomic (133) at 60° C. Ditchburn and Arnot [14] have shown that atomic potassium ions shot through a jet of potassium vapor become diatomic molecules with a probability nearly independent of their kinetic energy between 200 and 20 volts. They find, however, that the ions produced by the photo-electric ionization of potassium by an iron arc are purely atomic.

If in cæsium vapor the continuous absorption gives atomic ions and the line absorption gives molecules, the question arises as to whether the space-charge method gives directly the ratio of ions as we have assumed. In view of the fact that ions take a long time to produce their space-charge effect, it is probable that an equilibrium ratio of molecule and atom ions is reached which is quite independent of their initial state.

---

[13] Ives, J. Frank. Inst., **201**, p. 47; 1926.
[14] Ditchburn and Arnot, Proc. Roy. Soc., **123**, p. 516; 1929.

VI. SUMMARY

The results show that the ionization of cæsium vapor by light on the red side of the limit is the result of line absorption (neglecting a small effect between lines) in lines of a width of the order of 0.01 *A* or less below 0.01 mm pressure.

The subsequent ionization is independent of temperature and electrical conditions but depends on the vapor pressure in a manner which suggests that a collision with a normal cæsium atom must occur during the life of the excited state. The chance of ionization at a collision increases from a very low value for the 4 *P* state to nearly one for 16 *P*. The collision distance depends on the life of the excited state which is unknown, but this distance is certainly large compared with usual atomic dimensions.

WASHINGTON, January 4, 1930.

REGULARITIES IN THE SPECTRA OF LUTECIUM

By William F. Meggers and Bourdon F. Scribner

ABSTRACT

Up to the present time no significant regularities have been found in the spectra of any of the rare earth elements, 58 Ce to 71 Lu. A study of the arc and spark spectra of the last of these, lutecium, resulted in a separation of the lines into three distinct classes: (1) Those characterizing neutral atoms, constituting the Lu_I spectrum; (2) those due to singly ionized atoms, the Lu_{II} spectrum; and (3) a small number of lines ascribable to doubly ionized atoms, the Lu_{III} spectrum. Regularities have been discovered in each of these spectra. The normal state of neutral Lu atoms is represented by a ^2D spectral term arising from the electron configuration s^2d; its levels are separated by 1993.9 wave numbers. The normal state of Lu^+ atoms is described by a ^1S (ss), and metastable terms ^1D, ^3D (ds), ^3F (dd) have also been established. A ^2S (s) term describes the normal state of Lu^{++} atoms. There is no evidence of f electrons playing any part in the production of the spectra; it is concluded that the fourteen f electrons in Lu form a closed shell of considerable stability. The structures of Lu spectra resemble those of Y more closely than those of La or Sc.

CONTENTS

	Page
I. Introduction	73
II. The spectrum of neutral Lu (Lu_I)	75
III. The spectrum of singly ionized Lu (Lu_{II})	77
IV. The spectrum of doubly ionized Lu (Lu_{III})	79
V. Comparison of 21 Sc, 39 Y, 57 La, and 71 Lu spectra	79

I. INTRODUCTION

In 1927 when Hund [1] summarized the results of spectral classifications and developed the theory of their relation to atomic structure, he pointed out that typical spectra have been analysed in nearly all the periods, "Nur an einer Stelle des periodischen Systems klafft eine grosse Lücke. Von den *seltenen Erden* ist noch kein Spektrum in Terme geordnet."

The rare earth elements are found in the sixth period; according to Bohr their appearance is explained by the assumption that the building of the shell of 5*d* electrons beginning with 57 La is not continued with 58 Ce, but the number of 6*s* and 5*d* electrons remains constant from 58 Ce to 71 Lu while *f* electrons are added until a shell of 14 such electrons is completed. If this shell is stable like the rare gas shells 54 Xe, 36 Kr, and 18 A, we may expect the configuration of valence electrons and, consequently, the spectral structures for 71 Lu to resemble those of 57 La, 39 Y, and 21 Sc. In any of these cases the neutral atoms in their normal states involve two *s* and one *d* electron (s^2d), and the corresponding spectral term is ^2D. The configuration

[1] Hund, Linienspektren und Periodisches System der Elemente, p. 175, Julius Springer, Berlin; 1927.

d^2s is expected to yield a metastable ^4F term. Singly ionized atoms of this type will exhibit a singlet S term associated with the *ss* configuration, ^1D and ^3D terms for the *ds* configuration and a group of terms ^1S, ^1D, ^1G, ^3P, ^3F, arising from the *dd* configuration. The normal state of doubly ionized atoms will be represented by a ^2D or ^2S spectral term, according as the electron is bound most firmly in a *d* or in an *s* orbit.

Analyses of the spectra of Sc,[2] Y,[3] and La[4] have revealed all these theoretical terms, and the temptation to look for similar terms in the spectra of Lu could not be resisted. It was first necessary, however, to make new descriptions of the spectra, since the older data were too incomplete and unreliable. The authors have photographed both arc and spark spectra of Lu in the wave length interval 2,000 A to 9,000 A, and have succeeded in separating the Lu_I, Lu_{II}, and Lu_{III} lines characteristic of neutral, singly ionized and doubly ionized atoms respectively. Complete wave-length data and more extensive classification of the spectral lines will be presented in a subsequent paper. The main object of this paper is to describe and interpret certain regularities which have been discovered among the most prominent lines of the Lu spectra. We shall here retain the notation used for similar spectra cited above.

The arc spectrum of Lu was excited in a 220-volt direct-current arc between silver electrodes on which some Lu salt was fused. The same electrodes were then used in a condensed high-voltage discharge to excite the spark spectra. Both spectra were photographed on the same plate, and comparison of line intensities in the two sources made it easy to recognize the lines belonging to neutral and to ionized atoms. The lines of neutral Lu atoms are strongly developed in the arc, but are very weak in the spark. A small number of lines (about 50) occur with considerable intensity in the arc but, for the most part, somewhat enhanced in the spark. These are recognized as the lines involving the normal or metastable states of the singly ionized atoms. A larger number of lines appear only in the spark or greatly enhanced in this source when compared with the arc. These lines are usually somewhat hazy and unsymmetrical. They undoubtedly involve higher excited states in the ionized atoms. Within the range of the observations five lines are recognized as belonging to doubly ionized Lu atoms because they are strong in the spark, but are not excited at all in the 220-volt arc except near the negative electrode. In general, the properties of the Lu spectral lines closely parallel those of Y and La lines which have been studied in similar sources. Perhaps the most striking difference is the relatively greater simplicity of the Lu spectra. The number of strong lines in the Lu_I spectrum does not exceed 50, and, roughly, the same number of intense lines appear in the Lu_{II} spectrum, while in the corresponding Y_{II} and La_{II} spectra the numbers are much larger. The reasons for this difference will be discussed after the Lu regularities are exhibited.

It must be remembered that wave lengths and estimated relative intensities are the only data at hand for the analysis of Lu spectra.

[2] Russell and Meggers, B. S. Sci. Paper No. 558, **22**, p. 329; 1927.
[3] Meggers and Russell, B. S. Jour. Research, **2** (RP 55), p. 733; 1929.
[4] Meggers, J. Wash. Acad. Sci., **17**, p. 25; 1927. J. Opt. Soc. Am., **14**, p. 191; 1927; and extensive unpublished results.

no observations of Zeeman effects, temperature classes, absorption or reversal, and pressure effect have ever been made. The situation is similar to that which existed for Hf spectra,[5] so that the method of analysis which was used there was applied here. It consists, briefly, in systematically subtracting the wave numbers of groups of lines which are likely to be related, extending as far as possible a two-dimensional wave-number system representing combinations of spectral terms, and attempting to interpret the spectral terms on the basis of quantum theory. The combination principle, and the well-known rules governing quantum numbers, line intensities, and spectral-term intervals, make it possible to analyze any spectrum, provided that one has a reasonably good description of the spectrum.

II. THE SPECTRUM OF NEUTRAL Lu (Lu_I)

A half hundred of the most prominent arc lines of Lu were selected and the vacuum wave numbers were systematically subtracted from each other up to differences of 15,000 cm^{-1}. When these were tabulated it was seen that the only difference which occurred more than three times was 1,993.9 cm^{-1} which repeated 10 times, and must, therefore, be regarded as significant. This is regarded as the separation of $^2D_2$ and $^2D_3$, the two sublevels of the ^2D term describing the normal state of neutral Lu atoms. Combinations of this term with higher excited states are presented in Table 1, where the level combinations are represented by vacuum wave numbers, above which the measured wave length in air and estimated intensities are given. Two intensity numbers appear in parentheses after each wave length, the first is the intensity in the arc and the second the intensity in the spark. These numbers show that the lines are a homogeneous group, easily excited in the arc where a large percentage of atoms are neutral, but weak in the spark where most of the atoms are ionized. Guided by relative intensities and by reasonable level separations we have hazarded an identification of many of the excited states, but these term symbols are subject to correction. It is especially difficult to select the single combinations with any certainty, but it may be added that the only strong lines of the Lu_I spectrum not included in Table 1, are the following: 3,647.77 (50, 5), 4,518.58 (200, 40), 5,001.15 (100, 20).

Some of the unidentified levels may represent doublet-quartet intercombinations, but we have not succeeded as yet in completing any quartet multiplets. The metastable ^4F (d^2s) term is expected to be rather high in the energy diagram and its combinations are likely to consist mostly of weaker lines.

[5] Meggers and Scribner, J. Opt. Soc. Am., **17**, p. 83; 1928. B. S. Jour. Research, **4** (RP 139), p. 169; 1930.

TABLE 1.—*Multiplets in the Lu_I spectrum*

		$^2D_2$ 0.0	$^2D_3$ 1993.9
		5, 736. 55 (40, 5)	6, 477. 68 (4, ?)
$^2F_3$?	17, 427. 3	17, 427. 26	15, 433. 37
			6, 004. 53 (100, 10)
$^2F_4$?	18, 643. 4		16, 649. 49
		5, 402. 57 (50, 5)	6, 055. 03 (25, 3)
$^2D'_2$?	18, 504. 6	18, 504. 58	16, 510. 63
		4, 658. 03 (50, 10)	5, 135. 10 (100, 15)
$^2D'_3$?	21, 462. 3	21, 462. 31	19, 468. 41
		4, 498. 85 (8, 1)	4, 942. 34 (20, 3)
$^2P_2$?	22, 221. 6	22, 221. 69	20, 227. 70
		4, 904. 89 (50, 5)	
$^2P_1$?	20, 382. 1	20, 382. 14	
		4, 112. 67 (4, —)	4, 480. 16 (3, —)
	24, 308. 3	24, 308. 27	22, 314. 39
		4, 124. 73 (100, 15)	
$^2P_1$?	24, 237. 2	24, 237. 20	
		3, 567. 84 (80 10)	3, 841. 17 (100, 10)
$^2P_2$?	28, 020. 2	28, 020. 19	26, 026. 38
		3, 376. 51 (40, 8)	3, 620. 31 (3, —)
	29, 607. 9	29, 607. 91	27, 614. 10
		3, 312. 11 (40, 10)	3, 546. 39 (5, 1)
$^2F_3$?	30, 183. 6	30, 183. 58	28, 189. 66
			3, 359. 56 (50, 10)
$^2F_4$?	31, 751. 2		29, 757. 28
		3, 278. 97 (40, 4)	3, 508. 41 (20, 3)
	30, 488. 7	30, 488. 63	28, 494. 82
		3, 171. 36 (20, 4)	3, 385. 51 (25, 3)
	31, 523. 1	31, 523. 12	29, 529. 20
		3, 080. 11 (5, 2)	3, 281. 73 (40, 4)
	32, 456. 9	32, 456. 98	30, 462. 99
		2, 989. 28 (15, 3)	
$^2P_1$?	33, 443. 1	33, 443. 14	
		2, 903. 03 (5, 1)	3, 081. 45 (25, 5)
$^2P_2$?	34, 436. 7	34, 436. 70	32, 442. 86
		2, 728. 94 (8, 2)	2, 886. 02 (2, —)
$^2D'_2$?	36, 633. 5	36, 633. 44	34, 639. 66
		2, 692. 35 (2, —)	2, 845. 13 (10, 2)
$^2D'_3$?	37, 131. 3	37, 131. 27	35, 131. 47

III. THE SPECTRUM OF SINGLY IONIZED Lu (Lu II)

After selecting about 50 of the more intense spark lines (also strong in the arc) the corresponding vacuum wave numbers were systematically substracted, and three recurring differences (639.1, 1,763.8, 3,133.5) were at once recognized. These formed the nucleus of a wave-number system which was finally extended to that shown in Table 2. The structure of this table is similar to that of Table 1. The spectral term combinations are represented by vacuum wave numbers appearing directly below the observed wave lengths in air. The wave lengths are followed by arc and spark intensities in parentheses. Lines marked *d* are double or complex with hyperfine structure, and a few marked *l* are shaded to longer wave lengths. The latter involve rather high levels and begin to partake of the general character of lines which are more difficult to excite. The easily excited lines, such as a^3D–a^3P, appear with about equal intensity in arc and spark, but, in general, the other lines show increasing enhancement in the latter source as the values of the energy levels increase. Assuming that the three lines, 2,195.55, 2,615.43, and 3,507.39, arise from combinations of a $^1S_0$ term with levels having inner quantum number $j=1$, the inner quantum numbers of the remaining levels are determined from their combinations, and the levels are then grouped into terms. The combinations, intensities, and intervals have made it possible to identify all of the levels, and there can hardly be any question as to the correctness of the interpretation. Table 2 contains a homogeneous group of lines and practically all of the lines of this character. All of the expected terms of low energy content have been established except b^1S, b^1D, a^1G, and a^3P', which are probably so high in the energy diagram that their principal combinations lie far out in the infra-red.

TABLE 2.—*Multiplets in the Lu_{II} spectrum*

		a^1S_0 0.0	a^3D_1 11796.1	a^3D_2 12435.2	a^3D_3 14199.0	a^1D_2 17332.5	$a^1F'_3$ 29406.7	$a^3F'_3$ 30889.1	$a^3F'_4$ 32503.7
a^3P_0	27, 264. 3		6, 463. 11 (200, 200)						
		3, 507. 39 (100, 100)	15, 468. 16	6, 221. 88 (200, 200)					
a^3P_1	28, 503. 1	28, 503. 11	5, 983. 90 (100, 100 d)	16, 067. 88					
			16, 706. 89	4, 994. 14 (120, 120)	5, 476. 69 (200, 200)	6, 611. 61 (10, 10 d)			
a^3P_2	32, 453. 1		4, 839. 62 (30, 30 d)	20, 017. 90	18, 254. 14	15, 120. 74			
		2, 615. 43 (60, 250)	20, 657. 04						
				3, 876. 65 (100, 100)		4, 785. 42 (50, 60)			
a^1P_1	38, 223. 2	38, 223. 23		25, 788. 19		20, 890. 98			
			3, 397. 07 (50, 150)	3, 472. 48 (40, 120)		4, 184. 26 (100, 120)	8, 459. 2 (3, 7)		
a^3F_2	41, 224. 8		29, 428. 72	28, 789. 65		23, 892. 38	11, 818. 2		
				3, 077. 59 (50, 150)	3, 254. 32 (25, 90)	3, 523. 95 (20, 40)	6, 444. 87 (2, 3)	7, 125. 9 (6, 10 l)	
a^3F_3	44, 918. 7			32, 483. 55	30, 719. 56	27, 586. 14	15, 511. 94	14, 029. 5	
			2, 969. 81 (20, 40)	3, 027. 28 (4, 5)	3, 198. 12 (20, 50)	3, 554. 43 (90, 200)	6, 228. 14 (3, 4)		
$a^1D'_2$	45, 458. 4		33, 662. 39	33, 023. 37	31, 259. 37	28, 125. 90	16, 051. 73		
		2, 195. 55 (15, 30)	2, 963. 32 (30, 100)	3, 020. 53 (20, 50)			6, 199. 64 (6, 20 l)		
$a^3D'_1$	45, 532. 4	45, 532. 40	33, 736. 11	33, 097. 16			16, 125. 52		
			2, 847. 50 (25, 60)	2, 900. 30 (25, 100)	3, 056. 71 (25, 40)		5, 713. 45 (2, 3)	6, 242. 34 (10, 40l)	
$a^3D'_2$	46, 904. 3		35, 108. 23	34, 469. 12	32, 705. 43		17, 497. 63	16, 015. 21	
					2, 911. 39 (50, 200)			5, 664. 88 (1, 3)	6, 235. 36 (5, 20 l)
a^3F_4	48, 536. 8				34, 337. 82			17, 647. 74	16, 633. 14
				2, 754. 16 (25, 60)	2, 894. 84 (30, 150)	3, 183. 71 (3, 5)		5, 602. 55 (1, 2)	6, 159. 03 (8, 60 l)
$a^3D'_3$	48, 733. 2			36, 298. 00	34, 534. 13	31, 400. 84		17, 844. 07	16, 229. 47
			2, 619. 26 (20, 40)						
b^3P_0	49, 963. 4		38, 167. 54			3, 055. 71 (1, 2)	4, 843. 02 (2, 2)		
			2, 613. 40 (10, 30)	2, 657. 81 (25, 60)		32, 716. 83	20, 642. 52		
b^3P_1	50, 049. 0		38, 282. 92	37, 613. 78		2, 951. 68 (10, 50)	4, 586. 92 (2, 2)	4, 921. 69 (3, 5)	
			2, 526. 95 (5, 20)	2, 578. 79 (20, 80)	2, 701. 71 (30, 120)	33, 869. 14	21, 795. 03	20, 312. 57	
b^3P_2	51, 201. 6		39, 405. 58	38, 766. 28	37, 002. 64				
									4, 858. 77 (3, 4)
				2, 459. 65 (—, 6)	2, 571. 23 (10, 60)	2, 796. 62 (20, 80)	4, 223. 08 (1, ?)	4, 505. 20 (2, 2)	20, 575. 61
a^1F_3	53, 079. 3			40, 643. 89	38, 880. 25	35, 746. 93	23, 672. 76	22, 190. 37	

IV. THE SPECTRUM OF DOUBLY IONIZED Lu (Lu_{III})

Within the range of our observations five lines undoubtedly belonging to Lu^{++} atoms have been recorded. These lines are grouped in multiplets in Table 3, where an interpretation of the combining levels is given. The letter *e* after an arc intensity signifies that the line appeared only at the negative electrode. Two of the lines clearly show evidence of being afflicted with hyperfine structure.

TABLE 3.—*Multiplets in the Lu_{III} spectrum*

	$^2S_1$ 0.0	$^2D_2$ 6304.3	$^2D_3$ 8648.1
$^2P_1$	2,563.53(1*e*, 50)	3,057.90(3*e*, 100)	
3,8997.0	38,997.0	32,692.7	
$^2P_2$	2,236.19(3*ed*, 100)	2,603.34(5*ed*, 200)	2,772.58(4*e*, 125)
4,4705.0	44,705.0	38,400.7	36,056.9

The arrangement and interpretation of these Lu_{III} regularities may, perhaps, be questioned because of the abnormally large intensity of of 2,603.34 A ($^2D_2$–$^2P_2$), but the only other possibility is to interchange $^2S_1$ and $^2D_2$ which would make the separation of ^2D abnormally large. We hope to be able, ultimately, to confirm these terms with other combinations and more definitive intensities.

V. COMPARISON OF 21 Sc, 39 Y, 57 La AND 71 Lu SPECTRA

The lowest energy (normal state) in any atom with 3-valence electrons s^2d is represented by a ^2D spectral term and such a term has been found in every case. These terms for Sc_I, Y_I, La_I, and Lu_I spectra are collected in Table 4. A more or less regular increase in the separation of the ^2D levels accompanies the atomic number.

TABLE 4.—*Comparison of (s^2d) ^2D terms in Sc_I, Y_I, La_I, and Lu_I spectra*

Levels	Sc_I	Y_I	La_I	Lu_I
$^2D_2$	0. 0	0. 0	0. 0	0. 0
$^2D_3$	168. 3	530. 5	1, 053. 2	1, 993. 9

In order to compare the analogous first spark spectra of these four elements the relative terms for *ss*, *dd*, and *ds* electron configurations are collected in Table 5. There is a close resemblance between Y_{II} and Lu_{II} in the relative positions of the various terms, except that the separations in the latter case are much larger and the $^3F'$ term has reached a considerable altitude in the energy diagram. If this parallelism can be extended to the undiscovered terms ^1D, ^1G, and $^3P'$ they will be much higher and difficult to establish.

In the La_{II} spectrum the following additional middle terms have been found: (*sf*) ^1F, ^3F, (*df*) ^1P, $^1D'$, ^1F, $^1G'$, ^1H, ^3P, $^3D'$, ^3F, $^3G'$, ^3H. No evidence of these terms has been found in any of the other spectra;

their presence in La accounts for the relatively greater complexity of the La_{II} spectrum. 57 La is the last element just preceding the rare earths, 58 Ce–71 Lu, in which *f*-type electrons are added, and it appears that this feature of atom building is anticipated in La^+ so that in the excited state either a *d* or an *s* electron may occupy *f*-type orbits. The fact that *sf* and *df* terms do not appear in the Lu_{II} spectrum is evidence that the completed group of fourteen *f* electrons is a closed shell of considerable stability resembling the rare gas shells.

TABLE 5.—*Comparison of* (*ss*), (*dd*), *and* (*ds*) *terms in* Sc_{II}, Y_{II}, La_{II}, *and* Lu_{II} *spectra*

Electrons	Levels	Sc_{II}	Y_{II}	La_{II}	Lu_{II}
ss	$^1S_0$	11, 736. 4	0. 0	7, 394. 6	0. 0
dd	$^1D_2$	10, 944. 5	14, 832. 9	10, 094. 9	
	$^1G_4$	14, 261. 4	15, 683. 0	7, 473. 4	
	$^3P'_0$	12, 074. 0	13, 883. 5	5, 249. 8	
	$^3P'_1$	12, 101. 4	14, 018. 3	5, 718. 2	
	$^3P'_2$	12, 154. 3	14, 098. 2	6, 227. 5	
	$^3F'_2$	4, 802. 8	8, 003. 1	0. 0	29, 406. 7
	$^3F'_3$	4, 883. 4	8, 328. 0	1, 016. 0	30, 889. 1
	$^3F'_4$	4, 987. 6	8, 743. 4	1, 970. 8	32, 503. 7
ds	$^1D_2$	2, 541. 0	3, 296. 3	1, 394. 5	17, 332. 5
	$^3D_1$	0. 0	840. 2	1, 895. 1	11, 796. 1
	$^3D_2$	67. 7	1, 045. 1	2, 591. 6	12, 435. 2
	$^3D_3$	177. 6	1, 449. 9	3, 250. 4	14, 199. 0

Terms of the analogous second spark spectra of these four elements are collected for comparison in Table 6.

TABLE 6.—*Comparison of d, s, and p terms in* Sc_{III}, Y_{III}, La_{III}, *and* Lu_{III} *spectra*

Electron	Levels	Sc_{III}	Y_{III}	La_{III}	Lu_{III}
d	$^2D_2$	0	0. 0	0. 0	6, 304. 3
	$^2D_3$	198	724. 8	1, 603. 2	8, 648. 1
s	$^2S_1$	25, 537	7, 466. 2	13, 590. 8	0. 0
p	$^2P_1$	62, 102	41, 401. 2	42, 014. 9	38, 997. 0
	$^2P_2$	62, 576	42, 954. 7	45, 110. 6	44, 705. 0

If our interpretation of the Lu_{III} lines is correct it supports other evidence that in the period of 5*d* and 6*s* electrons the latter become more stable than the former. Attention is called to the fact that the (*ss*) ^1S terms of the first spark spectra (Table 5) show a trend very much like that of the (*s*) ^2S terms of the second spark spectra, being highest for Sc, considerably lower for La, and lowest for Y and Lu. The relatively small advantage of ^2S over ^2D in the Lu_{III} spectrum appears to account for the decided advantage of ^1S over ^3D as the lowest term in the Lu_{II} spectrum.

Finally, it will be of interest to compare the total intervals of related D terms of three successive spectra for each of the four elements discussed above. These are presented in Table 7.

TABLE 7.—*Total separation of lowest D levels in successive spectra of Sc, Y, La, and Lu*

Spectrum	Level separation	Sc	Y	La	Lu
I	$^2D_2$–$^2D_3$	168. 3	530. 5	1, 053. 2	1, 993. 9
II	$^2D_1$–$^2D_3$	177. 6	609. 7	1, 355. 3	2, 402. 9
III	$^2D_2$–$^2D_3$	198. 0	724. 8	1, 603. 2	2, 343. 8

The three successive D terms for each element are intimately connected according to the theory of series convergence to limits, and the total separations should be the same (to a first approximation) for the successive spectra of each element. The reality of this connection is obvious from the data in Table 7, and this may be regarded as a general verification of the term identifications and analyses of the Sc, Y, La, and Lu spectra.

WASHINGTON, March 7, 1930.

A NEW CONSISTOMETER AND ITS APPLICATION TO GREASES AND TO OILS AT LOW TEMPERATURES [1]

By Ronald Bulkley and F. G. Bitner

ABSTRACT

A consistometer is described which is suitable for determining the consistency of viscous and plastic materials in general, but which is more particularly advantageous in obtaining flow-pressure diagrams for materials which change rapidly in consistency with time or which show a breakdown of structure with mechanical working. The limitations of some commonly used instruments are discussed, and the sources of error in the present instrument are pointed out. Flow-pressure graphs of a cup grease at different temperatures and of various plastic oils at 0° C. are shown.

The importance and the significance of the unworked consistency of the undisturbed material and of the thoroughly worked consistency of the completely broken down material are discussed. The method of measuring these properties of the material with the new instrument are described in detail.

CONTENTS

	Page.
I. Introduction	83
II. Description of the instrument	84
III. Manner of operation	85
IV. Calibration of capillaries	86
V. Some advantages of the instrument and some sources of error	89
VI. Flow-pressure graphs of plastic lubricants	91
VII. Conclusions	96

I. INTRODUCTION

The consistometer to be described here is rugged, simple of construction, speedy in operation, and can be employed for either opaque or clear materials of a wide range of consistencies. It also possesses two features which are unusual in a consistometer, but which are of great importance in the testing of all such plastic materials as show a breakdown of structure with working, or which change in consistency with time.

The first of these features is that the test material may be passed successively back and forth through the capillary any number of times.[2] The second is that determinations of the rate of flow are made by passing only a very small volume of material through the capillary, thus minimizing the breakdown effect of the working which is incident to the measurement itself.

With the aid of these two features the unworked, as well as the thoroughly worked, consistency of the material may be closely approximated. With such forms of instrument as permit of flow in one direction only, and for which a large amount of material must be passed through the capillary for a single datum point, neither the unworked

[1] This paper was presented at the meeting of the Society of Rheology held at Washington, D. C., Dec. 19 and 20, 1929.

[2] Another consistometer embodying this feature has recently been described by Scott Blair, The Flow of Clay Pastes Through Narrow Tubes, J. Phys. Chem., 33, pp. 321-330; 1929. This paper first came to our attention about a year after our own instrument had been put into use.

nor the worked consistency is obtained, but only an intermedia consistency on partially worked and constantly changing materia The first of the two special features also makes it possible to obta flow-pressure graphs at a number of temperatures with a single fillin of the instrument, or without removing the instrument from th bath. There are no weighings to be performed and no auxiliar apparatus is required, such as pressure tanks, pressure regulators, etc

II. DESCRIPTION OF THE INSTRUMENT

The complete apparatus dismounted for photographing, togethe with all auxiliary appliances and two extra capillaries, is shown i Figure 1. Figure 2 is a schematic representation of the instrumen in operation.

Referring to Figure 2, the device shown on the right is a mercur leveling bulb equipped with two stopcocks and with a side arm o

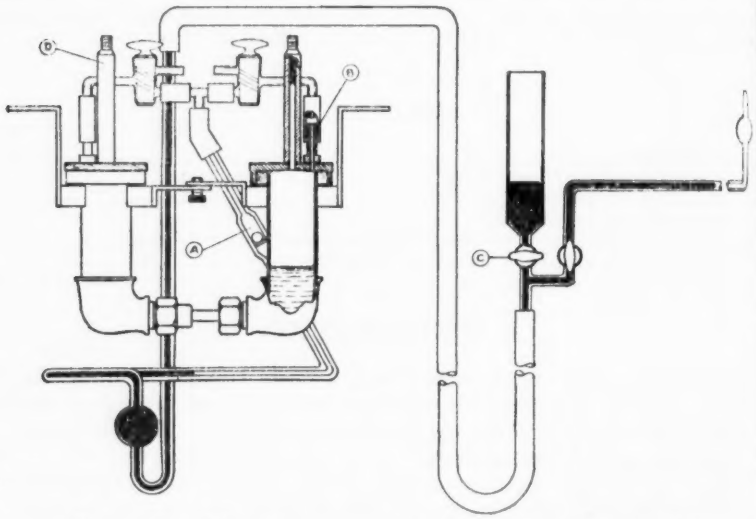

FIGURE 2.—*Schematic representation of instrument in operation*

small-bore glass tubing. Since the movement of the mercury surface in this tubing shows the volume of flow of the test material, the volume of mercury per unit length of the tube must be determined. If clean mercury is employed and if the pressure tubing of the system is of high-grade sulphur-free rubber, the bore of the glass side arm may safely be as great as 2.5 mm, without causing the mercury surface to assume an irregular form. This part of the apparatus is mounted on a clamp stand outside the bath. The side arm must be accurately horizontal.

The ball float valve *A* serves to prevent the passage of mercury into the consistometer in case of a sudden leak in the apparatus. It is joined to a second horizontal tube and then to a gooseneck with a safety bulb, and is connected by pressure tubing to the leveling device outside the bath. Merely to conserve space, it is bent at an angle to the horizontal tube below it. When this tube has been leveled,

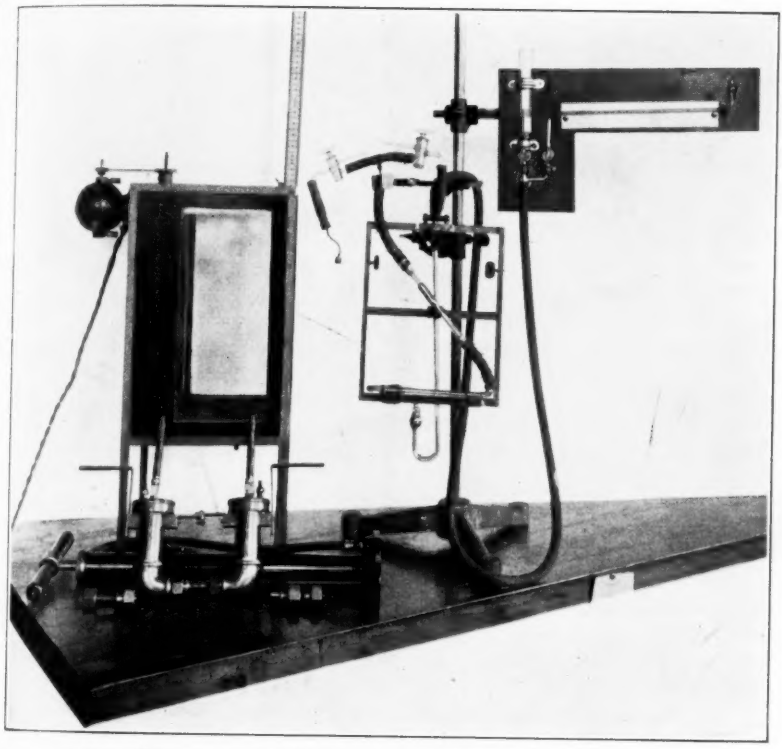

FIGURE 1.—*Bulkley consistometer and accessories*

the frame on which the piece is mounted is clamped rigidly in position in the bath once for all. The head of mercury effective in producing flow is the vertical distance between the two horizontal tubes, and is measured on a millimeter scale attached to the bath.

The consistometer proper is made entirely of metal. It consists essentially of two similarly constructed reservoirs to contain the test material, joined at the bottom by the capillary through which the flow is to be measured, and fitted with screw covers having suitable outlets for pressure connections. The instrument is hung in the bath by side arms of brass straps. Similar straps connect the two containers at the top. The capacity of each container need not be greater than 25 cm^3.

The capillaries are interchangeable. They are equipped on one end with a rigidly attached hexagonal nut and on the other with a collar and gland nut, which permits ready dismounting and reassembling of the instrument.

Each cover has two openings. The one centrally placed is closed by an ordinary automobile tire valve, while the other is joined through a 3-way stopcock to the mercury float valve.

III. MANNER OF OPERATION

Sufficient mercury is poured into the leveling bulb to fill the pressure system from some point on the lower horizontal tube to a corresponding point on the upper tube, as shown in Figure 2. At higher pressures slightly more mercury will be required than at low pressures, on account of the expansion of the rubber tubing. This adjustment of the mercury volume is very easily and quickly made through the leveling bulb in either direction as desired. Most of the mercury remains permanently in the pressure system for several months or until fouled.

To prevent blowing air through the capillary and to reduce the total volume of air in the apparatus, slightly more of the test material should be put into the consistometer than the amount required to fill one container. Suppose the left-hand container to be more than half full and the right one to be less than half full of the material to be tested. The covers are fitted tightly, the instrument is suspended in the bath and connected to the pressure system through the flexible joints *B*. When all is in readiness for a run, both cocks of the leveling device being open, the 3-way cocks above the float valve *A* are turned into such position as to connect both containers of the instrument with *A*. The leveling device is raised sufficiently to give a head of mercury equivalent to the highest pressure desired in the run. By a tire pump, pressure is now applied through either of the tire valves *D*. There will be no appreciable flow of the test material during this procedure, since the air pressure will be equal in both containers, but the mercury in *A* will be forced out and up into the leveling device. When the pressure is just great enough to keep the mercury surfaces in the two horizontal tubes, stopcock *C* is closed. Flow of the test material through the capillary is started by relieving the pressure in the right-hand container of the instrument by connecting this container to the atmosphere through its 3-way stopcock. The test material flows through the capillary of the consistometer from left to right. As flow proceeds the mercury surface in the lower hori-

zontal tube of the pressure system moves to the right, that in the upper tube to the left. Conditions at this instant are depicted in Figure 2.

Since the two horizontal tubes are approximately 2.5 mm in diameter, no correction for the surface tension of the mercury is required. The slight pressure resulting from the difference of level of the test material in the two containers may be neglected except in the work of calibration and in such instances as demand the highest accuracy.

The volume of flow of test material is equal to the volume of mercury displaced after the run has commenced. The rate of flow is therefore calculated by timing the motion of the upper mercury surface along a scale mounted behind the side arm. The volume of flow for one point on the flow-pressure graph need not be greater than 0.5 cm^3 to procure ample accuracy of measurement. After the time reading has been taken the run is allowed to proceed while the head is being measured and while the data are being recorded. To obtain a reading at a second pressure, it is not necessary to use the pump again or to disturb the setting of the stopcock. The leveling bulb is simply lowered to such a position that the mercury surfaces are again in the proper portions of the horizontal tubes, when the frame is again clamped into position and the rate of flow again timed.

By the above procedure data for a great many points are obtained very speedily. If the air pressure in the system is partially relieved between runs by manipulating one of the 3-way stopcocks, greater decrements of pressure result. This method of operation is, perhaps, preferable to the first, since a much greater range of pressures may be covered in a given length of time.

Data for the first flow-pressure relation having been obtained, those for any number of others at the same temperature or at other temperatures may be obtained by forcing the material back and forth through the capillary, taking readings as the material flows in either direction.

If the material is a simple viscous liquid or if no concern is felt as to a possible breakdown in structure with working, the time required to establish thermal equilibrium before commencing the first run may be greatly lessened by forcing the material through the capillary with the pump. During this procedure the float valve and leveling bulb are cut out by the appropriate stopcock to permit the use of higher pressures. As the material passes through the capillary it is exposed to its environment in a thin stream, and in only one or two passages it has all acquired the proper test temperature.

IV. CALIBRATION OF CAPILLARIES

A method which is frequently employed for the calibration of the diameter of large capillary tubes, such as are ordinarily used for plastic materials, is the direct microscopic examination of the ends of the tube. This method, however, involves the somewhat doubtful assumption that the mean of the observed diameters of the two ends is the true effective diameter under conditions of flow.

A more reliable method [3] consists in calculating the true effective diameter from the results of flow tests with liquids of known viscosity.

[3] Herschel and Bulkley, Calibration of the Buret Consistometer. Ind. & Eng. Chem., **10**, pp. 134–139; 1927.

This procedure seems particularly commendable in the present instance, where it is desired to check not only the diameter of the capillary but also the general performance of the apparatus as a whole.

Figures 3 and 4 show flow-pressure graphs for two capillaries for mineral oils whose viscosity at the different temperatures had been determined on a Bingham viscometer. The general accuracy of the data may be inferred from the manner in which the points fall upon a straight line passing through the origin. From the slope of each

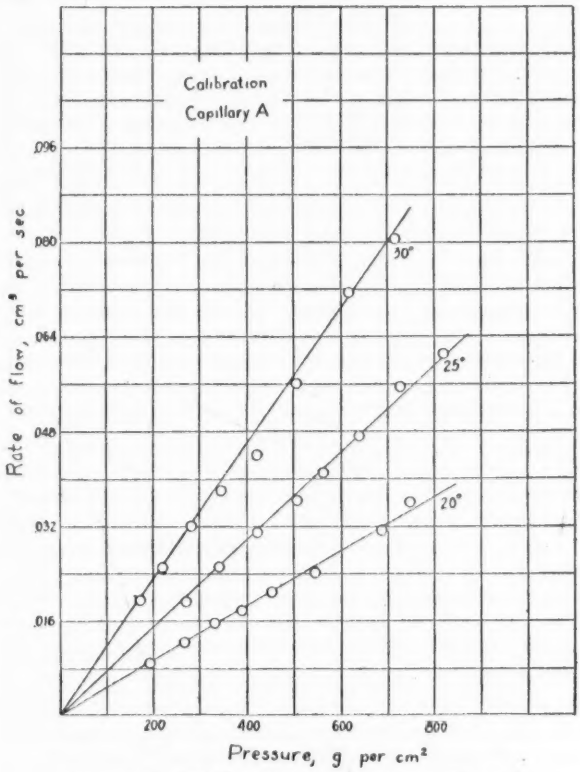

FIGURE 3.—*Calibration graphs for capillary A*

graph the diameter of the capillary may be calculated and compared with the diameter as measured directly. Since the kinetic energy correction is negligible here, we write from the ordinary equation for viscous flow

$$d^4/l = \frac{128\mu}{\pi g}\left(\frac{q}{p}\right)$$

where

μ = viscosity in poises.
d = diameter of capillary, cm.
l = length of capillary, cm.
g = acceleration of gravity, cm/sec.^{2}.
q = rate of flow, cm^3 per sec.
p = pressure difference producing flow, g per cm^2.

The quotient, q/p, is obtained directly from the diagram as the slope of the flow-pressure graph.

The agreement between values of d^4/l as calculated from different graphs for the same capillary is an index of the dependability of the apparatus and general procedure. The following table shows the agreement which is obtained between values of this quotient as calculated from flow tests and from direct measurement. The values calculated from the graphs are considered the more reliable and have been used in later work. All of the data for the three graphs of Figure

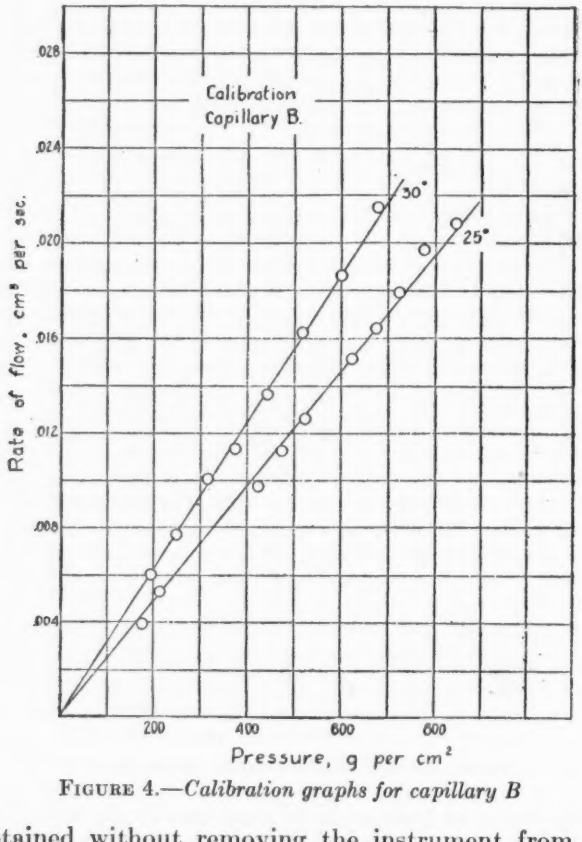

FIGURE 4.—*Calibration graphs for capillary B*

3 were obtained without removing the instrument from the bath. The same is true for the two graphs of Figure 4.

	Capillary A			Capillary B	
	20° C.	25° C.	30° C.	25° C.	30° C.
Viscosity of oil poises	49.7	30.7	19.5	0.560	0.429
$q/p \times 10^5$	4.61	7.41	11.4	2.44	3.12
$d^4/l \times 10^7$, calculated	952	945	924	5.68	5.56
Average $d^4/l \times 10^7$, calculated		940.4		5.620	
Measured length, centimeters		7.54		7.39	
Measured diameter, centimeters		.163		.0445	
$d^4/l \times 10^7$ from measured diameter and length		936		5.31	

V. SOME ADVANTAGES OF THE INSTRUMENT AND SOME SOURCES OF ERROR

Of the various devices commonly employed for determining the consistency of a plastic material, the capillary-tube type of instrument has been more thoroughly investigated than any other, both experimentally and from a theoretical point of view. Many forms of this type of instrument are in use, but practically all of them are suitable only for such materials as show no change of consistency either with time or with mechanical working.

F. L. Browne and Don Brouse [4] have emphasized the importance of the change of casein glue with time, and have shown the limitations of the Herschel consistometer for this kind of material. The same disadvantages are inherent in the Bingham and Green plastometer, of which the Herschel instrument is a modification. In a later paper Brouse [5] has also mentioned the necessity for testing over a wide range of temperatures. For the above instruments a period of two hours in the bath is required after each change of temperature for the material to acquire the temperature of test. Casein glue is only one example of a great variety of substances which show a more or less rapid change of consistency with time, and flow-pressure graphs of other plastic materials are frequently desired at several temperatures. While the ideal instrument "with which measurements of flow under several different pressures can be made simultaneously" is not realized in the present case, the consistometer used by the present authors, nevertheless, does permit the worked material to be brought in a few minutes to the test temperature, and data for five or six points on a flow-pressure graph can then be obtained in approximately the same time as required for a single point by the instrument Browne and Brouse employed.

Theoretically, an instrument equipped with a flow meter, after the manner of Henry Green,[6] gives an instantaneous reading of the rate of flow. Practically, however, this offers very little saving of time in procuring data because of the relatively large amount of time which must still be used in taking readings, adjusting the pressure, etc. The calibration of a flow meter of the Green type is laborious, and a separate thermostat for the flow meter is desirable, if not utterly essential, where tests are to be conducted at more than one temperature. The calibration of the horizontal measuring tube of the present instrument is exceedingly simple, and the readings of rate of flow are obtained in a short enough time to make the instrument satisfactory for the testing of rapidly changing materials as well as materials which break down in structure with working.

P. M. Giessey and S. Arzoomanian [7] have described a modification of the simple buret consistometer whereby the principle of the latter instrument may be applied to stiff substances, such as greases and dental pastes. The material used by these investigators possessed "some structure," and on making a check run on material which remained in the instrument from a previous determination they found an increase of 50 per cent in the mobility. This very considerable

[4] The Consistency of Casein Glue, Colloid Symposium Monograph, **5**, pp. 229–242; 1928.
[5] Consistency of Animal Glue, Ind. & Eng. Chem., **21**, pp. 242–247; 1929.
[6] Further development of the Plastometer and Its Practical Application to Research and Routine Problems, Proc. Am. Soc. Test. Mats., **20**, pt. 2, pp. 451–494; 1920.
[7] A New Rapid Extrusion Plastometer, Colloid Symposium Monograph, **5**, pp. 253–258; 1928.

change in consistency had evidently been produced by mechanical working of the material in the container of the instrument while the first run was proceeding. Presumably a much greater breakdown of structure would have been noted had the material been tested again after its passage through the capillary, where the shearing is much more severe than in the container. The indications are therefore that the first run, certainly, and the check run, perhaps, were both made on material which was constantly changing. In this event neither run truly represents the consistency either of the unworked or the thoroughly worked material.

This instance is cited not as a criticism of a particular investigation, but merely as an example of the practice, which has been more or less common in the past, of submitting a material possessing structure to a single passage through the capillary. The results of such a procedure are usually of little practical value, since, in general, either the unworked or the thoroughly worked consistency is desired. Thus when starting an engine in cold weather, if the oil is congealed in the feed lines and bearings, its unworked consistency is of paramount importance. After a few minutes' running, however, the structure of the oil is completely broken down and the worked consistency is desired. The consistency in an intermediate condition is of little significance.

For many materials this breakdown of structure is, of course, well recognized, and in the case of greases the American Society for Testing Materials [8] has tentatively specified a definite procedure for working the material before test. The structure may be present in many other materials, however, where its existence would remain unsuspected unless tested for directly. It is known to develop in certain paint pastes,[9] and in enamel slips containing a small percentage of clay, if these materials are allowed to stand undisturbed for some time after working. As will be shown later, oils which have become plastic at a low temperature also manifest this behavior. The same phenomenon has been observed in the case of many other colloidal systems by Freundlich [10] and has been called by him thixotropy.

Strictly speaking, the experimental determination of the unworked consistency of a plastic material is an impossibility. It is conceivable that some method of testing could be devised whereby the unworked consistency could be approximated through a backward extrapolation. A more practical expedient, and one which gives a sufficiently accurate approximation for many purposes, is to make several observations of the rate of flow over a range of pressures by the passage of only a small amount of material through the capillary. As shown by Giesy and Arzoomanian, and as will be shown here later, the breakdown of structure in the container is often so great that when several grams of material are passed for a single datum point even an approximation of the unworked consistency is impossible.

If a material increases in stiffness only slowly after working, its thoroughly worked consistency may be determined at room tem-

[8] Tentative Method of Test for Penetration of Greases, Proc. Am. Soc. Test. Mats., **26**, pt. 1, pp. 834–839; 1926.

[9] H. L. Beakes, Settling of Pigments in House Paints, Ind. & Eng. Chem., **21**, pp. 1118–1121; 1929.

[10] H. Freundlich and L. L. Bircumshau, Thixotropic Behavior of Aluminum Hydroxide Gels, Kolloid Z., **40**, pp. 19–22; 1926.

perature on practically any of the instruments commonly employed. When the plastic properties exist largely as a result of cooling, however, as in the case of a frozen oil or gelatin, the broken-down consistency in the cooled condition can be measured only with an instrument in which the material is maintained at the test temperature continuously while being worked and tested. The effects of any working received by a plastic oil at 0° C., for instance, are completely destroyed by exposing the oil to the temperature of the room while weighing the oil and returning it to the consistometer, as must be done in the Bingham instrument and its various modifications.

The instrument herein described is well adapted for the purpose of determining the consistency of plastic materials in general, and more particularly for the special materials considered in this section. It is also suitable for the determination of the viscosity of true liquids which are too opaque or too viscous to be handled readily in viscometers of the Ostwald or the Bingham type. At the present time there is a great dearth of instruments with which viscosities higher than 30 or 40 poises can be measured to an accuracy of 5 per cent without an excessive consumption of time. With the present instrument the rapid measurement of viscosities of several thousands of poises to an accuracy of ± 2 per cent is entirely feasible.

The chief source of error in the instrument is the change of volume which is brought about in the air in the system by a change either of temperature or of pressure. Since the volume of flow which is measured is small, a given percentage change in the volume of air during a test produces a relatively large percentage error in the observed rate of flow.

As a numerical example, if the total volume of the air in the apparatus is 20 cm^3 and if the head of mercury producing flow is 24 cm, then for a volume of flow of 1 cm^3 a change of pressure of 1 mm of mercury will result in a 2 per cent error in the observed rate of flow if the change takes place during the timed interval. Similarly, a change of temperature of 0.1° C. during a timed interval produces an error of about 0.8 per cent in the observed rate of flow. This emphasizes the necessity for using great care in leveling the horizontal tubes and in accurately controlling the temperature of the bath. It also indicates the desirability of having the volume of air in the system as small as practicable.

VI. FLOW-PRESSURE GRAPHS OF PLASTIC LUBRICANTS

The data for the graphs shown in this section were taken on an earlier form of the instrument in which a safety reservoir was employed in place of the float valve. The degree of accuracy of the data is therefore not as high as that obtained in the calibration of the capillaries.[11] In most cases the graphs are straight lines throughout the greater portion of their length, and the method of treatment proposed by Bingham [12] is apparently the most satisfactory for obtaining numerical constants for the consistency of the material. However, since the present purpose is merely to illustrate the utility of the instrument in procuring consistency data, discussion of the significance of these constants in lubrication practice, not only for

[11] We are indebted to E. F. Mueller, of the Bureau of Standards, for the suggestion to substitute a float valve for the safety reservoir.
[12] Fluidity and Plasticity, McGraw Hill; 1922.

greases but for oils at low temperatures as well will be reserved for subsequent publication.

Figure 5 is an example of the use of the instrument in obtaining flow-pressure diagrams on cup greases. The grease used here was of medium grade, showing a penetration of 241 at 77° F. on the standard A. S. T. M. penetrometer.[13] All of the data shown on Figure 5 were obtained without removing the instrument from the bath.

Before filling the consistometer to obtain the data of Figure 5 the grease was broken down in an A. S. T. M. grease worker to a constant

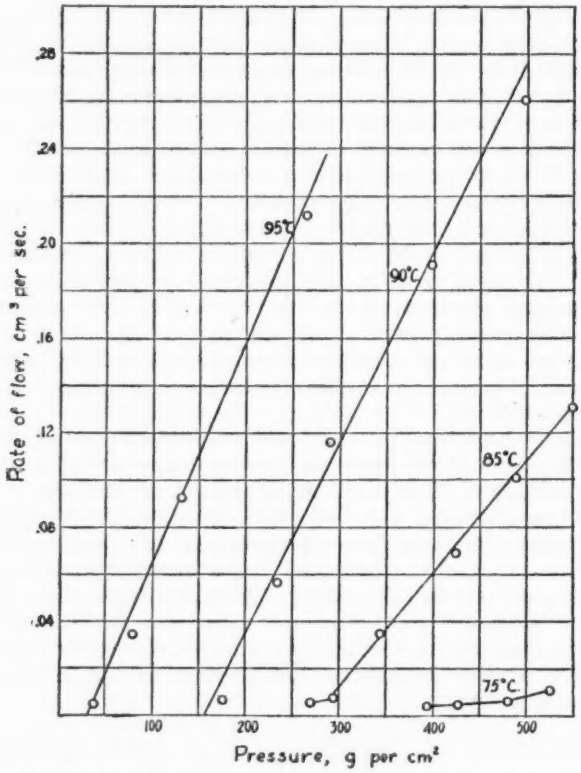

FIGURE 5.—*Flow-pressure graphs on medium cup grease*

consistency at room temperature. There was, consequently, no further breaking down of the grease as it passed through the capillary at the higher temperatures where the tests were made. Such would not be the case, however, for an oil or a grease cooled to a low temperature before test. To illustrate the unique utility of the instrument in such cases, Figures 6, 7, and 8 are given.

H. K. Griffin and S. A. McKee, in an unpublished investigation at the Bureau of Standards, have shown that a plastic oil cooled below its pour point does not at first flow at a steady rate through a consistometer capillary, even when the pressure producing flow is maintained

[13] See footnote 8, p. 90.

constant. The rate instead gradually increases over a considerable period of time, but ultimately acquires a steady value, greatly in excess of that initially observed. This behavior was explained by Griffin and McKee as due to a breaking down of the structure of the congealed oil in the body of the consistometer before the material had yet arrived at the entrance to the capillary. The observations of Giesey and Arzoomanian, which must be explained in the same manner, have already been cited.

Figure 6 shows a test of a heavy paraffin-base oil with the instrument here described. The oil was cooled in the instrument without any

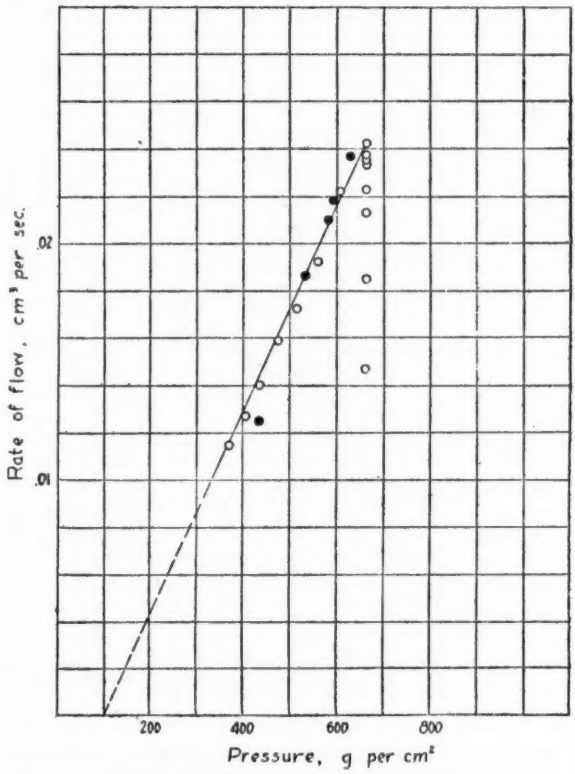

FIGURE 6.—*Breakdown of a plastic oil before passing through capillary*

disturbance for two hours before commencing the first test. An initial pressure of about 660 g per cm² was applied and maintained while nine observations of the rate of flow were taken. The rate increased to about 170 per cent of its initial value before it became even approximately constant. The pressure was lowered through successive stages to give the graph represented by the empty circles, and was then increased and again lowered by steps to give the solid circles, all the points on the figure representing a single passage through the capillary. These graphs and many more of a similar nature which have been taken completely confirm the phenomenon observed by Griffin and McKee, as well as the interpretation they gave.

In the instrument used by these investigators it was not possible to follow the breakdown process further. In the ordinary plastometer even this primary breakdown of structure completely escapes detection.

The far greater breakdown produced by passing the material through the capillary is shown by the triangles and crosses of Figure 7, which represent, respectively, the first and fifth passages of a plastic oil through the same capillary as employed in Figure 6. The hook at the upper end of the graph represented by triangles is due to the

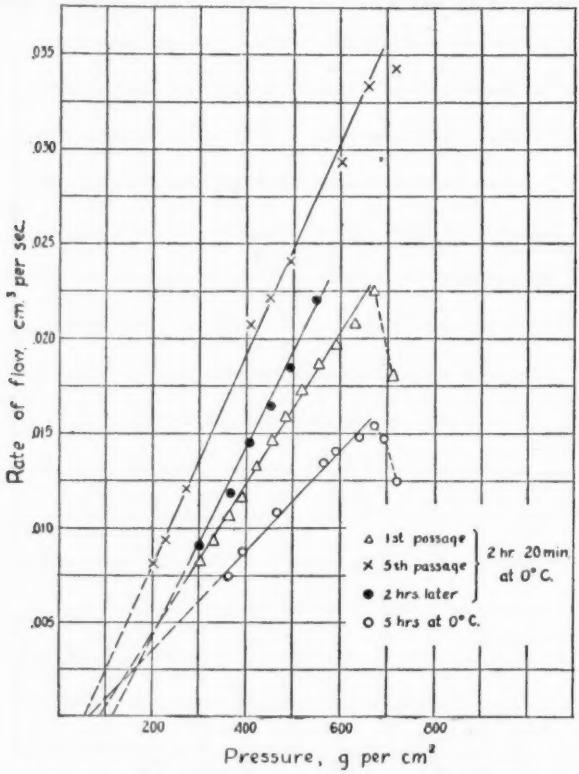

FIGURE 7.—*Breakdown due to successive passages through capillary; also time effect of cooling*

phenomenon shown in Figure 6, and indicates that the breakdown of the material is so great for the first part of the run that the rate of flow actually increases at first even though the pressure has been lowered somewhat. The same behavior has been observed in many other instances.

The solid circles of Figure 7 show that at a low temperature this oil possesses the property of thixotropy as already mentioned. Thus, after taking the data represented by crosses, the broken-down oil was allowed to stand at the same temperature undisturbed for two additional hours, when its resistance to flow was found to be greatly increased. The data represented by the empty circles were taken on a fresh sample of the same oil and show that the oil behaves somewhat like a glue or jelly in requiring a considerably longer time to

reach its maximum stiffness than that required for it merely to assume the temperature of test. While, by actual measurement, it was known that less than 2 hours' standing in the bath was ample for all the oil to come to 0° C., yet a sample cooled for 5 hours shows a much higher resistance to flow than the same oil cooled 2 hours and 20 minutes. These features emphasize the necessity of a standardized period of cooling for any lubricant on which a viscometric investigation is to be conducted at a low temperature.

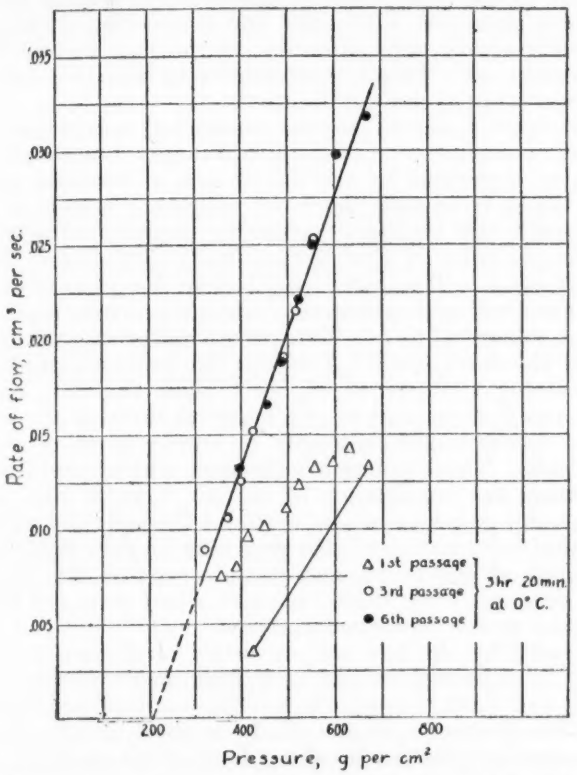

FIGURE 8.—*Manner of obtaining both unworked and completely worked consistency*

Before proceeding to Figure 8 it should be pointed out that of all the graphs on Figures 6 and 7 the only one which may possess any value whatsoever as a reproducible index of the consistency of the oil under test is the one shown by crosses on Figure 7, representing the fifth passage through the capillary. All the other graphs on these two figures represent data taken on a constantly changing material. For a graph to be of value as representing the consistency of a plastic oil under reproducible conditions, it must show either the consistency of the solid, undisturbed material or that of the oil thoroughly worked and broken down to a constant consistency.

Figure 8 shows how flow-pressure graphs for both these sets of circumstances may easily be obtained on the new instrument. Admittedly, the cooling period should be much longer than the three

hours employed here if the data were to be used for other than illustrative purposes. The oil is cooled in the instrument the desired length of time without being disturbed. A single point is taken at a suitable pressure by forcing as small an amount of material as practicable through the capillary. The flow is stopped while the pressure is raised to a somewhat higher level and a second point is taken, again on a small amount of material. The total volume of flow for both points need not be in excess of 0.5 cm^3. Since the flow-pressure graph of a grease or plastic oil is usually linear except at the lowest pressures, a straight line connecting these two points affords a satisfactory approximation to the true consistency of the solid, unworked oil. This is represented by the two triangles connected with a straight line on Figure 8.

A closer approximation to the unworked consistency could be obtained by correcting each of these two points downward, according to the scheme suggested by the data taken at constant pressure for Figure 6. That is to say, the total volume of material which has passed through the capillary might be determined when each of several separate rates of flow is measured, all the time keeping the pressure constant. The rates could then be plotted against the respective total volumes measured, and this curve extrapolated backward to zero volume of flow. The corresponding rate would represent very closely the starting rate of flow at the pressure employed.

The remaining triangles of Figure 8 show the data obtained by continuing the first passage of the material through the capillary in the manner which would ordinarily be employed to procure a flow-pressure graph. These points are the ones which would be regarded as representing the consistency of the oil, were it not possible to make successive passages of the material through the capillary. It is evident that information of this type may be very misleading, since both the slope of the graph and its intercept on the pressure axis are vastly different from those obtained when tests are made either on the worked or the unworked material.

As illustrated by the two sets of circles on Figure 8, the worked consistency is measured on the new instrument simply by passing the oil back and forth through the capillary a number of times before taking the flow-pressure graph. To be assured that further working will not produce any further breaking down of the material, additional graphs may be taken as checks.

VII. CONCLUSIONS

1. The consistometer described is speedy in operation and permits the taking of any number of flow-pressure graphs at the same or different temperatures without refilling or removing from the bath. It is suitable for materials which change in consistency with time or with mechanical working. It possesses the unusual advantage that it can be used to measure either the unworked or the worked consistency of plastic materials at any temperature. These are the properties generally recognized as most useful in characterizing such materials.

2. Certain oils at low temperatures show the property of thixotropy, and require a standardized period of cooling to assume a reproducible consistency.

WASHINGTON, November 19, 1929.

METHOD OF MEASURING STRAINS BETWEEN GLAZES AND CERAMIC BODIES

By H. G. Schurecht and G. R. Pole[1]

ABSTRACT

A new test was developed for comparing the strains existing between different glazes or other ceramic finishes and the bodies to which they are applied. By its use these strains may be so adjusted that the finishes will be in sufficient compression to prevent crazing from subsequent expansion of the body without causing initial shivering. The new test is particularly valuable because the measurements are made on combinations of glaze and body prepared and treated almost exactly like those intended for regular use and because of the simplicity and cheapness of the apparatus required. A modification of the test provides a comparison of the moisture expansions of different bodies.

CONTENTS

	Page
I. Introduction	97
II. Experimental methods	98
III. Results of tests on newly fired ware	100
IV. The ring test as a means of measuring moisture expansions of ceramic bodies	102
V. Summary and conclusions	104

I. INTRODUCTION

In selecting glazes or other finishes for ceramic bodies it is essential to know to what extent the finish may be in compression or in tension without causing delayed crazing [2] or shivering. If a glaze is in strong compression on newly fired bodies it is not likely to be thrown into tension from the subsequent expansion of the body. It is therefore less apt to develop delayed crazing than a glaze in tension or only under slight compression. If a ceramic finish is under excessive compression it may shiver.

The purpose of this work was to develop a simple, cheap, and rapid means for measuring the strains existing between glazes and the bodies to which they are applied. This test will also be of assistance in developing new glazes and bodies on which the glaze should be in adequate compression to prevent crazing, but still should not be in sufficient compression to cause shivering.

[1] Research associates of the National Terra Cotta Society at the National Bureau of Standards.
[2] Method of Testing Crazing of Glazes Caused by Increases in Size of Ceramic Bodies, J. Am. Ceram. Soc., 11, pp. 271-272; 1928.

II. EXPERIMENTAL METHODS

The specimens used for these tests are 2-inch diameter hollow cylindrical rings with the glaze or other ceramic finish to be tested applied to the outside only. (See fig. 1.) Care must be taken not to glaze the inside surface or edges, otherwise an error would be introduced.

After firing, two grooves or holes are cut in one edge of the ring approximately one-fourth inch apart and large enough to hold glass capillary tubes one-eighth inch long and one thirty-second inch in diameter. These thin capillary tubes are prepared by heating thicker tubes and drawing them down to a thread to make the

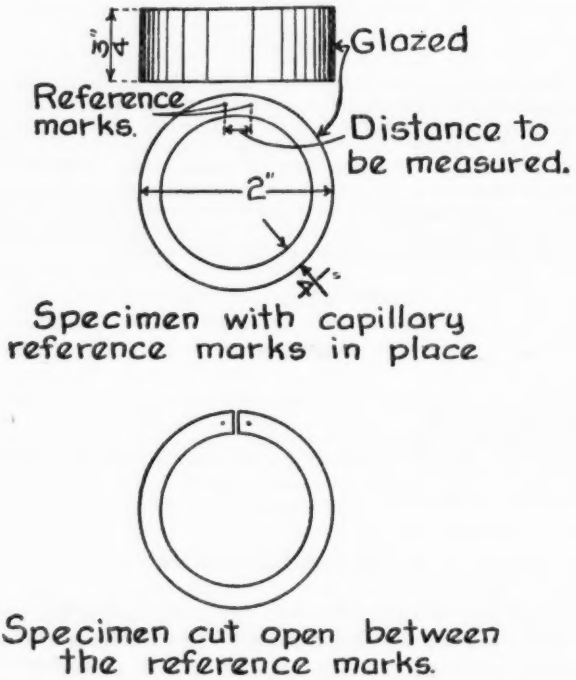

FIGURE 1.—*Sketch of ring specimen*

capillary holes small, and thus provide sharp reference marks when observed under the microscope. They are cemented in the holes or grooves with a litharge glycerin mixture or other suitable adhesive. The distance between the two reference marks is then measured as accurately as possible with a micrometer microscope similar to that shown in Figure 2.[3]

The rings are then cut open between the reference marks with a diamond saw or a narrow crystalon grinding wheel. By remeasuring these distances after cutting, the expansions or contractions of the rings may be observed. The expansions or contractions of rings with no glaze are also determined, and these are subtracted from the

[3] In making these measurements it is important to keep the reference marks as nearly parallel to the horizontal cross hair or direction of measurement as possible.

measurements obtained on the corresponding glazed rings to obtain the true expansions or contractions caused by partially releasing the strains between the glaze and body.

If the glazes are in tension the ring will expand when cut open, but if in compression it will contract. Hence, the expansion or contraction of the rings may be used as approximate measurements of whether the glazes are in tension or compression.

In the work reported in this paper the expansion or contraction of the rings was determined as described above by one measurement without attempting to determine the actual stresses in the glazes.

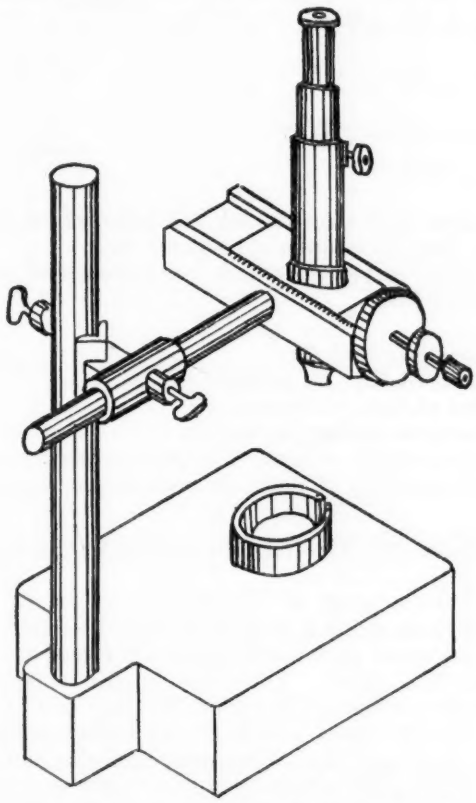

FIGURE 2.—*Apparatus used to measure the expansion or contraction of rings*

To determine the actual stresses in the glazes would be too involved for plant control and most laboratory work, in which cases it is merely desired to know if the glaze is in tension or compression and approximately how much.

The maximum stresses which have been released in the body and glaze by cutting the rings open may be also determined with Merriman's [4] curved beam formula.

In Figure 3, *ab* represents the change in length of the inside, while *AB* represents the change in length of the outside of the curved beam

[4] Merriman, M., Mechanics of Materials, p. 435, John Wiley & Sons, New York; 1916.

due to cutting the ring open. These changes in length may be measured directly between short distances on the outside and inside of the rings by means of the micrometer microscope. From these data the angle between Aa and Bb may be calculated. The curved beam formulas for calculating the maximum fiber stresses in this case are as follows:

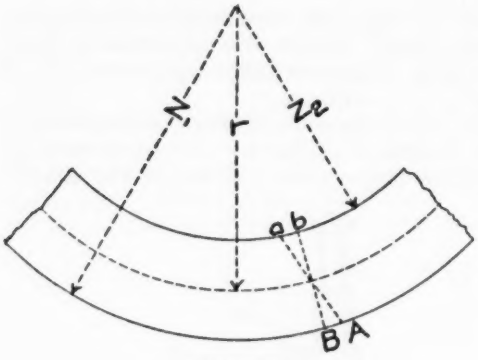

FIGURE 3

$$S_1 = E_1 \frac{d\theta}{\theta} \frac{z_1 - r}{z_1} \quad (1)$$

$$S_2 = E_2 \frac{d\theta}{\theta} \frac{z_2 - r}{z_2} \quad (2)$$

S_1 = maximum fiber unit stress which was released on glaze by cutting open the ring, in pounds per square inch.
S_2 = maximum fiber unit stress which was released on body, in pounds per square inch.
$\theta = 360°$.
$d\theta$ = angle between Aa and Bb.
z_1 = outside radius of ring, in inches.
z_2 = inside radius of ring, in inches.
r = radius of neutral surface, in inches.
E_1 = modulus of elasticity of glazes, in pounds per square inch.
E_2 = modulus of elasticity of body, in pounds per square inch.

III. RESULTS OF TESTS ON NEWLY FIRED WARE

To determine how much a slip finish may be in tension before it crazes and also how much it may be in compression before it shivers, 24 bodies were prepared with coefficients of thermal expansion varying from 5×10^{-6} to 13.2×10^{-6}. These coefficients were calculated from interferometer measurements between 20° and 600° C. made on the separate burned clays from which the 24 bodies were compounded. These were molded into ring specimens and the same vitreous slip finish applied to all, after which they were fired to cone 6.

The average results of strain tests made on five duplicate rings are given in Table 1 and plotted in Figure 4. It is apparent that a slip finish may be in compression sufficient to cause a contraction of the ring of 0.0308 cm in circumference without shivering. The values obtained where the slip had crazed are too low, since some of the strain between body and slip has been relieved through crazing of the slip. By examining results which show the slip to be in tension but still sound, it is apparent that the slip may cause the rings to expand 0.0071 cm in circumference without crazing. If, however, the expansion is higher, it may develop crazing. It is apparent that this slip can be under considerable compression before it shivers, but crazing may occur when under a comparatively small tension.

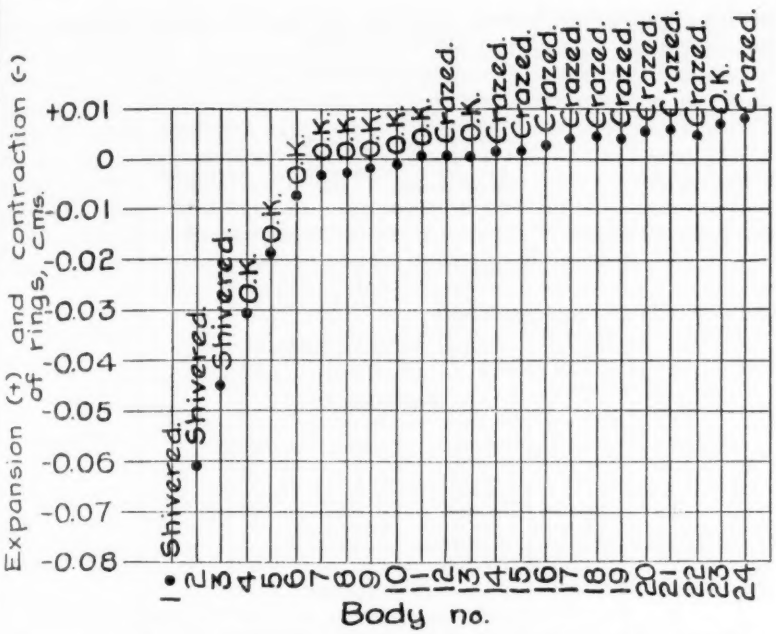

FIGURE 4.—*Relation between expansions and contractions of rings and the tendency of glazes to craze or shiver*

TABLE 1.—*The relation between ring tests and the tendency of a slip finish to craze or shiver*

Special bodies	Expansions (+) or contractions (−) of rings with no glaze *A*	Expansions (+) or contractions (−) of glazed rings after cutting *B*	Expansions (+) or contractions (−) of glazed rings due to strains between glaze and body (*B*−*A*)	Condition of glaze when removed from kiln
	cm	*cm*	*cm*	
1	+0.0004	−0.0844	−0.0848	Shivered.
2	−.0026	−.0631	−.0605	Do.
3	+.0008	−.0446	−.0454	Do.
4	−.0003	−.0311	−.0308	O. K.
5	−.0009	−.0197	−.0188	O. K.
6	−.0021	−.0097	−.0076	O. K.
7	+.0006	−.0029	−.0035	O. K.
8	+.0012	−.0009	−.0021	O. K.
9	−.0001	−.0016	−.0015	O. K.
10	+.0015	+.0006	−.0009	O. K.
11	−.0013	−.0004	+.0009	O. K.
12	+.0007	+.0009	[1] +.0002+	Crazed.
13	+.0009	+.0010	+.0001	O. K.
14	+.0004	+.0018	+.0014+	Crazed.
15	+.0006	+.0020	+.0014+	Do.
16	+.0009	+.0031	+.0022+	Do.
17	−.0002	+.0034	+.0036+	Do.
18	−.0006	+.0037	+.0043+	Do.
19	+.0006	+.0039	+.0033+	Do.
20	−.0006	+.0049	+.0055+	Do.
21	−.0004	+.0056	+.0060+	Do.
22	+.0009	+.0057	+.0048+	Do.
23	+.0015	+.0086	+.0071	O. K.
24	+.0015	+.0096	+.0081	Crazed.

[1] The expansions of rings which were crazed when removed from the kiln are marked plus, since some of the strain between the body and slip has been relieved by crazing of the slip.

TABLE 2.—*The relation between ring tests and the tendency of different ceramic finishes to craze*

	Expansions (+) or contractions (−) of glazed rings due to strains between glaze and body	Condition of glaze when removed from kiln	Condition of glaze after treatment with steam at 150 lbs./in.² for 1 hour
	cm		
1	−0.0063	O. K.	O. K.
2	−.0033	O. K.	O. K.
3	.0018+	Crazed	
4	.0080+	do	
5	.0012+	do	
6	.0130+	do	
BRIGHT GLAZES			
1	−0.0140	O. K.	O. K.
2	−.0106	O. K.	O. K.
3	−.0103	O. K.	O. K.
4	−.0043	O. K.	O. K.
5	−.0005	O. K.	Crazed.
6	.0030+	Crazed	
7	.0033+	do	
MAT GLAZES			
1	−0.0066	O. K.	O. K.
2	.0020+	Crazed	
3	.0040+	do	
4	.0063+	do	
5	.0090+	do	
SLIP FINISHES			

The results of similar tests with different glazes and slip finishes are given in Table 2. It is evident from these that glazes or slips in strong compression on newly fired bodies do not craze even when treated with steam at 150 lbs./in.² for one hour. However, all glazes which were in tension when removed from the kiln were crazed. It seems, therefore, that the use of glazes which are under strong compression on newly fired ware would tend to obviate delayed crazing due to moisture.

These tests confirm previous work done on glazes by the autoclave [5] and interferometer methods.[6]

In general, the mat glazes were found to be in greater compression than the other ceramic finishes tested, although some mat glazes were not as good in this respect as certain bright glazes. This apparently shows that the mat glazes tested have a lower thermal expansion than the other glazes.

IV. THE RING TEST AS A MEANS OF MEASURING MOISTURE EXPANSIONS OF CERAMIC BODIES

Since certain ceramic bodies expand when treated with water while the glaze remains relatively constant in size, it is obvious that open glazed rings may be used to obtain an approximate measure-

[5] H. G. Schurecht, Methods of Testing Crazing of Glazes Caused by Increase in Size of Ceramic Bodies, J. Am. Ceram. Soc., **11**, No. 6; 1928.

[6] George Merritt, Application of the Interferometer to Measurements of the Thermal Dilatation of Ceramic Materials, B. S. Sci. Paper No. 485; 1924.

ment of the moisture expansions of ceramic bodies. Rings and bars of the same body were prepared for the purpose of comparing the expansions obtained in the two tests when the specimens were subjected to the same treatments. They were completely immersed in water for seven days, after which the distances between the reference marks were measured while wet and also after drying at 110° C. for 12 hours. These distances were also measured subsequent to subjecting them to steam at a pressure of 150 lbs./in.^{2} for one hour. By this means the same ring can be used as a measure of the strain and also as an approximation of the moisture expansion.

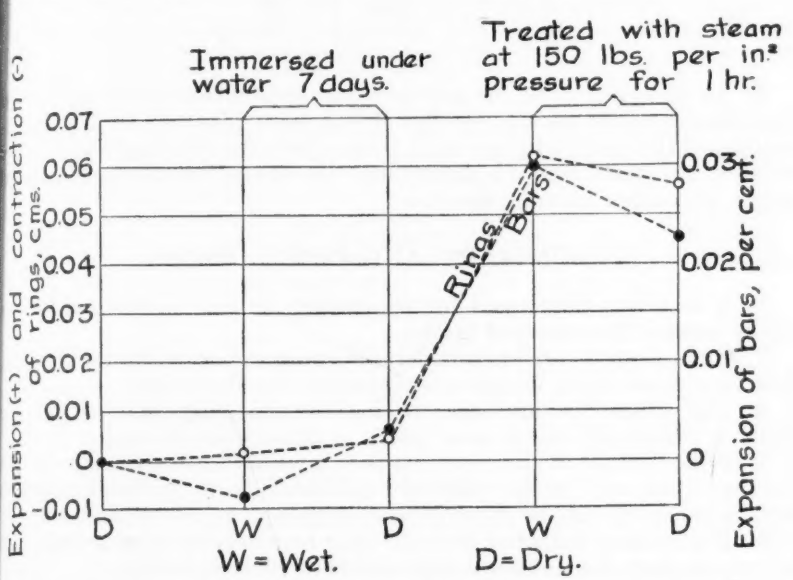

FIGURE 5.—*A comparison of the moisture expansions of a ceramic body and the expansion of rings*

The results obtained with glazed rings, cut open between the reference marks, and bars made of the same body have been plotted in Figure 5. It is evident that the expansions of the rings are approximately proportional to those of the bars.

Similar data for a number of other bodies are given in Table 3. From these data it is again evident that the expansions of the rings, in general, increase as the expansions of the bars increase. Although the ring moisture expansion test is not as accurate as the bar moisture expansion test, it can be conducted in less time and with inexpensive equipment.

TABLE 3.—*Expansions of rings and bars caused by autoclave treatment*

	Treated in an autoclave at a steam pressure of 150 lbs./in.² for 1 hour	
	Expansion of rings	Expansion of bars
	cm	*Per cent*
1	0.0040	0.033
2	.0064	.039
3	.0111	.057
4	.0089	.042
5	.0113	.083

As an illustration of further possible applications of ring tests in ceramics it might be stated that it has been planned to use modifications of this test in future work to compare the resistance of ceramic finishes to strain and to determine the annealing temperatures of glazes and other ceramic finishes.

V. SUMMARY AND CONCLUSIONS

1. A test was developed for measuring strains between glazes or other ceramic finishes and bodies.

2. Glazes can be under considerable compression without shivering, but they craze when under comparatively small tension.

3. The simplicity and ease of making the ring test on ceramic finishes admirably suit it as a means of plant control work.

4. With the aid of the ring test it is possible to fit glazes to bodies so that they will be in sufficient compression to prevent moisture crazing and still not be in compression enough to cause shivering.

5. It was demonstrated that the ring test may be used to compare approximately the moisture expansions of ceramic bodies.

6. In general, it was found that mat glazes, owing to their lower thermal expansions, are in stronger compression on ceramic bodies than bright glazes and hence are more resistant to crazing.

WASHINGTON, October 16, 1929.

THE PREPARATION OF FIBER TEST SHEETS

By Merle B. Shaw, George W. Bicking, and Leo W. Snyder

ABSTRACT

The need in the paper-making research at the bureau for a laboratory test that is analogous to paper-mill processes has led to the construction of a suction sheet machine and the development of a method of preparing fiber sheets. The test procedure relates to the forming of the sheet on the mold and the subsequent operations of couching, pressing, and drying. A complete description of the equipment and technic employed is given.

Test data on the finished papers show that the fibers are uniformly distributed in sheets made by the method described, and that the different sheets of a series made from a given sample of stock are in close agreement, and can be duplicated as desired. The personal equation is reduced to a minimum and comparable results are obtained by different operators.

The size of the finished sheets is adequate to supply specimens for each kind of test ordinarily made to evaluate the quality of paper.

The results obtained warrant the view that the method is practical and is useful for mill control or paper-making research.

CONTENTS

	Page
I. Introduction	105
II. Description of apparatus	106
1. Agitator	106
2. Sheet machine	106
3. Couching plate and felt	107
4. Sheet press	110
5. Sheet dryer	111
III. Operation of apparatus	111
IV. Test data on finished hand sheets	112
V. Summary	114

I. INTRODUCTION

In investigating new materials for paper it is often desirable to study the behavior of the fibers under paper-manufacturing conditions without actually making paper-machine runs, which are costly and require considerable quantities of fibrous materials. Several laboratory methods for evaluating the quality of pulp for paper-making purposes have been proposed,[1] but none has as yet been adopted as a standard procedure. This paper describes the method which has been developed[2] in the paper laboratory of the Bureau of Standards and is used in the preparation of fiber test sheets.

The determination of the strength of fibers for paper making includes several different operations—sheet forming, pressing, drying, and testing—and all need to be standardized in order to obtain a method that is reliable as a whole. The pulp used in making fiber

[1] The Bibliography of Wood Pulp Strength Testing, W. F. Moore, Paper Trade J., **89**, No. 12, pp. 62-72, Sept. 19, 1929, gives very complete abstracts of many of the published articles on this work.

[2] Method of Making Uniform Fiber Sheets for Test Purposes, Merle B. Shaw and George W. Bicking, Paper Trade J., **79**, No. 21, pp. 51-53; Nov. 20, 1924. Also included in B. S. Tech. Paper No. 340, Caroá Fiber for Paper Making, pp. 326-332.

sheets at the bureau is in most cases taken from stock prepared in the semicommercial beaters of the mill equipment. The sheet-making method adopted and described relates to the forming, couching, pressing, and drying of the sheet.

II. DESCRIPTION OF APPARATUS

1. AGITATOR

An agitator is used to separate the clots of fibers without beating action and to mix the pulp and water preparatory to forming the sheet. The agitator (fig. 1) consists of a vertical shaft having a 2-blade propeller fitted in the lower end, and is driven by a ⅛-horsepower motor at a speed of 1,750 revolutions per minute. It is mounted on a board free to move up and down in vertical guides on either side.

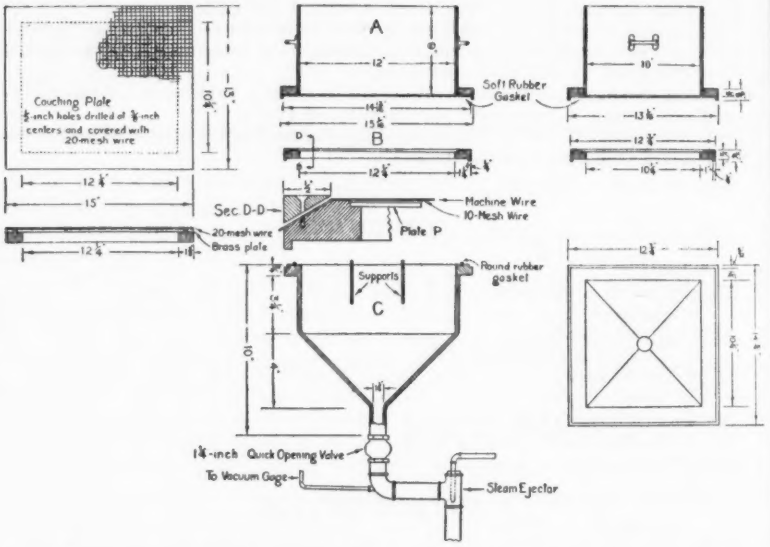

FIGURE 2.—*Working drawing of sheet machine and couching plate*

A counterweight facilitates the movement and keeps the apparatus in the position desired. A stop watch used to indicate the duration of the mixing is started and stopped simultaneously with the motor by means of a lever bar tripped by the motor switch. The watch can also be operated by hand.

The mixing vessel has a capacity of 1½ gallons. A baffle plate, *B*, 1 inch in width, extending from top to bottom and fastened to the side wall, breaks up the swirl of the liquid and produces the necessary turbulent motion.

2. SHEET MACHINE

The sheet machine is a suction mold. It consists of 3 sections, 2 brass and 1 aluminum (fig. 2, *A*, *B*, and *C*, respectively).

Fitted into the casting of the top section, *A*, is a 10 by 12 inch sheet brass box (18 gage brass), open at top and bottom and forming a

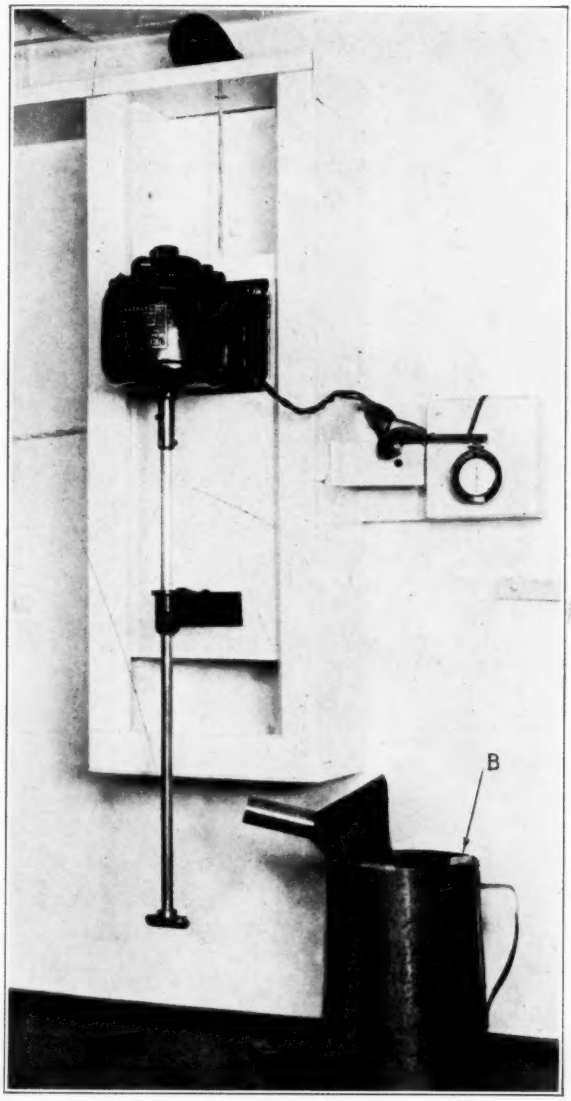

FIGURE 1.—*Agitator and mixing vessel*

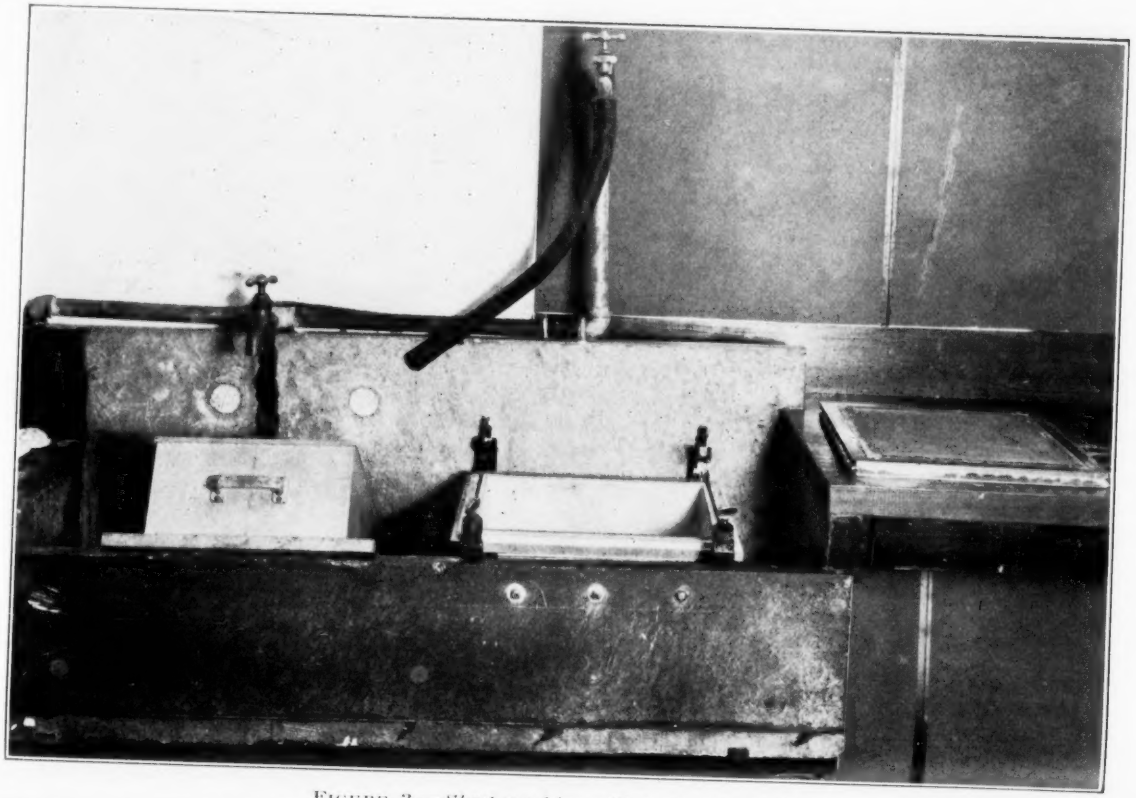

FIGURE 3.—*Sheet machine with parts separated.*

deckle box.[3] On the under side of the casting a rubber gasket is cemented (with shellac) to effect a tight seal when the mold is assembled and the top is clamped down. With a 10 by 12 inch deckle area a trimmed sheet 8 by 10½ inches in size is obtained. From a sheet of this size test specimens may be cut for each kind of test ordinarily made to evaluate the quality of paper. Since no difficulty is encountered in making 10 by 12 inch sheets of uniform formation and weight, these dimensions are believed to be the most satisfactory and economical.

In the mold casting, *B*, is a perforated brass plate, *P*, drilled with ½-inch holes at ⅝-inch centers. The plate is covered first by No. 10 brass wire cloth, soldered to it at the edges, and then by No. 80, stretched taut over the mold and held securely by a frame screwed to the casting. A mixture of litharge and glycerine poured on the edges of the mold makes the joint tight and thus prevents leakage. The mold plate supporting the screens must be level if a uniform sheet is to be secured.

The lower casting, or mold support, *C*, has a water outlet fitted with a quick-opening gate valve. A steam ejector is placed in the discharge pipe below to accelerate the suction. Two vertical ⅛-inch aluminum plates across the casting prevent sagging of the mold plate. A rubber tube fitted in a groove in the top of the casting makes a tight seal with the mold when the machine is in operation.

In most of the sheet-making machines now in use the clearance between the wire on which the sheet is formed and the suction outlet is small. The rate of drainage for these machines is nearly always specified, and is nearly always very slow. If much suction is applied during the forming of the sheets the fibers are drawn to the area over the suction opening and the sheet formed is therefore of uneven thickness and weight. If a baffle plate is placed above the suction opening the fibers are then drawn to the edges of the sheet, causing, as before, resultant inequalities in the substance of the sheet. These conditions are prevented and uniform fiber distribution is obtained with the bureau's sheet machine by increasing the height of the mold plate above the outlet valve and changing the form of the base casting. The casting (fig. 2, *C*) consists of a rectangular box perpendicular to the mold plate, a truncated pyramid, and a cylindrical section for pipe connections, the heights of which are 4 inches, 4 inches, and 2 inches, respectively.

FIGURE 3.—*Sheet machine with parts separated.*

3. COUCHING PLATE AND FELT

A perforated brass plate (fig. 2) is used in transferring, or "couching," the sheet from the mold for the subsequent pressing and drying operations. The plate, which is ⅛-inch thick and drilled with ½-inch holes at ⅝-inch centers, is similar to the mold plate and is mounted in a frame of the same size as the mold casting. A No. 20 wire screen is stretched over the plate and soldered to it at the edges.

Hand sheets have generally been couched by placing an absorbent material, such as a blotter or felt, over the web of pulp, pressing it lightly against the molded sheet, and lifting it and the adhering sheet from the mold. This procedure requires extreme care in removing the sheet to prevent any undue stresses that might disturb the original

[3] A deckle box is a frame laid upon a wire mold to confine the paper pulp to a definite area, thus limiting the size of the sheet.

position of the fibers, particularly in lightweight sheets, because of their tendency to tear and leave portions adhering to the screen. By use of the perforated plate the sheet with couching felt and plate superposed can be inverted, returned to the sheet machine, and transferred to the felt by suction. This modification simplifies the couching procedure considerably.

Blotters and felts are the couching materials generally used in removing hand sheets from the screen. Experimental data as to their comparative value were not available, however, and tests were therefore made to determine the number of times each could be used, ease with which they could be handled, and their comparative effect on the strength of the finished fiber sheets. The blotting paper used had the following properties.[4]

Weight:		
25 by 40 inches, 500 sheets	pounds	266.0
19 by 24 inches, 500 sheets	do	121.3
Thickness	inch	.028
Bursting strength	points	34.4
Fiber composition:		
Rag	per cent	50.0
Chemical wood	do	50.0
Absorption (1 cc distilled water)	seconds	41.0

The felt was similar in quality to paper-machine felts, smooth, napless, and of a weave that permitted ready passage of air through it when suction was applied. Other physical properties were:[5]

Weight per square yard	ounces	19.2
Thread count per inch, warp		70
Thread count per inch, filling		40
Thickness	inch	.040

In preparing the stock for the hand sheets the pulp was beaten only until it was free from clumps of fibers, no attempt being made to develop its maximum strength. The standard procedure, described hereinafter (III), was used in the sheet-making operations except in the couching with the blotters. Couching by suction was tried but the close texture of the blotting paper rendered it too impermeable to air and prevented effective action of the suction on the web of pulp. The couching plate could not be used therefore, and the sheets had to be removed by hand. The sheet on the mold was covered with a blotter and over it a 4½-inch brass pipe was rolled. The sheet and blotter were then lifted together from the plate, and laid sheet up on another blotter placed on a metal plate. Two more blotters and another metal plate were laid on the sheet and the unit was ready for pressing.

Pressures ranging from 30 to 240 lbs./in.^{2}, increasing by 30-pound steps, were employed. In each case two sets of five sheets each—one couched with blotters, the other with felts—were used, the pressure being applied for three minutes. Other sheets were weighed after being pressed and then dried to constant weight to determine the amount of moisture in the pressed sheets. The results are recorded graphically in Figure 4. It will be noted that less water was left in the sheets couched and pressed with blotters. In no case, however, was the amount present in excess of that in paper going to the dryers

[4] The tests were made according to the official methods of the Technical Association of the Pulp & Paper Ind.

[5] Methods of measurements are described in U. S. Government Master Specification No. 345a, General Specification for Textile Materials (Methods of Physical and Chemical Tests).

leaving the last press) of a commercial paper machine. The amount of moisture removed from the hand sheets will, of course, depend not only on the type of couching material used, but also on the number of thicknesses employed and the duration of the pressing.

Since the differences in the comparative moisture content of the sheets pressed with blotters and felts were as great as 10 per cent, it was thought that they might affect the strength of the finished papers. Tests made on the sheets indicate, however, that the final strength was not affected by the amount of moisture in the sheet when ready

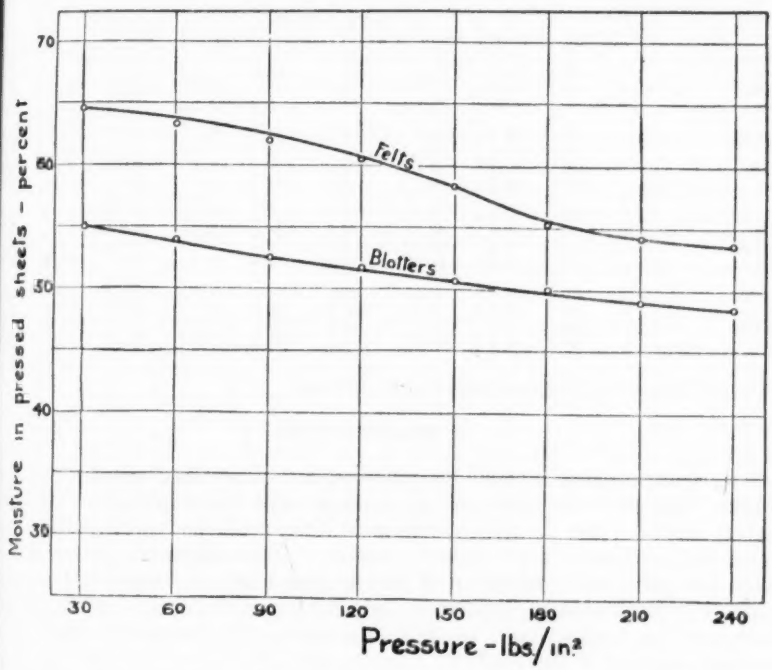

FIGURE 4.—*Comparative moisture content of sheets pressed with blotters and felts*

for drying. The measurements (Table 1) show very good agreement in the results obtained with the blotters and felts.

As to the relative serviceability of the two couching materials, however, felts were found to be preferable to blotters. Blotters become unsatisfactory after being used a few times in preparing hand sheets. Although subsequent drying and pressing smooths the surface and permits their being employed again, they are not as satisfactory as when new, and the number of times they can be used is limited. Felts, on the other hand, are easily kept in good condition, and when properly cared for their period of service has practically no determinate limitation.

TABLE 1.—*Comparative strength of hand sheets pressed with blotters and felts*

Material between which sheets were pressed	Pressure	Physical tests on finished hand sheets							
		Weight (25 by 40 inches, 500 sheets)	Bursting strength	Folding endurance		Tensile strength (strip 15 by 100 mm)		Tearing strength	
				Long direction [1]	Short direction [1]	Long direction [1]	Short direction [1]	Long direction [1]	Short direction [1]
	Lbs./in.[2]	*Pounds*	*Points*	*Double folds*	*Double folds*	*kg*	*kg*	*g*	*g*
Blotters	30	65.6	28.4	53	40	3.2	3.3	62.8	63.6
Felts	30	64.5	27.0	53	55	3.1	3.3	66.0	64.4
Blotters	60	64.4	31.3	85	76	3.4	3.3	65.6	62.6
Felts	60	63.2	31.0	67	70	3.4	3.4	65.2	66.8
Blotters	90	64.8	32.5	58	55	3.8	4.2	64.8	64.0
Felts	90	61.5	32.0	60	58	3.4	4.0	65.2	66.4
Blotters	120	67.4	33.1	142	92	4.2	4.2	62.0	66.0
Felts	120	66.2	33.5	75	87	4.2	4.1	67.2	65.2
Blotters	150	69.0	32.3	98	86	4.3	4.3	62.0	66.0
Felts	150	70.1	32.0	88	91	4.2	4.3	65.2	64.8
Blotters	180	70.1	32.8	88	75	4.5	4.6	70.4	74.0
Felts	180	69.3	34.0	89	93	4.2	4.1	64.8	67.2
Blotters	210	68.2	34.8	102	95	4.8	4.8	73.6	74.4
Felts	210	69.9	34.0	87	85	4.8	4.5	68.8	69.2
Blotters	240	70.8	35.3	163	132	5.1	4.9	78.0	77.6
Felts	240	65.1	35.0	128	135	4.6	4.5	69.2	70.0

[1] Test strip cut from the hand sheet in the direction indicated.

4. SHEET PRESS

A hydraulic press is used for pressing the fiber sheets before drying them. The press is operated by means of a hand pump. The two platen surfaces are 12 by 14 inches in size, and the vertical displacement of the lower surface is 8 inches. This distance gives ample space for pressing a number of hand sheets at one time. The ram has a sectional area of approximately 50 square inches, and sufficient force can be transmitted to it to maintain on the hand sheets any pressure up to 800 lbs./in.^{2}

5. SHEET DRYER

The dryer consists of a steam-heated cylinder and a carrying felt which covers most of the cylindrical surface. The diameter and the length of the cylinder are 12 and 14 inches, respectively. A thermometer placed between the carrying felt and the cylinder in preliminary experimental tests showed the temperature used to be approximately 90° C. A pressure gauge attached to the dryer is of value in preventing excessive temperature by showing when steam pressure develops within the cylinder.

III. OPERATION OF APPARATUS

Sheets are frequently made at the bureau in connection with the semicommercial work to note changes in the strength of the pulp during the progress of the beating operation. The tabular data given herein are on stock taken from the semicommercial beater.

A 2-quart dipper of stock is withdrawn from the beater as a sample, which is sufficient for several hand sheets, and to it 6 dippers of water are added. A measured volume of the diluted stock is made into a hand sheet, and from the weight of the dried sheet the volume of stock required for the desired test sheets is determined. The quantity of stock requisite for a test sheet of the specified weight is then taken and is diluted further to approximately 1 gallon in the 1½-gallon container used with the agitator. (Fig. 1.) The concentration of the final mixture is approximately 0.15 per cent.

The base, or mold support, of the sheet machine is filled with water, the mold and deckle box are set in place, and the assembled parts are clamped together. Water is run into the deckle box to a height of 4 inches, making about 2 gallons above the screen. The propeller shaft of the agitator is lowered into the container of diluted stock and operated for one-half minute. The stock is then immediately poured into the assembled sheet-making apparatus, the container being continuously moved back and forth, criss-crossing the mold, to insure uniform distribution. The dilution of the stock in the deckle box is about 0.05 per cent, which is ample for good felting of the fibers.

The steam-ejector valve and the quick-opening gate valve, respectively, are opened immediately after the transfer of the stock, to prevent settling of the fibers. The water and pulp are drawn down, and the sheet of fibers is formed on the wire. The length of time required for emptying the sheet machine depends on the rate at which water drains from the pulp—the "slowness" of the stock. When the machine contains only water the time is five seconds. Quick emptying is necessary to prevent unequal distribution of the fibers. It has been found desirable to continue the suction at least one minute after the water has been discharged from the base in order to facilitate the subsequent drying of the sheet.

After the sheet is formed the deckle box is removed, a felt is laid over the sheet, and the couching frame is placed on it. The couching frame, felt, sheet of pulp, and mold are then removed as a unit, inverted, and replaced on the mold base. Suction is again applied, and the fiber sheet is thus transferred to the felt.

The fiber sheet and the felt on which it rests are removed together from the mold and placed sheet up on a metal plate. Another felt and another plate are laid on the sheet of pulp. A number of sheets are prepared in this manner and stacked one above the other. The completed stack of fiber sheets, felts, and plates is placed in the hydraulic press and subjected to a pressure of 200 lbs./in.^{2} for three minutes.

The pressure applied for compacting the sheet has considerable influence on the ultimate strength of the paper. To obtain comparative data in testing the strength of pulp it is imperative that a standard pressure be used. Previous tests by other investigators [6] have shown that strength increases with increase in pressure, the rate of change being more rapid, however, at the lower pressures. Since 200 lbs./in.^{2} gives reliable results for all pulps and is the pressure recommended as

[6] The Determination of the Effect of Pressure on the Strength of Test Sheets in the Strength Testing of Pulp, E. P. Cameron, Pulp & Paper Mag. of Canada, **21**, No. 5, pp. 127-135; Feb. 1, 1923. The Effect of Pressure on the Strength of Test Sheets in the Strength Testing of Pulp, E. P. Cameron and J. M. Payne, Pulp & Paper Mag. of Canada, **22**, No. 3, pp. 53-60; Jan. 17, 1924.

a tentative standard by the Technical Association of the Pulp and Paper Industry it was the pressure adopted. The duration of the pressure has no appreciable effect on the strength of the sheet. Holding the load constant for three minutes gives very satisfactory results, and this period of time was adopted as standard.

The drying is accomplished by feeding the sheets between the cylinder and the carrying felt of the dryer and turning the cylinder slowly by hand. If the paper-making stock is "free" the sheet is removed after two revolutions of the cylinder, turned over, and replaced in the dryer, care being taken to avoid wrinkling the paper. If the stock is "slow," however, the sheet is not turned over, because of its tendency to cockle and wrinkle. In either case the cylinder is turned until the paper is apparently dry.

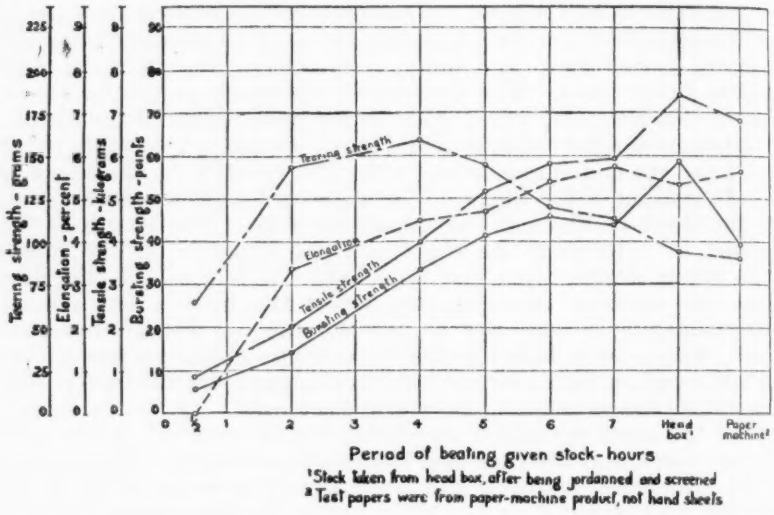
Tearing strength - grams
Elongation - percent
Tensile strength - kilograms
Bursting strength - points
Tearing strength
Elongation
Tensile strength
Bursting strength
Head box[1]
Paper machine[2]
Period of beating given stock - hours
[1] Stock taken from head box, after being jordanned and screened
[2] Test papers were from paper-machine product, not hand sheets

FIGURE 5.—*Comparison of strength properties of fiber sheets*

(Stock from beater run No. 1122)

The dried sheets are trimmed to 8 by 10½ inch size, and the various strength properties of the paper are determined. The measurements are made by the official methods of the Technical Association of the Pulp and Paper Industry,[7] under the standard atmospheric conditions for paper testing, 65 per cent relative humidity and 70° F. temperature.

IV. TEST DATA ON FINISHED HAND SHEETS

Measurements on hand sheets made by the method described are given in Tables 2 and 3. The stock for the sheets of Table 2 was taken at the recorded intervals of beating in connection with a research problem in which it was desired to know the change in strength as the beating progressed. Data on paper made on the semicommercial Fourdrinier paper machine from the same stock at the completion of

[7] Paper Testing Methods, published by the Technical Association of the Pulp & Paper Ind., 18 East Forty-first Street, New York, N. Y.

the beating are included for comparison. Two different beaters of stock, Nos. 1122 and 1123, were used and two different weights of hand sheets were made. As the measurements show, the fibers were uniformly distributed, and sheets of practically constant weight were produced regardless of the condition of the pulp being tested. The results of some of the tests on the lighter-weight papers are also shown graphically in Figure 5. The data for the heavier papers would give curves similar in slope but placed higher on the vertical scale.

TABLE 2.—*Measurements for sheets made from different samples of stock* [1]

Beater run No.	Beating interval [2]	Weight (25 by 40 inches, 500 sheets)	Bursting strength	Ratio of bursting strength to weight (25 by 40, 500 sheets)	Thickness	Folding endurance		Tensile strength (strip 15 by 100 mm)		Elongation (strip 15 by 100 mm)		Tearing strength	
						Long direction [3]	Short direction [3]	Long direction	Short direction	Long direction	Short direction	Long direction	Short direction
	Hours	*Lbs.*	*Points*	*Per cent*	*Inch*	*Double folds*	*Double folds*	*kg*	*kg*	*Per cent*	*Per cent*	*g*	*g*
1122	½	54.8	5.9	10.8	0.0069	0	0	0.89	0.84	0.00	0.00	65.6	62.4
1122	2	57.4	14.3	24.9	.0063	16	19	2.01	2.03	3.30	3.50	140.0	142.4
1122	4	56.7	33.6	59.2	.0056	623	518	4.03	4.08	4.56	4.50	154.4	162.4
1122	5	54.3	41.7	76.9	.0053	2,207	1,619	5.15	5.13	5.00	4.50	134.4	162.4
1122	6	55.8	45.9	82.2	.0051	3,627	3,728	5.86	5.79	5.35	5.45	115.2	120.8
1122	7	57.3	44.0	76.9	.0051	3,359	3,330	5.72	6.23	5.55	5.90	112.8	112.8
1122	(4)	56.4	59.0	104.9	.0048	-------	-------	7.30	7.57	5.15	5.55	93.6	91.2
1122	(5)	56.5	39.4	69.7	.0036	4,418	5,480	8.24	5.39	3.05	8.23	88.0	90.4
1122	½	105.1	15.8	15.0	.0125	7	7	2.45	1.88	3.05	2.85	213.6	196.0
1122	2	115.7	41.7	36.1	.0110	127	145	4.64	4.85	4.30	4.60	337.6	344.0
1122	4	113.9	70.2	61.7	.0095	8,028	7,888	8.93	8.87	5.50	5.90	362.4	323.2
1122	5	112.4	83.2	74.0	.0090	10,098	10,974	10.20	10.00	6.20	6.35	300.0	297.6
1122	6	113.7	102.5	90.3	.0089	15,184	16,113	12.01	11.89	7.20	7.00	278.4	284.8
1122	7	118.0	100.8	85.5	.0094	-------	-------	12.70	12.10	7.35	7.05	280.0	309.6
1123	½	57.8	8.0	13.8	.0074	0	0	.94	1.07	.00	.00	84.8	88.8
1123	2	57.2	21.1	36.8	.0060	50	33	2.54	2.24	3.50	3.60	164.0	169.6
1123	4	57.2	40.1	70.2	.0055	999	1,246	3.92	4.33	5.04	5.02	164.0	176.8
1123	5	57.1	44.6	78.0	.0053	3,075	3,575	4.65	5.09	5.36	6.20	148.0	143.2
1123	6	56.8	46.7	82.2	.0053	3,187	3,380	5.01	5.21	5.39	5.92	133.6	136.0
1123	7	56.7	53.7	94.6	.0050	2,488	2,747	5.50	5.68	5.93	5.68	126.6	108.6
1123	(4)	59.6	56.0	94.0	.0049	-------	-------	7.08	6.77	5.82	5.56	98.4	105.6
1123	(5)	57.5	37.2	64.6	.0038	3,080	2,688	9.20	4.85	2.48	7.63	98.4	108.0

[1] Hand sheets were made by Martin J. O'Leary, assistant paper maker.
[2] Reckoned from beginning of furnishing. Time required for furnishing was 15 minutes.
[3] Samples were taken from the sheets in the direction indicated. The values in the long and short directions, which should be equal in the ideal case, are given separately merely to indicate the uniform formation of the sheets.
[4] Head box: Sample taken from head box, after being jordanned and screened, during paper-machine run.
[5] Test papers were from paper-machine product, not hand sheets.

As there is no definite relation between the data obtained on lightweight and heavyweight papers made from the same stock, it is necessary to standardize the weight of the test sheets when adopting a standard method. A number of investigators have recommended that hand sheets of relatively heavy weight be made for test purposes. Since the quality of the heavier sheets bears little relation to the strength values of the usual machine-made paper, it is desired in the work at the bureau that the weight of the hand sheets correspond to that of the paper-machine product, and, therefore, the lighter-weight sheets are regularly made.

Table 3 reports the values obtained on the individual sheets made from a given sample of stock and test samples taken from the machine product made from the same stock after being run through the Jordan. The measurements for the different hand sheets are in good agreement, the variations being hardly greater than the usual experimental errors of the measuring instruments, and no larger than for the different test samples of the machine-made paper. The results show that the method permits duplication of sheets as many times as desired.

TABLE 3.—*Measurements for different sheets made from one sample of stock*

Test paper	Bursting strength	Tensile strength (strip 15 by 100 mm)		Elongation (strip 15 by 100 mm)		Tearing strength (4 ply)	
		Long direction	Short direction	Long direction	Short direction	Long direction	Short direction
	Points	*kg*	*kg*	*mm*	*mm*	*g*	*g*
Hand sheet [1]	53	5.6	6.2	7.5	6.0	29	29
Do	49	5.2	6.0	6.5	6.0	32	27
Do	54	5.0	6.1	6.0	6.0	33	26
Do	56	5.8	5.5	5.4	4.5	32	29
Do	54	6.1	6.2	7.0	5.8	32	25
Do	56	5.0	5.9	4.3	6.0		
Do	57	5.7	4.9	5.3	4.8		
Do	55	5.5	5.5	6.0	5.9		
Do	51	5.6	5.3	5.8	6.0		
Do	52	5.5	5.2	5.5	5.8		
	53.7	5.50	5.68	5.93	5.68	31.6	27.3
Machine made [1]	37	10.0	4.7	2.5	7.2	24	28
Do	35	9.6	4.9	2.7	8.5	24	25
Do	43	8.8	5.3	2.5	8.5	24	25
Do	36	9.8	4.8	2.7	8.0	26	29
Do	41	9.1	4.7	2.2	7.5	29	26
Do	35	8.9	5.0	2.0	6.7	23	26
Do	35	9.7	5.0	2.5	8.0	23	30
Do	36	9.6	4.6	2.5	7.7	24	30
Do	33	9.4	4.4	2.5	5.7	26	26
Do	41	7.1	5.1	2.5	8.2	23	25
	37.2	9.20	4.85	2.46	7.60	24.6	27.0

[1] From stock of beater No. 1123; beating interval 7 hours. Stock for machine-made paper was jordanned and screened.

V. SUMMARY

A laboratory method for making small sheets of fibers in studying the paper-making quality of pulp has been developed, and a suction sheet machine has been designed. The method relates to the forming of the sheet of fibers on the screen and the subsequent operations of couching, pressing, and drying. The finished sheet is adequate to supply specimens for each kind of test ordinarily made to evaluate the quality of paper.

With the equipment and procedure described, sheets uniform in quality—formation, weight, etc.—can be made by an operator of average skill. Measurements of the physical properties show that the different sheets made from a given sample of stock are in good agreement and that the sheets can be duplicated as desired. The personal equation is reduced to a minimum, and truly comparable results can be obtained by different operators. The data warrant the view that the method is practical and is useful for pulp quality measurements.

WASHINGTON, March 3, 1930.

THE GEIGER TUBE ELECTRON COUNTER

By L. F. Curtiss

ABSTRACT

Experiments are described which show that the sensitive surface of the Geiger tube counter is not on the wire electrode, but on the inner surface of the tube. This result explains the previously observed result that the operation of the counter is only slightly affected by the condition of the surface of the wire electrode. An explanation of the operation of the counter is offered which takes account of this additional information.

CONTENTS

		Page
I.	Introduction	115
II.	Recent experiments on the location of the sensitive surface	117
III.	Discussion of operation of counter	119

I. INTRODUCTION

Recently the writer has reported [1] the results of experiments which were undertaken to discover the effect on the operation of the Geiger tube counter of subjecting the central wire electrode to different treatments. It was apparent from these experiments that neither the kind of wire nor the condition of its surface made much difference in the behavior of the counter. The writer has extended these experiments and has obtained information which indicates that the sensitive surface is on the inner wall of the tube which serves as the negative electrode. This paper describes the results which have been obtained and gives a qualitative discussion of the problems involved in attempting a complete explanation of the operation of the counter consistent with current ideas regarding the nature of gas discharges in general. In any attempt of this kind one is confronted with the problem of the conflicting theories of the conduction of electricity in gases which makes the development of a quantitative theory, which may be tested numerically, exceedingly difficult. Even in a discussion such as is offered here it is necessary to make more or less arbitrary assumptions regarding the elementary processes which are responsible for the formation of an electrical discharge through a gas. As an example of the kind of difficulty referred to, one may consider the fundamental problem of the rôle of the positive ion in the production of ions. There is to date no definite answer to the question whether it does or does not form new ions by impact under conditions which usually obtain in a discharge tube. In spite of numerous uncertainties of this kind it is possible to develop qualitatively an explanation which accounts for the main facts so far known about tube counters by making use only of assumptions with fairly strong experimental evidence supporting them.

The problem of the action of the counter involves considerations quite apart from those of a simple electrical circuit containing capacity and resistance. As can be seen from the diagram shown in Figure 1

[1] B. S. Jour. Research, 4 (RP167), p. 601; May, 1930.

of a typical arrangement of a tube counter, it is in reality a cylindrical condenser in series with a resistance of the order of several megohms. Any electrical discharge occurring in the counter will be controlled to a great extent by the values of the capacity and the resistance of this circuit, and certain features of the action of the counter depend on a proper adjustment of these values. These may be regarded as subsidiary to the successful operation of a counter, however, since not every circuit of this kind can be made to function as a counter.

A brief description of the operating characteristics of a counter will suffice to make clear the difference between it and a simple discharge tube. The most prominent feature in this connection is the existence of a range of voltage which, when applied to the counter, making the tube negative, does not cause an appreciable current to flow, not more than 10^{-9} amperes in most cases. With the voltage so adjusted, however, if the counter is working properly the entrance of a high-speed electron causes this current to jump up momentarily to about

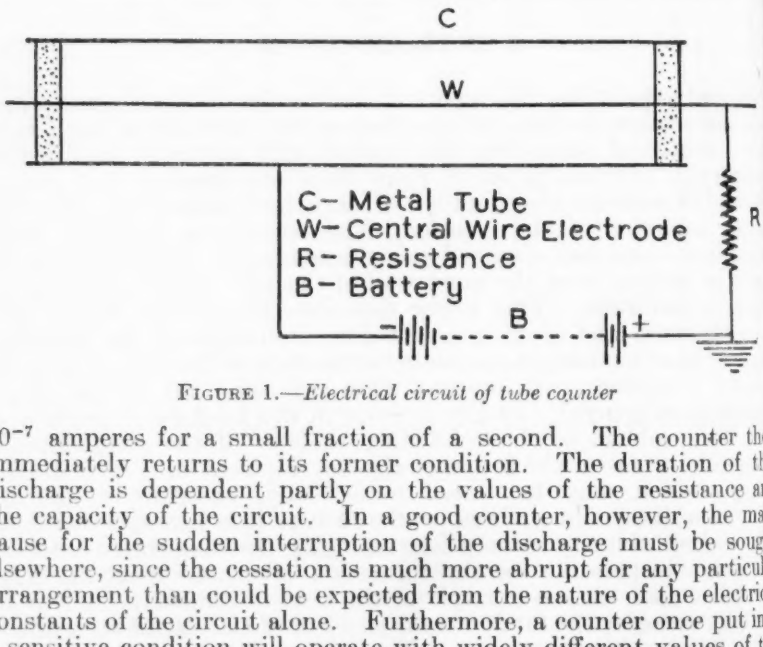

FIGURE 1.—*Electrical circuit of tube counter*

10^{-7} amperes for a small fraction of a second. The counter then immediately returns to its former condition. The duration of this discharge is dependent partly on the values of the resistance and the capacity of the circuit. In a good counter, however, the main cause for the sudden interruption of the discharge must be sought elsewhere, since the cessation is much more abrupt for any particular arrangement than could be expected from the nature of the electrical constants of the circuit alone. Furthermore, a counter once put into a sensitive condition will operate with widely different values of the resistance whereas a counter not sensitive for any one value of the resistance can not, in general, be made to work with any other resistance. It is the problem of what might be called the sensitizing of the counter which is primarily considered here. A further examination of methods of preparation which appear to produce counters sensitive to single electrons, as well as methods of preparation which fail to produce sensitive counters, has been made and an explanation of the results has been attempted along lines consistent with the present ideas concerning ordinary electric discharges in gases at the pressures used in the counter.

II. RECENT EXPERIMENTS ON THE LOCATION OF THE SENSITIVE SURFACE

It is important for the development of the explanation to be offered here to consider some facts concerning the behavior of tube counters which seem so far to have escaped observation. It has been assumed by Geiger [2] that the surface of the wire is the sensitive surface since it seems to require special treatment for successful operation of the counter. Kniepkamp [3] and also the writer [4] have been able to operate counters quite successfully using wires with no special treatment whatever. In fact, the writer has been unable to find any kind of wire or surface which will not work successfully for the central electrode. Experiments in this laboratory [5] have shown, however, that these counters are susceptible to adsorptive poisoning and this result has been interpreted by the writer to mean that the ordinary adsorption occurring on all surfaces exposed to gas is sufficient to provide a sensitive surface. A review of these experiments on the effect of poisons reveals, however, that the same effects would be observed if the sensitive surface were not on the wire, but on the inner wall of the tube. Although this seemed improbable at first, the writer is now convinced that such is the case, and this explains why any kind of wire or surface will serve as a central electrode. Attention was accidentally drawn to the possible importance of the inner surface of the tube when a brass tube counter, which had recently been "polished" with emery paper to remove radioactive contamination, failed to respond to the presence of a gamma ray source in the neighborhood. In consequence of this observation a

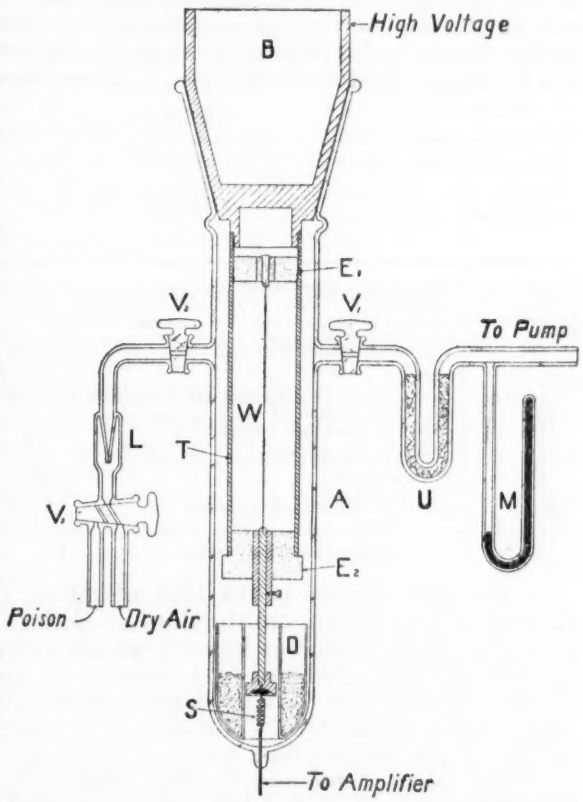

FIGURE 2.—*Apparatus for testing sensitive condition of tube counters*

[2] Geiger, H., and Müller, W., Phys. Z. S., **29**, p. 839; 1928; **30**, p. 489; 1929.
[3] Kniepkamp, H., Phys. Z. S., **30**, p.237; 1929.
[4] See footnote 1, p. 115.
[5] See footnote 1, p. 115.

considerable number of trials have been made of various kinds of surfaces. As a result it has been found that the nature of the surface on the inner wall of the chamber is important. Although the preparation of this surface is not as critical as the preparation of a point for a point counter, it seems to play a very similar rôle in the operation of the counter.

For investigating the effect of various surfaces, the apparatus described in the work[6] referred to above was used since it makes it relatively easy to change the counters and evacuate them. It is shown in Figure 2. The experiments, which were mainly qualitative in nature, consisted in evacuating the counter to a suitable pressure of dry air, say 3 cm, and then adjusting the voltage between 1,000 and 2,000 volts, and noting whether at any voltage it would respond to the presence of a gamma ray source when brought up to within a few feet of it. A summary of these trials has been arranged in Table 1.

TABLE 1

Metal	Treatment	Kicks per minute	
		Source present	Source removed
Copper	Polished with emery paper	99	
Brass	Untreated	150	
Copper	Heated in flame	165	
Brass	Lacquered inside	32	
Do	Lacquered as above; then coated with a layer of soot from a flame	31	
Steel	Oxidized	118	
Do	Oxidized as above and coated with a thin layer of vaseline	(1)	(1)
Copper	Coated with sodium silicate	(2)	(2)
Do	Coated as above then with soot	133	
Steel	Oxidized in flame, left in moist air over night	52	
Do	Freshly oxidized	143	
Do	Coated with soot	182	
Copper	Oxidized and reduced in hydrogen	89	

[1] No kicks could be obtained. [2] No kicks.

In the first column is the kind of metal; the second gives the method of preparation and the third gives the number of kicks when a radium preparation was brought within a definite distance of the counter and when removed to a considerable distance behind a wall. It is at once obvious that the inner wall does not seem to require a very careful preparation. However, it is equally obvious that the nature of the surface does have an effect on the operation of the counter. Most significant in this connection are the experiments with counters lacquered inside and those coated with sodium silicate. It might be argued that the insulating properties of the lacquer prevented the counter from responding and that the soot was sufficiently conducting to permit it to operate. Sodium silicate, however, is a fairly good conductor so the only way that the soot played a part in this case was to alter the nature of the surface. The behavior of so-called bare metal surfaces is also peculiar, although very little can be said on this point without more experiments. Apparently a metal surface prepared in approximately the same way does not always yield a sensitive surface. This is not surprising when one considers the rapidity with which oxide films form on the surfaces of freshly cut metals.

[6] See footnote 1, p. 115.

When dealing with such a large surface, it is very difficult to make certain that all parts have received the same treatment and are in the same condition from the standpoint of adsorption. Consequently, it is not surprising that at times effects are not always definitely reproducible. For our present purpose, it is sufficient to know that some surfaces are not satisfactory for the inside of the tube in these counters and that we are, therefore, justified in assuming that the sensitive surface is in this case not on the wire, but on the inner wall of the tube.

The results mentioned above become more significant when it is recalled that clean metal surfaces emit electrons with great difficulty under bombardment by electrons or positive ions. Coating such metals with alkali earth oxides increases the facility with which they emit electrons under bombardment.[7] This and other similar effects suggests that a secondary process is involved in the operation of the counter. This process may be supposed to be the liberation of electrons from the outer wall of the counter, the ionization produced by these electrons, as they are drawn to the central electrode, constituting the major part of the ionization current which is necessary in order that the counter may respond. The following discussion assumes the existence of such a secondary process.

III. DISCUSSION OF OPERATION OF COUNTER

The operation of the counter can now be explained on the basis of the following assumptions, both of which have some experimental support: (1) Ionization by impact is produced only as a result of collisions of electrons with gas molecules. (2) Positive ions contribute to the production of ions by releasing electrons from the surface of the negative electrode.

Since these assumptions may appear entirely arbitrary, it may be well to point out what justification exists for them. As regards ionization by impact, it is generally agreed that most of the ionization produced in a gas when a current flows results from the collision of electrons with molecules. For currents produced at voltages below the sparking potential, the entire current can be accounted for in this way.[8] When the sparking potential is approached, however, there is a well-known more rapid increase in the current that can not be accounted for as the result of collisions of electrons with gas molecules. As Townsend points out in the paper last referred to, this additional ionization may be accounted for in several ways. It may be attributed to the impact of positive ions with gas molecules; it may result from the release of additional electrons from the negative electrode by the positive ions; or it may result from the photoelectric action of radiation falling on the negative electrode and thus releasing additional electrons. Each one of these views has been supported by some experimental evidence by various investigators. Townsend favors the view that the additional ionization is produced by impact of positive ions on gas molecules. There is at present, however, little or no direct evidence to confirm this view so that one may feel justified in excluding it. There are,

[7] H. D. Arnold, Phys. Rev., **16**, p. 70; 1920.
[8] Townsend, J. S., Phil. Mag., **45**, p. 444; 1923.

however, numerous recent experiments [9] [10] which give strong support to the idea that positive ions only produce additional ionization by releasing electrons from the negative electrode. The particular way in which this release of electrons occurs has been strongly debated by various authorities.

The writer favors the view that this release occurs as a result of electrostatic attraction between the negative and positive ions. The difficulty with the other obvious mode of release—bombardment of the cathode by positive ions—is illustrated by the example cited by Townsend to show that such an effect is impossible. He refers to the experimental fact that, in the case of a radial field of force between a wire and a coaxial cylinder, there is a critical value X_1 of the electrical field at the surface of the wire with which a small continuous glow discharge is maintained between the wire and cylinder. Let a be the radius of the wire, b that of the cylinder. It has been found experimentally that X_1 is independent of b, provided b is greater than a certain radius c. The value of c, of course, depends on a and the pressure of the gas. As Townsend remarks, in order to account for the fact that X_1 is independent of b, it is necessary to assume that, in the case of a positive current flowing from the wall to the cylinder, which is the case exemplified by the counter, either no electrons are set free from the surface of the cylinder or that the same number are liberated from a cylinder of large diameter as from one of small diameter. The electric field at the surface of the cylinder is $\frac{a}{b} X_1$, neglecting a distortion of the field due to accumulated charges on the surface; and, by increasing b, the intensity of the electric field near the surface of the cylinder may be reduced so that the positive ions would move with such small velocities that they could neither generate ions nor excite radiation on impact with the wall. There seems to be no escape from this argument. Consequently, the obvious solution to the problem thus presented is that the positive ions do not liberate electrons from the walls by impact, but by virtue of their electrostatic attraction for electrons on the walls. This idea is supported by Holst and Oosterhuis.[11] It is then very easy to see how the same number of electrons may be liberated from a cylinder of large diameter as from one of small diameter, since the number of electrons released is not directly connected with the velocity of the positive ion at the moment of impact. The only requirement is that the velocity of the positive ion should be great enough to prevent recombination and immediate neutralization of the electron as soon as liberated. This requirement is easily met, since Mohler and Boeckner [12] have been able to show that even the velocity of thermal agitation is sufficient to prevent recombination.

Since the experiments described in this paper show that the nature of the surface of the tube is the important factor in the operation of the counter, it is fairly certain that the gas layer on the tube wall and not that on the wire forms the sensitive surface which is disturbed by gas poisons. This renders the explanation given by the writer in a previous article no longer in accordance with the facts.

[9] Klemperer, O., Z. S. f. Physik, **52**, p. 650; 1928.
[10] Müller, W., Z. S. f. Physik, **48**, p. 624; 1928.
[11] Holst, H., and Oosterhuis, E., Phil. Mag., **46**, p. 1117; 1923.
[12] Mohler, F. L., and Boeckner, C., B. S. Jour. Research, **3**, p. 303; 1929.

since it was there assumed that the sensitive surface was located on the wire. With this new fact available and using assumptions (1) and (2) it is now possible to give an explanation which more nearly agrees with that offered for the point counter. It will be noted that in both cases the sensitive surface may now be assumed to be on the negative electrode. The chief difference between the two counters as regards principle of operation is that it is usually more satisfactory to use the point counter with the point negative while the tube counter only seems to work well with the tube negative. Thus in the case of a point we have a cathode of very small area in a very intense electric field while in the case of the tube the cathode has a very large area and is in a relatively weak field. This important structural difference is responsible, in the writer's opinion, for most of the differences in behavior between the two types of counters.

The stages of the process by which a count is registered may be outlined as follows: The electron to be counted produces a few pairs of ions as it passes through the gas of the chamber. This primary ionization is entirely too small to register on any of the usual instruments used for detecting the electrical impulse produced by counting. The positive ions move to the tube wall and the negative ions, presumably mainly electrons, go to the wire. As they pass to the wire they pass through the region of intense electric field and produce ions by impact, but even this ionization will be relatively feeble, representing currents which are only a small fraction of those observed when a count is registered. The amplification to be accounted for is of the order of 10^8. To account for the total ionization an additional supply of electrons is required. These come, according to the views set forth here, from the negatively charged tube; being released from the gas layer on the surface of the tube by the electrostatic attraction of the positive ions as they approach the walls of the tube. It is important to note, as shown above, that not all surfaces of the tube are sensitive, and this can be expected since it is reasonable to suppose that only certain types of surface will provide a layer of gas such that electrons may be released from it by positive ions. In such a case the additional ionization current required to register a count can not be obtained and the counter fails to function. It is also likely that a variety of surfaces would work here, since the electric fields are relatively weak and the time during which electrons are within a strong attractive field from the positive ion is relatively much longer than in the case of a point counter with positive points. This may be the explanation for the fact that a negative point must have a very careful preparation, whereas many kinds of surface will work in the case of the negative tube.

Such a discharge process as that outlined in the preceding paragraph should be self-sustaining. The counter, however, when it is properly registering counts, maintains a discharge for a very short period of time for each high-speed photoelectron which enters it, a period estimated as of the order 1/1000 second.[13] To interrupt the discharge in this way it is necessary to suppose that for some reason the positive ions very suddenly lose their ability to pull electrons from the cathode surface. Since our experiments point to a special condition of the surface required for operation, it is logical to conclude that the operation of the counter in registering a count so alters this

[13] Bothe, W., ZS. f. Phys., **59**, p. 1; 1929.

special surface that, after the discharge has proceeded for this ver brief space of time, it is no longer in the sensitive condition at th particular location on the chamber wall. The layer of adsorbe gas is so modified or disturbed that no electrons are released. A soon as the discharge stops, however, the cathode restores itself to it former condition by adsorption and is then in condition again t respond. This disturbed area of the surface probably is a small par of the total area of the tube, but owing to the relatively great surfac of the tube wall affected, as compared with that of a point, thi restoration does not need to occur quickly to register counts in rapi succession. This provides another reason why one would not expec the condition of the surface of the tube to be as critical as that of th point.

This explanation requires that a sensitive surface should have th property of releasing electrons on the approach of positive ions mor readily than an insensitive surface. It might be expected that sensitive counter would function at a voltage lower than the sparkin potential for an insensitive counter. This seems to be true in general but, if our assumption that the release of electrons by positive ions i independent of the mean kinetic energy of the positive ion, the applie voltage would not be affected. Furthermore, any small change o the applied voltage will not greatly affect the mean kinetic energy o the positive ions near the surface of the tube, since this is a region o weak electric fields. The mean kinetic energy of the positive ions i given by the product of the field strength and the mean free path. Since the mean free path is inversely proportional to the pressure, th mean kinetic energy may be expressed in terms of volts per centimete divided by the pressure in centimeters of mercury. For the usual tub counter the mean kinetic energy expressed as $\left(\text{kv/cm} \times \frac{1}{\text{cm of Hg}}\right)$ for the positive ions near the walls is from 0.1 to 0.01. Klemperer[14] has analyzed data on gas discharges and shows that, in the range o mean kinetic energies from 0.5 to 10 in the above units, the ratio o liberated electrons to incident positive ions increases by a factor o nearly a hundred. Since the mean kinetic energies used in his analysi are considerably higher than those existing in a counter it may b that at such higher energies impact is effective in releasing electron from the gas layer.

On the other hand, extrapolating his figures to the values of kineti energy of positive ions in the counter, the ratio of liberated electron to incident positive ions becomes a very small fraction, of the order o 1/100,000. This seems to show that in the counter impact can n longer be effective in releasing electrons from the walls. Nothin definitely is known concerning the surfaces of the ionization vessel in which the measurements which he has analyzed were made, and i might be that these figures refer to a wall surface similar to that of an insensitive counter. If we are to accept Townsend's argument supporting the view that the number of electrons liberated from th negative outer electrode by positive ions is independent of the diam eter of the outer electrode, it is clear that the effect that Klemperer deduces does not exist, since the experiment which Townsend cites would seem to prove conclusively that if positive ions do liberate

[14] Klemperer, O., ZS. f. Physik., 52, p. 650; 1928.

electrons the number liberated is independent of the velocity of the positive ion.

In addition to giving more information regarding possible explanations for the action of the tube counter, the experiments here discussed appear to throw additional light on the nature of certain kinds of gas discharges themselves. Considerable support seems to be offered the idea that the release of electrons from the cathode may occur by electrostatic attraction, since by such an assumption a satisfactory explanation is readily obtained for the operation of the counter. There are strong reasons, as has been pointed out, for making the release of electrons from the cathode the important feature in the operation of the counter. It does not appear obvious how this may be accomplished by impact of positive ions under the conditions discussed. The release by electrostatic attraction, on the other hand, provides a method which avoids all difficulties associated with the kinetic energy of the positive ion in relation to its efficiency in releasing electrons. In conclusion the writer wishes to thank L. L. Stockman and H. L. Martin for helping in preparing and testing various kinds of counters, and Dr. J. H. Hibben for valuable suggestions.

WASHINGTON, January 25, 1930.

FLOW CHARACTERISTICS OF SPECIAL Fe–Ni–Cr ALLOYS AND SOME STEELS AT ELEVATED TEMPERATURES

By H. J. French, William Kahlbaum,[1] and A. A. Peterson

ABSTRACT

The results of "creep" tests at different temperatures are given for three groups of alloys. The 11 metals in the first group included commercial alloys of nickel, chromium, and iron, both with and without tungsten, and low chromium steels containing also tungsten, vanadium, or molybdenum. The second group comprised two carbon steels, a 3½ per cent nickel steel and two low nickel chromium steels which were tested only at 700° F.; the 12 alloys of the third group were melted in a high-frequency induction furnace, and their compositions were selected to show the general trends at 1,000° F. in the load-carrying ability of castings of the nickel-chromium-iron system. A metallographic study of the creep-test specimens revealed intercrystalline weakness in some of the wrought nickel-chromium-iron alloys especially at temperatures between 1,160° and 1,390° F. A study was also made of the effect of deformation in the creep tests at different temperatures on the hardness and impact resistance of a chromium vanadium steel at atmospheric temperatures.

CONTENTS

	Page
I. Introduction	125
II. Test methods	126
III. Materials tested	130
IV. Results and discussion	131
1. General relations between stress, temperature, deformation, and time	131
2. Commercial nickel-chromium-iron alloys	143
3. Carbon and low alloy steels	174
4. Effect of prolonged stress at different temperatures on hardness and impact resistance at atmospheric temperatures	175
5. Trends at 1,000° F. in the system Ni–Cr–Fe	177
V. Summary	181
VI. Acknowledgments	183

I. INTRODUCTION

Considerable attention is now being given in both this country and Europe to "creep" tests (or flow tests) in which the time-deformation relationship is determined for metals subjected to constant loads for long periods at approximately constant temperatures. Previous tests at the Bureau of Standards have related jointly to the development of a testing technique and to the procurement of data intended to assist engineers in the selection of safe working stresses for equipment designed to operate at elevated temperatures. Correlations have also been made between the laborious flow tests and short-time tension tests with the object of finding, if possible, rapid methods of determining approximately the load-carrying ability of metals at different temperatures.

[1] Research associate, The Midvale Co., Philadelphia, Pa.

So far, data have been published for only five steels, and the purpose of this report is to present the results of additional tests extending over several years so that comparisons can be made of a wider range of metals, based on data secured under comparable conditions in one laboratory. The work simply represents the extension to more materials of the methods of test already described in detail.[2] [3] [4]

Tests were made of three groups of metals; the first, comprising commercial nickel-chromium and nickel-chromium-iron alloys and low-chromium steels containing tungsten, vanadium, or molybdenum, were tested, with one exception, under the research associate plan[5] with a research associate from The Midvale Co., Philadelphia, Pa. The second group consisting of two carbon steels, a 3½ per cent nickel steel and two low nickel-chromium steels were tested at 700° F. to assist the Bethlehem Steel Co., Bethlehem, Pa., and the Combustion Engineering Corporation, New York, N. Y., in the selection of a composition suited for particular requirements of power-plant construction. The metals of the third group were used in a study of the flow characteristics at 1,000° F. of alloys of the nickel-chromium-iron system.

II. TEST METHODS

The test methods employed were substantially the same as those used previously, but subsequently to the last published descriptions a number of modifications were incorporated in the equipment and test procedure. Four of the ten horizontal loading machines were replaced by vertical units (fig. 1) in which the frictional losses of the mechanical lever system were materially reduced. The new units were, therefore, better adapted than the old horizontal units for tests at the highest temperatures where the applied loads were the smallest.

The temperature fluctuations within the test specimens were reduced by placing the control thermocouples at the furnace windings instead of in the test specimens. Resistors of improved form (fig. 2) were installed in the furnaces of the vertical test units to reduce the temperature gradients from top to bottom in the test specimens. In order to secure greater accuracy in the length measurements with the metals which oxidized most readily, the practice was followed of using platinum or silver wire (32 B. & S. gage) in small grooves as reference points for length measurements with an optical micrometer instead of the edge of the enlarged end section of the specimen.

Only a limited quantity of some of the metals was available. The desire to secure the maximum information under such conditions led to the adoption of a specimen having two different diameters within the customary 2-inch gage length as is shown in Figure 3. A given applied load produced different unit stresses in the two halves of the gage length of such a specimen, and this was equivalent to two of the customary specimens. However, the use of the modified test specimen is not advocated under ordinary conditions. It is disadvan-

[2] H. J. French and W. A. Tucker, Flow in a Low-Carbon Steel at Various Temperatures, B. S. Tech. Papers No. 296; 1925.
[3] H. J. French, Methods of Test in Relation to Flow in Steels at Various Temperatures, Proc. Am. Soc. Test. Matls., **26**, p. 7; 1926.
[4] H. J. French, H. C. Cross, and A. A. Peterson, Creep in Five Steels at Different Temperatures, B. S. Tech. Papers, No. 362; 1928.
[5] Described in Circular No. 296 of the Bureau of Standards

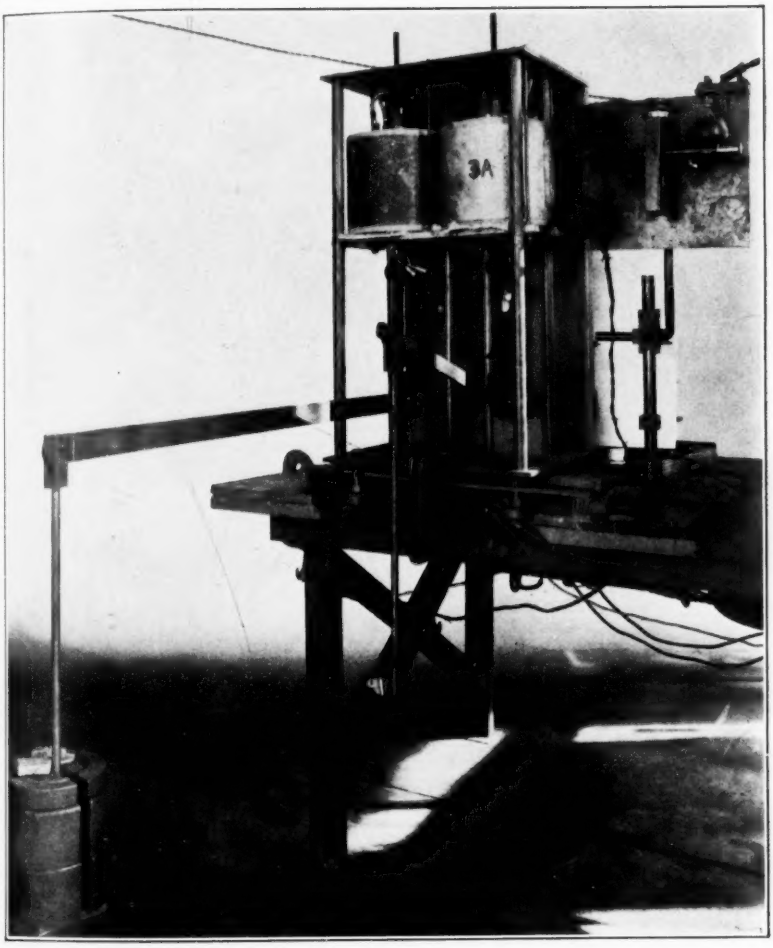

FIGURE 1.—*Two of the vertical test units for flow tests at different temperatures*

Four vertical and six horizontal test units constituted the testing equipment for the flow tests. The optical micrometer used in making length measurements is shown on the stand at the right.

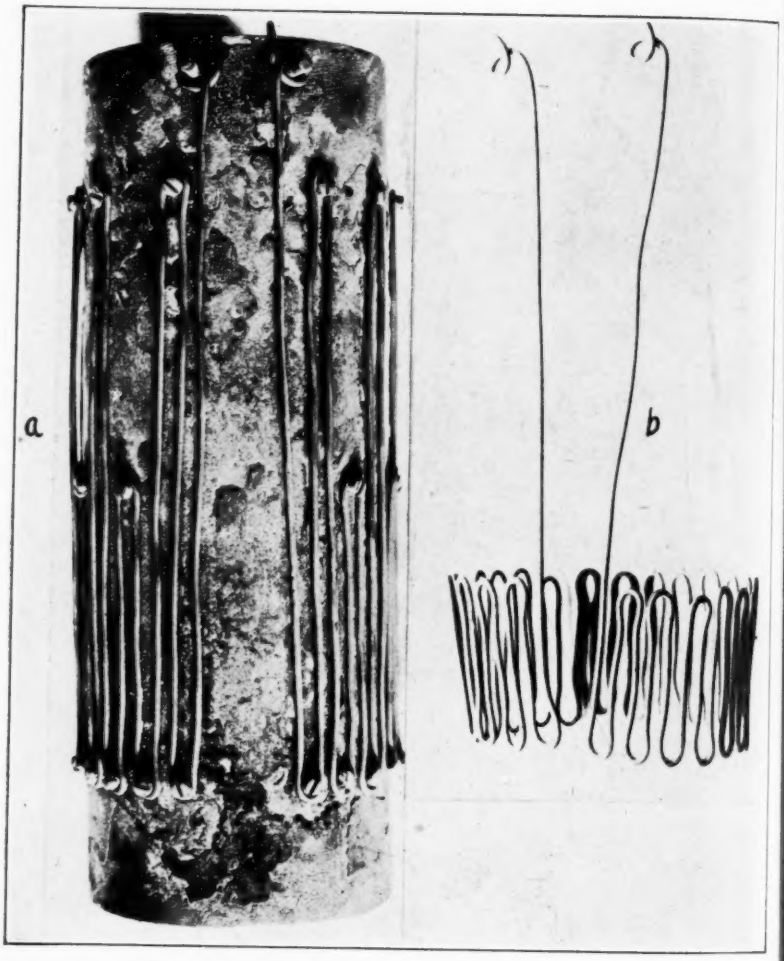

FIGURE 2.—*Improved resistors of the heating units*

a, The main resistor on the forming fixture; *b*, auxiliary resistor placed outside and at the lower end of the main resistor.

...geous to reduce the measured length from 2 inches to 1 inch and ...e abrupt change in section at the center of the 2-inch gage length ...ay introduce stress concentrations and also tend to increase the ...mperature variations in the test sections. As a result, the flow

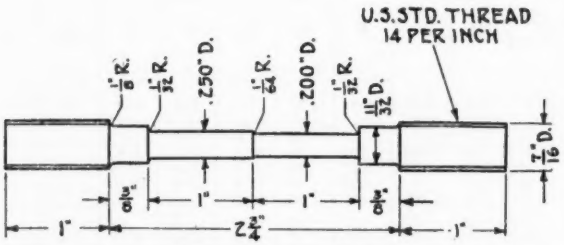

FIGURE 3.—*Modified flow test specimen used in some of the tests*

The flow under two different stresses can be followed on the one test specimen. See text for discussion.

...roduced by a given stress in the large half was not always as close as ...ould reasonably have been expected to that produced by the same ...tress in the small half of the gage length. In cases of doubt many ...f the tests were repeated on test bars having a gage length of uniform ...iameter.

TABLE 1.—*Chemical composi*

Group I.—TESTED AT DIFFERENT TEMPERATURES

Designation	Chemical composition											
	C	Mn	P	S	Si	Ni	Cr	W	Mo	V	Fe	Cu
	Per cent [1]	*Per cent* [1]	*Per cent* [1]	*Per cent* [1]	*Per cent* [1]	*Per cent* [1]	*Per cent* [1]	*Per cent* [1]	*Per cent* [1]	*Per cent* [1]	*Per cent* [1]	*Per cent* [1]
K4	0.31	2.79			0.27	76.0	18.8				0.80	
E1894	.25	1.40	0.028	0.020	.06	60.8	10.75	2.8				
FS-1, lot A	.19	1.62	.028	.027	.10	57.6	10.28	3.19				
FS-1, lot B	.20	1.66	.026	.029	.08	57.4	10.34	3.30				
FS-2, lot A	.32	1.52	.028	.038	.03	34.9	12.93	tr.				
FS-2, lot B	.28	1.45	.032	.027	.03	35.9	11.12	.34				
E1567	.28	1.50	.024	.018	.07	38.6	10.64	1.77				
EE1114	.29	.50			1.18	8.0	19.86	4.5				
E1912	.15	.35	.020	.021	.22	8.46	17.32					
10-518, lot A	.40	.57			.25		2.26			0.20		
10-518, lot B	.40	.57			.25		2.26			.20		
EE1139	.46	.37			.19		2.2	1.65		.25		
E1549	.53	.95	.037	.015	.23		1.07		0.44			
E1490	.75	.52	.028	.016	.31	.15	1.45		.54	.27		
Group II.—TESTED AT 700° F. (370° C.)												
4H451	0.23	0.48	0.015	0.024	0.18	0.05						
2H384	.45	.55	.016	.027	.15	.24						
4H247	.37	.68	.018	.023	.21	3.46						
1H391	.36	.63	.014	.022	.19	1.25	0.62					
1H396	.35	.49	.017	.017	.19	1.66	0.99					
Group III.—TESTED AT 1,000° F. (540° C.)												
1000A	0.19	0.75			0.69						Bal.[3]	
1001D	.25	.80			.89	Bal.						
1002A	.24	.88			.52	68.5					Bal.[3]	
1003A	.18	.75			.57	30.6					Bal.[3]	
1004A	.37	.67			.53		14.5				Bal.[3]	
1004B	.24	.59			.39		14.6				Bal.[3]	
1005B	.38	.73			.82		30.2				Bal.[3]	
1006B	.49	.68			1.01		55.3				Bal.[3]	
1007B	.51	.74			.75	78.2	18.3					
1008B	.24	.88			1.14	49.7	46.3					
1009A	.41	.53			.78	58.7	14.8					
1010A	.11	.54			.77	25.5	16.4					
1011A	.11	.59			.87	35.4	27.2				Bal.[3]	
Group IV.—STEELS PREVIOUSLY TESTED (INCLUDED FOR CONVENIENCE OF GENERAL COMPARISONS)												
K3	0.24 .39	0.37 .51	0.021 .015	0.028 .029	0.01 .19		0.87		0.21			
A336	.77	.24	.031	.035	.42	0.14	3.9	13.6		1.9		
A340	.28	.38	.026	.013	.17		20.5					0.98
A347	.24	.53	.009	.005	2.96	23.3	18.05					

[1] As reported by the maker for Groups I and II; by the Bureau of Standards, H. A. Bright, for Groups III and IV.

[2] Specimens cut at 90° to the direction of rolling, half way between center and surface of blooms at some distance from the ends.

and other details of the metals

Group I.—TESTED AT DIFFERENT TEMPERATURES

Specimens taken from—	Treatment before test	Properties at room temperature				
		Yield point	Tensile strength	Elongation in 2 inches	Reduction of area	Brinell No.
		1,000 lbs./in.[2]	*1,000 lbs./in.*[2]	*Per cent*	*Per cent*	
Rolled ¾-inch bars	1,900° F., 3 hours air cooled	39.5	116.5	37.5	50.3	
Riser from casting	Annealed 1,470° F	23.0	75.2	10.0	11.5	
Rolled bars	As rolled	63.0	112.5	30.0	36.9	207
....do	Annealed 1,650° F	57.5	110.0	31.0	51.6	200
....do	As rolled	68.0	100.0	33.0	54.1	181
....do	Annealed 1,650° F	54.0	99.5	33.0	47.7	172
As rolled		69.0	120.5	24.0	44.9	
Experimental melt, forged.						
Rolled bars	Lot A	40.0	95.0	45.0	60.0	
	Lot B, 1,850° F., water	64.8	112.2	[3] 54.5	[3] 63.5	
....do	1,575° F., 1 hour slow cool; 1,375° F., 1 hour furnace.	54.2	87.2	28.3	69.2	
....do	1,575° F., 1 hour air; 1,300° F., 1 hour furnace.	86.0	105.6	23.7	68.2	
Experimental melt, rolled.	1,400° F., 2 hour slow cool; 1,740° F., 1 hour oil; 1,000° F., 1 hour air cool.	207.0	231.5	7.8	22.8	444
Forged bars	1,550° F., 1 hour oil; 1,200° F., 4 hours slow cool.	124.0	143.0	[4] 18.7	[4] 56.0	
....do	1,550° F., 1 hour oil; 1,100° F., 4 hours slow cool.		174.0	[4] 7.5	[4] 16.7	

Group II.—TESTED AT 700° F. (370° C.)

6 by 6 inch rolled blooms.[2]	1,650° F., 4 hours furnace; 1,600° F., 4 hours air; 1,330° F., 4 hours furnace.	39.0	60.0	17.5	29.2	
5 by 5 inch rolled blooms.[2]	1,650° F., 4 hours furnace; 1,500° F., 4 hours air; 1,330° F., 4 hours furnace.	42.5	80.0	17.0	27.5	
6 by 5 inch rolled blooms.[2]	1,650° F., 4 hours furnace; 1,500° F., 4 hours air; 1,360° F., 4 hours furnace.	57.0	97.0	16.0	25.1	
6 by 6 inch rolled blooms.[2]	1,650° F., 4 hours furnace; 1,500° F., 4 hours air; 1,280° F., 4 hours furnace.	55.0	94.0	15.0	17.0	
5 by 4 inch rolled blooms.[2]	1,650° F., 4 hours furnace; 1,500° F., 4 hours air; 1,320° F., 4 hours furnace.	52.0	93.0	24.0	47.7	

Group III.—TESTED AT 1,000° F. (540° C.)

1½ inch octagonal ingots weighing about 3 pounds.	1,650° F., ½ hour air cool					150
	1,500° F., ½ hour air cool					114
	1,650° F., ½ hour air cool					131
	1,450° F., 1 hour furnace cool					147
	1,650° F., 2 hours furnace cool					298–319
	....do					219–222
	1,800° F., 2 hours air cool					217
	1,900° F., 3 hours air cool					363–388
	....do					183
	....do					285
	....do					138
	2,000° F., 1 hour air cool					113
	1,900° F., 3 hours air cool					144

Group IV.—STEELS PREVIOUSLY TESTED (INCLUDED FOR CONVENIENCE OF GENERAL COMPARISONS)

1-inch hot-rolled plate		33.0	66.7	30.0	59.2	
1⅛-inch diameter rolled bars.	1,625° F., 2 hours air; 1,550° F., 1½ oil; 1,300° F., 2 hours oil.		98.5	22.0	70.9	
1-inch diameter rolled bars.	Tested "as received," probably annealed.	95.7	110.1	[3] 17.0	[3] 36.5	
½-inch diameter rolled bars.	1,830° F., water; 1,200° F., air	67.3	89.8	[3] 21.5	[3] 55.6	
1⅛-inch diameter rolled bars.	1,450° F., 2 hours furnace cool	49.0	110.0	33.0	47.5	

[3] Determined on tensile-test specimens with a diameter of about 0.25 inch and a gage length of 2 inches.
[4] Determined on tensile-test specimens with a section ⅝ by 0.1565 inch.
[1] Containing impurities, such as small amounts of phosphorus and sulphur.

III. MATERIALS TESTED

The composition and other details of the metals tested are summarized in Table 1. The 11 metals of the first group may be divided into three classes; the first comprised the one alloy, K–4, which was prepared for the Joint Research Committee on Effect of Temperature on the Properties of Metals [6] to represent the alloy 80 nickel, 20 chromium, widely used as resistance wire. Its composition is actually not representative of the bulk of the metal used in such wires, but it should serve to indicate in a general way the flow characteristics of this class of material. The second class in the first group comprised nickel-chromium-iron alloys both with and without appreciable proportions of tungsten, while the third class consisted of low-alloy steels having not more than 4 per cent of alloying elements.

The six nickel-chromium-iron alloys in the first group represent compositions which have been used industrially in the construction of chemical or engineering equipment operating at high temperatures. Alloys E1894 and E1567 were made in this country and the test bars from heat E1894 were taken from the riser of a casting and do not represent the best properties obtainable at either room or elevated temperatures (Table 1.) The similar alloys, marked FS–1 and FS–2 were made abroad.

Alloy E1912 is an austenitic steel of the type of Krupp's V2A and the English corrosion resistant steel called Stabrite. Since austenitic steels are often said to retain a high proportion of their room temperature strength at elevated temperatures, this nickel-chromium steel was included for comparison with the high-chromium "stainless" steels previously tested. Alloy EE1114 is similar to alloy E1912 with the exception that it has somewhat higher carbon and silicon and 4.5 per cent of tungsten.

The materials designated as E1894, FS–1, FS–2 and E1567 have been used extensively abroad and to a lesser degree in this country, the first two chiefly in the form of castings, the latter pair largely as forgings. Alloy EE1114 which has been used both in castings and in forgings, is claimed to be resistant to softening at elevated temperatures and to resist scaling, even in oxidizing and sulphurous atmospheres at temperatures as high as 2,000° F.

The chromium-vanadium steel, No. 10–518, Table 1, has been used widely for autoclaves, and, especially with a somewhat lower carbon content, for vessels for ammonia synthesis. The treatments to which this steel was subjected before test were intended to produce conditions comparable to those existing in the walls of forgings too large to quench and too thick to harden effectively in the air.

Steels EE1139, E1549, and E1490 are compositions used in cylinders for the extrusion of metals. Such cylinders, or the liners for such cylinders, are subjected to severe service. The material must flow only very slowly under fairly high pressures at temperatures as high as 1,200° or 1,300° F. and at the same time exhibit sufficient toughness to resist cracking.

The two carbon steels and the three low-alloy steels comprising the second group of metals in Table 1 were made in 75-ton basic open-hearth furnaces and cast into large-end-up, hot-top ingots.

[6] A committee sponsored by the American Society for Testing Materials and the American Society of Mechanical Engineers.

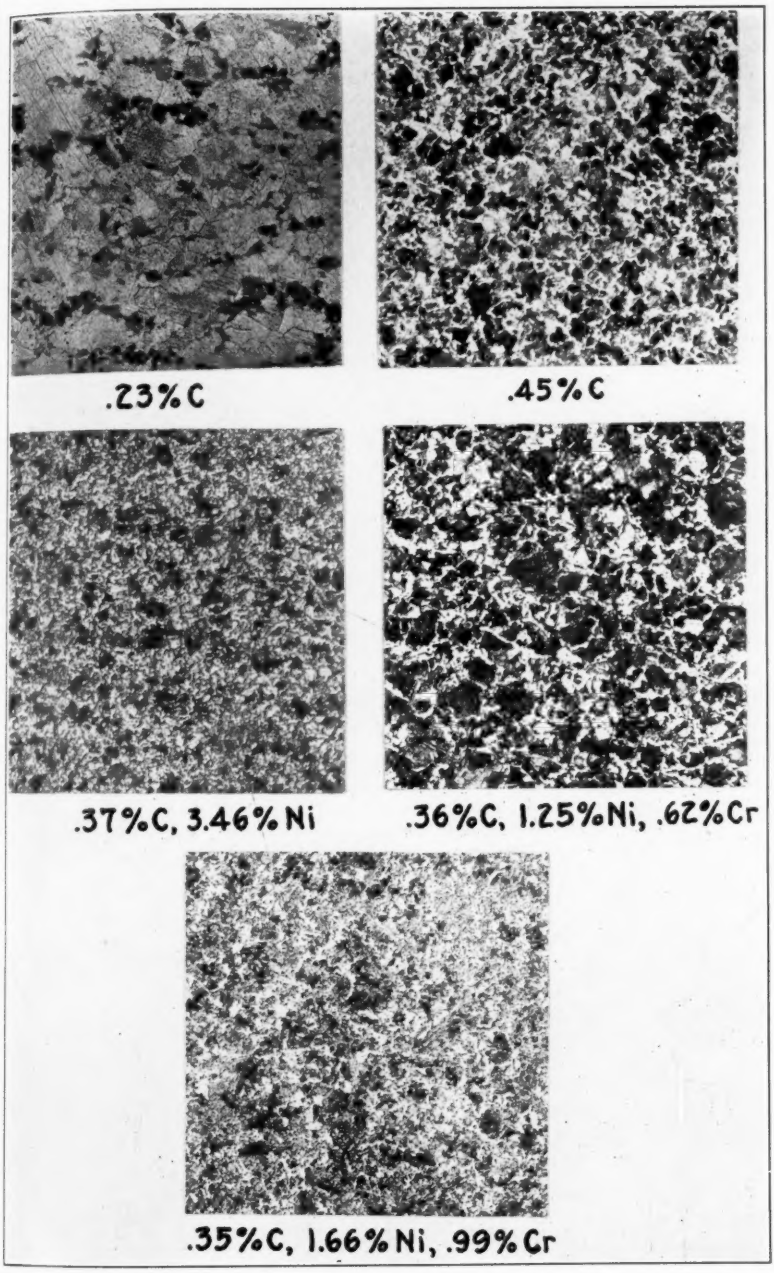

FIGURE 4.—*Micrographs of the steels of Group II, Table 1, in the conditions tested,* $\times 100$

These photographs supplied by the maker. Etched with 3 per cent HNO_3 in alcohol.

The ingots were charged hot into the soaking pits, and after being brought to the proper rolling temperatures, rolled to the bloom sizes shown in Table 1. After heat treatment, as indicated, flow test specimens were cut from the blooms, the long axis being at 90° to the direction of rolling, at points halfway between the center and surface, but at an appreciable distance from the ends. The heat treatment and the method of taking the flow test specimens were selected to represent the metal in large forgings for high-temperature, high-pressure, power-plant equipment, and the tests at 700° F., were made to assist in the selection of a steel to meet special design requirements. The specified heat treatments did not reduce the strengths of the steels at atmospheric temperatures to the desired values in all cases, and it was necessary to repeat the treatments for some of the steels in order to obtain the desired properties.

In view of the fact that some of these steels were heat treated more than once, the structural condition of the material as tested is shown in the micrographs of Figure 4.

The metals of the third group, Table 1, were melted in a high-frequency induction furnace, the charges being based on a carbon content of about 0.25 per cent, manganese of 0.5 per cent, and silicon of about 0.5 per cent. As far as was practicable, the nickel and chromium contents of the different alloys were selected to conform to those found in typical commercial alloys, but the primary basis of selection was a widespread scattering over the nickel-chromium-iron ternary diagram, so that the general trend of effects of composition on the flow characteristics at 1,000° F. could be determined. The alloys were all tested in the cast condition after being heat-treated as shown in Table 1.

The results of tensile tests at atmospheric temperatures or Brinell hardness tests are given in Table 1 for many of the materials in order to define better the conditions in which the different metals of the several groups were tested. Since the properties of the metals in Groups I and II are compared with those of five steels previously reported upon the chemical compositions and preliminary treatments of the latter have been included for convenience in Table 1.

IV. RESULTS AND DISCUSSION

1. GENERAL RELATIONS BETWEEN STRESS, TEMPERATURE, DEFORMATION, AND TIME

The flow of the metals of Groups I and II, Table 1, when loaded at different temperatures, is shown graphically in Figures 5 to 17, inclusive. The relations between stress, temperature, deformation, and time are similar to those observed in the steels previously tested and the time-elongation curves fall into three classes which depend upon the metal and the temperature.

At atmospheric and slightly elevated temperatures, initial changes in dimensions (initial flow) are not necessarily followed by continuous flow but, due to strain hardening, the rates of flow may decrease with time. In many cases the flow rates subsequent to the initial period (second stage of flow), may be considered to be zero for all practical purposes and determination of allowable working stresses is therefore a function of the permissible initial deformation.

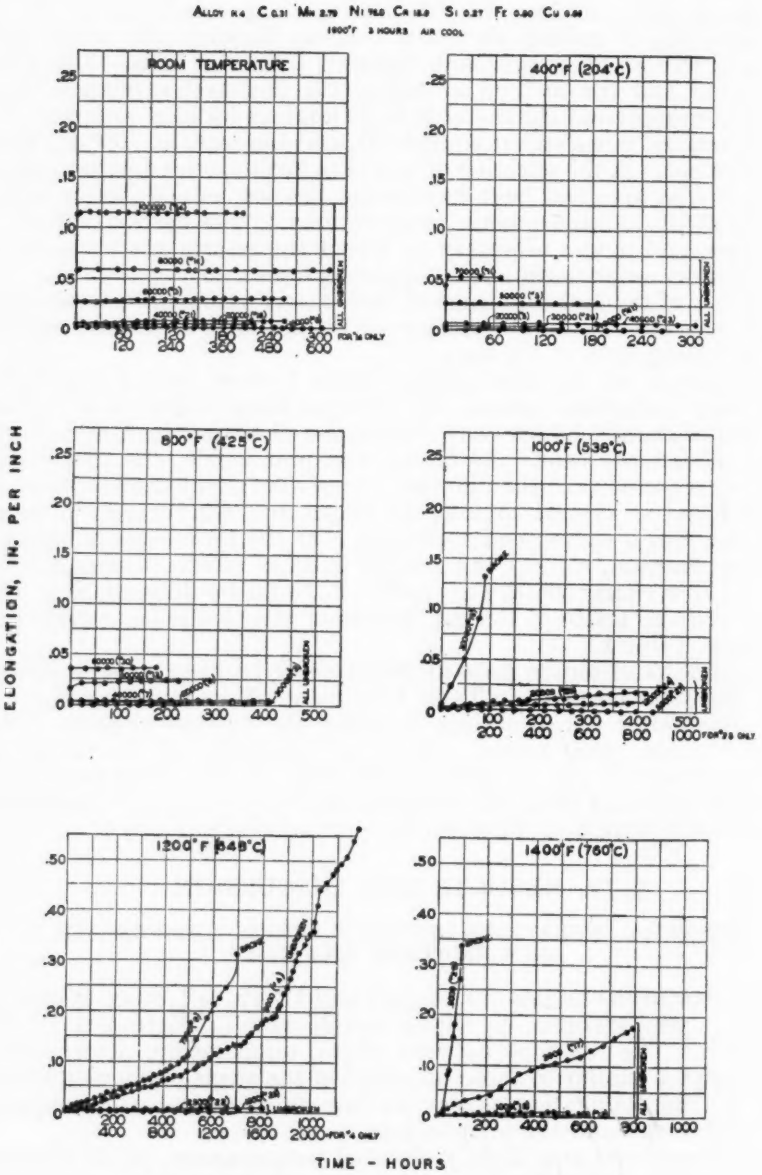

FIGURE 5.—*Time-elongation curves for the alloy K–4*

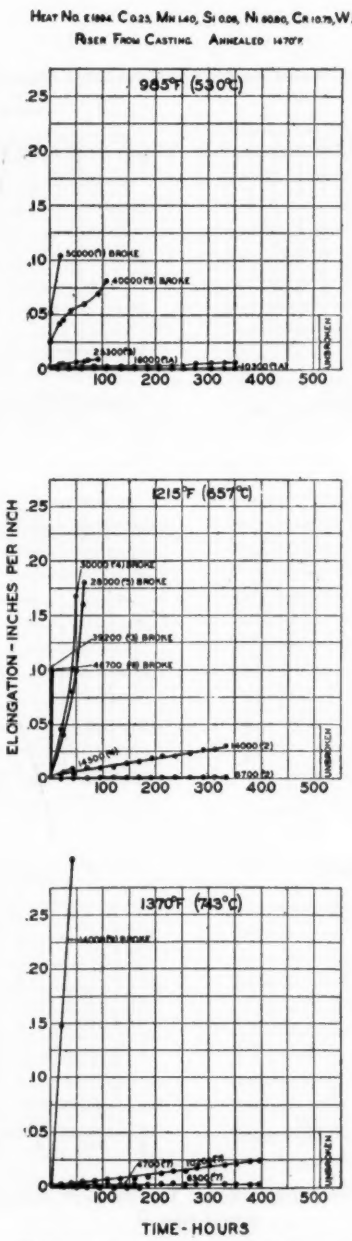

FIGURE 6.—*Time-elongation curves for the Ni-Cr-Fe alloy E1894*

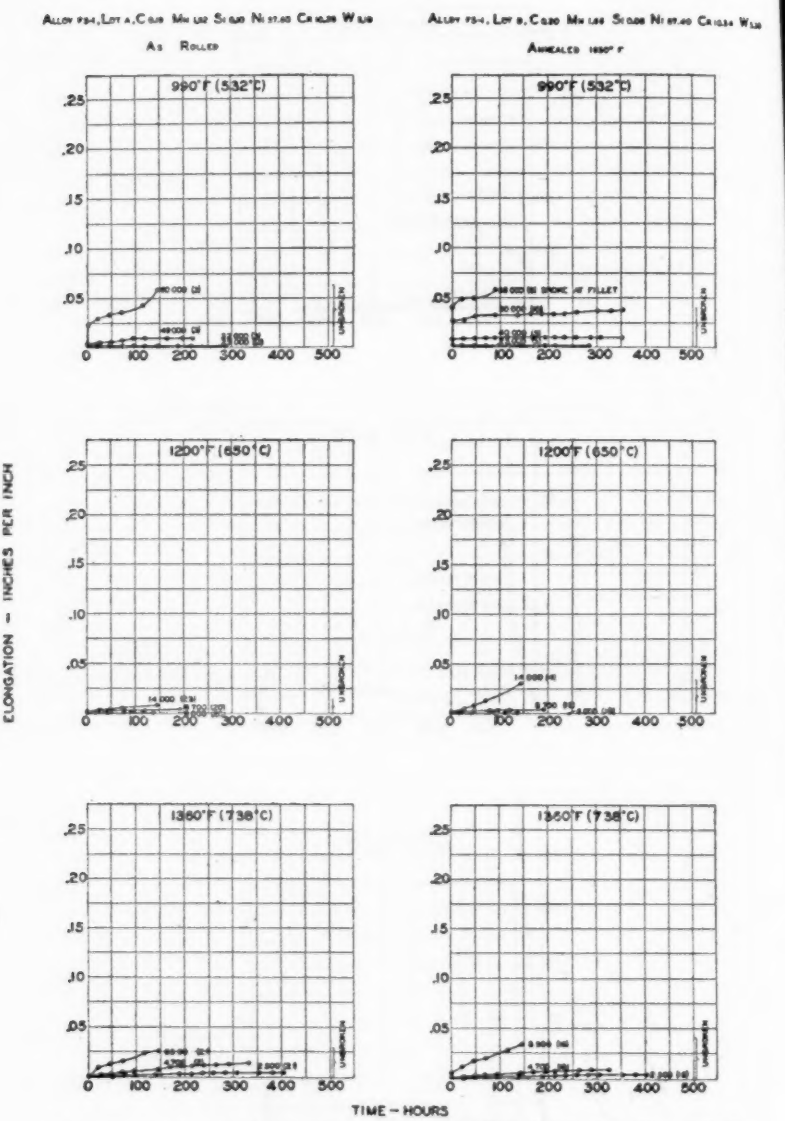

FIGURE 7.—*Time-elongation curves for the Ni-Cr-Fe-W alloy FS–1, lots A and B*

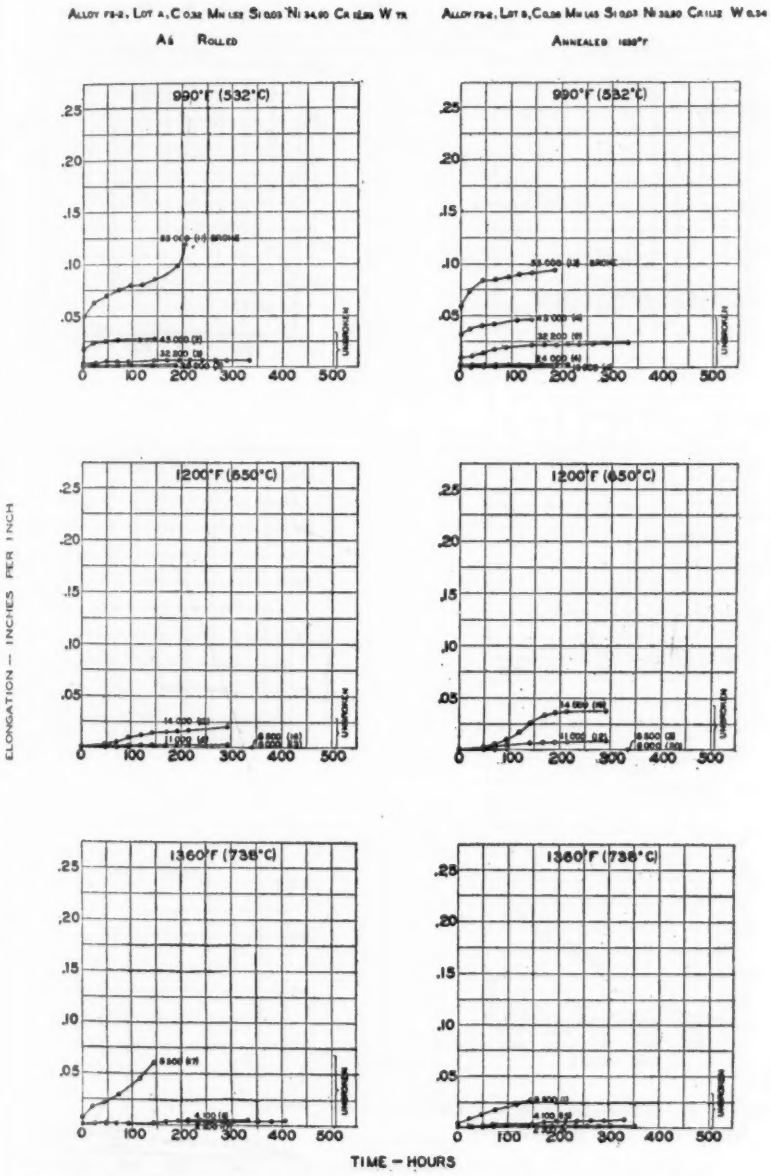

FIGURE 8.—*Time-elongation curves for the Ni-Cr-Fe alloy FS–2, lots A and B*

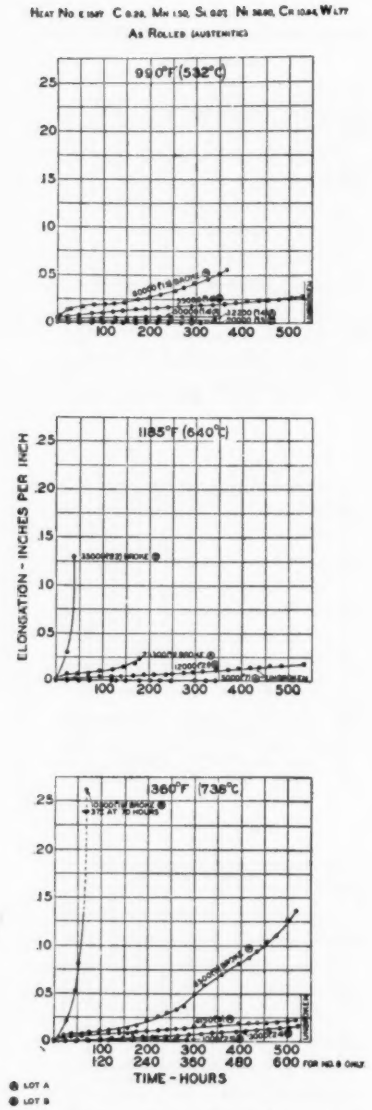
HEAT NO E 1567 C 0.20, MN 1.50, SI 0.07, NI 36.60, CR 10.04, W 1.77
AS ROLLED (AUSTENITIC)
990°F (532°C)
1185°F (640°C)
ELONGATION - INCHES PER INCH
1360°F (736°C)
TIME - HOURS
LOT A
LOT B

FIGURE 9.—*Time-elongation curves for the Ni-Cr-Fe alloy E1567*

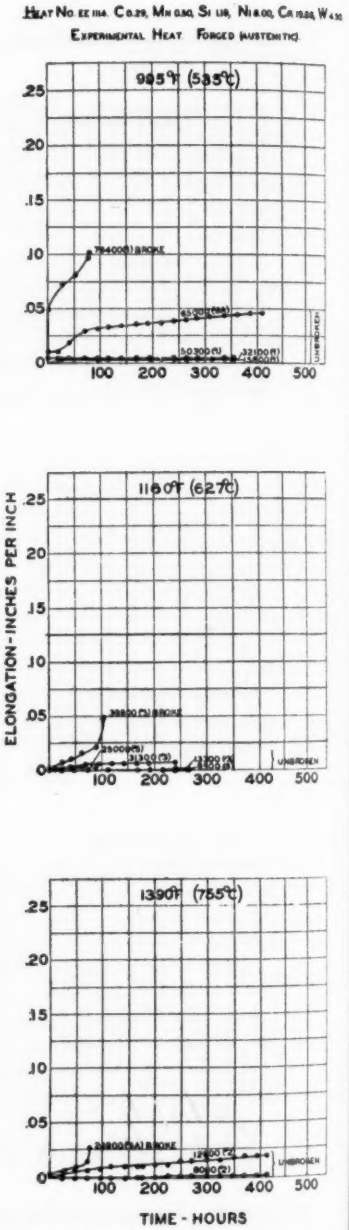
HEAT NO. EE 1114. C 0.29, MN 0.90, SI 1.18, NI 8.00, CR 13.06, W 4.10
EXPERIMENTAL HEAT FORGED (AUSTENITIC)
985°F (535°C)
1160°F (627°C)
ELONGATION - INCHES PER INCH
1390°F (755°C)
TIME - HOURS

FIGURE 10.—*Time-elongation curves of the steel EE1114*

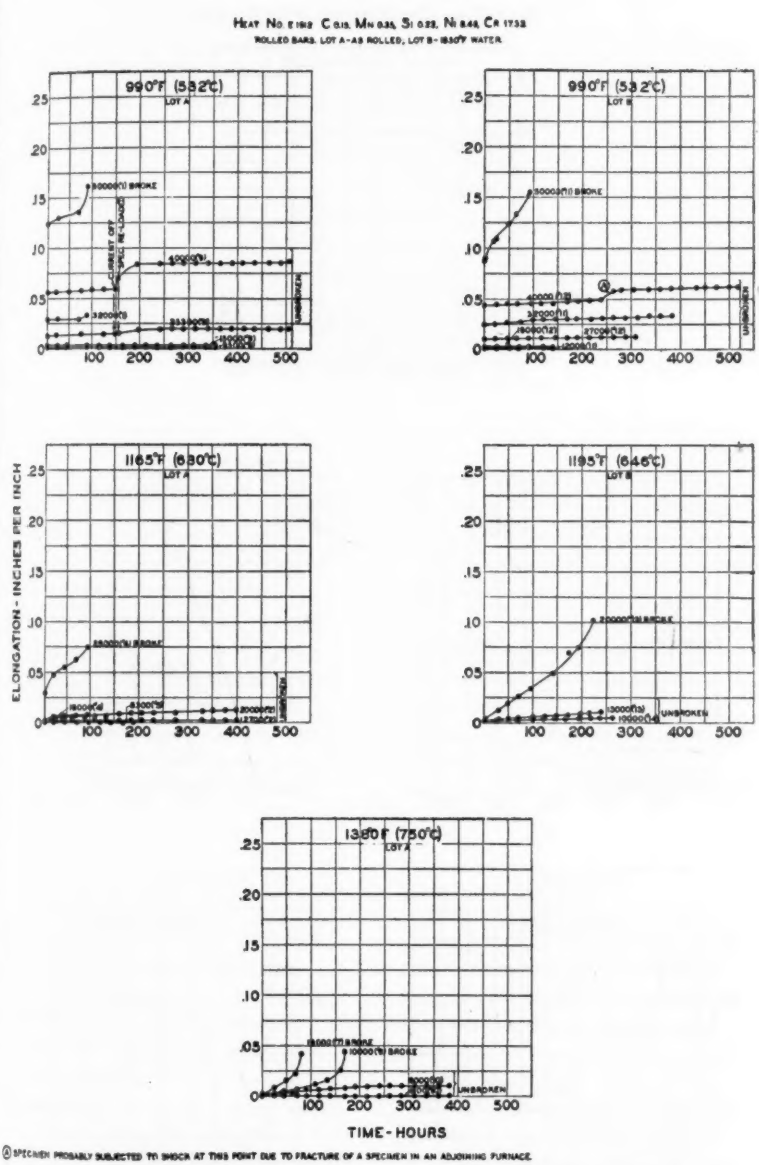

(A) SPECIMEN PROBABLY SUBJECTED TO SHOCK AT THIS POINT DUE TO FRACTURE OF A SPECIMEN IN AN ADJOINING FURNACE

FIGURE 11.—*Time-elongation curves of the steel E1912*

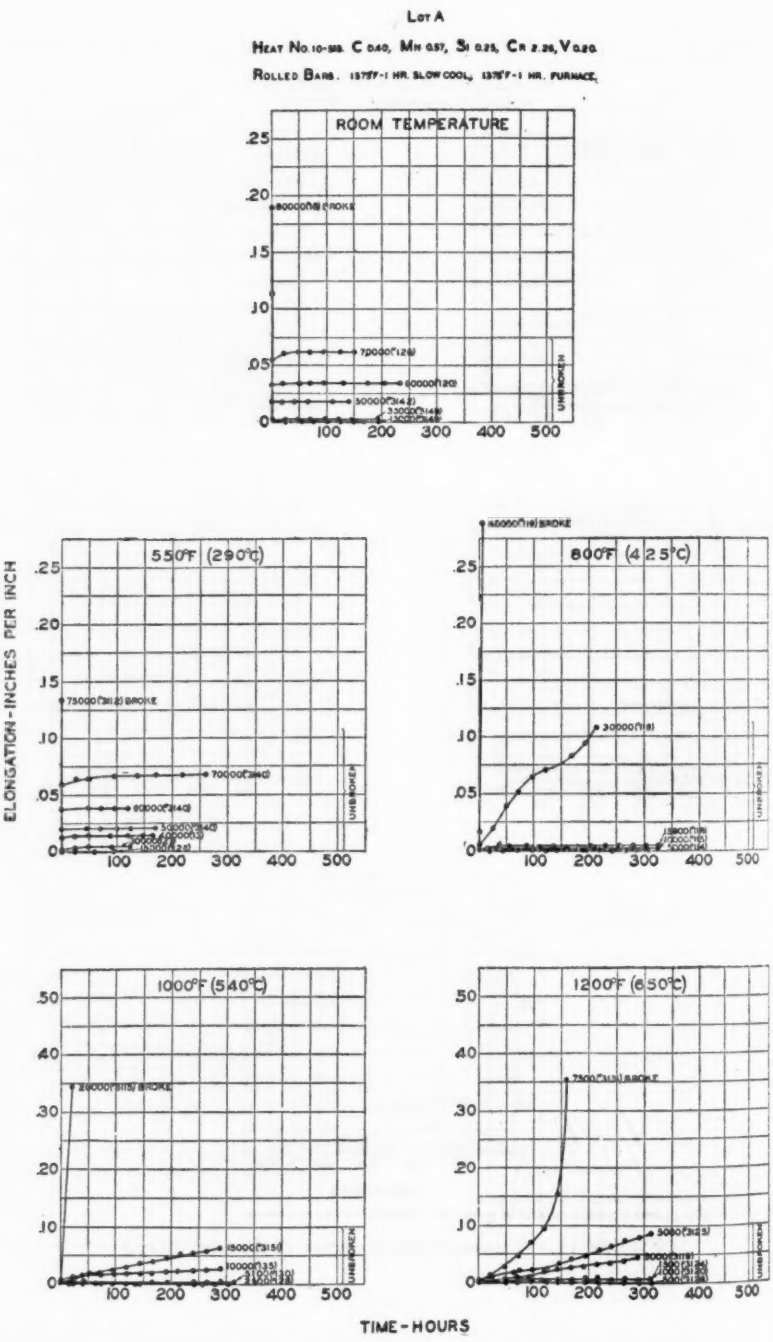

FIGURE 12.—*Time-elongation curves of steel 10–518, lot A*

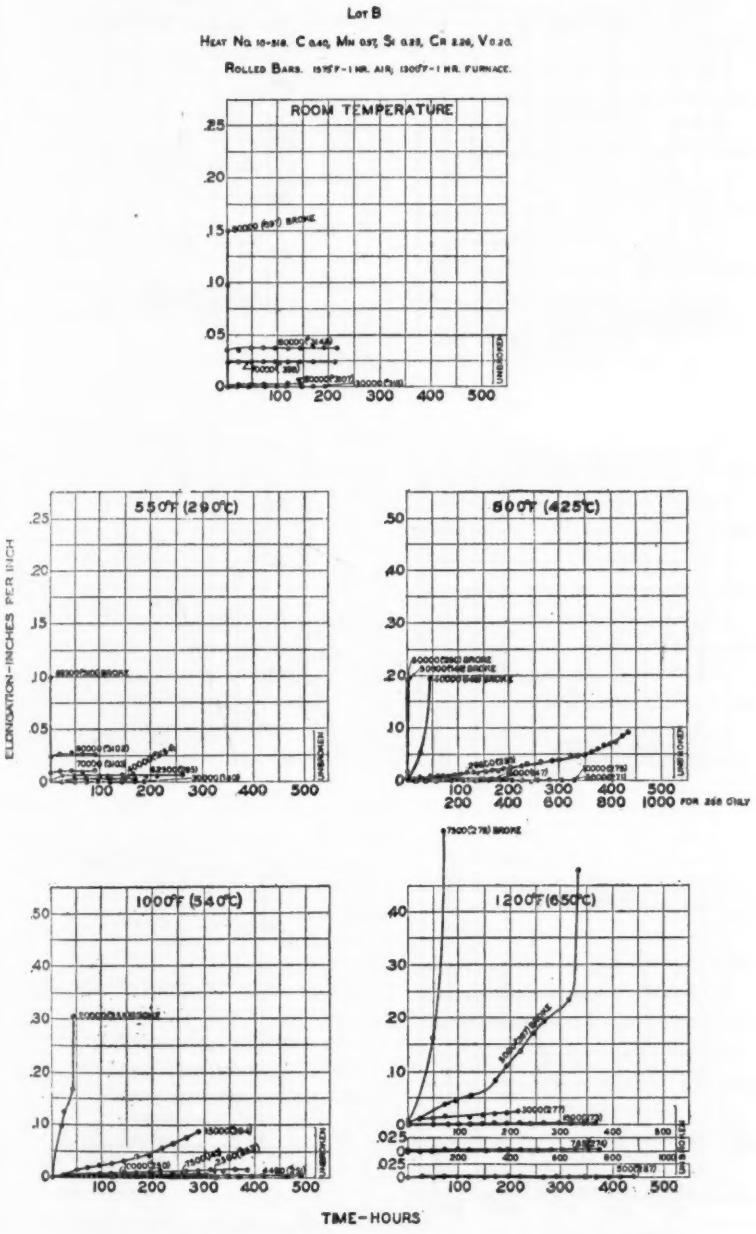

FIGURE 13.—*Time-elongation curves of steel 10–518 lot B*

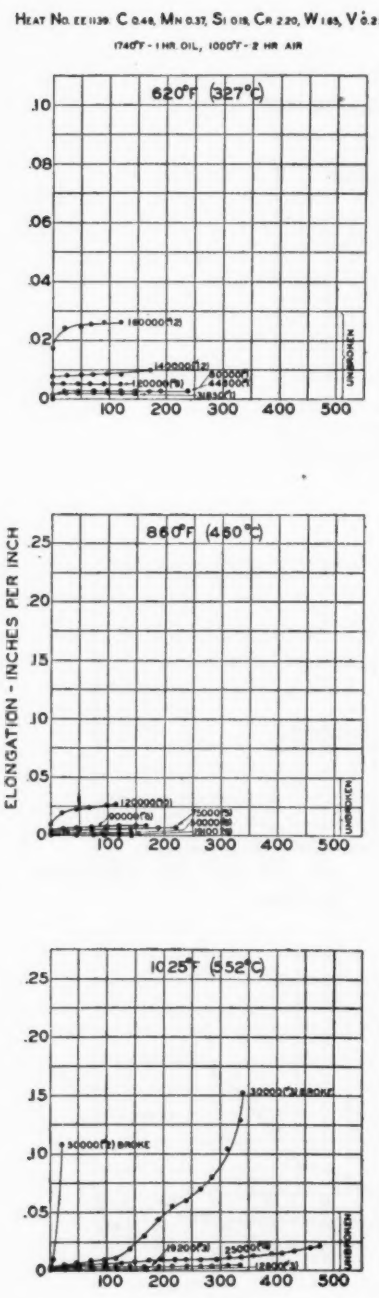
HEAT NO. EE 1139 C 0.48, MN 0.37, SI 0.18, CR 2.20, W 1.85, V 0.25,
1740°F - 1 HR. OIL, 1000°F - 2 HR. AIR
620°F (327°C)
860°F (460°C)
1025°F (552°C)
ELONGATION - INCHES PER INCH
TIME - HOURS
UNBROKEN

FIGURE 14.—*Time-elongation curves of steel EE1139*

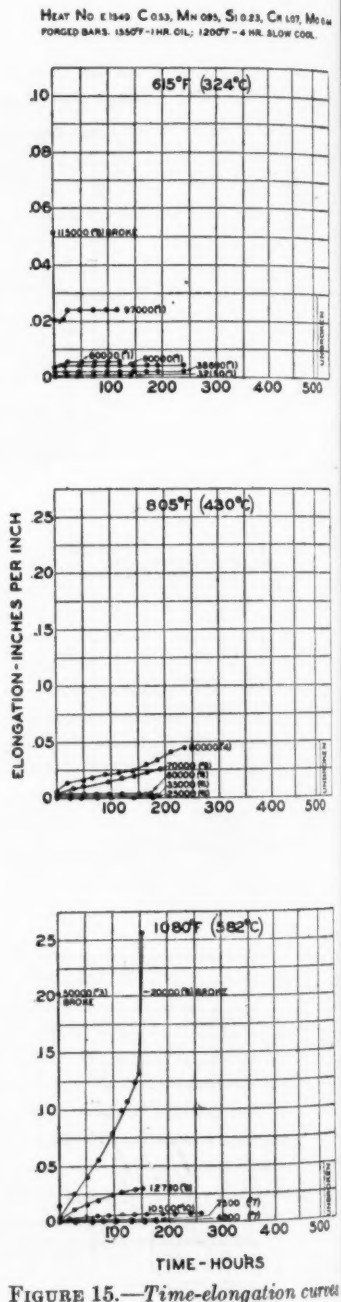
HEAT NO. E 1549 C 0.53, MN 0.95, SI 0.23, CR 1.07, MO 0.14
FORGED BARS. 1550°F - 1 HR. OIL; 1200°F - 4 HR. SLOW COOL
615°F (324°C)
805°F (430°C)
1080°F (582°C)
ELONGATION - INCHES PER INCH
TIME - HOURS
UNBROKEN

FIGURE 15.—*Time-elongation curves of the steel E1549*

At temperatures above those at which strain hardening is observed, any appreciable initial flow is followed by further and continuous deformation which may take place at approximately the same rate, a higher or a lower rate, depending upon the conditions of test. At such high temperatures the flow ordinarily increases with time and the allowable working stresses usually become a function of the rate of deformation subsequent to any initial changes in dimensions (secondary flow rates).

At intermediate temperatures, the time-elongation curves may show some of the characteristics of each of the two classes of curves mentioned. In other words, the transition from the relations typical of temperatures at which marked strain hardening is observed to the relations typical of much higher temperatures is most often gradual. The time-elongation curves may show appreciable initial deformation followed by decreases in flow rates, but the flow may be continuous so that fracture occurs in relatively short time.

In ductile materials appreciable elongation eventually results in appreciable contraction in area. This, in turn, results in stress concentration and the rates of flow are greatly increased just before fracture (final flow).

Different methods have been used in summarizing the results of flow tests, but probably the most acceptable to engineers are those which show the relations between deformation, stress, temperature, and time, since the selection of allowable working stresses is usually not solely a function of the time for fracture but demands consideration of the allowable deformation during any selected life. The desired life and the maximum allowable deformation will vary with different classes of structures and the viewpoints of individual designers and are likewise affected by the details of construction and operation. For this reason, the results are summarized in terms of per cent deformation per thousand hours at the different temperatures as is shown in Figures 30 to 41, inclusive, and in Table 2.

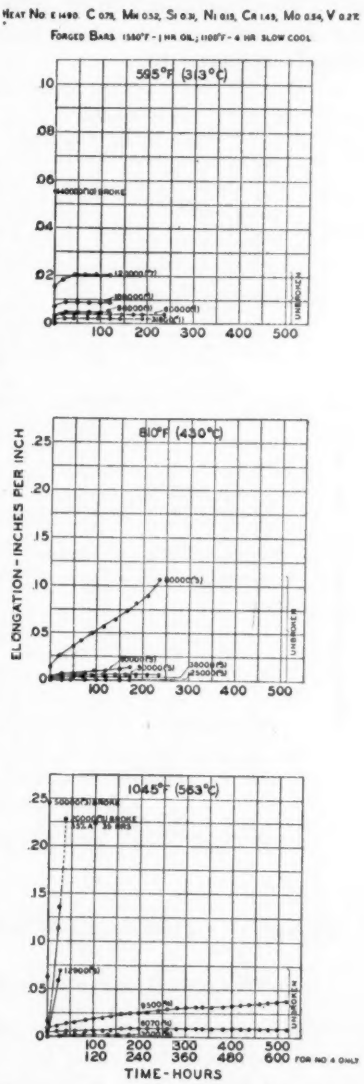
HEAT NO. E 1490 C 0.12, Mn 0.52, Si 0.31, Ni 0.15, Cr 1.43, Mo 0.54, V 0.22
FORGED BARS 1550°F - 1 HR OIL; 1100°F - 4 HR SLOW COOL
595°F (313°C)
810°F (430°C)
1045°F (563°C)
ELONGATION - INCHES PER INCH
TIME - HOURS
UNBROKE

FIGURE 16.—*Time-elongation curves of the steel E1490*

The stresses producing the deformation rates shown in Figures 30 to 41 were determined from charts giving the relations between the applied load and the initial flow or secondary flow rates, shown in Figures 18 to 29, inclusive. The methods by which Figures 30 to 41 were obtained from data in Figures 18 to 29 and Table 2, and the assumptions involved, have been discussed in detail in reports already referred to.

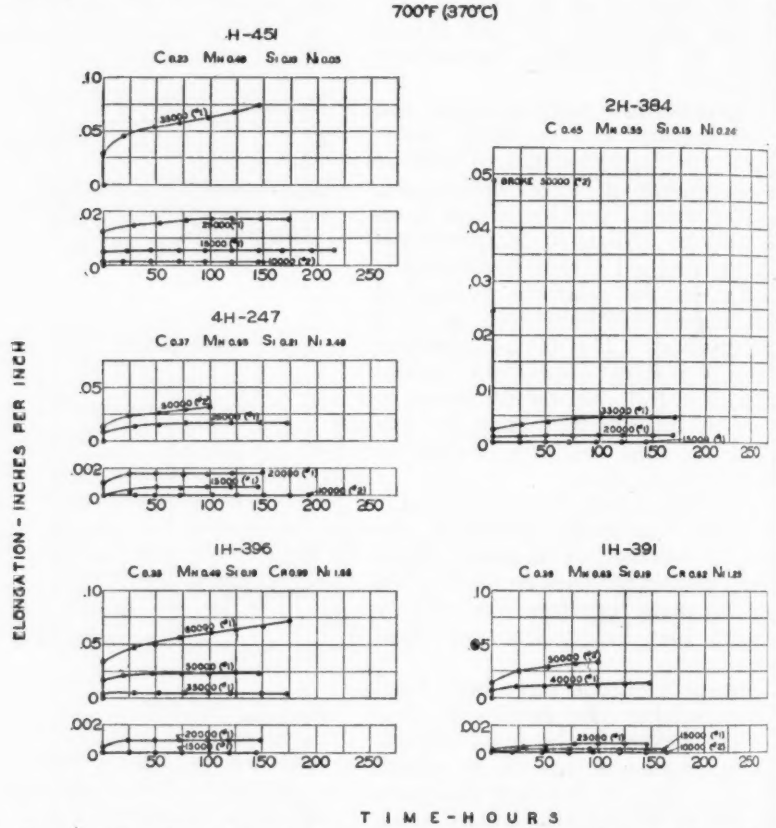

FIGURE 17.—*Time-elongation curves at 700° F. of two carbon and three alloy steels*

Table 1 contains details of chemical composition and preliminary heat treatments.

Where comparisons are made with the metals of Group IV, Table 1, the required flow data for these steels were taken from previously reported tests which were carried out under comparable conditions.[7]

One important point, which has not been given much consideration in the interpretation of flow tests, is that the numerical values obtained on one bar, lot, or melt of a given alloy may not coincide closely with the values obtained on other bars, lots, or melts. Similar variations in the properties of metals at atmospheric temperatures are well recognized and should likewise be given consideration in the

[7] See footnotes 2, 3, and 4, p. 126.

application of flow-test data. The extent of these variations is not now accurately known, but it has been shown [8] that the differences in load-carrying ability, from heat to heat of steel, may be large. Without additional data, it is not safe to assume that the reported values represent the average, maximum, or minimum of the range characteristic of a given metal and safety factors must still be employed.

TABLE 2.—*Flow-test data for five steels tested at 700° F.*

Steel No.	Type composition [1]	Load	Initial flow	Secondary flow	Stress producing flow per 1,000 hours of—	
					0.1 per cent	1 per cent
		Lbs./in.²	*in./in.*	*in./in./hr.*		
4H451	0.23 C	10,000	0.0012	0	9,500	19,500
		15,000	.0054	0		
		25,000	.017	0		
		35,000	.03	.0002		
2H384	0.45 C	15,000	0	0	19,000	[3] [38,000]
		20,000	.0012	0		
		35,000	.0046	0		
		50,000	Continuous.	----------		
4H247	0.37 C, 3.46 Ni	10,000	0	0	17,300	31,400
		15,000	.0006	0		
		20,000	.0016	0		
		35,000	.016	0		
		50,000	.021	.00011		
1H391	0.36 C, 1.25 Ni, 0.62 Cr	10,000	0	0	26,000	32,000
		15,000	.0002	0		
		25,000	.0005	0		
		40,000	.011	.00002		
		50,000	.026	[4] .00008		
1H396	0.35 C, 1.66 Ni, 0.99 Cr	15,000	0	0	20,500	38,000
		20,000	.0009	0		
		35,000	.0051	0		
		50,000	.022	.000015		
		60,000	.043	.00017		

[1] For details of chemical composition and heat treatment refer to Table 1.
[3] Bracketed values estimated.
[4] Or less.

2. COMMERCIAL NICKEL-CHROMIUM-IRON ALLOYS

In Figure 42, comparisons are given at 700°, 1,000°, 1,125°, and 1,350° F. of the metals in Groups I and II, Table 1, and the five steels previously tested, Group IV. The stresses producing 0.1 and 1 per cent initial elongation and also 0.1 and 1 per cent secondary elongation (calculated per 1,000 hours) are represented by the lower and upper limits, respectively, of the blocks in the chart and serve as a basis of comparison of the flow characteristics of the different metals. Comparisons can be made at lower temperatures in some cases and likewise at higher rates of flow from data given in Figures 30 to 41, inclusive.

In the relation of stress to total deformation for alloys at certain temperatures, it is necessary to consider both the initial and the secondary flow. These differences can be studied in detail from data given in Figures 18 to 29 and Table 2.

[8] See footnote 3, p. 126.

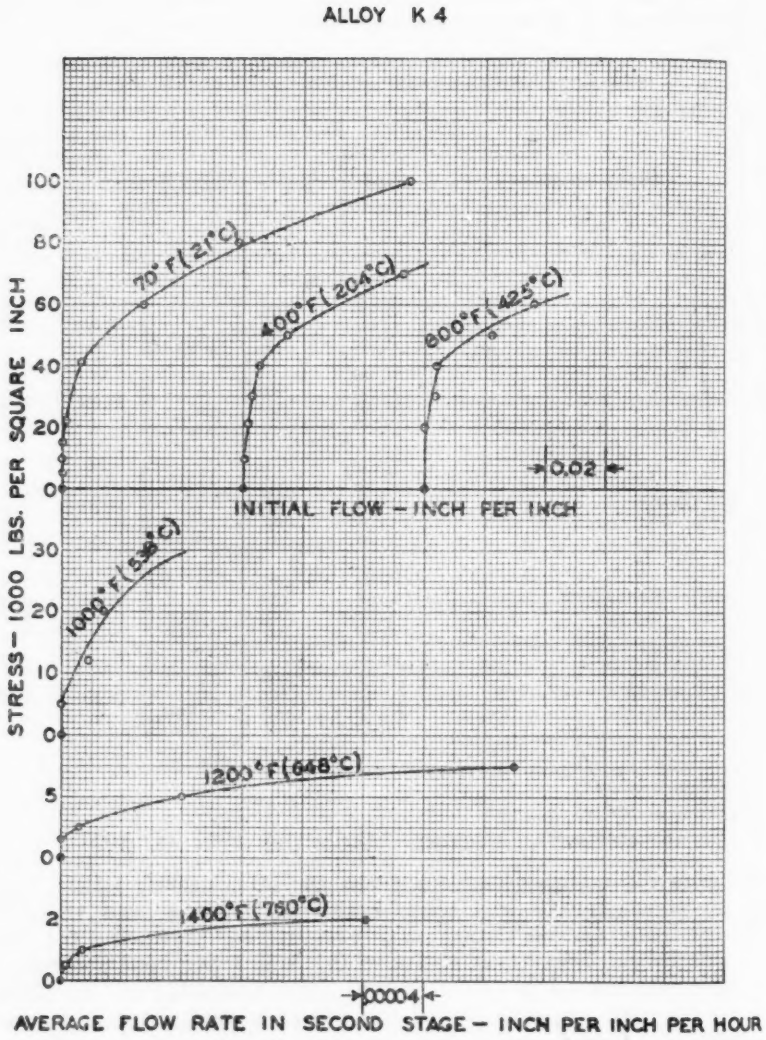

FIGURE 18.—*Flow data for Ni-Cr alloy K–4, at different temperatures*

Obtained from Figure 5.

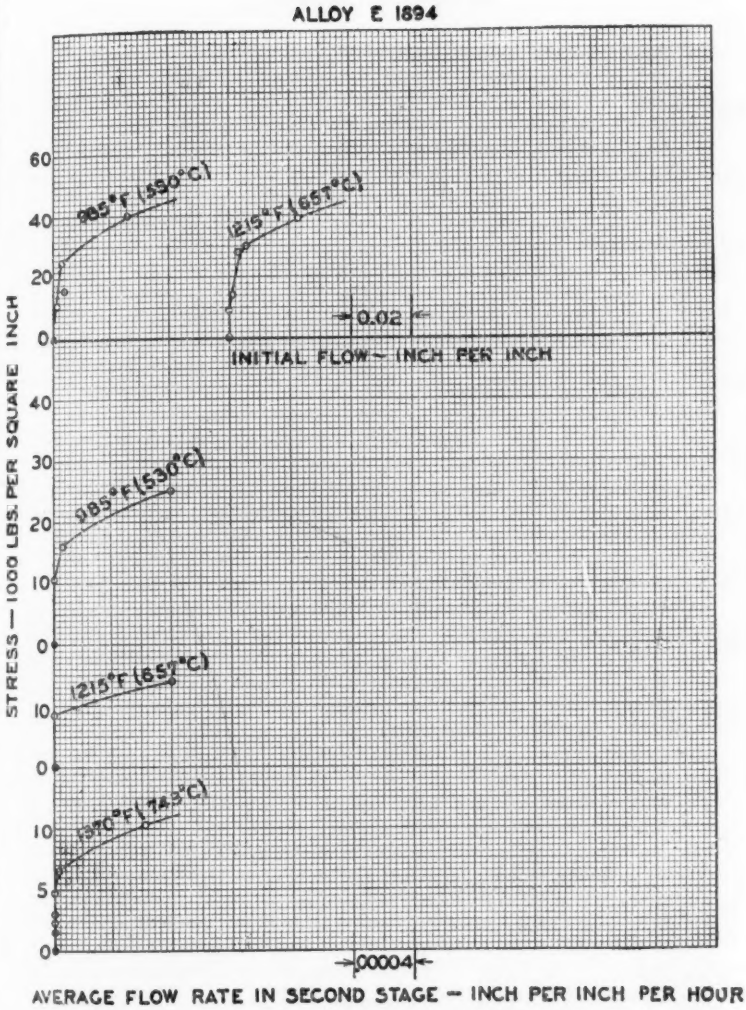

FIGURE 19.—*Flow data for Ni-Cr-Fe-W alloy E1894, at different temperatures*

Obtained from Figure 6.

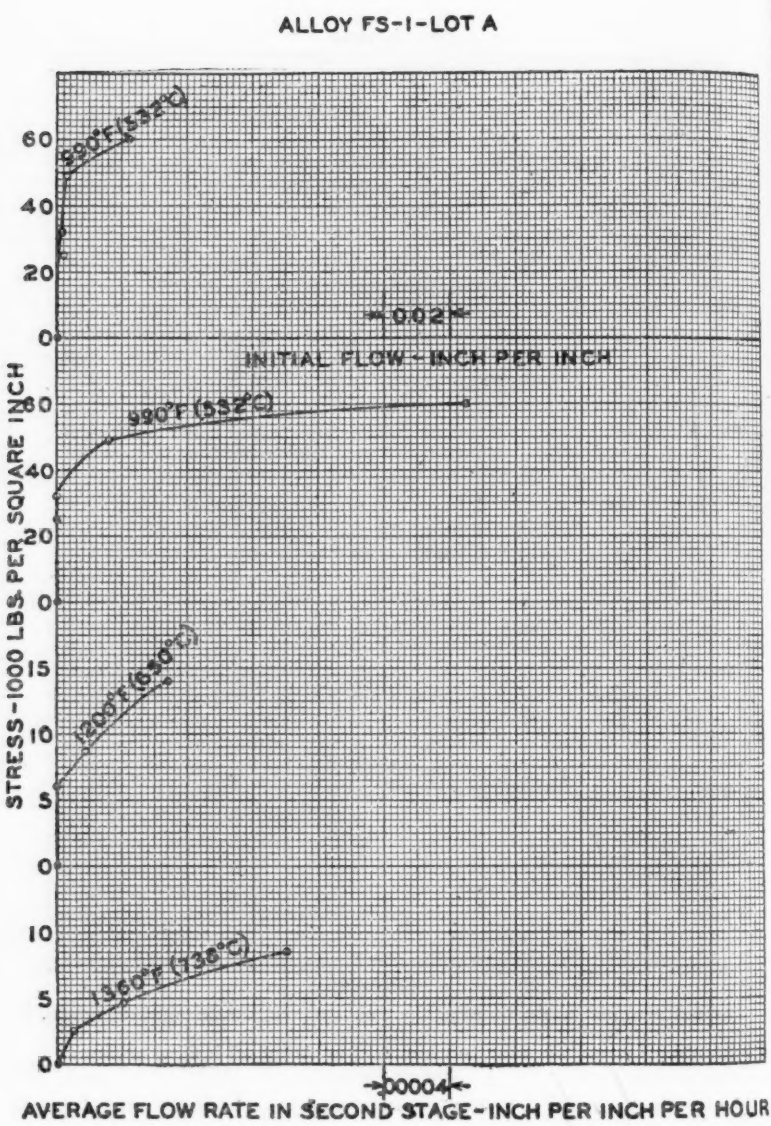

FIGURE 20.—*Flow data for the high Fe-Cr-Ni-W alloy FS–1, lots A and B, at different temperatures*

Obtained from Figure 7.

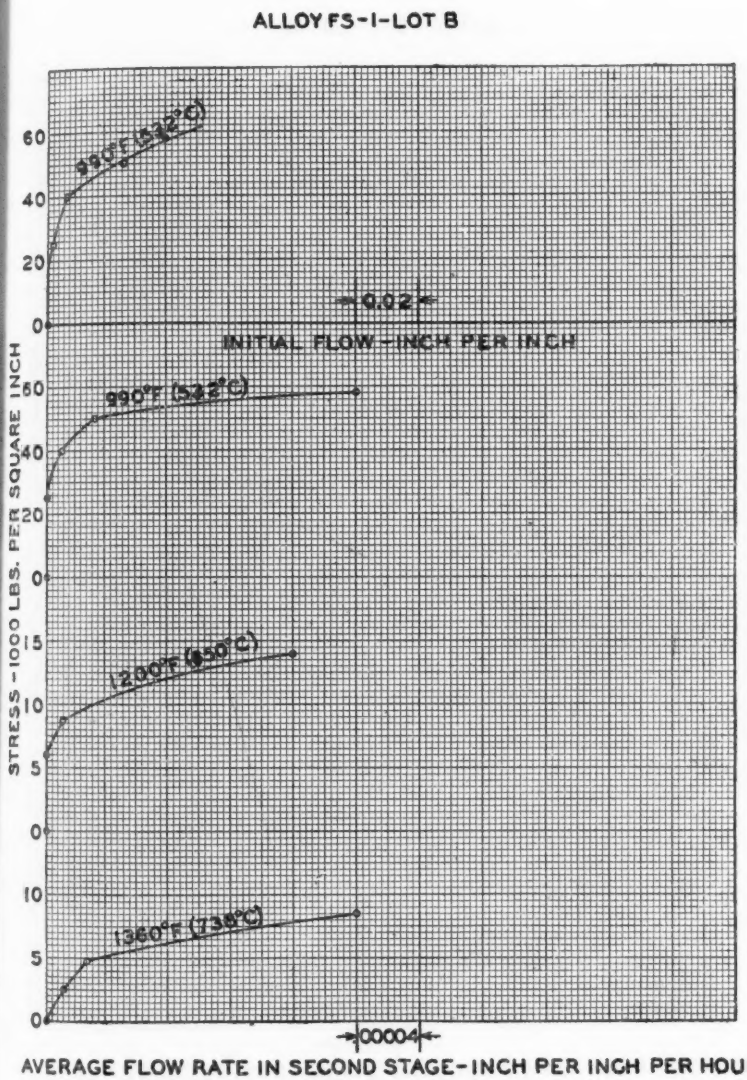

FIGURE 20.—*Flow data for the high Fe-Cr-Ni-W alloy FS1, lots A and B, at different temperatures*—Continued

Obtained from Figure 7.

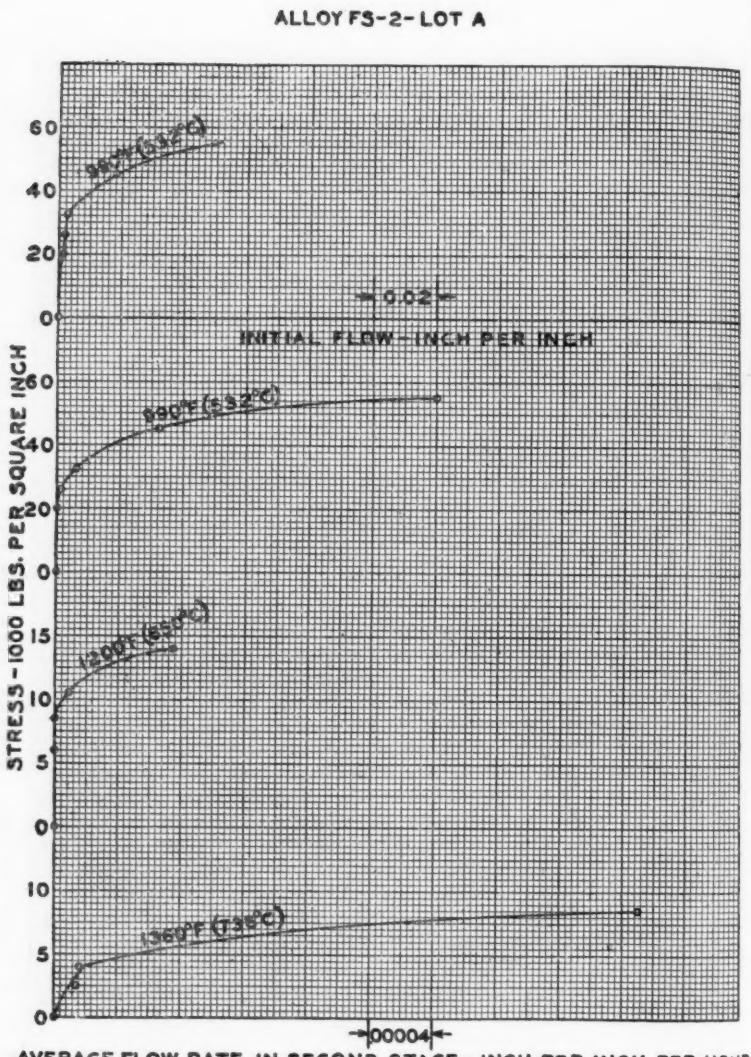

FIGURE 21.—*Flow data for the high Fe-Cr-Ni alloy FS-2, lots A and B, at different temperatures*

Obtained from Figure 8.

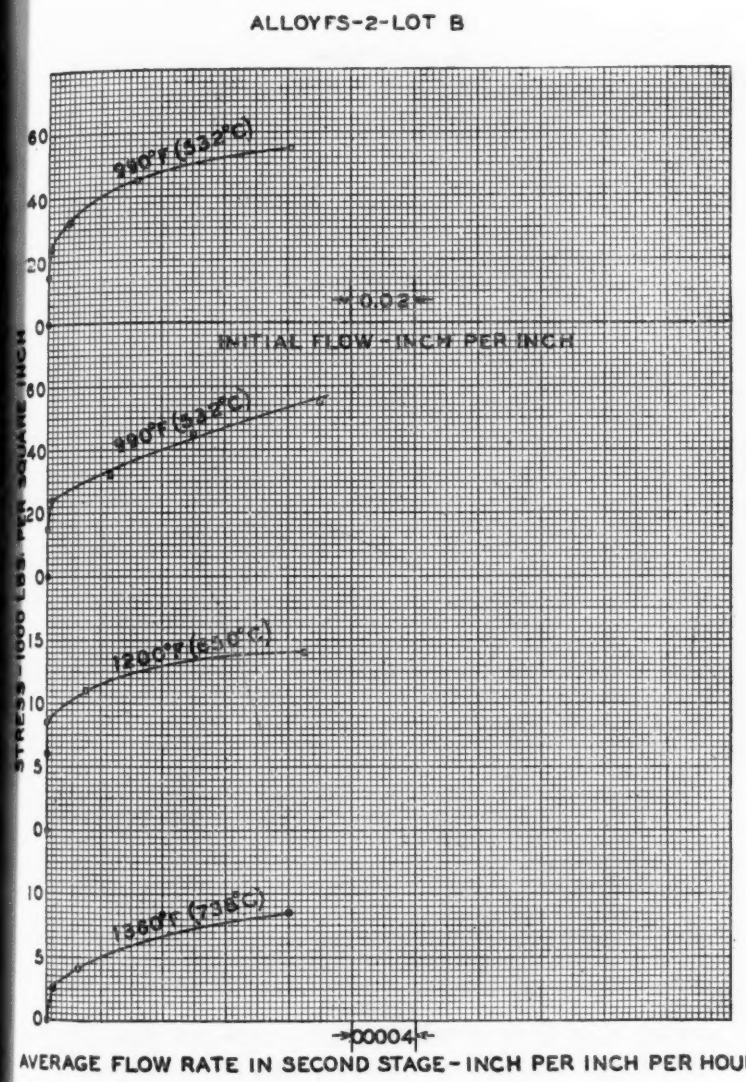

FIGURE 21.—*Flow data for the high Fe-Cr-Ni alloy FS–2, lots A and B, at different temperatures*—Continued

Obtained from Figure 8.

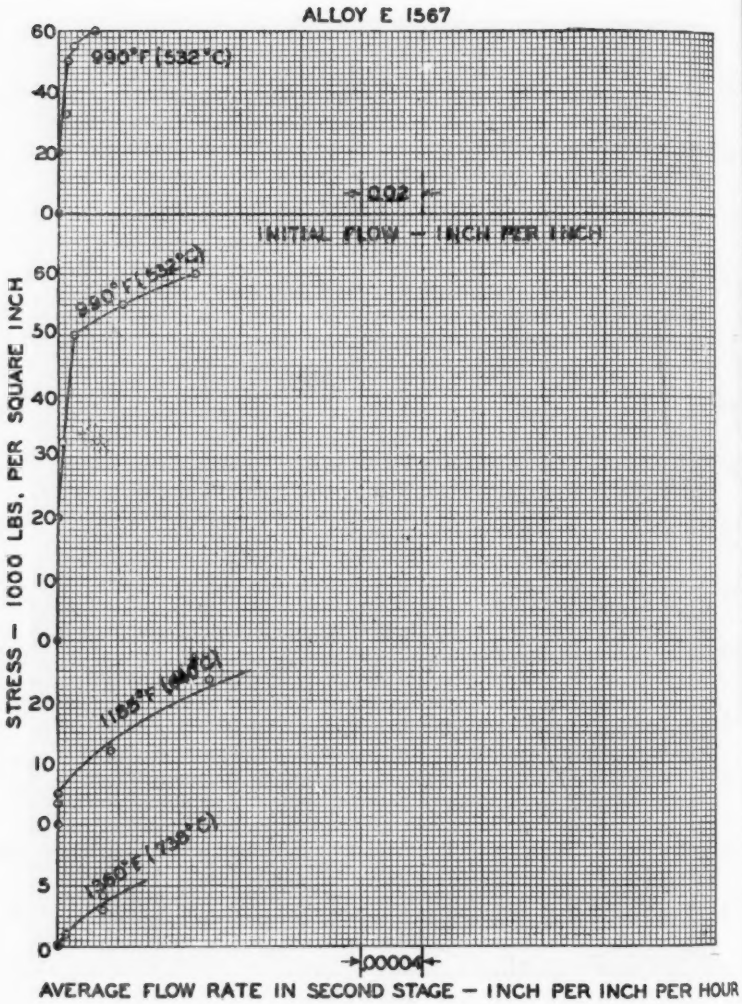

FIGURE 22.—*Flow data for Ni-Cr-Fe-W alloy E1567, at different temperatures*

Obtained from Figure 9.

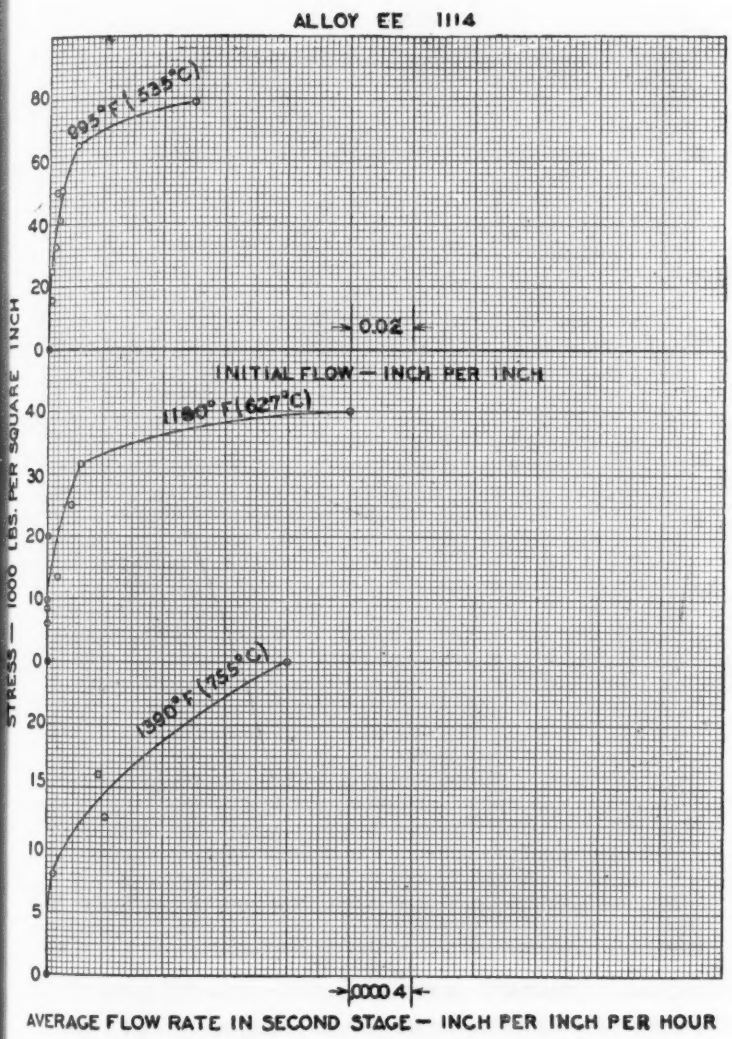

FIGURE 23.—*Flow data for the high chromium-nickel-tungsten steel EE1114, at different temperatures*

Obtained from Figure 10.

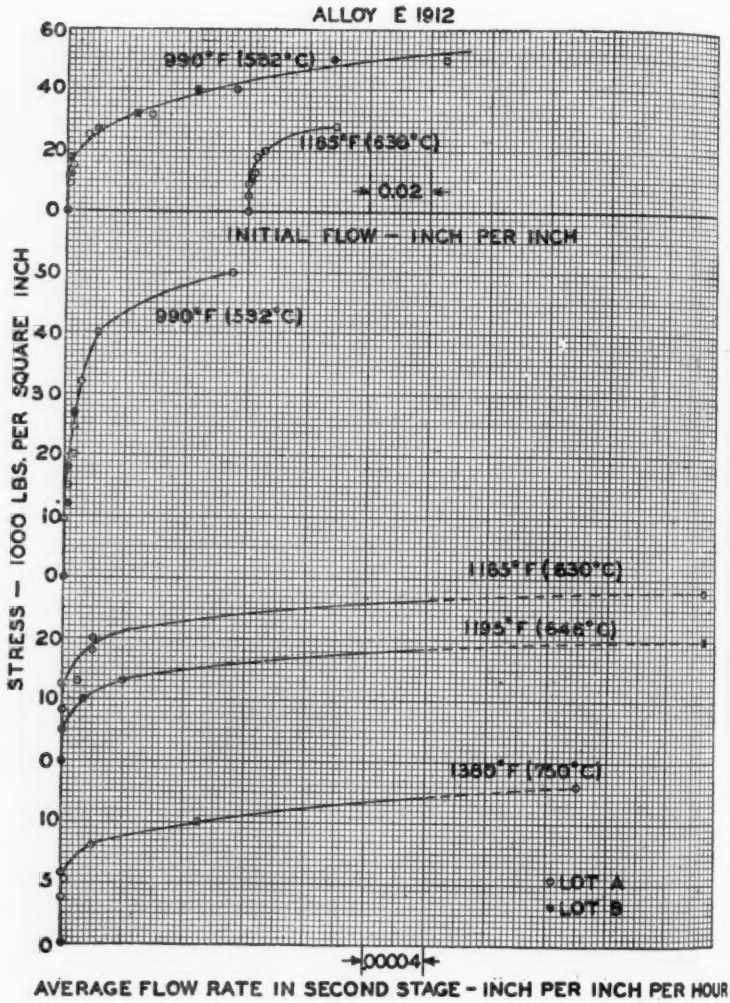

FIGURE 24.—*Flow data for the high chromium-nickel steel E1912, at different temperatures*

Obtained from Figure 11.

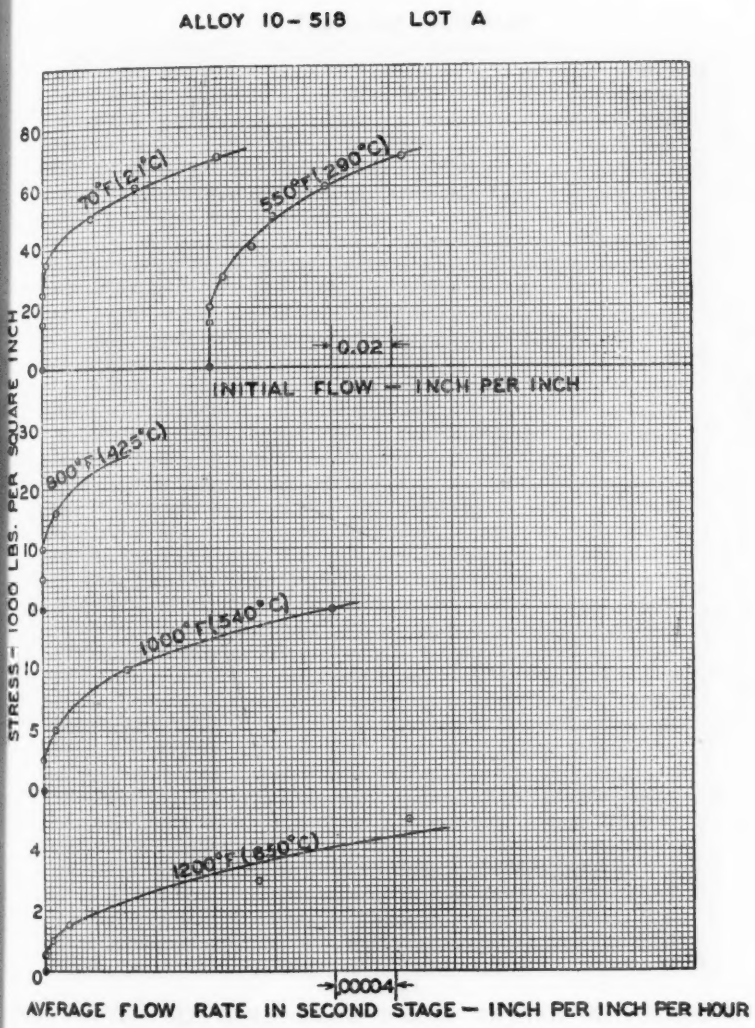

FIGURE 25.—*Flow data for the Cr-V steel 10–518, lot A, at different temperatures*

Obtained from Figure 12.

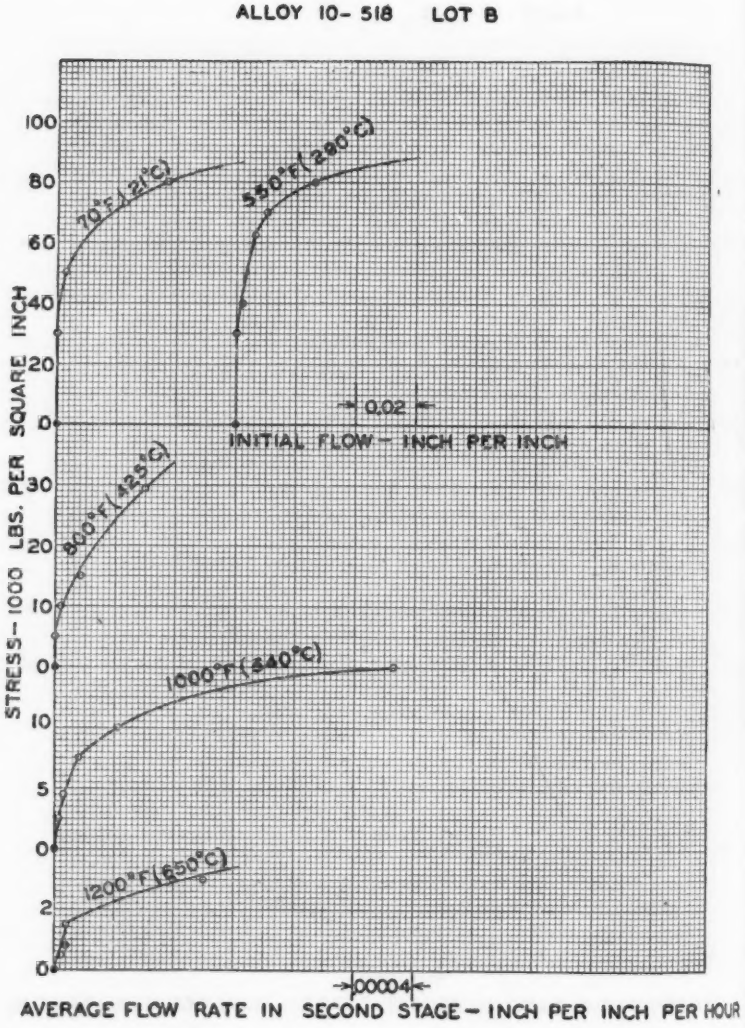

FIGURE 26.—*Flow data for the Cr-V steel 10–518, lot B, at different temperatures*

Obtained from Figure 13.

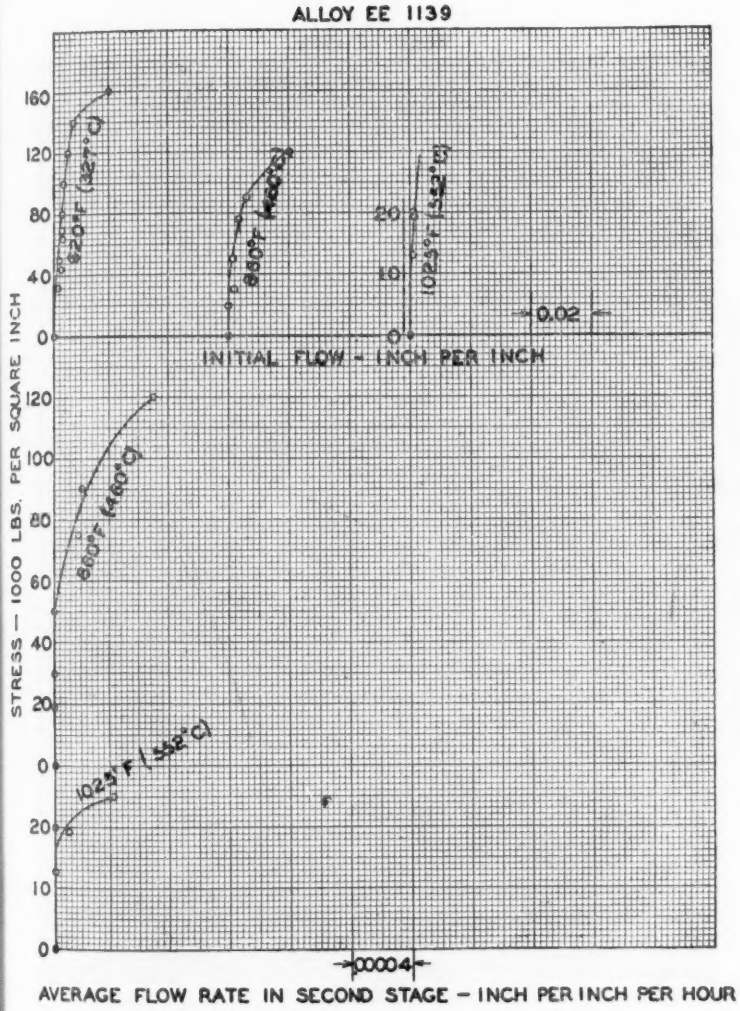

FIGURE 27.—*Flow data for the Cr-V-W steel EE1139, at different temperatures*

Obtained from Figure 14.

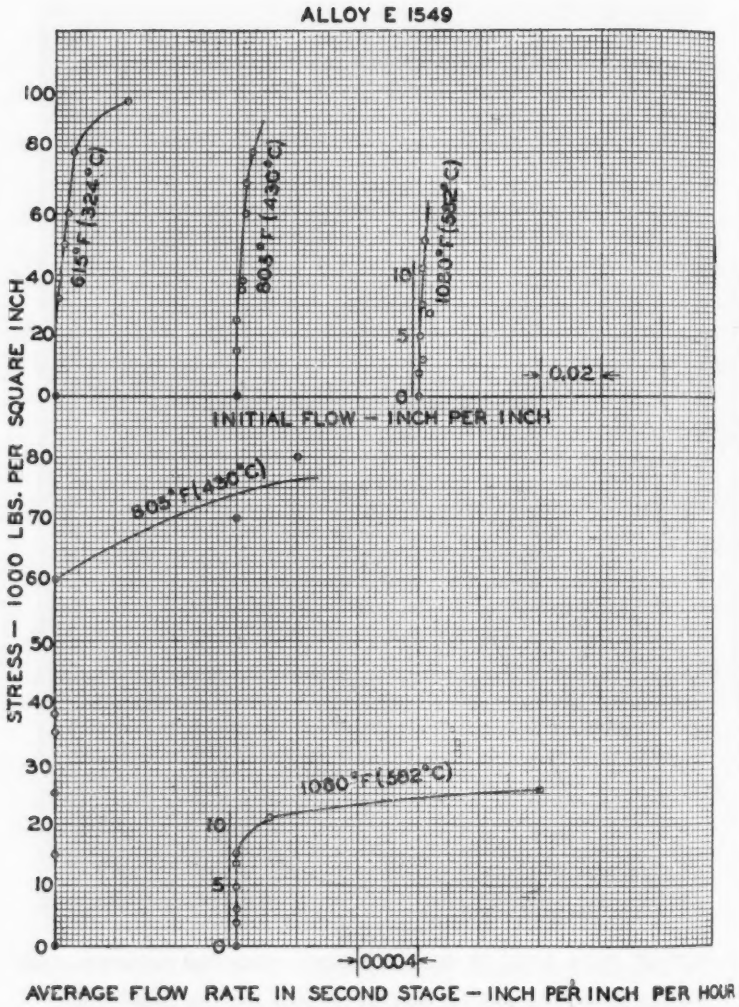

FIGURE 28.—*Flow data for the Cr-Mo steel E1549, at different temperatures*

Obtained from Figure 15.

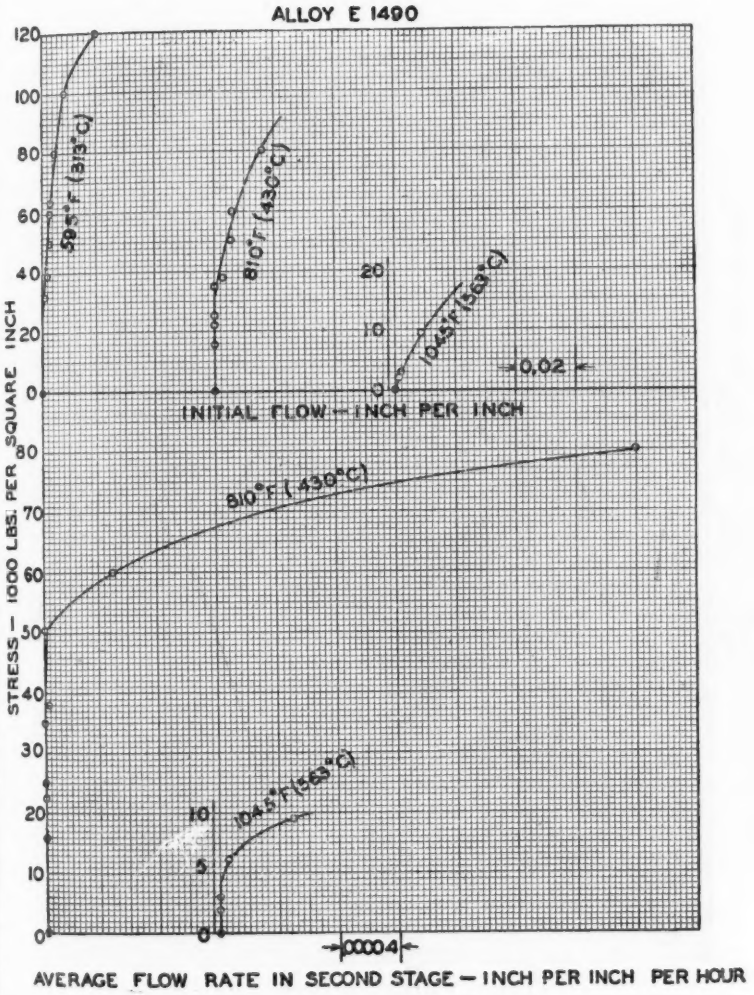
ALLOY E 1490
STRESS — 1000 LBS. PER SQUARE INCH
INITIAL FLOW — INCH PER INCH
AVERAGE FLOW RATE IN SECOND STAGE — INCH PER INCH PER HOUR
595°F (313°C)
810°F (430°C)
1045°F (563°C)
0.02
0.0004

FIGURE 29.—*Flow data for the Cr-Mo-V steel E1490, at different temperatures*

Obtained from Figure 16.

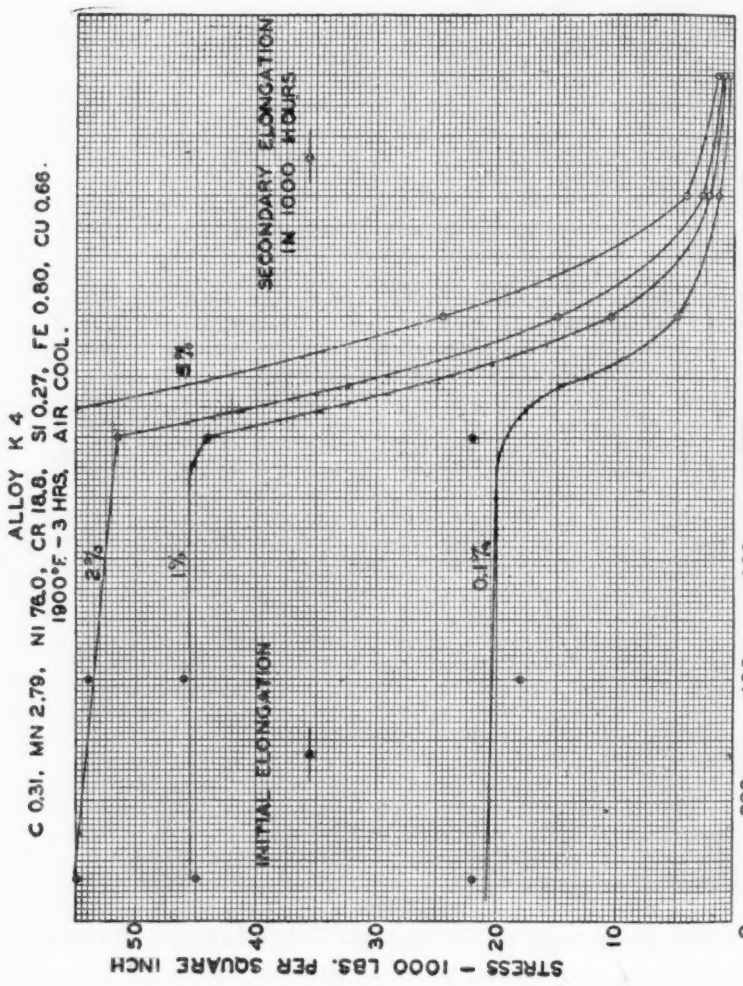

FIGURE 30.—*Flow chart for alloy K–4*

HEAT NO. E 1894 • C 0.25 • MN 1.40 • SI 0.05 • NI 60.80 • CR 10.75 • W 2.80
RISER FROM CASTING ANNEALED 1450°F

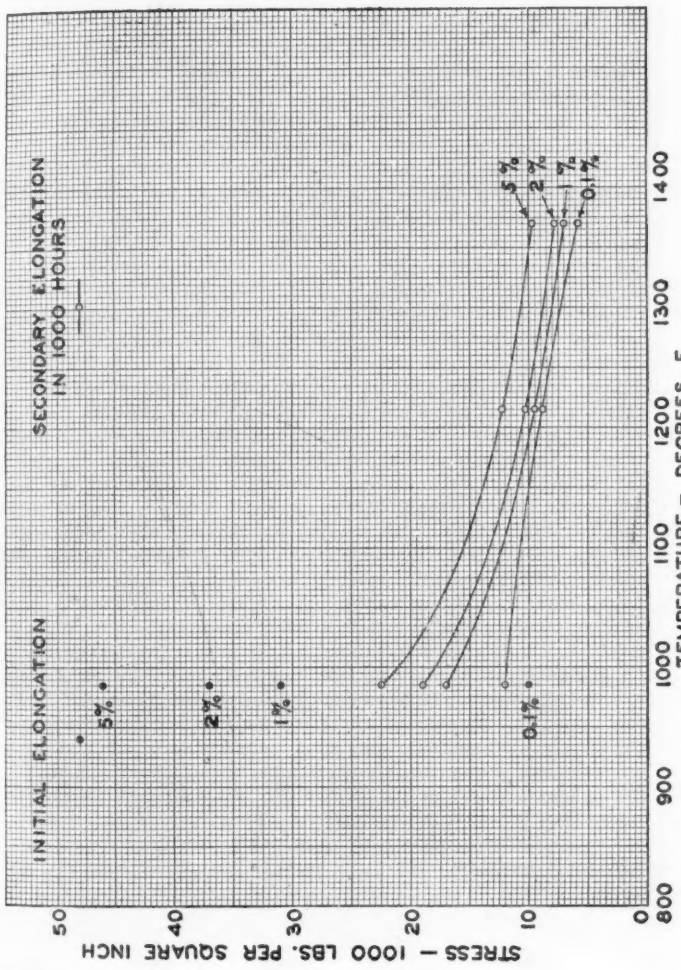

FIGURE 31.—*Flow chart for alloy E1894*

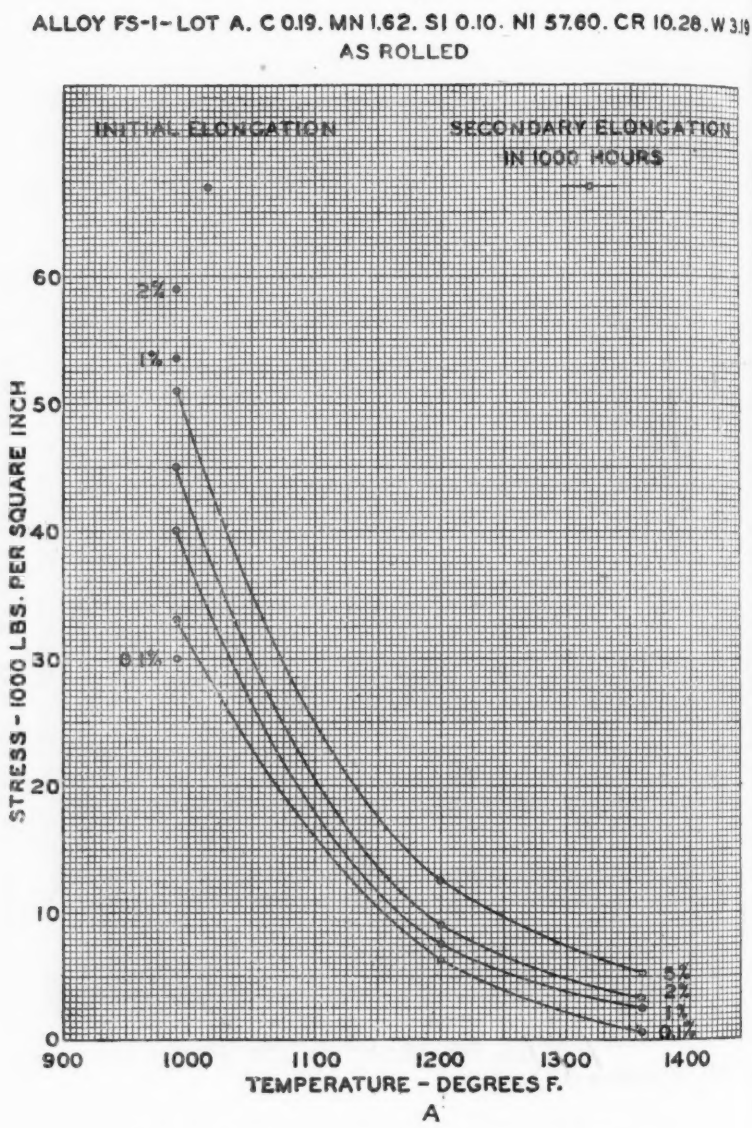

FIGURE 32.—*Flow data for alloy FS–1, lots A and B*

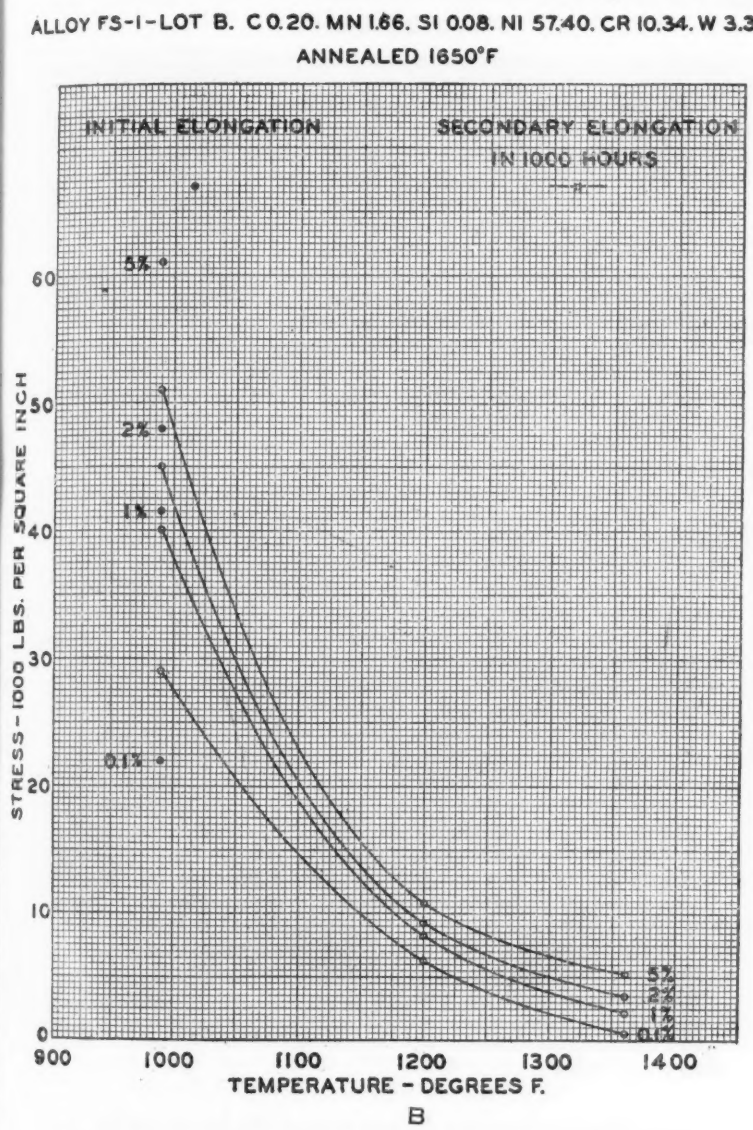

FIGURE 32.—*Flow data for alloy FS-1, lots A and B*—Continued

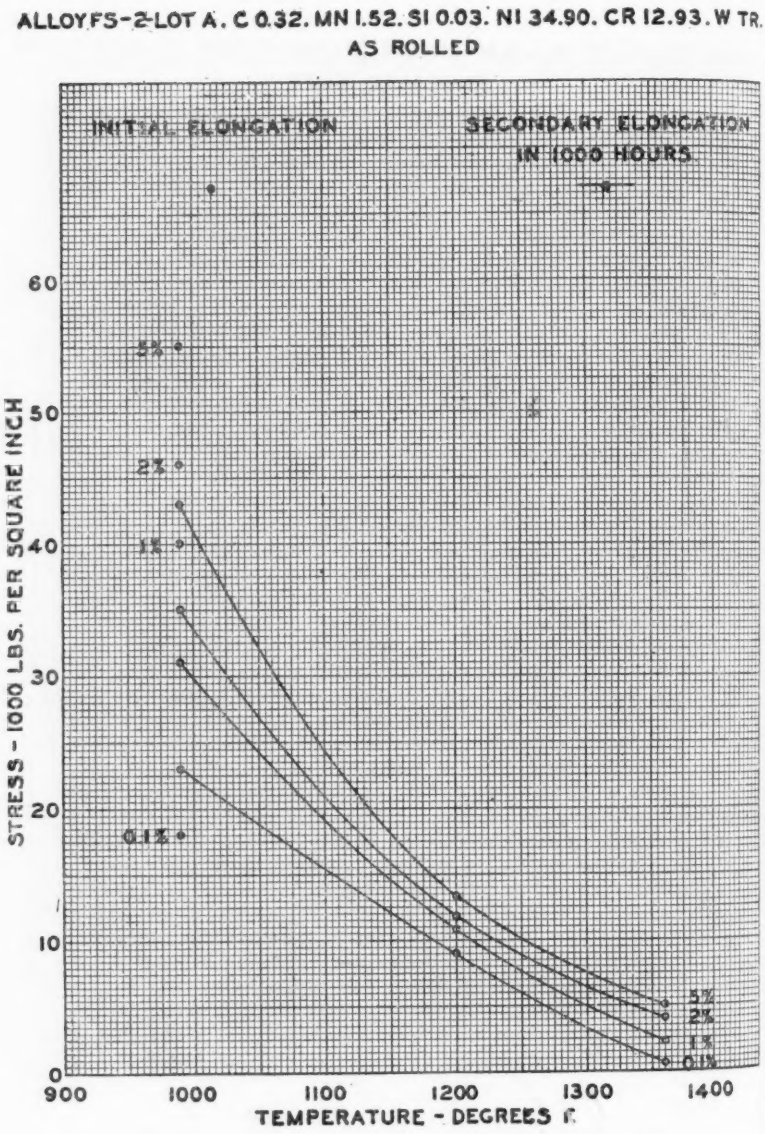

FIGURE 33.—*Flow data for alloy FS–2, lots A and B*

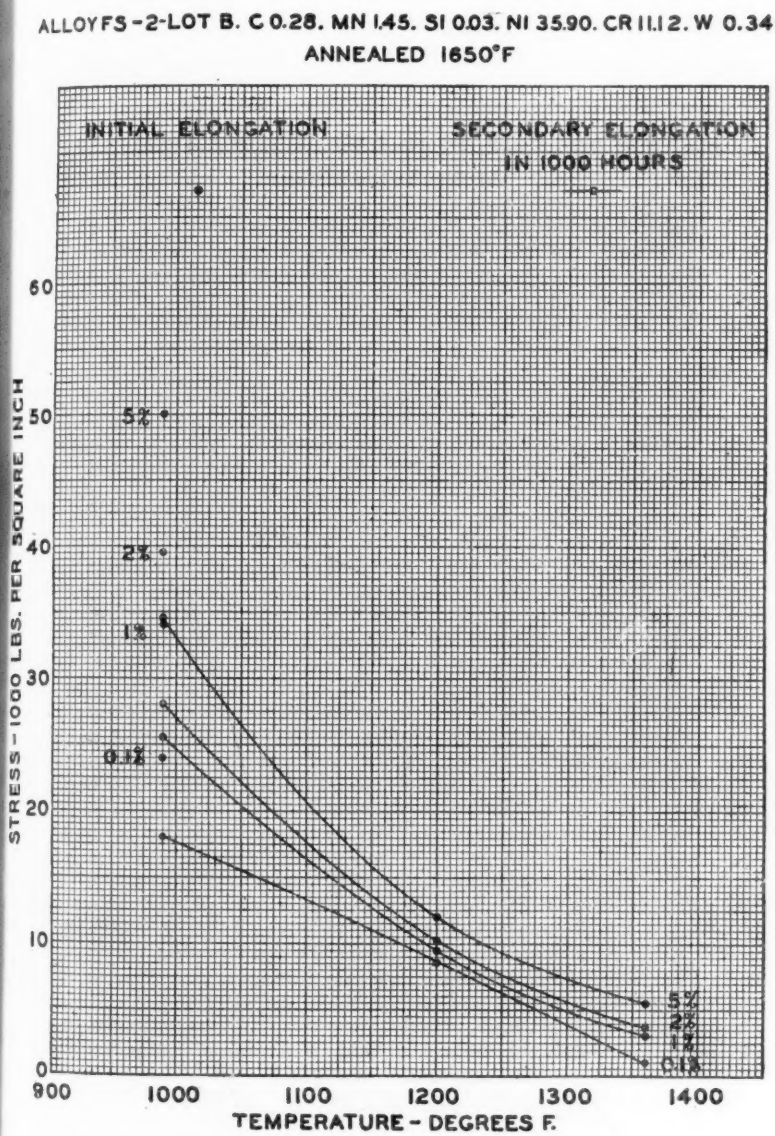

FIGURE 33.—*Flow data for alloy FS–2, lots A and B*—Continued

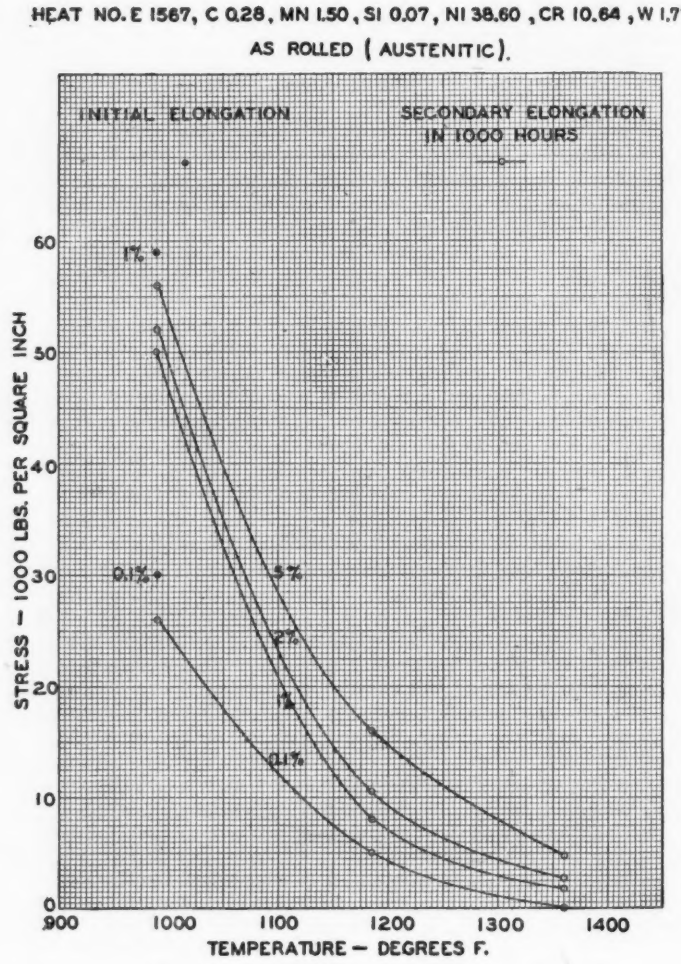

FIGURE 34.—*Flow chart for alloy E1567*

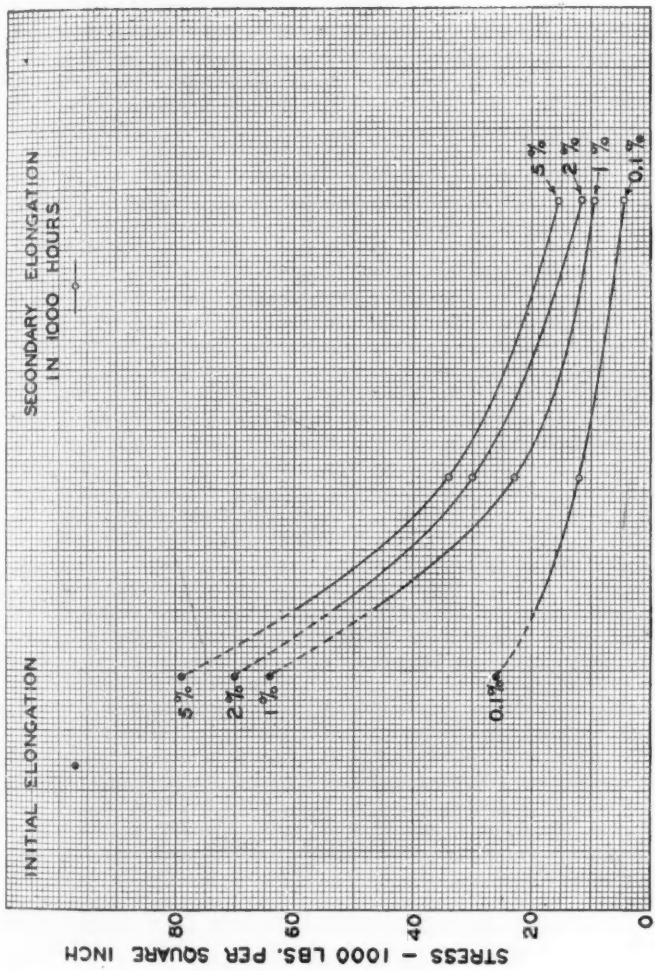

FIGURE 35.—*Flow chart for steel EE1114*

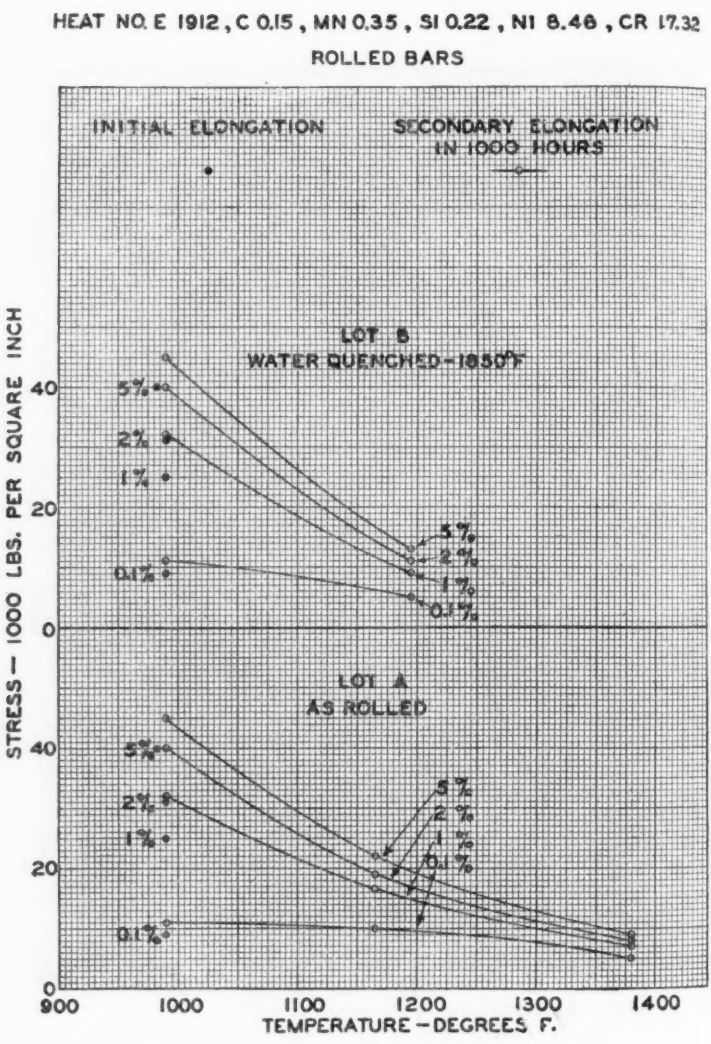

FIGURE 36.—*Flow chart for steel E1912*

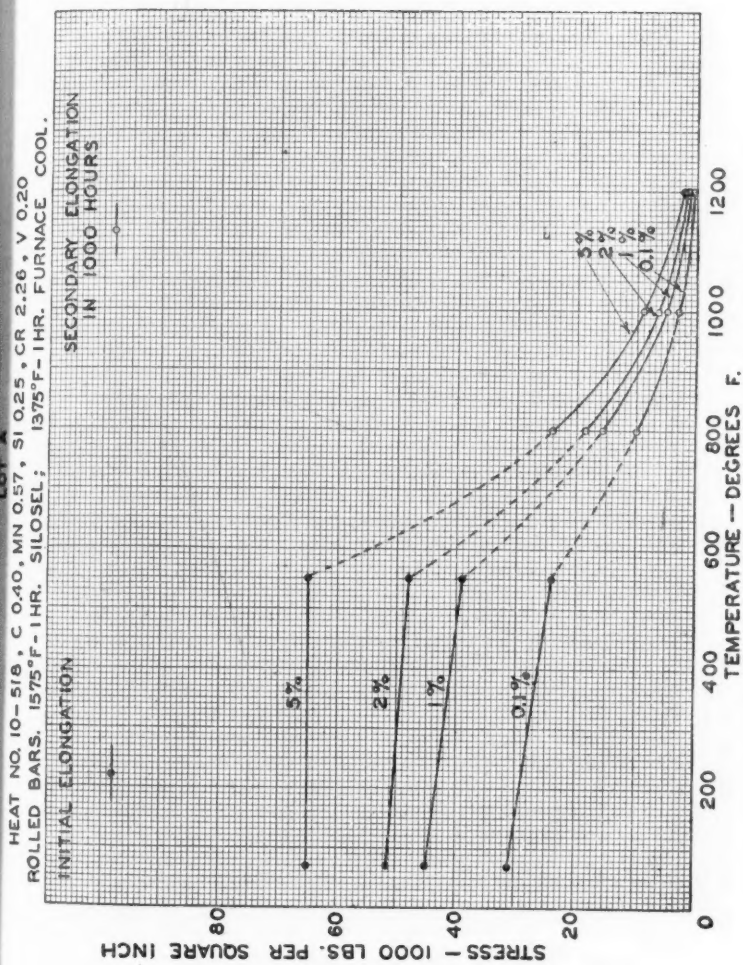

FIGURE 37.—*Flow chart for steel 10–518, lot A*

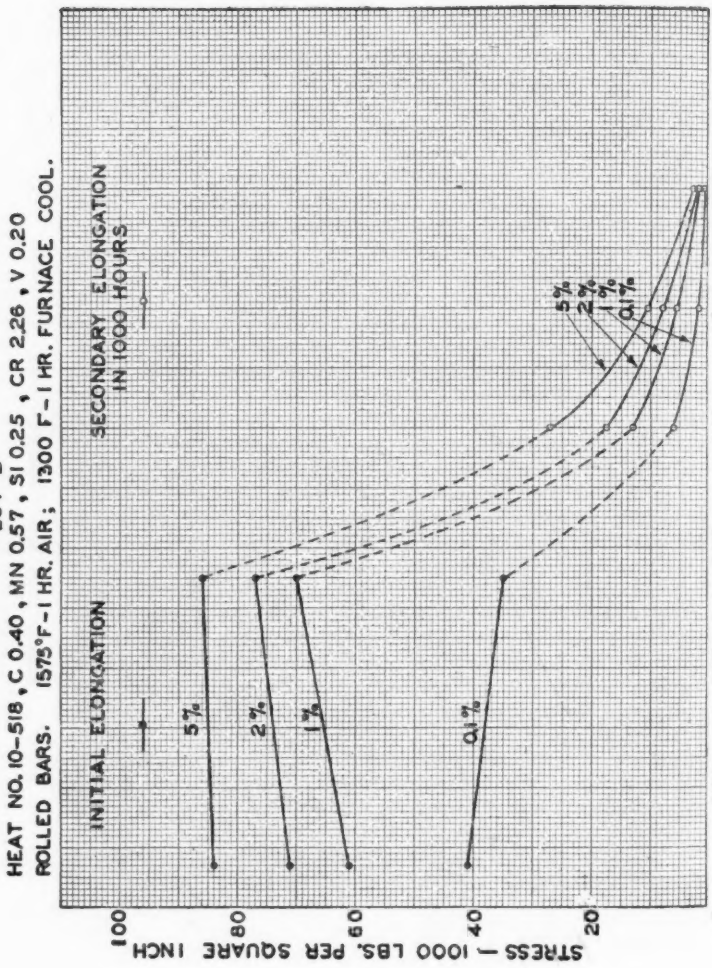
LOT B
HEAT NO. 10-518, C 0.40, MN 0.57, SI 0.25, CR 2.26, V 0.20
ROLLED BARS. 1575°F-1 HR. AIR; 1300 F-1 HR. FURNACE COOL.
INITIAL ELONGATION
SECONDARY ELONGATION IN 1000 HOURS
5%
2%
1%
0.1%
STRESS — 1000 LBS. PER SQUARE INCH
TEMPERATURE — DEGREES F.
100
80
60
40
20
0
200
400
600
800
1000
1200

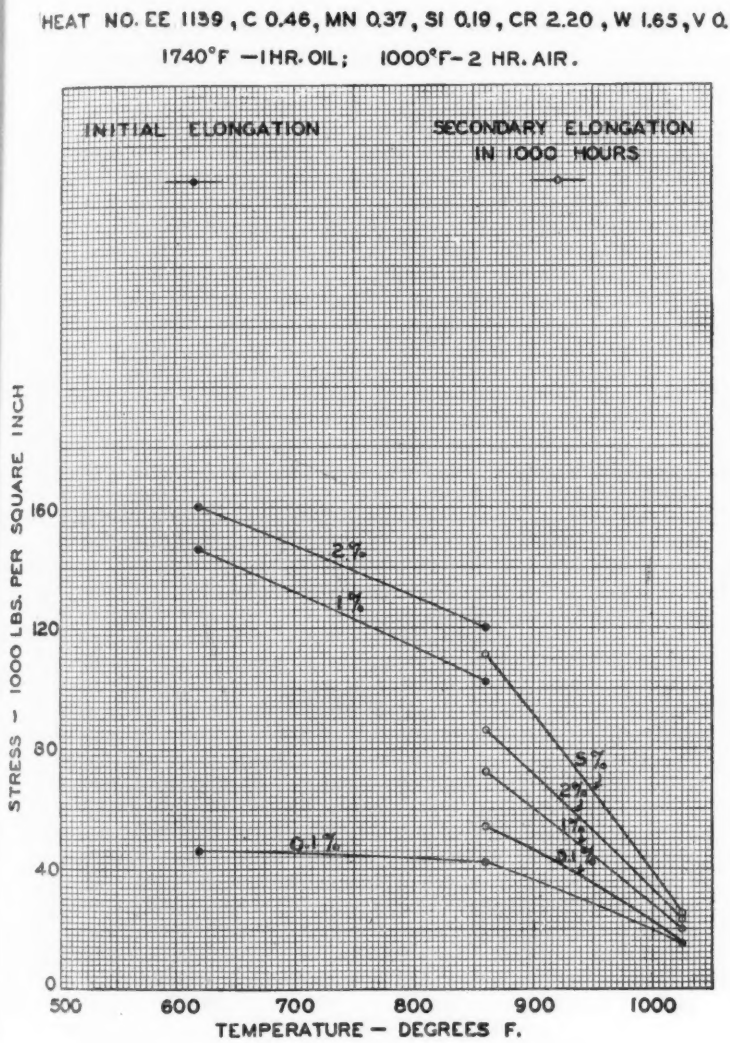

FIGURE 39.—*Flow chart for steel EE1139*

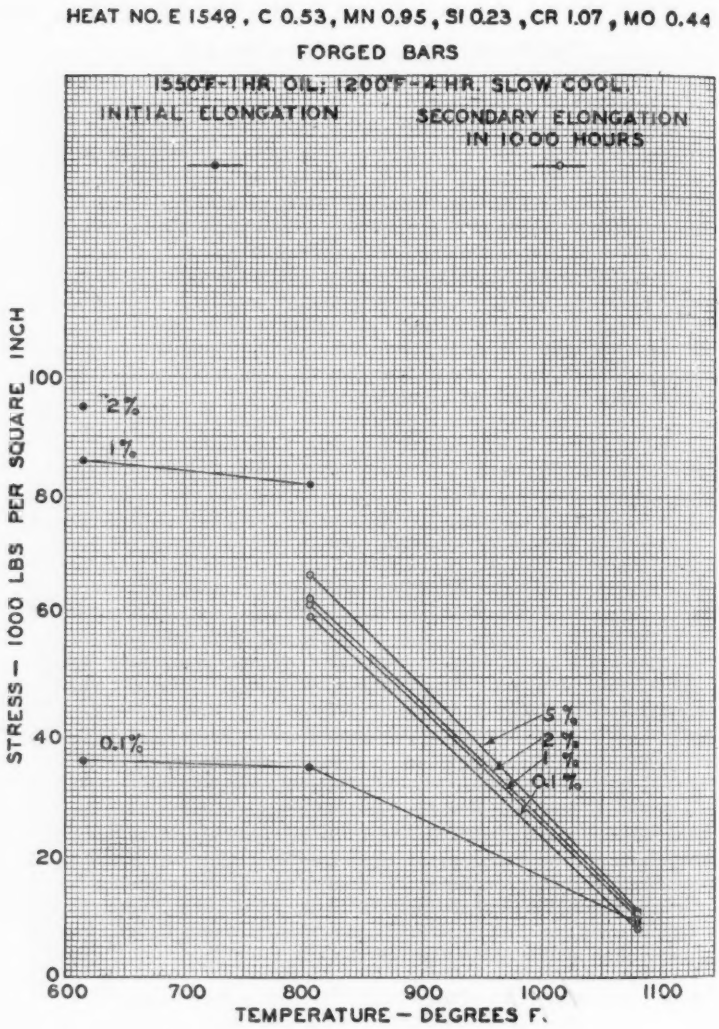

FIGURE 40.—*Flow chart for steel E1549*

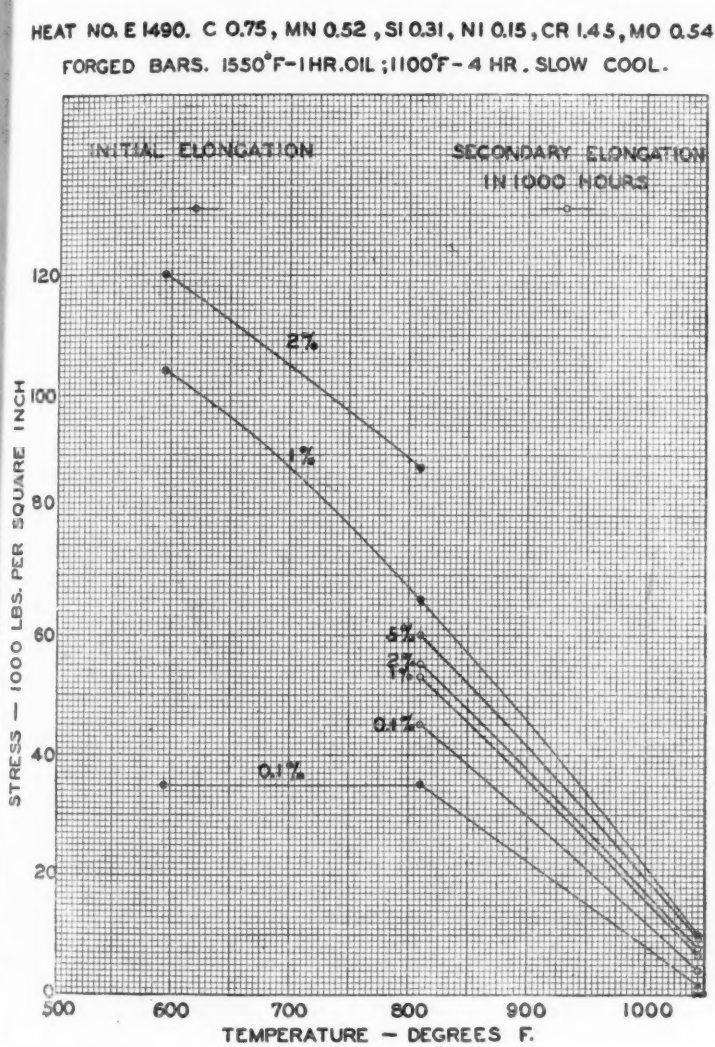

FIGURE 41.—*Flow chart for steel E1490*

The data given in Figure 42 confirm some of the facts developed from practical experience, but, in addition, show certain features which have not been given much, if any, attention. At temperatures between 1,125° and 1,350° F., the high nickel-chromium steels were generally superior to the carbon and low-alloy steels, but if the deformation per thousand hours at the higher temperatures is limited to 1 per cent or less, the maximum allowable stresses drop to low values even for the high-alloy steels.

The outstanding alloy of the group at temperatures between 1,000° and 1,350° F. was the one containing about 0.3 per cent carbon, 1 per cent silicon, 20 per cent chromium, 8 per cent nickel, and 4.5 per

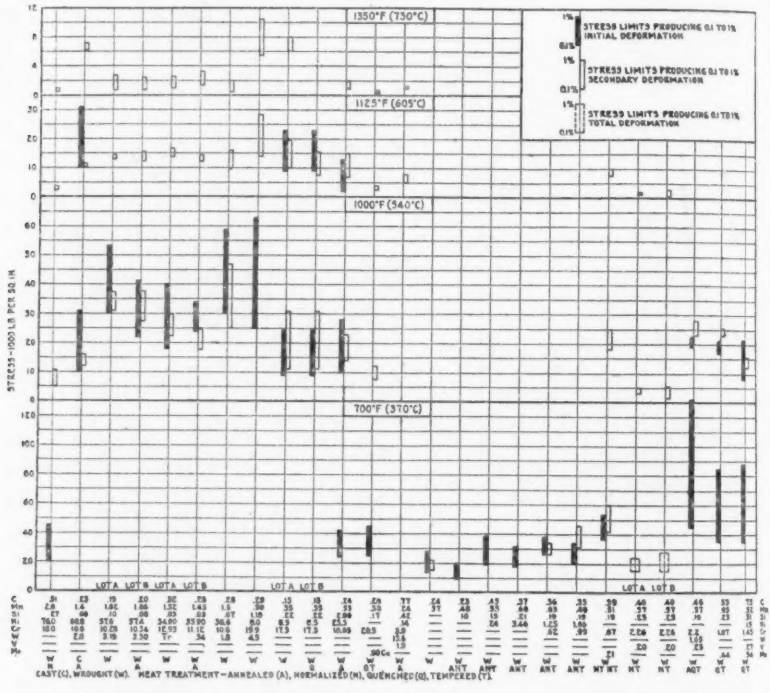
1350°F (730°C)
1125°F (605°C)
1000°F (540°C)
700°F (370°C)
STRESS LIMITS PRODUCING 0.1 TO 1% INITIAL DEFORMATION
STRESS LIMITS PRODUCING 0.1 TO 1% SECONDARY DEFORMATION
STRESS LIMITS PRODUCING 0.1 TO 1% TOTAL DEFORMATION
STRESS - 1000 LB PER SQ IN
LOT A LOT B LOT A LOT B
LOT A LOT B
CAST (C), WROUGHT (W). HEAT TREATMENT - ANNEALED (A), NORMALIZED (N), QUENCHED (Q), TEMPERED (T).

FIGURE 42.—*Comparisons of alloys on the basis of the stresses producing both initial and secondary deformation*

NOTE.—Secondary deformation is over period of 1,000 hours.

cent tungsten; it showed as high or higher load-carrying ability than any of the other alloys. Its superiority was most marked at 1,350° F., but tended to decrease with decrease in the permissible rates of flow and with decrease in temperature.

With this one exception, alloys showing superior properties at 1,350° F. did not necessarily show superiority at lower temperatures. At 1,350° F. superior load-carrying ability was shown by the alloys, 20 Cr, 8 Ni, 1 Si, 4.5 W; 18 Cr, 8 Ni; and 61 Ni, 11 Cr, 2.8 W; at 1,000° F. superiority was shown by the alloys 20 Cr, 8 Ni, 1 Si, 4.5 W; 38 Ni, 11 Cr, 1.8 W, and 57 Ni, 10 Cr, 3 W (FS–1 lot A; as rolled).

These different alloys all represent compositions used industrially for service at different temperatures and it was not practicable to

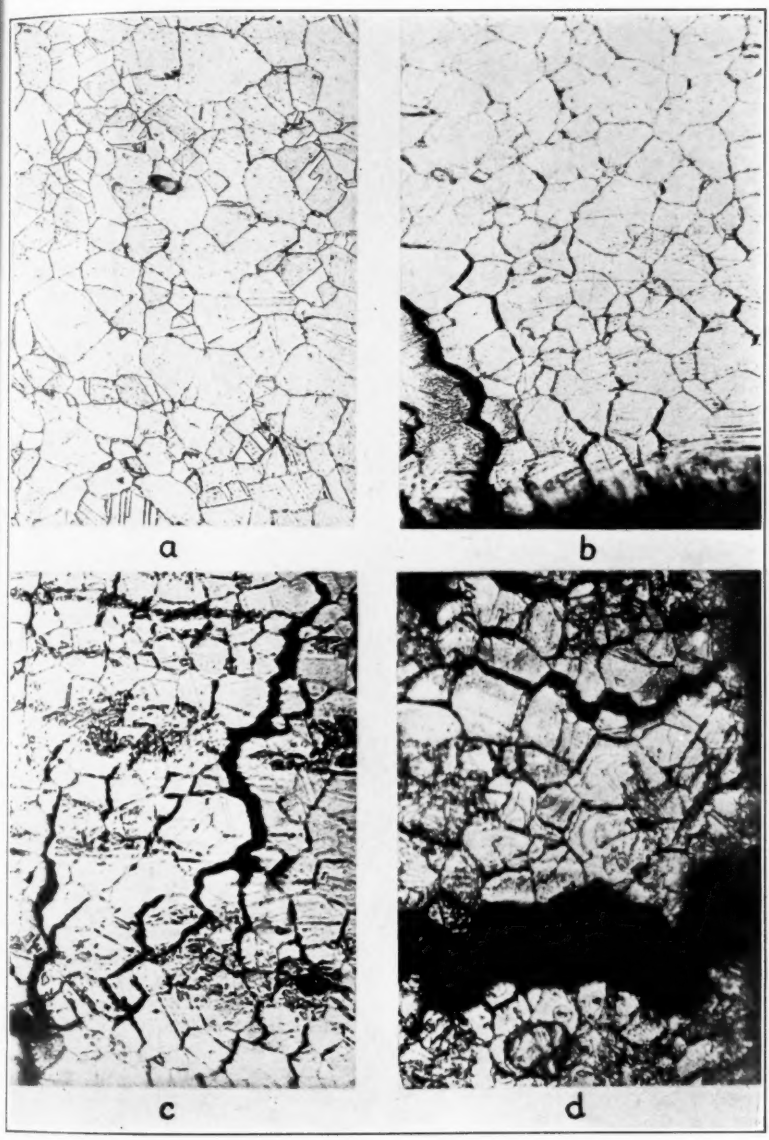

FIGURE 43.—*Structures of the rolled bars (lot A) of alloy E1912, after test at different temperatures,* × *250*

a, 40,000 lbs./in.² at 990° F. for 560 hours; *b*, 50,000 lbs./in.² at 990° F. for 90 hours; metal ¼ inch back of fracture at surface of specimen Total elongation, 15.5 per cent; *c*, 28,000 lbs./in.² at 1,165° F. for 93 hours; metal ⅛ inch back of fracture at surface of specimen. Total elongation, 7.7 per cent; *d*, 10,000 lbs./in.² at 1,380° F. for 168 hours; metal ⅛ inch back of fracture at surface of specimen. Total elongation, 4.4 per cent. Etched with 2 parts concentrated HCl, 1 part concentrated HNO_3, 1 part H_2O_2 and 2 parts glycerin.

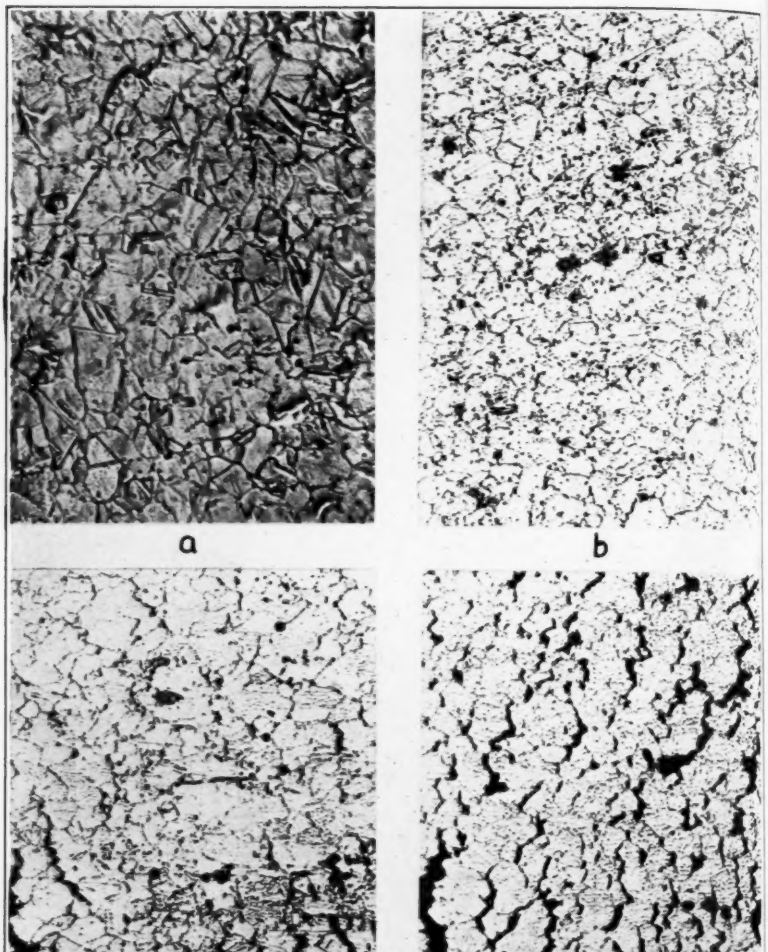

FIGURE 44.—*Structures of the water quenched bars (lot B) of alloy E1912 before and after test at different temperatures*

a, Original quenched bar; *b*, 40,000 lbs./in.² at 990° F. for 520 hours, unbroken with 6.1 per cent elongation; *c*, 50,000 lbs./in.² at 990° F. for 93 hours; metal ¼ inch back of fracture at surface of specimen. Total elongation, 15.5 per cent; *d*, 20,000 lbs./in.² at 1,195° F. for 223 hours, metal ⅛ inch back of fracture at surface of specimen. Total elongation, 10.1 per cent. Etched as indicated in Figure 43.

attempt to determine the effects of variations in important elements, such as nickel, chromium, and silicon upon their high temperature flow characteristics, since in only a few cases were the differences in composition of any two alloys restricted to a single element. For example, the effect of tungsten on the alloy nominally containing 18 per cent chromium and 8 per cent nickel can not be established from data in Figure 42, since the alloy with tungsten contains about twice the carbon and five times the silicon in the alloy without tungsten. Such circumstances do not affect the usefulness of the flow-test data, but made it necessary to depend upon the experimental melts, Group III, Table 1, to show the general trends in the system, nickel-chromium-iron.

The two lots of alloy E1912, containing about 18 per cent chromium and 8 per cent nickel with 0.15 per cent carbon offer some interesting comparisons. It was originally intended to test this alloy only in the hot-worked condition as represented by lot A, Table 1. However, more samples were required before the tests were completed and the bars of the second lot (B) were found to have a higher tensile strength at atmospheric temperatures than bars of lot A, due quite probably to a somewhat lower finishing temperature in rolling. Therefore, lot B was softened by water quenching from 1,850° F. and subsequently tested although its room temperature tensile strength was still somewhat higher than that of lot A. Also, the grain size of the quenched samples was smaller than that of the hot finished samples as is shown in Figures 43 and 44.

At 990° F., these two lots of alloy E1912 exhibited about the same load carrying ability but at 1,180° F. the fine-grained (water quenched) steel was weaker than the coarse-grained material. (Fig. 36.) Comparisons of the two lots were not made at higher temperatures, but the evidence available gives interesting confirmation of the view that fine-grained metals having more intercrystalline material than corresponding coarse-grained metals should be stronger at atmospheric temperatures, but weaker at high temperatures.

There is some evidence, however, that coarsely crystalline metals may be dangerous from other viewpoints. While they may flow at lower rates than corresponding fine-grained metals, fracture may occur with less total elongation. There is also the possible added disadvantage of weakness in resisting shock at high temperatures as well as at atmospheric temperatures.

In the case of the steel nominally containing 18 per cent chromium and 8 per cent nickel, a marked intercrystalline weakness was observed at temperatures between 1,165° and 1,380° F. and to some extent also at 990° F., in both fine-grained and coarse-grained samples, though the latter seemed to show the more marked tendency in this direction. When the specimens were allowed to remain under load at 1,165° to 1,195° or 1,380° F., until fracture occurred the fracture was intercrystalline and grain separations were to be observed at some distance back of the fractures, especially at the surface. These fractures are shown in Figures 43 and 44. There is no clear evidence that this intercrystalline weakness is associated with carbide precipitation at the grain boundaries.

According to one manufacturer [9] there is decided difference in behavior of this nickel-chromium steel which depends upon whether

[9] Private communication.

the carbon content is below or above 0.07 per cent. Quenching from around 2,100° F. has been recommended to bring the carbides into solution, but if subsequently reheated to above 990° F. embrittlement of steels with over 0.07 per cent carbon has been reported to occur and has been attributed to the reprecipitation of carbides at the grain boundaries.

The steel containing about 0.3 per cent carbon, 1 per cent silicon and 4.5 per cent tungsten, in addition to 20 per cent chromium and per cent nickel, showed intercrystalline weakness, 1,160° and 1,30 F., but, so far as could be determined from the usual metallographic examination, this was less marked than in the 0.15 per cent carbon steel with 18 per cent chromium, 8 per cent nickel, and no tungsten. (Figs. 43, 44, and 45.)

Intercrystalline weakness, possibly associated in some cases with grain growth, was observed in two of the samples of the alloy E150 containing 38 per cent nickel, 11 per cent chromium, and 1.8 per cent tungsten when subjected continuously to stress at 1,185° F. (Fig. 46.) No similar effects were found in the alloy, E1894, containing about 60 per cent nickel, 11 per cent chromium, and 2.8 per cent tungsten which was tested in the cast (annealed) condition. The structure of this latter alloy was exceedingly coarse, as is shown in Figure 47 and in tests at 1,370° F. there was evidence of either carbide precipitation or the formation of a eutectic at the grain boundaries. (Fig. 47 (*b*) and (*c*).) Further attention to constitutional changes and intercrystalline weakness of the high-nickel chromium alloys when subjected continuously to stress at high temperatures with comparisons of the alloys nominally containing 18 per cent chromium and 8 per cent nickel with both more and less than 0.07 per cent carbon, would seem to be merited.

3. CARBON AND LOW ALLOY STEELS

If the load-carrying ability is judged by the stresses producing 0.1 to 1 per cent deformation in 1,000 hours, as in Figure 42, the low-alloy steels show promising properties at 700° to 1,000° F. and even up to 1,125° F.

Figure 42 shows a number of factors which tend to improve the load-carrying ability of carbon and low-alloy steels. The first is increase in carbon content. The steel with 0.45 per cent carbon showed much better load-carrying ability than that with 0.23 per cent carbon and resisted flow at 700° F. about as well as the steel with 0.35 per cent carbon and either 3½ per cent nickel or a combination of 1¼ to 1¾ per cent nickel and ½ to 1 per cent chromium.

A comparison of the stresses producing 0.1 to 1 per cent deformation in 1,000 hours for 0.35 per cent carbon steel obtained by interpolation of values for the 0.23 and 0.45 per cent carbon steels with the load-carrying ability of the nickel and nickel chromium steels of similar carbon content indicates that the addition of 3½ per cent of nickel or 1¼ to 1¾ per cent nickel and ½ to 1 per cent chromium is relatively ineffective in increasing the resistance to flow at 700° F. At least the load-carrying ability was no higher than that of a plain carbon steel of somewhat higher carbon content (0.45 per cent) when the metal was placed in a "soft" condition corresponding to that in

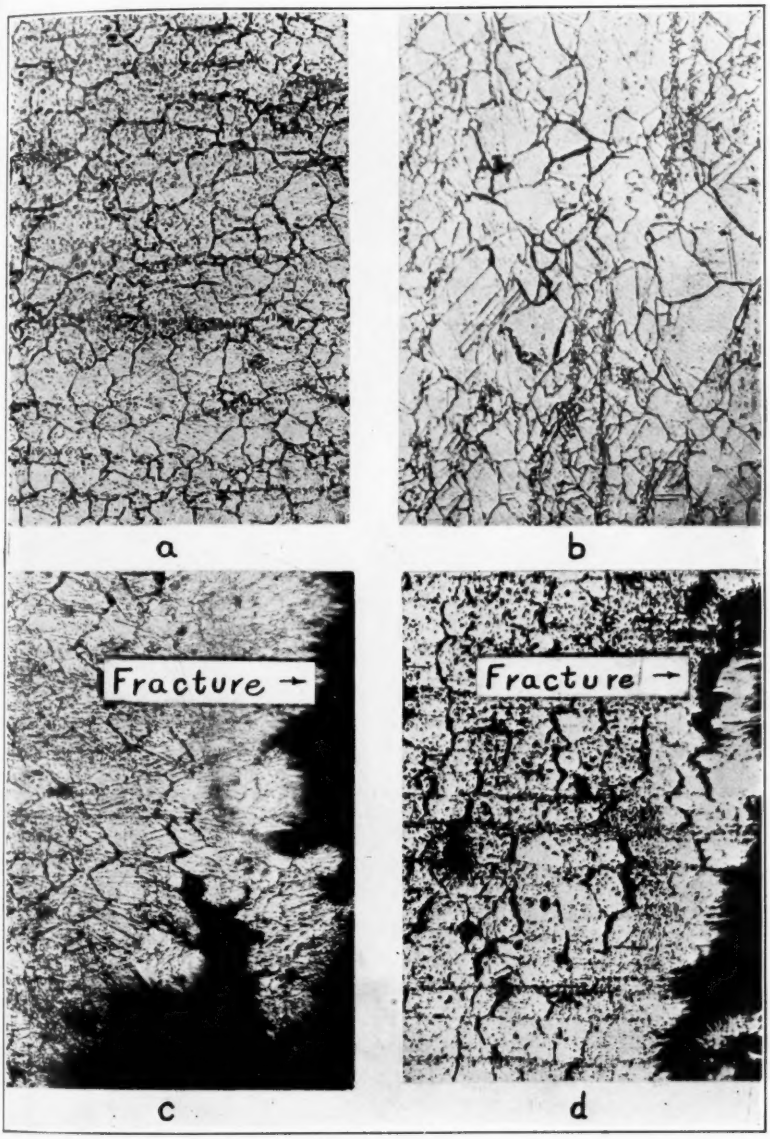

FIGURE 45.—*Structures of the forged bars of alloy EE1114, after test at different temperatures,* × *250*

a, 78,400 lbs./in.² at 995° F. for 79 hours; metal ⅛ inch back of fracture near center of bar. Total elongation, 10.2 per cent; *b*, 25,000 lbs./in.² at 1,160° F. for 106 hours. Unbroken with total elongation of 0.32 per cent; *c*, 39,800 lbs./in.² at 1,160° F. for 106 hours; section at fracture. Total elongation, 4.9 per cent; *d*, 24,900 lbs./in.² at 1,390° F. for 77 hours; section at fracture. Total elongation, 2.7 per cent. Etched as indicated in Figure 43.

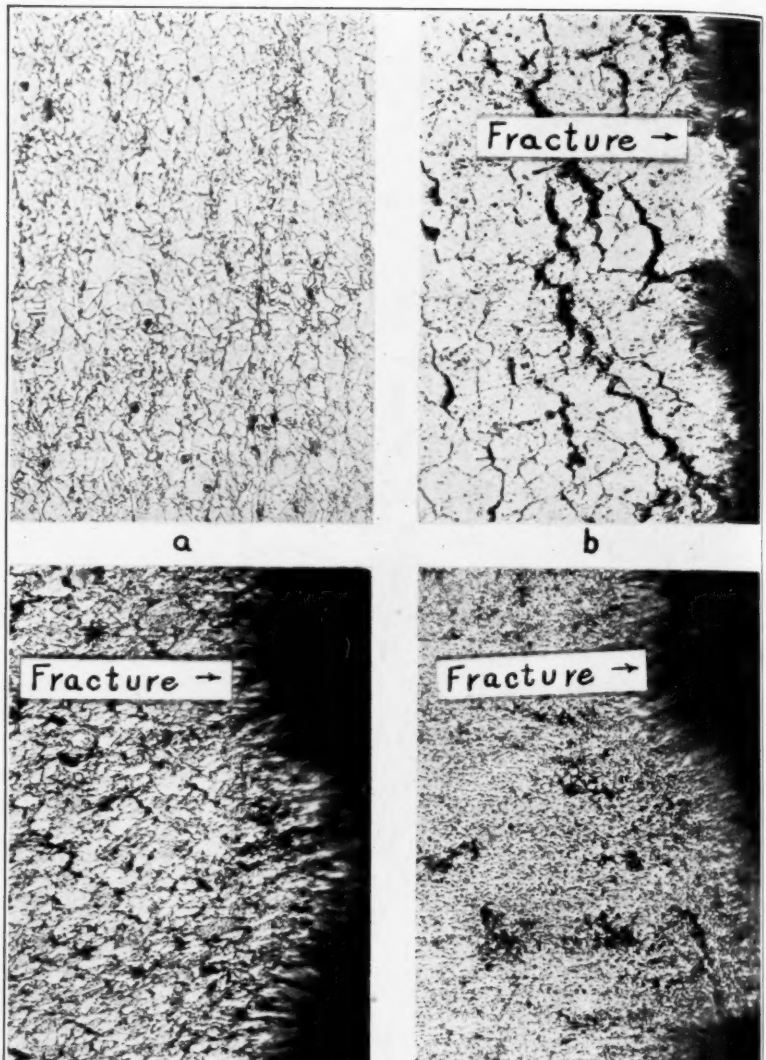

FIGURE 46.—*Structures of the rolled bars of alloy E1567, before and after test at different temperatures,* × *250*

a, Original bar of lot B; *b*, 23,300 lbs./in.² at 1,185° F. for 180 hours; metal at fracture. Total elongation, 2.4 per cent (lot A); *c*, 35,000 lbs./in.² at 1,185° F. for 38 hours; metal at fracture. Total elongation, 13 per cent; *d*, 10,000 lbs./in.² at 1,360° F. for 70 hours; metal at fracture. Total elongation, 37 per cent. Etched as indicated in Figure 43.

large forgings. However, other characteristics of the alloy steels may give them superiority, such, for example, as superior resistance to grain growth on recrystallization which results from deformation and subsequent heating in cyclic temperature operations.

The outstanding feature with respect to the low-alloy steels is the effectiveness of quenching in raising the resistance to flow at temperatures around 700° to 1,000° F. It may be said, a priori, that quenching should be followed by tempering at temperatures at, or preferably above, those of subsequent operation if stability is to be expected, but it is significant that at 700° and 1,000° F. (in one case at 1,125° F.), the quenched and tempered steels showed load-carrying ability proportionately much higher than that produced by small additions of any of the alloying elements considered. It is largely for this reason that it was considered impracticable to attempt to develop the magnitude of the effects of tungsten additions to the chromium or other alloy steels (fig. 42) since the heat treatments were not all comparable.

One other item of interest is to be found in the comparison of the results obtained on the chromium-vanadium steel, No. 10–518, Table 1, subjected to two different preliminary heat treatments. At atmospheric and slightly elevated temperatures the samples with the higher tensile strengths, as determined at room temperature, showed the higher load-carrying ability but at 1,200° F. the order of superiority was reversed although the differences between the two sets of samples were not marked. It is probable that this reversal is analogous to that found in the high chromium nickel steel, E1912, Table 1, already discussed. Once again evidence has been obtained to indicate that high tensile strength at ordinary temperatures does not necessarily signify high load-carrying ability at high temperatures.

4. EFFECT OF PROLONGED STRESS AT DIFFERENT TEMPERATURES ON HARDNESS AND IMPACT RESISTANCE AT ATMOSPHERIC TEMPERATURES

One question which may arise in the practical application of metals at high temperatures is whether prolonged loading will produce appreciable changes in their properties at either atmospheric or elevated temperatures. Aside from precipitation of carbides, claimed to embrittle high chromium or high nickel chromium steel similar to E1912, Table 1, deformation at high temperatures followed by cooling and reheating, which may be encountered in cyclic operation of high-temperature equipment, may result in grain growth and changes in impact resistance or other properties.[10]

Recently Rosenhain and Hanson[11] reported an appreciable increase in the Brinell hardness of mild steel strips containing 0.11 per cent carbon when subjected for about five years at 570° F, to loads equivalent to one-third to two-thirds of their tensile strength determined at ordinary temperatures. This hardening was observed despite the fact that the samples were reported to have undergone only a very small amount of deformation in the specified interval.

No satisfactory explanation was offered for these effects, but if appreciable hardening can take place generally in steels without

[10] F. P. Fischer, Rekristallisationsversuche Allgemeiner Art und zahlenmässige Feststellungen über Festigkeitseigenschaften rekristallisierten Flusseisens (Weicheisens) Kruppsche Monatshefte, **4**, p. 77; 1923.
[11] W. Rosenhain and D. Hanson, The Behavior of Mild Steel Under Prolonged Stress at 300° C., J. Iron & Steel Inst., **116**, p. 117; 1927.

deformation, when they are subjected to prolonged stresses at high temperatures, this matter must be considered in the interpretation of flow-test data. On this account hardness and notched bar impact tests were made on samples of the chromium-vanadium steel, No. 10–518, Table 1, after they had been stressed for long periods in the flow tests.

The impact specimens were prepared from the reduced sections of the flow-test specimens, the notch being placed in the center of the gage length. On account of the small size of the specimens used in the flow tests (0.25-inch diameter) a standard impact test specimen could not be obtained. Instead, specimens were prepared for a low-range Charpy impact testing machine and had a length of 2.1 inches, a thickness of 0.1 inch and widths varying from 0.14 to 0.2 inch, depending upon the diameters of the tested flow test specimens. Whenever possible, specimens having a width of 0.2 inch were used. However, the results were all converted [12] to equivalent values for specimens having a width of 0.2 inch.

Rockwell hardness tests were also made on the broken impact specimens, a $\frac{1}{16}$-inch ball and 100 kg load (B scale) being used. The results are summarized, together with pertinent flow test data in Tables 3 and 4.

TABLE 3.—*Effect of prolonged stress at different temperatures on subsequent hardness and impact resistance at atmospheric temperatures of the Cr–V steel, No. 10–518, Lot A, Table 1*

[1,575° F., slow cool; 1,375° F., furnace cool]

Specimen No.	Flow test		Duration of flow test	Final elongation in flow test	Reduction of area in flow test	Tests at room temperatures subsequent to flow tests	
	Temperature	Load				Impact resistance	Rockwell (B scale) hardness
	° F.	*Lbs./in.²*	*Hours*	*Per cent*	*Per cent*	*Ft./lbs.*	
3149	70	25,000	96			5.10	85.8
3149	70	35,000	195	0.17		5.00	95.9
3142	70	50,000	140	1.87		4.68	87.4
120	70	60,000	94	3.47		4.55	90.5
120	70	70,000	148	6.24		4.48	98.4
126	550	20,000	96			4.97	83.3
127	550	30,000	121	.43		4.93	86.1
13	550	40,000	164	1.40		5.11	86.0
3140	550	50,000	168	2.07		4.22	90.8
3140	550	60,000	121	3.84		3.08	94.0
3140	550	70,000	168	6.40		3.53	98.8
C114	800	5,000	308			4.85	85.1
C115	800	10,000	327			5.07	93.3
C118	800	15,900	327	.06		3.23	86.1
116	800	30,000	218	10.13	14.6	3.58	88.5
C128	1,000	2,500	305			5.26	84.5
C130	1,000	5,100	313			5.30	84.5
C135	1,000	10,000	291	1.89	2.04	4.45	85.2
C138	1,000	15,000	194	4.10	4.50	4.23	85.7
3151	1,000	15,000	288	6.24	5.30	4.36	84.9
C3126	1,200	500	315			5.21	83.4
C3120	1,200	1,000	313			5.11	84.5
3124	1,200	1,500	312			5.21	82.7
3119	1,200	3,000	288			4.99	81.9
C3125	1,200	5,000	315	7.8		5.18	83.9

[12] Since the thickness of the specimens was the same in all cases, the impact values vary directly with the width.

TABLE 4.—*Effect of prolonged stress at different temperatures on subsequent hardness and impact resistance at atmospheric temperatures of the Cr–V steel, No. 10–518, Lot B, Table 1*

[1,575° F., air cool; 1,300° F., furnace cool]

Specimen No.	Flow test		Duration of flow test	Final elongation in flow test	Reduction of area in flow test	Tests at room temperatures subsequent to flow tests	
	Temperature	Load				Impact resistance	Rockwell (B scale) hardness
	° F.	*Lbs./in.²*	*Hours*	*Per cent*	*Per cent*	*Ft./lbs.*	
C3111	70	30,000	194	0.08		5.12	95.0
3107	70	50,000	143	.38		4.47	98.0
C3105	70	70,000	143	.39		4.84	97.3
308	70	70,280	214	1.77	1.20	4.21	97.8
C3148	70	80,000	216	3.13	3.15	3.88	98.5
140	550	30,000	187			4.18	98.3
C142	550	37,750	187	.02		4.13	97.9
3154	550	40,000	168			4.22	93.0
C265	550	62,500	260	.33		4.25	96.4
C3103	550	70,000	91	.74		4.10	97.7
C3102	550	80,000	91	2.19		3.20	100.6
266	800	5,000	308			2.74	97.2
271	800	5,000	327			3.42	95.7
C262	800	9,440	197			2.20	97.1
C275	800	10,000	327	.10		2.46	97.3
C147	800	15,000	191	.18		2.61	97.2
C259	800	22,000	282	.55		2.50	96.6
C268	800	29,600	866	8.99	1.43	3.78	95.4
252	1,000	2,500	322	.33		4.19	98.2
C251	1,000	4,490	489	.10		4.47	96.7
C143	1,000	7,500	305	.52		4.65	95.3
C250	1,000	10,000	383	1.49		4.45	97.1
C394	1,000	15,000	288	8.52	13.06	4.46	95.7
287	1,200	500	441	.18		4.95	92.3
C274	1,200	785	750	1.13		5.25	88.7
C273	1,200	1,500	367	.57		4.92	90.1
C277	1,200	3,000	218	2.77		5.06	93.4

No measurable changes were found in the hardness or impact resistance at atmospheric temperatures so long as no appreciable deformation was produced in the previous flow tests. Deformation at temperatures at which strain hardening occurs in the flow tests was accompanied quite generally by an increase in the hardness and a decrease in the resistance to impact. In all cases, however, the changes were small. At higher temperatures, 1,000° to 1,200° F., no measurable changes were produced in the impact resistance or hardness by deformation in the flow tests. The flow tests were not continued for such long periods as in the tests reported by Rosenhain and Hanson and a steel of very different composition was studied. The results indicated, however, that no changes occurred other than those which might normally be expected from strain hardening.

5. TRENDS AT 1,000° F. IN THE SYSTEM NI-CR-FE

In the tests of the commercial alloys of nickel, chromium, and iron, it was impracticable to determine the effects of variations in nickel or chromium on the load-carrying ability of the alloys at high temperatures, since the variations in composition were not restricted to these individual metals. It was largely on this account that the 12 metals of Group III, Table 1, were prepared. Their

approximate locations in the nickel-chromium-iron ternary diagram are shown in Figure 48.

The flow tests were not continued for such long periods as those made on the commercial alloys, since the principal object was to determine general trends in the system, nickel-chromium-iron, rather than to secure numerical values of the load-carrying ability of the different alloys.

The metals were melted in zirconia crucibles in a high-frequency induction furnace, cast in iron molds (preheated to approximately 390° F.), and subsequently heat treated as indicated in Table 1. The heat treatments were selected to produce at least a partial grain

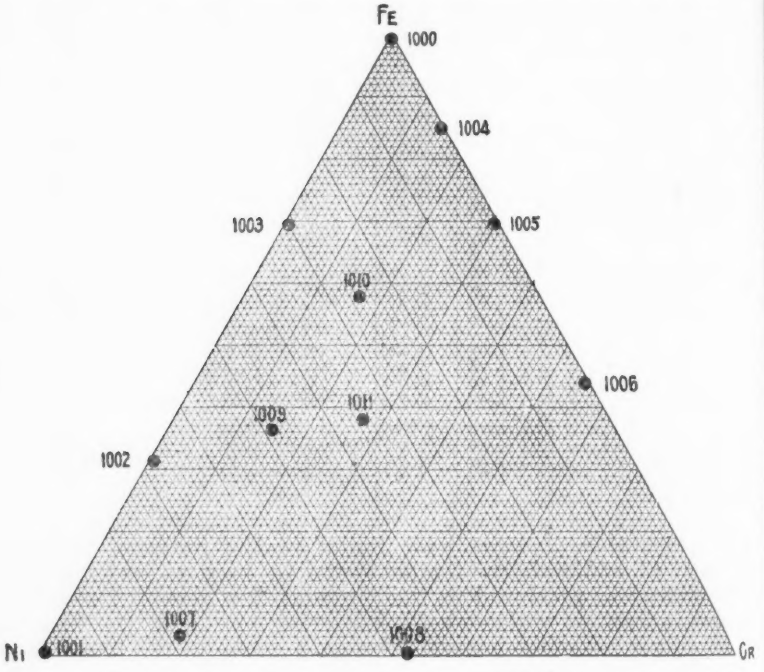

FIGURE 48.—*Locations of the alloys of Group III, Table 1, on the nickel-chromium-iron ternary diagram*

The melt numbers given in the chart correspond to those given in Table 1.

refinement, promote diffusion, and leave the alloys in a "softened" condition.

The alloys tested were not pure in the sense that they were free from all elements except nickel, chromium, and iron, since intentional additions were made of carbon, silicon, and manganese. The presence of appreciable proportions of the last three elements probably exerted a pronounced effect upon numerical values of the flow at 1,000° F., and by acting in different ways in different alloys may have modified somewhat the magnitude of the changes existing in the pure nickel-chromium-iron system. However, it is hardly probable that the general trends were upset by the presence of the carbon, silicon, or manganese and, since most industrial alloys castings of this general

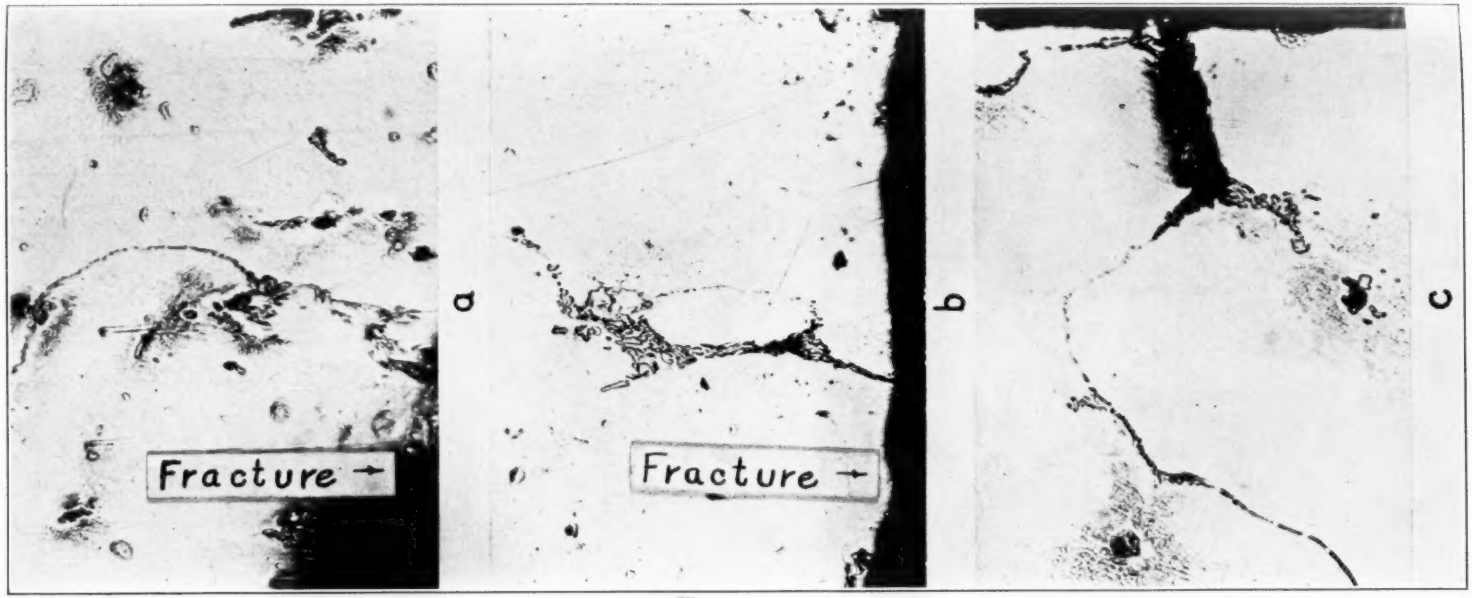

FIGURE 47.—*Structures of the cast and annealed specimens of alloy E1894 after test at different temperatures,* × *100*

a, 28,000 lbs./in.² at 1,215° F. for 64 hours; metal at fracture. Total elongation 18 per cent; *b*, 14,000 lbs./in.² at 1,370° F. for 41 hours; metal at fracture. Total elongation 35.4 per cent; *c*, same as *b*, but at surface ⅛ inch back of fracture. Etched as indicated in Figure 43

type contain appreciable amounts of these three metals, the results are probably closer to those obtainable in practice than would be the case with pure metals.

Table 1 shows that not all of the alloys contained the desired amounts of carbon, silicon, and manganese. The carbon contents were 0.20 to 0.35 per cent in most cases, but some of the alloys contained as much as 0.50 per cent or as little as 0.11 per cent. The manganese was between 0.6 and 0.9 per cent, but the silicon varied from about 0.5 to 1.1 per cent. These variations probably affected the numerical values of the flow appreciably, but, in general, may be disregarded since only the major trends in the nickel-chromium-iron system are to be considered.

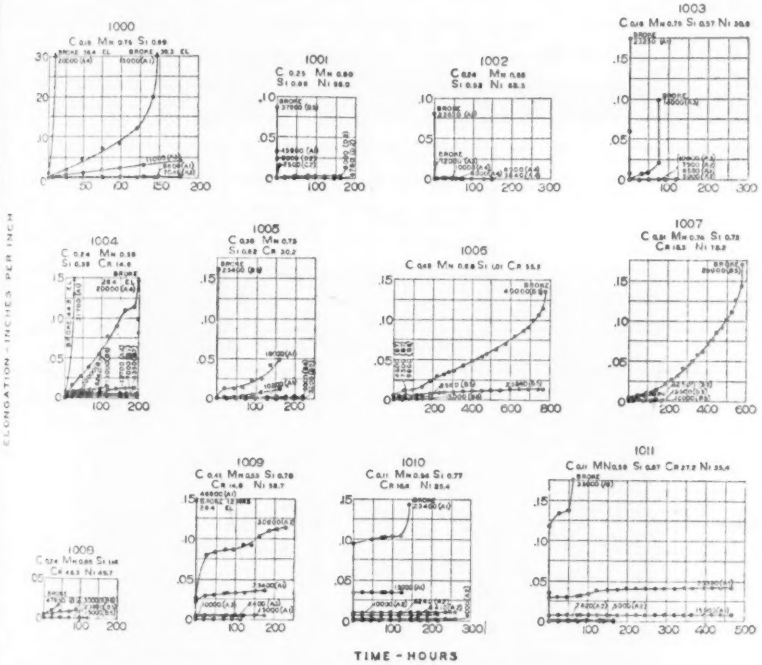

FIGURE 50.—*Time-elongation curves from tests at 1,000° F. of the alloys of Group III, Table 1*

The specimens for the flow tests were cut from the castings at points midway between the outside and the center in the direction of the long axis. The Brinell hardness values subsequent to the recorded heat treatments are given in Table 1, and have been used as the basis of the 3-dimension model in Figure 49 to give a better picture of the conditions in which the metals were tested. The time-elongation curves from the flow tests at 1,000° F., are given in Figure 50 while the relations between the flow and the applied loads are summarized in Figure 51.

As in the case of the alloys of Groups I and II, Table 1, the load-carrying ability may be represented by the stresses producing 1 per cent elongation in the first thousand hours and a comparison of the metals on this basis is given in the 3-dimension ternary model in

Figure 52. Figure 52 shows that the addition of nickel to the iron containing about 0.2 per cent carbon, etc. (Table 1), resulted in no marked changes in the stresses producing 1 per cent elongation in the first thousand hours.

The addition of chromium to iron containing about 0.2 per cent carbon, etc. (Table 1), did not improve the load-carrying ability at 1,000° F. appreciably until the chromium content was in the neighborhood of 50 per cent. In fact, the iron alloy with 30 per cent chromium showed the lowest resistance to flow of all of the alloys tested and that with 14 per cent chromium, representing the composition of "stainless steel," was about on a par with steel containing no chromium.

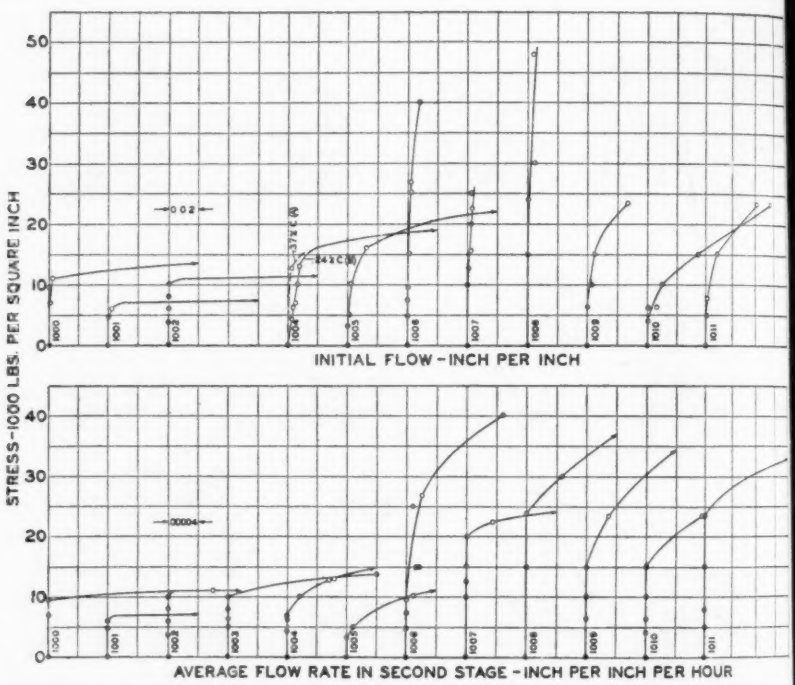

FIGURE 51.—*Flow data for tests at 1,000° F. on the alloys of Group III, Table 1*

Obtained from Figure 50.

On the other hand, the addition of a little chromium to the iron alloys with 40 per cent or more of nickel produced a marked increase in the load-carrying ability. The most effective proportions of chromium were between 5 and 20 per cent; higher proportions produced further increases, but not in the same degree.

These results explain in part the popularity of the commercial iron-nickel-chromium casting alloys containing about 60 to 65 per cent of nickel and 10 to 20 per cent of chromium. This composition is in the range of high load-carrying ability, although it does not have the best resistance to flow.

The strongest of the alloys at 1,000° F. were those with little or no iron, 50 to 80 per cent nickel, and 50 to 20 per cent chromium. The

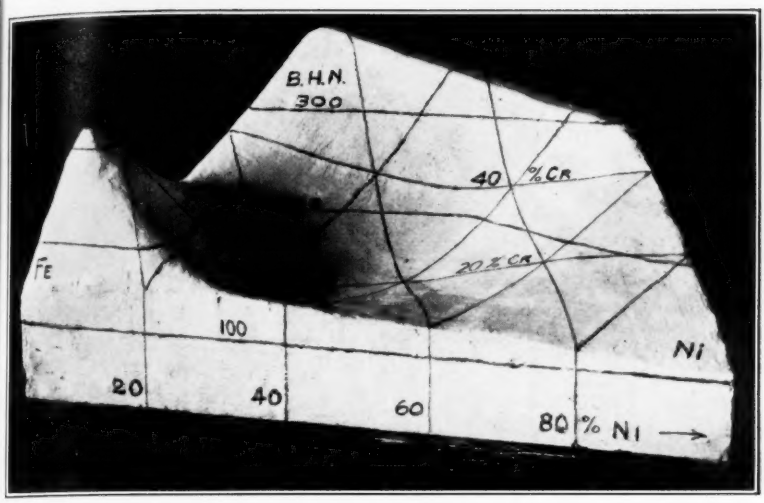

FIGURE 49.—*Summary of the Brinell hardness of the alloys in Group III, Table 1, in the conditions tested*

This model is based on data given in Table 1.

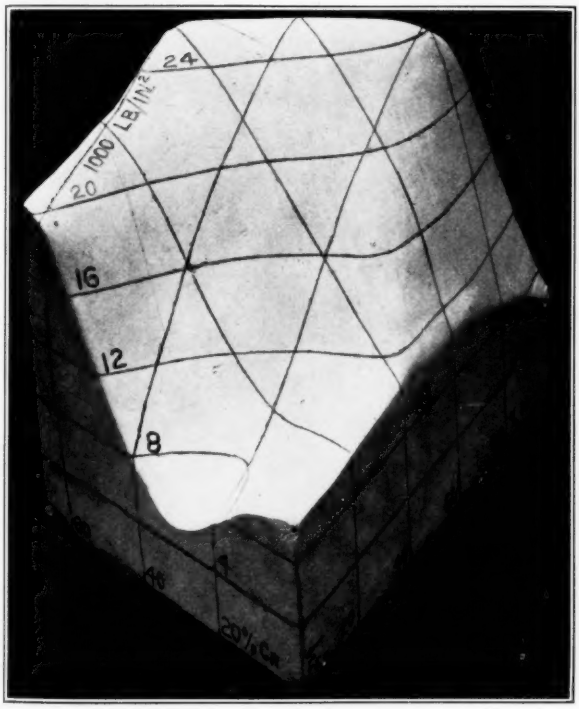

FIGURE 52.—*Stresses producing 1 per cent elongation in the first 1,000 hours at 1,000° F. in cast alloys of the system, nickel-chromium-iron*

As explained in the text, this model is intended only to show the general trends in the system.

highest load-carrying ability was obtained in the castings containing about 50 per cent each of nickel and chromium (alloy 1008, Table 1), but this alloy would be expected to offer difficulties in the foundry and had the serious disadvantage of fracturing with low elongation. (Fig. 50.) The remedy for this latter condition may be in decrease in the impurities, but foundry difficulties would be expected to persist under such conditions. A more practical solution of the problem of securing higher resistance to flow at high temperatures would probably be in additions of other elements to the alloys containing 60 to 65 per cent of nickel, 10 to 20 per cent of chromium. Tungsten is one of the additions used industrially for this purpose as is shown by the composition of the commercial alloys of Group I, Table 1.

In the alloys containing 50 per cent or more of nickel and 10 to 20 per cent of chromium, it would seem to be advisable to keep the chromium close to 20 per cent, since a decrease to 15 per cent or less brings the metal into a range of rapidly decreasing load-carrying ability as is shown in Figure 52. This means that the composition variations ordinarily encountered in commercial production would result in wider variations in properties in the nickel-iron alloys with 5 to 15 per cent chromium than in those with 15 to 20 per cent. Furthermore, lowering the chromium would also tend to lower the oxidation resistance of the metal.

It is of interest to note that the iron-nickel-chromium alloy having the nominal composition of 18 per cent chromium and 8 per cent nickel, which is now so widely used in the wrought condition, is in the field of low load-carrying ability at 1,000° F. It can not compete with some of the other alloys in castings for service requiring high resistance to flow, but is attractive on account of excellent resistance to oxidation and because it can be formed either hot or cold.

While this and some of the other alloys in the nickel-chromium-iron system were found to have relatively low resistance to flow at 1,000° F., it should be recognized that improvement may be obtained through modifications in heat treatment or by varying the proportions of elements, such as carbon, silicon, etc. An example is found in the iron alloy containing 14 per cent chromium. Tests on two different ingots containing, respectively, 0.24 and 0.37 per cent carbon showed (fig. 51) that the alloy with 0.37 per cent carbon had a much better resistance to flow at 1,000° F. than the alloy with 0.24 per cent carbon.

It should be recognized that variations in the general structure (cast or wrought metal), in heat treatment, or in the proportions of elements, such as carbon and silicon, may affect the load-carrying ability to a greater degree than appreciable variations in the proportions of nickel, chromium, or iron at least in some parts of the system. (Fig. 52.)

V. SUMMARY

Flow tests were made at different temperatures on three groups of alloys. The 11 metals of the first group comprised 1 nickel-chromium alloy, 6 nickel-chromium-iron alloys, with or without tungsten, and 4 low chromium steels containing also vanadium, tungsten, or molybdenum. The flow characteristics of these metals are summarized in charts given in the report.

Two carbon steels, two low nickel-chromium steels, and a 3½ per cent nickel steel comprised the second group of metals which were

tested at 700° F. When annealed so as to reproduce the conditions existing in large forgings the plain carbon steel containing 0.45 per cent carbon showed better load-carrying ability than that with 0.2 per cent carbon and resisted flow at 700° F. about as well as the steels with 0.35 per cent carbon and either 3½ per cent nickel or a combination of 1¼ to 1¾ per cent nickel and ½ to 1 per cent chromium.

The third group of metals consisted of nickel-chromium-iron alloy castings melted in a high-frequency induction furnace. Their chemical compositions were selected to cover a broad area in the nickel-chromium-iron system, and the tests of these metals were made at 1,000° F. after annealing or normalizing to produce softening, grain refinement, and diffusion.

It was found that the addition of nickel to iron containing about 0.20 per cent carbon, 0.75 per cent manganese, and 0.7 per cent silicon resulted in no marked changes in the stresses required to produce 1 per cent elongation in the first 1,000 hours. The addition of chromium to the iron did not greatly improve its load-carrying ability until the chromium content reached about 50 per cent. In fact, the iron alloy with 30 per cent chromium showed the lowest resistance to flow of all of the alloys tested at 1,000° F. and the one with 14 per cent chromium, representing the composition of "stainless steel," was about on a par with steel containing no chromium.

On the other hand, the addition of a little chromium to the iron alloys with about 40 per cent or more of nickel produced a marked increase in the load-carrying ability. The most effective amounts of chromium were between 5 and 20 per cent; higher proportions produced further increases, but these were not commensurate with the increases produced by additions below 20 per cent.

The highest load-carrying ability was obtained in the castings containing about 50 per cent each of nickel and chromium, but this alloy would be expected to offer difficulties in the foundry and, with the proportions of carbon, silicon, and manganese present, had the serious disadvantage of low ductility.

In the case of the wrought commercial alloy containing 0.15 per cent carbon, 18 per cent chromium, and 8 per cent nickel, intercrystalline weakness was observed at temperatures between 1,165° and 1,380° F. and to some extent also at 990° F. This was noted in both fine-grained and coarse-grained samples, although the latter seemed to show the greater tendency in this direction. A similar tendency, but in a smaller degree, was observed at 1,160° and 1,390° F. in the alloy containing 0.3 per cent carbon, 1 per cent silicon, 4.5 per cent tungsten, 20 per cent chromium, and 8 per cent nickel, and at 1,185° F. in an alloy containing 38 per cent nickel, 11 per cent chromium, and 1[illegible] per cent tungsten.

In the case of the wrought alloy containing about 0.15 per cent carbon, 18 per cent chromium, and 8 per cent nickel, fine-grained and coarse-grained samples showed about equal load-carrying ability at 990° F., but the fine-grained samples were weaker than the coarse-grained at 1,180° F. This should not be taken as a recommendation of coarse-grained metals for high-temperature service, since fracture may occur with less total elongation than in the corresponding fine-grained metals and so counteract any advantages from lower rates of flow. There is also the possible added disadvantage of weakness in resisting shock.

With one exception the wrought commercial alloys of nickel, chromium, and iron which showed superiority at about 1,380° F. did not necessarily show superiority at lower temperatures. This exception was the alloy containing about 20 per cent chromium, 8 per cent nickel, 4.5 per cent tungsten, 0.3 per cent carbon, and 1 per cent silicon, which had the highest load-carrying ability of all of the alloys of Group I.

A study was made of the effect of deformation in the flow tests at different temperatures on the hardness and impact resistance of a chromium-vanadium steel at ordinary temperatures. No marked changes were found in the hardness or impact resistance so long as no measurable deformation was produced in the prior flow tests. At temperatures at which strain hardening occurs, deformation in the flow tests produced a small increase in the hardness and a decrease in the impact resistance of the steel at atmospheric temperatures; deformation in the flow tests at higher temperatures did not affect these properties at atmospheric temperatures.

VI. ACKNOWLEDGMENTS

The authors are indebted to H. K. Herschman, associate metallurgist, for the micrographs included in this report; to H. A. Bright, chemist, for the chemical analysis of the alloys; and to H. C. Cross, junior metallurgist, for carrying out the hardness and impact tests on the flow-test specimens and for assistance, from time to time, in the flow tests. The very efficient aid of Dr. R. L. Dowdell, senior metallurgist, and W. A. Tucker, senior laboratory assistant, has contributed greatly to the progress of the work in its later phases and is gratefully acknowledged.

WASHINGTON, February 25, 1930.

THE CHARACTERISTICS OF TWO-BLADE PROPELLER FANS

By H. L. Dryden and P. S. Ballif

ABSTRACT

Seven 2-blade propeller fans, 8 feet in diameter and of pitch/diameter ratios 0.250, 0.375, 0.500, 0.625, 0.750, 0.938, and 1.063, respectively, were tested in a duct especially constructed to simulate the operating conditions encountered in cooling towers. Each fan was tested for two operating conditions: (1) With the fan operating as a blower, and (2) with the fan exhausting air from the duct. Each fan was operated at constant speed of rotation against resistance conditions which were varied by steps, from a completely blocked passage to as nearly as open passage as the conditions in the duct permitted. The relation between the volume of air moved in unit time, the head developed, and the power absorbed by the fan was determined for each resistance condition. The results are expressed in the form of coefficients and are plotted so as to facilitate their use in estimating the performance of fans of other diameters and rotational speeds. The chief effect of variation of pitch/diameter ratio is to increase the range of head and volume coefficients with increase in pitch/diameter ratio up to pitch/diameter ratio of 0.938. The blower condition shows a slightly higher efficiency throughout. There is little variation in maximum efficiency between pitch/diameter ratios of 0.375 and 0.938. Pitch/diameter ratios greater than 1.0 should not, in general, be used.

Two-blade propeller fans are suitable for moving large volumes of air against pressures that do not exceed 1.0 inch of water. For pressures greater than 1.0 inch of water the rotational speeds become inconveniently large. The speed of rotation and the fan diameter should be carefully chosen to obtain maximum efficiency.

CONTENTS

	Page
I. Introduction	185
II. General plan of the investigation	186
III. Description of apparatus	186
IV. Remarks on the location of the static pressure holes	189
V. Test procedure	192
VI. Reduction of observations	193
VII. Results	200
VIII. Accuracy of results	210
IX. Conclusion	211
X. Acknowledgment	211

I. INTRODUCTION

The investigation described in this report was undertaken as a cooperative project between the Paragon Engineers (Inc.), of Baltimore, Md., and the National Bureau of Standards for the purpose of obtaining for the industry data on the performance of 2-blade propeller fans. Recently there has been a trend toward the use of fans of this type in cooling-tower installations, and their use has also been considered for other applications where it is desired to move large volumes of air against relatively low pressures. Since no data were available as to the operating characteristics of 2-blade propeller fans, the importance of this information to the manufacturer and user is obvious.

The Paragon Engineers (Inc.) furnished the fans used and supplied funds for the construction of a test duct at the Bureau of Standards where the experiments were performed. Members of the staff of the Bureau of Standards installed the apparatus and conducted the tests. This report contains a brief description of the apparatus and methods employed and presents a summary of the results of the investigation, together with such comments and discussion as seem necessary.

II. GENERAL PLAN OF THE INVESTIGATION

In regard to any one fan the object of the experiments is to determine the relation between the power absorbed and the quantity of air delivered against various resistance conditions. When this relation has been found and expressed in suitable form, it can be used to predict the performance of similar fans operating under similar conditions. It is important to remember the restriction stated in the last clause, since the test duct was arranged to simulate the special conditions encountered in cooling-tower applications.

Each fan was operated at constant speed of rotation against resistance conditions which were varied by steps, from a completely blocked passage to as nearly an open passage as conditions in the test duct permitted. The temperature and barometric pressure of the free atmosphere, the static pressure and velocity of the air flowing through the duct, and the power furnished by the motor were measured. The quantity of air delivered by the fan in unit time was calculated from the observed value of the mean air velocity and the area of the duct.

Observations were made on each fan at two speeds of rotation, viz, 585 and 700 r. p. m., except for two fans of low pitch where it was necessary to use speeds of 800 and 900 r. p. m. in order to stay within the efficient working range of the motor. These speeds were selected as representative motor speeds. As will be explained later, the measurements at two speeds are, in effect, check measurements and serve to indicate the accuracy of the work.

Data were obtained for two operating conditions: (1) With the fan operating as a blower, and (2) with the fan exhausting air from the duct.

III. DESCRIPTION OF APPARATUS

The test duct (figs. 1, 2, 10, 11) is circular in cross section, 10 feet in diameter, and 26 feet 3½ inches long, with the axis of the duct about 8 feet above the ground. The duct is out of doors, a control room built at the side of the duct serving to house the instruments and control apparatus. In the duct there is a honeycomb partition consisting of hollow sheet-metal cylinders 3 inches in diameter and 12 inches long with their axes parallel to the axis of the duct. In addition to serving its usual function of straightening the air stream, the honeycomb serves as a support for holding the materials used to increase the resistance of the duct. When the fan is operated as a blower, the honeycomb is located 13 feet 11½ inches from the plane of the fan. (Fig. 10.) For the exhaust condition (fig. 11) the honeycomb is located 21 feet 6⅝ inches from the plane of the fan. Eight static wall plates, 45° apart in a plane normal to the axis of the duct and 13 feet 9⅛ inches from the plane of the fan. are located in the duct wall. The

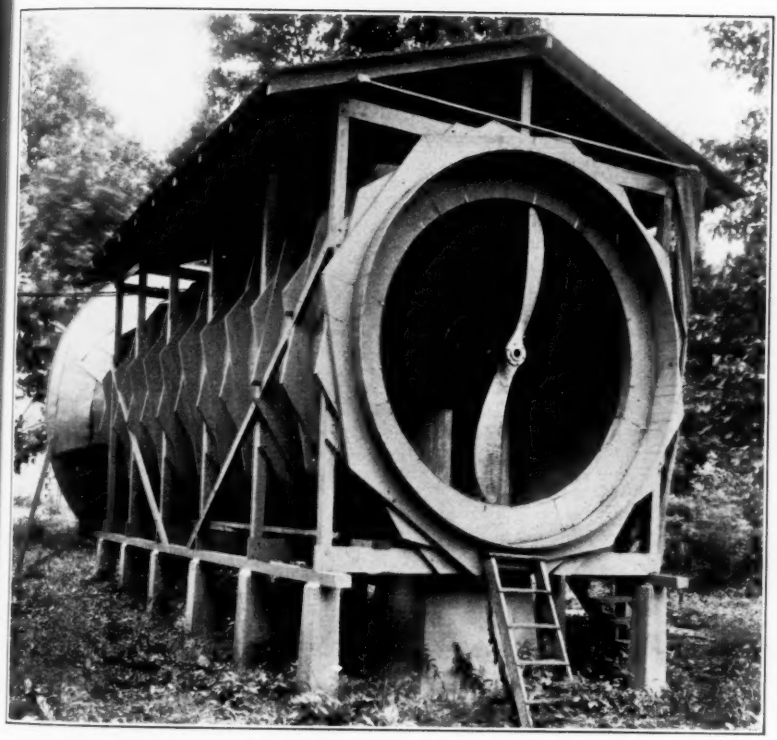

FIGURE 1.—*Front view of test duct*

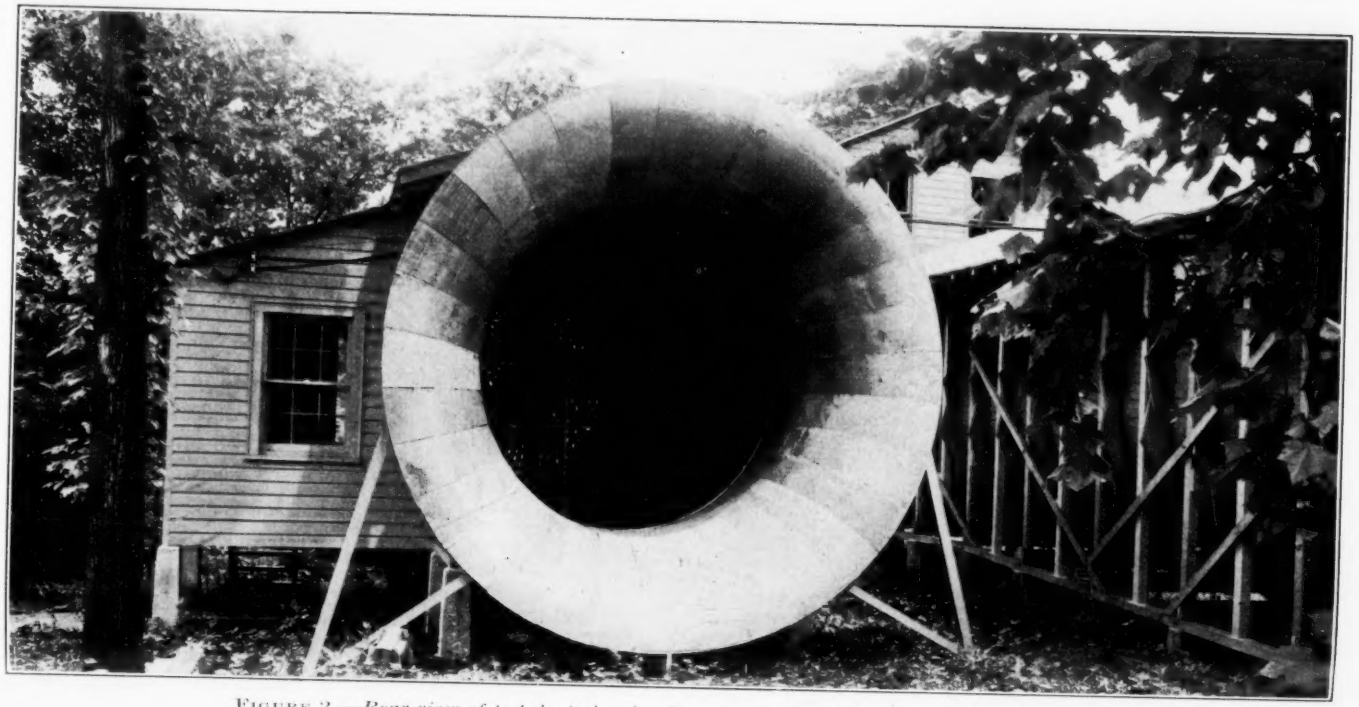

FIGURE 2.—*Rear view of test duct showing honeycomb, faired section, and control room*

all plates are connected through one-eighth inch galvanized pipe to single header. Each lead contains a valve so that any wall plate may connected through the header to a sloping manometer while the st are closed off.

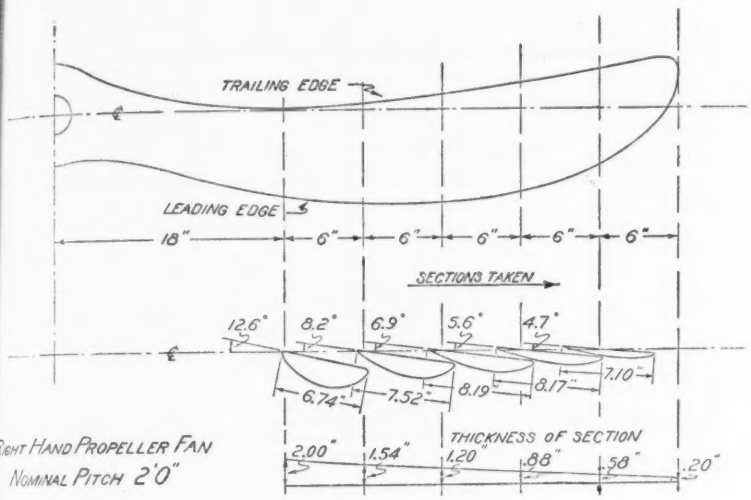

FIGURE 3

A 25-horsepower direct-current variable-speed motor is mounted on two streamlined concrete columns inside the duct. The motor is substantially cylindrical and about 35 inches in diameter. The

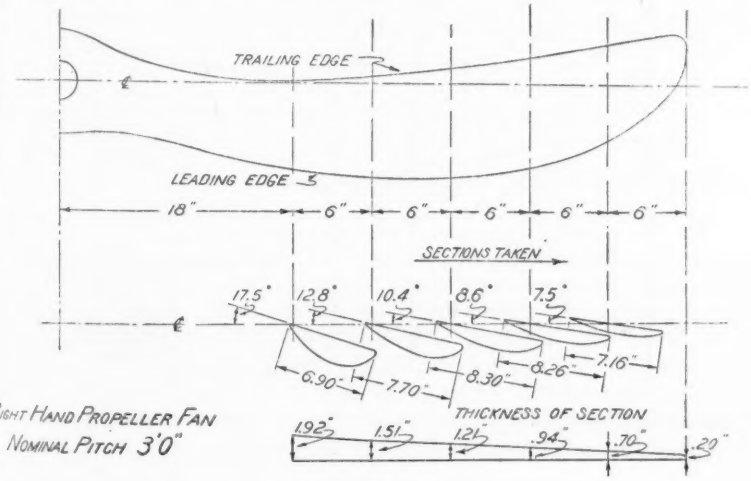

FIGURE 4

streamlined columns are about 3½ feet high and 2½ feet long, with a maximum thickness of about 8 inches.

The air speed at any point was measured by a 4-inch Richard electrically signaling anemometer, which had been calibrated on the mounting used. The anemometer was fastened, as indicated in

Figures 10 and 11, to an arm that could be turned in a plane normal to the axis of the duct, and it could be set at any distance from the axis

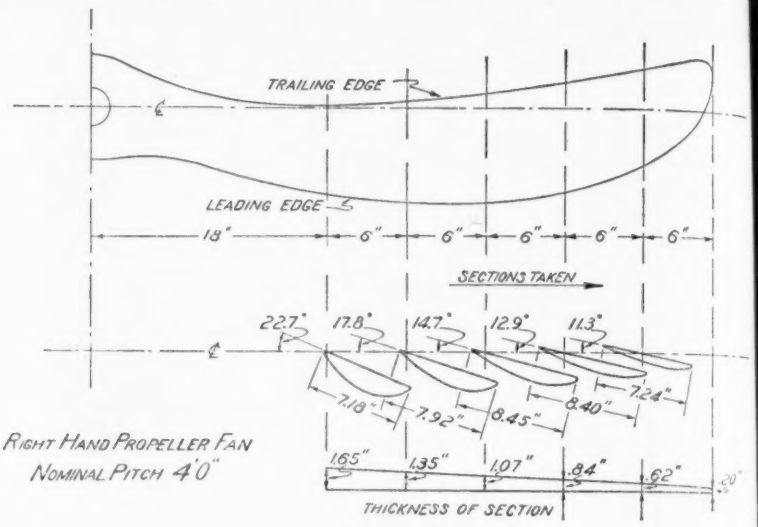

FIGURE 5

hence, it was possible to place the anemometer at any point on the circle swept out when the arm was turned.

The speed of rotation was measured by a Weston electric tachometer directly connected to the motor shaft. The power input was measured

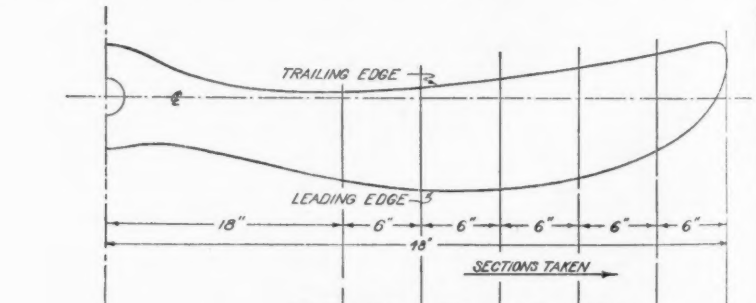

FIGURE 6

by means of a portable-type ammeter and voltmeter accurate to one-half of 1 per cent.

Seven 8-foot 2-blade propeller fans of laminated wood construction were used in the investigation. The nominal pitch of the fans was

3, 4, 5, 6, 7½, and 8½ feet, respectively. The measured geometric pitch at several radii is given in Table 1. Figures 3 to 9 show the approximate shape and dimensions of the fans. It should be noted that the fans are not all of one family, since the plan form, blade width, and blade section vary considerably.

TABLE 1.—*Measured pitch of fans at various radii*

Nominal pitch	Radius in feet				
	1.5	2.0	2.5	3.0	3.5
4-foot	2.14	1.80	1.86	1.80	1.74
5-foot	3.02	2.91	2.98	2.94	2.90
6-foot	3.94	4.03	4.12	4.32	4.40
7-foot	4.40	4.64	4.85	4.97	5.08
8-foot	4.40	5.02	5.44	5.74	5.73
7½-foot	5.18	6.45	7.32	7.55	7.51
8½-foot	6.83	7.85	8.33	8.52	8.36

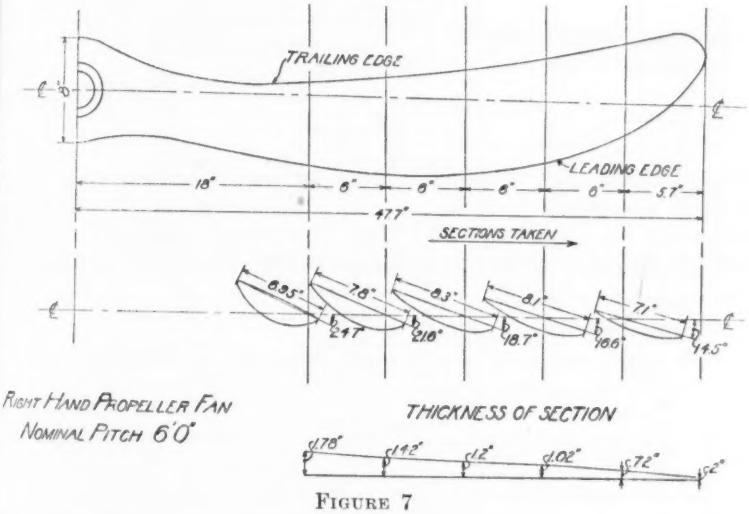

FIGURE 7

The diameter of the duct was made 2 feet larger than the diameter of the fan so as to approximate the condition in a particular cooling-tower installation. That installation has several fans located in the walls of the tower. The cross-sectional area of the tower is 1.56 times the total fan disk area; hence, in reproducing this condition, the ratio of the diameter of the outlet duct to the diameter of the fan was made $\sqrt{1.56}$, or 1.25. A cylindrical ring 4½ inches long and 8 feet 1 inch inside diameter was centered in the plane of the fan to simulate the wall condition.

IV. REMARKS ON THE LOCATION OF THE STATIC PRESSURE HOLES

The static pressure holes were originally located 3⅜ inches downstream from the plane of the fan. With the 5-foot pitch fan operating as a blower at 585 r. p. m., the static pressure was found to be 0.25

inch of water less than the atmospheric pressure. It seemed sur
prising at first that the fan operating as a blower should develop
decreased static pressure, but further investigation showed it to be
perfectly natural phenomenon, as explained below. A longitudin

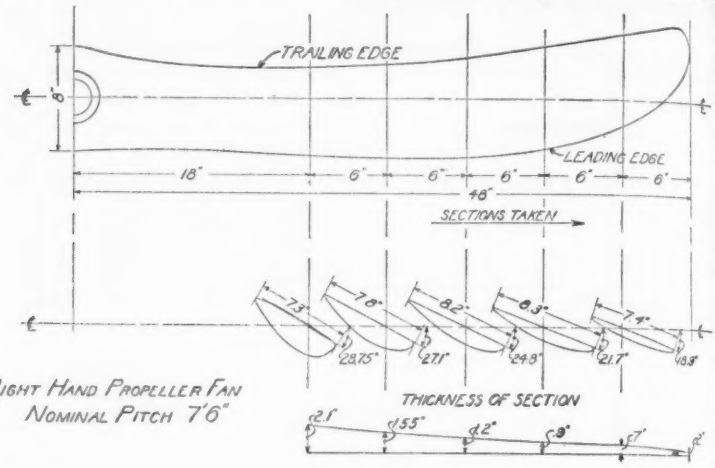

FIGURE 8

traverse of the duct was made, observations of static pressure being taken at the points *1*, *2*, *3*, ... *24* of Figure 10. The results are plotted in Figure 12. The fan produces a condition of reduced pressure on its inlet side which causes the air to flow into the fan

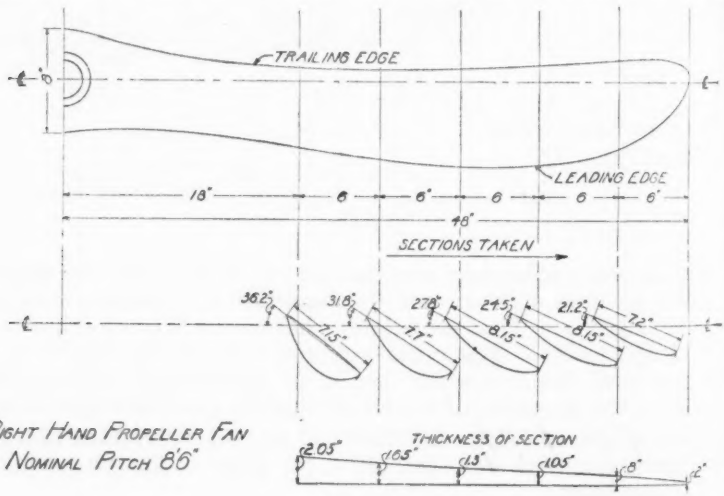

FIGURE 9

Referring to the curve, we see that the static pressure at this section is 0.57 inch of water less than the atmospheric pressure. The fan boosts the pressure to 0.25 inch of water less than the atmospheric pressure and the air is discharged into the duct which is of larger cross section than the inlet ring. The air tends to fill the duct,

lowing up and thus converting velocity pressure into static pressure. The obstruction of the duct by the motor and its supporting columns

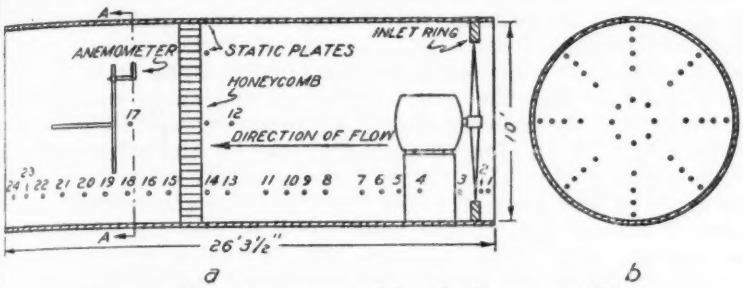

FIGURE 10.—*Arrangement of duct for blower condition*

a, Longitudinal section. b, Section A–A, showing points of observation for velocity.

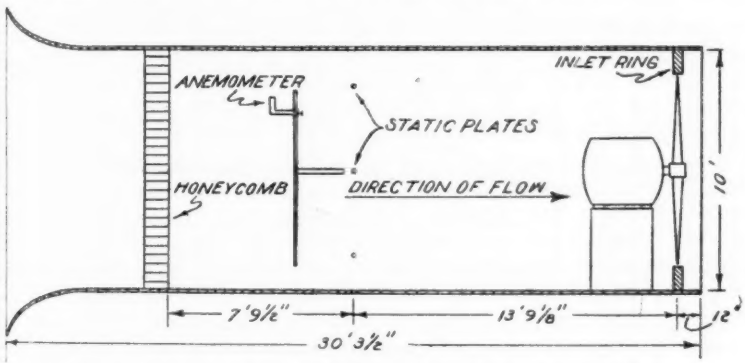

FIGURE 11.—*Longitudinal section of duct, exhaust condition*

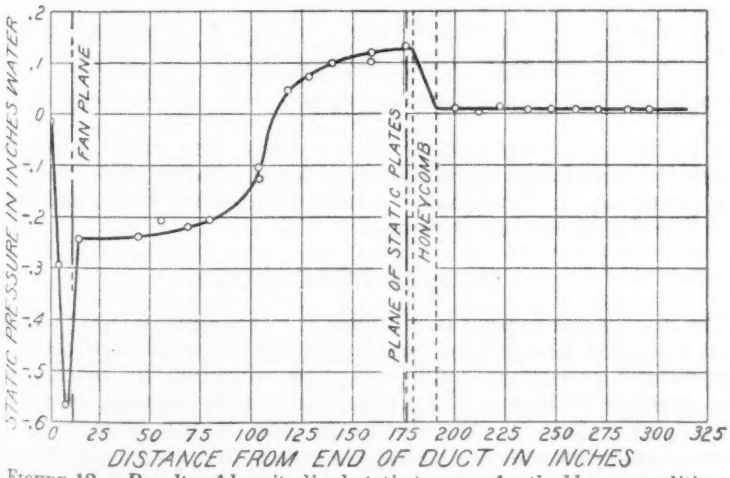

FIGURE 12.—*Results of longitudinal static traverse for the blower condition*

inders the process until the obstruction has been passed, when we nd the pressure rising rapidly to a maximum value just in front of he honeycomb. There is a sharp drop in pressure through the

honeycomb, and a fairly constant value is then maintained to the end of the duct. The pressures measured near the fan are probably greatly in error because of the very turbulent and nonaxial motion of the air. The curve shows clearly that the most desirable location of the static pressure holes is just in front of the honeycomb. Since in the blowing tests some spiral motion persists right up to the honeycomb, we feel that the measurement of the static pressure is less satisfactory in the blowing tests than in the exhaust tests.

The results of the longitudinal traverse for the exhaust condition are shown in Figure 13. In front of the honeycomb the static pressure is about 0.06 inch of water less than the atmospheric pressure. There is a drop through the honeycomb to about 0.1 inch of water less than the atmospheric pressure, and this value is maintained until the obstruction of the passage by the motor and its supports causes the velocity to increase and the pressure to decrease. The fan boosts the pressure to about atmospheric pressure and the air is discharged

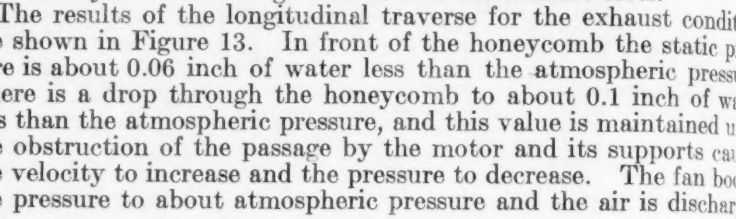

FIGURE 13.—*Results of the longitudinal static traverse for the exhaust condition*

at a relatively high velocity. It is readily seen that the position of the static holes is not so restricted as for the blower-fan arrangement. The pressures for the exhaust arrangement were very much steadier than for the blower arrangement.

V. TEST PROCEDURE

The duct is not housed in a building, but stands in the open. Runs were not made when there was any precipitation or appreciable wind. The desired resistance conditions were obtained by placing a suitable number of layers of material (mosquito netting, cheese cloth, batiste, or paper) on the upstream side of the honeycomb. The several fans were run at the speeds mentioned above for each resistance condition; the resistance was then changed, and the procedure repeated. Measurements of the velocity for each resistance condition were made at the 40 points indicated in Figure 10 (*b*), the points being at the centers of equal areas of the cross section. Each reading of the anemometer took about one minute and represented an inte-

gration of the velocity over this period of time. The velocity in feet per minute was computed from the time (measured by a stop watch) required for the anemometer to make a counted number of revolutions, the calibration curve being used.

The first set of data was taken with the fan operating as a blower; Figure 10 shows the arrangement in the duct. For the exhaust condition, a faired section 4 feet long and 14 feet maximum diameter (fig. 2) was placed at the opposite end of the duct from the fan so as to secure a more even flow. Also, the honeycomb was moved to the position shown in Figure 11, the anemometer mounting was moved to the opposite side of the honeycomb, the fans were reversed on their hubs, and the direction of rotation of the motor reversed. Observations were taken as described for the blower fan.

At the beginning of the test the efficiency of the motor at the various speeds was obtained by means of a Prony brake. Curves of the efficiency against power input were plotted and used to compute the power delivered to the fan from the observed power input to the motor. Check runs made at the end of the tests showed an apparent change of about 5 per cent in the power absorbed by the fans. Check measurements of the pitch showed no apparent change in the fans, and, therefore, the Prony brake was again rigged up, and several efficiency runs were made. The results showed that the efficiency of the motor had changed during the tests. Since there was no way of knowing when the change took place, all of the fans were run again at the various speeds and against the various resistance conditions. Observations were made as before, except that the velocity readings were omitted. This omission was justified because the head-volume relation was not affected by the change in the efficiency of the motor. In plotting the power-volume curve, the head-volume curve obtained in the original tests was used to obtain the volume corresponding to the observed head. To guard against errors due to further changes in the efficiency of the motor, measurements of the power required to turn the motor without fan load were made at frequent intervals, and since the efficiencies measured by the Prony brake were in good agreement with those determined from the no-load power and the electrical losses, the power absorbed by the fan was computed by subtracting the electrical and mechanical losses.

VI. REDUCTION OF OBSERVATIONS

When a fan is operated at various rotational speeds to move air through a given duct system, the volume of air moved varies directly as the speed of rotation N; the static pressure developed varies as the square of the speed of rotation, and the power required varies as the cube of the speed of rotation. The static pressure and the power also vary directly as the air density, if the volume transferred per minute is the same in all cases, as may be secured by suitably adjusting the speed of rotation. For geometrically similar installations, the average velocity of the moving air is proportional to the tip speed, hence to the product of speed of rotation (N) and diameter (D). The volume, therefore, varies as ND^3 (air speed times area of duct), the head as N^2D^2 (square of the tip speed), and the power as N^3D^5 (product of head and volume). It is assumed that the reader

is familiar with these relations, which form the basis of practically all fan tables.

The resistance of a given duct system is not constant, but is a function of the air speed, varying approximately as the square of the volume of air flowing. When the speed of rotation of a fan delivering air to the system is increased, the volume increases directly as the speed of rotation, and the pressure developed by the fan increases as the square of the speed of rotation, hence, as the square of the volume flowing. The pressure developed by the fan keeps in step with the increasing resistance of the duct and, therefore, except for the small and usually negligible deviations from the relations stated, no additional information is obtained by changing merely the speed of rotation of the fan that is delivering air to, or removing it from, a fixed duct system.

A fixed value of the ratio of the resistance of the duct to the square of the volume flowing may be spoken of as a given resistance ratio. To make a satisfactory test of the fan, this ratio must be varied from infinity (a closed duct) to nearly zero (an open duct). The method of doing this has already been explained. With a closed duct, the fan builds up a static pressure in the duct, but there is no flow of air through the duct system. As the resistance to flow is decreased, the speed of rotation of the fan remaining constant, the volume of air flowing increases and the static pressure decreases until finally, when the difference in static pressure between the inlet and outlet side of the fan is zero, the fan moves the greatest volume of air. Curves of the static pressure and power against air volume for a constant speed of rotation represent one method of giving the characteristics of the fan.

The useful work of the fan is usually defined as the work done in moving the observed volume of air against the observed static pressure. With this definition the efficiency of a fan operating either in a closed duct or in the open is zero. Often, but not always, the work required to impart the observed velocity to the air is included in the useful work. We have included it. A volume, Q cu. ft./min., moving in a duct of diameter, d feet, corresponds to a mean speed of $\frac{Q}{0.7854\ d^2 \times 60}$ ft./sec. The kinetic energy imparted per second is one-half the product of the mass of air moved per second times the square of the mean speed. The mass moved per second is the product of the density (ρ slugs/ft.^{3}) by the volume per second $\left(\frac{Q}{60}\text{ cu. ft.}\right)$. Hence the kinetic energy imparted per second is $\frac{1}{2}\rho\frac{Q}{60}\left(\frac{Q}{0.7854\ d^2\times 60}\right)^2$ ft. lbs./sec. The power required to move the volume $\frac{Q}{60}$ cu. ft./sec. against a static pressure of h inches of water ($=5.2\ h$ lbs./ft.^{2}) is $\frac{5.2\ Qh}{60}$ ft. lbs./sec. Hence, the total useful power is $\frac{Q}{60}\left\{(5.2h+\frac{1}{2}\rho\left(\frac{Q}{0.7854\ d^2\times 60}\right)^2\right\}$ ft. lbs./sec. The second term in the bracket is the velocity pressure, and the sum of the two terms is the total pressure, both expressed in lbs./ft.^{2} We have adopted, then, as the useful

power the power required to move the observed volume from the total pressure on the inlet side of the fan to the total pressure on the outlet side.

We do not intend to suggest that the above definition of useful work is the "true" or "best." The practical problem is generally to circulate a definite quantity of air through a given duct system with the minimum power. The use of the conception of efficiency may or may not be helpful in securing the desired result.

All observations were reduced to the standard air conditions adopted by the Fan Manufacturers Association,[1] that is, to air weighing 0.07488 lbs./ft.^{3}. This weight corresponds to air having a barometric pressure of 29.92 inches of mercury, standard gravity, a dry-bulb temperature of 68° F., and 50 per cent relative humidity.

In view of the approximate laws previously stated and to facilitate the use of the results in estimating the performance of fans of other diameters and rotational speeds, the results are given in terms of the coefficients defined as follows:

$$K_H = 10^8 \frac{H}{N^2 D^2}$$

$$K_Q = \frac{Q}{N D^3} \qquad (1)$$

$$K_P = 10^{12} \frac{P}{N^3 D^5}$$

$$\text{Efficiency} = \frac{5.2\ QH}{33{,}000\ P} = \frac{10^4 \times 5.2\ K_H K_Q}{33{,}000\ K_P}$$

where, K_H = total pressure coefficient, K_Q = volume coefficient, K_P = power coefficient, N = rotational speed (r. p. m.), D = diameter of fan (ft.), Q = volume of air (cu. ft./min.), P = horsepower absorbed by fan, and H = increase in total pressure produced by fan (inches of water), that is, the sum of the increase in the static pressure plus the increase (or minus the decrease) in the velocity pressure.

The increase in static pressure is measured on the manometer gage. The velocity pressure in a duct of diameter, d, is computed from the expression already given,

$$\frac{\frac{1}{2}\rho}{5.2}\left(\frac{Q}{0.7854\ d^2 \times 60}\right)^2$$

inches of water. The standard value of ρ is $\frac{0.07488}{32.156} = 0.002329$ slugs/ft.^{3}. Combining the numerical factors, we find that the velocity pressure is

$$0.0000001008 \frac{Q^2}{d^4} = \frac{N^2 D^2}{10^8}\left(10.08\ K_Q{}^2 \frac{D^4}{d^4}\right)$$

inches of water, ρ having its standard value.

[1] J. A. S. H. V. E., **29**, p. 371; 1923.

For the blower condition, the air starts from rest at atmospheric pressure, and H is the excess of the total pressure in a 10-foot duct above that pressure. As D is 8 feet, the increase in velocity pressure is $\frac{N^2D^2}{10^8}(4.13\ K_Q^2)$, and $H=H_S+\frac{N^2D^2}{10^8}(4.13\ K_Q^2)$, H_S being the excess of the static pressure in the duct above one atmosphere. Hence, $K_H=\frac{10^8H_S}{N^2D^2}+4.13\ K_Q^2$.

For the exhaust condition, D being 8 feet, the increase in the velocity pressure in passing from the 10-foot duct, where the static pressure is H_S below atmospheric, to the outside air (atmospheric pressure) at an opening 8 feet 1 inch in diameter will be $\frac{N^2D^2}{10^8}$ $(10.08\ K_Q^2D^4)\left\{\frac{1}{(8.083)^4}-\frac{1}{10^4}\right\}=\frac{N^2D^2}{10^8}(5.55\ K_Q^2)$, provided that the average air speed is the same at every point of the 8 foot 1 inch opening. Then $H=H_S+\frac{N^2D^2}{10^8}(5.55\ K_Q^2)$, and $K_H=\frac{10^8H_S}{N^2D^2}+5.55\ K_Q^2$. (Actually, the flow will not be distributed uniformly over the discharge opening, and this will modify the results.)

When the coefficients, K_H, K_Q, and K_P are known, it is easy to determine whether given conditions can be met, and if so, what rotational speed, diameter, and pitch are required. This is facilitated by combining these equations in various ways and by the use of suitable graphs. For example—

$$D^4=\frac{Q^2K_H}{10^8HK_Q^2} \tag{2}$$

$$N=\frac{Q}{D^3K_Q}$$

are convenient for use with a slide rule. These two equations may be used in the solution of many types of selection problems. For special problems it may be convenient to plot the characteristic curves in terms of new variables so chosen that the independent variable involves only known quantities. For example if Q, N, and H are the known quantities, some convenient power of $\frac{K_Q^2}{K_H^3}$ is chosen as the independent variable, for by the relations given in equation (1)

$$\frac{K_Q^2}{K_H^3}=\frac{Q^2N^4}{10^{24}H^3}$$

and, hence, its value is determined completely by the known quantities Q, N, and H. The reader is referred to a paper entitled "Characteristics of Centrifugal Fans," by T. G. Estep and C. A. Carpenter, appearing in the Proceedings of the Engineering Society of Western Pennsylvania, volume 43, 1927–28, page 306, for illustrations of the use of this independent variable.

If Q, D, and H are the known quantities, a convenient power of $\frac{K_Q^2}{K_H}$ is chosen as the independent variable, for by the relations given in equation (1)

$$\frac{K_Q^2}{K_H} = \frac{Q^2}{10^8 D^4 H}$$

and, hence, its value is determined completely by Q, D, and H. This variable forms the basis of the so-called Hagen chart described in Marks Mechanical Engineers Handbook, second edition, page 1643 (McGraw-Hill, 1924).

TABLE 2.—*Blower fan*

(*a*) 2-FOOT PITCH (PITCH/DIAMETER RATIO 0.250)

800 r. p. m.				900 r. p. m.			
K_H	K_Q	K_P[1]	Efficiency	K_H	K_Q	K_P[1]	Efficiency
			Per cent				*Per cent*
0.245	0.1870	0.33	21.9	0.233	0.1848	0.33	20.6
.511	.1377	.34	32.6	.506	.1375	.34	32.2
.662	.1123	.33	35.5	.674	.1128	.33	36.3
.938	.0672	.29	34.2	.945	.0676	.29	34.7
1.075	.0346	.24	24.4	1.065	.0346	.24	24.2
1.233	0	.21	0	1.224	0	.21	0

(*b*) 3-FOOT PITCH (PITCH/DIAMETER RATIO 0.375)

0.404	0.2447	0.58	26.8	0.414	0.2410	0.58	27.1
.815	.1743	.58	38.6	.815	.1757	.58	38.9
1.073	.1309	.57	41.5	1.062	.1375	.56	41.1
1.362	.0811	.48	36.2	1.352	.0701	.46	32.5
1.449	.0463	.42	25.2	1.467	.0469	.42	25.8
1.695	0	.34	0	1.700	0	.34	0

(*c*) 4-FOOT PITCH (PITCH/DIAMETER RATIO 0.500)

585 r. p. m.				700 r. p. m.			
K_H	K_Q	K_P[1]	Efficiency	K_H	K_Q	K_P[1]	Efficiency
			Per cent				*Per cent*
0.580	0.2740	0.81	30.9	0.563	0.2775	0.81	30.4
1.089	.2090	.81	42.4	1.060	.2005	.81	41.4
1.362	.1552	.76	43.8	1.366	.1575	.77	44.0
1.568	.1015	.69	36.3	1.551	.1051	.70	36.7
1.855	.0420	.60	20.5	1.854	.0442	.60	21.5
2.031	0	.52	0	2.012	0	.52	0

(*d*) 5-FOOT PITCH (PITCH/DIAMETER RATIO 0.625)

0.659	0.297	1.04	29.6	0.655	0.299	1.04	29.7
.968	.258	1.03	38.2	.951	.256	1.03	37.3
1.277	.208	1.01	41.5	1.275	.209	1.01	41.6
1.528	.129	.93	33.4	1.497	.135	.94	33.9
1.800	.070	.81	24.5	1.780	.074	.81	25.6
2.110	0	.68	0	2.140	0	.68	0

[1] These values of K_P taken from faired curves.

TABLE 2.—*Blower fan*—Continued

(*e*) 6-FOOT PITCH (PITCH/DIAMETER RATIO 0.750)

585 r. p. m.				700 r. p. m.			
K_H	K_Q	K_P[1]	Efficiency	K_H	K_Q	K_P[1]	Efficiency
			Per cent				*Per cent*
0.712	0.3185	1.15	31.1	0.683	0.3090	1.14	29.2
.714	.3068	1.14	30.3	.695	.3075	1.14	29.5
1.288	.2151	1.06	41.2	1.313	.2161	1.06	42.2
1.033	.2597	1.11	38.1	1.048	.2577	1.10	38.7
1.521	.1529	.98	37.4	1.508	.1562	.98	37.9
1.343	.2055	1.05	41.4	1.345	.2125	1.06	42.5
1.611	.0992	.92	27.4	1.645	.1006	.92	28.3
1.516	.1332	.96	33.2	1.515	.1361	.96	33.9
1.988	.0449	.83	16.9	1.981	.0475	.84	17.6
1.837	.0621	.86	20.9	1.871	.0596	.86	20.4
2.100	0	.75	0	2.108	0	.75	0
2.062	0	.75	0	2.080	0	.75	0

(*f*) 7.5-FOOT PITCH (PITCH/DIAMETER RATIO 0.938)

0.949	0.3525	1.60	32.9	0.876	0.3505	1.60	30.2
1.290	.2923	1.60	37.1	1.314	.3014	1.60	39.0
1.830	.2250	1.60	40.5	1.847	.2220	1.60	40.4
1.928	.1499	1.50	30.4	1.947	.1505	1.50	30.8
2.357	.0972	1.39	25.9	2.285	.0988	1.39	25.6
2.673	0	1.31	0	2.695	0	1.31	0

(*g*) 8.5-FOOT PITCH (PITCH/DIAMETER RATIO 1.063)

				0.977	0.3740	1.99	28.9
0.992	0.3670	1.98	29.0	.988	.3660	1.98	28.8
1.332	.3068	1.94	33.2	1.355	.3058	1.94	33.6
1.696	.2423	1.88	34.5	1.704	.2368	1.88	33.8
2.003	.1486	1.68	27.9	1.949	.1505	1.68	27.5
2.019	.1455	1.68	27.5	1.951	.1524	1.68	27.9
2.055	.1418	1.67	27.5	2.041	.1396	1.66	27.1
2.384	.0901	1.64	20.6	2.366	.0960	1.64	21.8
2.629	0	1.59	0	2.610	0	1.59	0

TABLE 3.—*Exhaust fan*

(*a*) 2-FOOT PITCH (PITCH/DIAMETER RATIO 0.250)

800 r. p. m.				900 r. p. m.			
K_H	K_Q	K_P[1]	Efficiency	K_H	K_Q	K_P[1]	Efficiency
			Per cent				*Per cent*
0.338	0.1561	0.34	24.5	0.325	0.1555	0.34	23.4
.538	.1234	.33	31.7	.523	.1236	.33	30.9
.640	.0997	.32	31.4	.644	.1004	.32	31.8
.858	.0688	.30	31.0	.859	.0697	.30	31.4
.968	.0509	.28	27.7	.969	.0524	.28	28.6
1.165	0	.22	0	1.165	0	.22	0

(*b*) 3-FOOT PITCH (PITCH/DIAMETER RATIO 0.375)

0.522	0.1978	0.58	28.0	0.512	0.1970	0.58	27.4
.818	.1554	.57	35.1	.807	.1546	.57	34.5
.953	.1282	.55	35.0	.952	.1284	.55	35.0
1.181	.0924	.50	34.4	1.191	.0901	.50	33.8
1.391	.0632	.47	29.5	1.375	.0648	.47	29.9
1.614	0	.36	0	1.612	0	.36	0

[1] These values of K_P taken from faired curves.

TABLE 3.—*Exhaust fan*—Continued

(*c*) 4-FOOT PITCH (PITCH/DIAMETER RATIO 0.500)

585 r. p. m.				700 r. p. m.			
K_H	K_Q	K_P[1]	Efficiency	K_H	K_Q	K_P[1]	Efficiency
			Per cent				*Per cent*
0.683	0.2277	0.81	30.2	0.660	0.2228	0.81	28.6
.690	.2267	.81	30.4	.687	.2268	.81	30.3
1.036	.1772	.80	36.1	1.023	.1772	.80	35.7
1.245	.1347	.77	34.3	1.231	.1391	.78	34.6
1.473	.1024	.75	31.7	1.426	.1038	.75	31.1
1.648	.0616	.69	23.2	1.651	.0651	.70	24.2
1.927	0	.55	0	1.912	0	.55	0

(*d*) 5-FOOT PITCH (PITCH/DIAMETER RATIO 0.625)

0.778	0.2388	1.03	28.4	0.784	0.2399	1.03	28.8
.939	.2138	1.02	31.0	.926	.2192	1.02	31.4
1.090	.1861	1.00	32.0	1.072	.1878	1.00	31.7
1.280	.1533	.98	31.5	1.260	.1544	.98	31.3
				1.584	.1071	.91	29.4
1.563	.1060	.91	28.7	1.538	.1107	.92	29.2
1.753	.0717	.84	23.6	1.747	.0752	.85	24.3
2.040	0	.69	0	2.030	0	.69	0

(*e*) 6-FOOT PITCH (PITCH/DIAMETER RATIO 0.750)

0.756	0.2353	1.08	25.9	0.751	0.2363	1.08	25.9
.891	.2121	1.07	27.8	.897	.2148	1.07	28.4
1.037	.1816	1.05	28.3	1.030	.1828	1.05	28.3
1.171	.1506	1.03	27.0	1.184	.1517	1.03	27.4
1.518	.1036	.97	25.6	1.507	.1075	.97	26.3
1.713	.0696	.91	20.6	1.695	.0748	.92	21.7
1.950	0	.81	0	1.932	0	.81	0

(*f*) 7.5-FOOT PITCH (PITCH/DIAMETER RATIO 0.938)

1.058	0.2797	1.60	29.1	1.066	0.2816	1.60	29.6
1.216	.2507	1.63	29.5	1.212	.2508	1.63	29.4
1.337	.2106	1.65	26.9	1.328	.2123	1.65	26.9
1.577	.1683	1.61	26.0	1.572	.1720	1.62	26.3
1.976	.1292	1.51	26.6	1.949	.1307	1.52	26.4
2.210	.0801	1.40	19.9	2.160	.0844	1.40	20.5
2.392	0	1.30	0	2.380	0	1.30	0

(*g*) 8.5-FOOT PITCH (PITCH/DIAMETER RATIO 1.063)

1.110	0.2865	1.93	25.9	1.088	0.2845	1.93	25.3
1.264	.2552	1.96	25.9	1.246	.2541	1.96	25.5
1.384	.2190	1.98	24.1	1.375	.2181	1.98	23.9
1.703	.1743	1.85	25.3	1.668	.1770	1.86	25.0
2.018	.1359	1.72	25.1	1.978	.1378	1.72	25.0
2.129	.0758	1.64	15.5				
2.154	.0831	1.65	17.1	2.116	.0869	1.65	17.5
2.269	0	1.59	0	2.238	0	1.59	0

[1] These values of K_P taken from faired curves.

Each of these independent variables has advantages in a particular type of problem, eliminating methods of trial and error which may be necessary with the characteristic curve involving K_H and K_Q. To avoid possible confusion due to a number of methods of procedure, we will make use of the relations of equations (2) and the K_H–K_Q curves in the illustrative problems given in this paper.

VII. RESULTS

The results obtained are summarized in Tables 2, (*a*) to (*g*), and 3 (*a*) to (*g*), and in Figures 14 to 31. As the pitch/diameter ratio is increased, the curve of efficiency *v.* volume coefficient becomes pro-

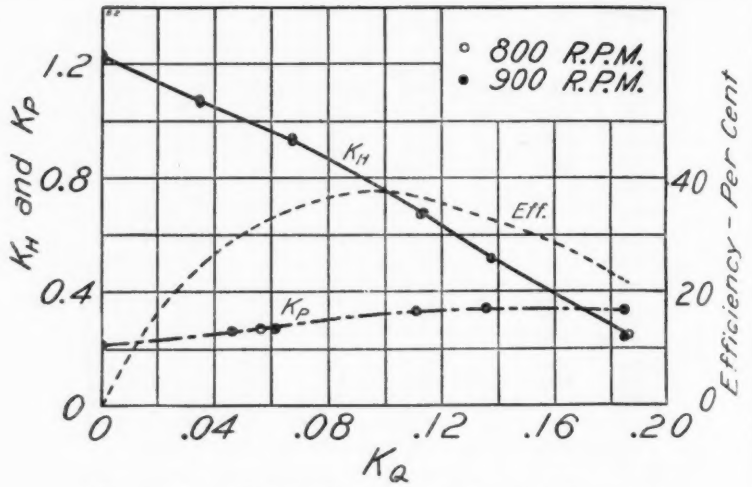

FIGURE 14.—*Characteristics of 8-foot by 2-foot blower fan*
Diameter, 8 feet; pitch, 2 feet; pitch/diameter ratio—0.250.

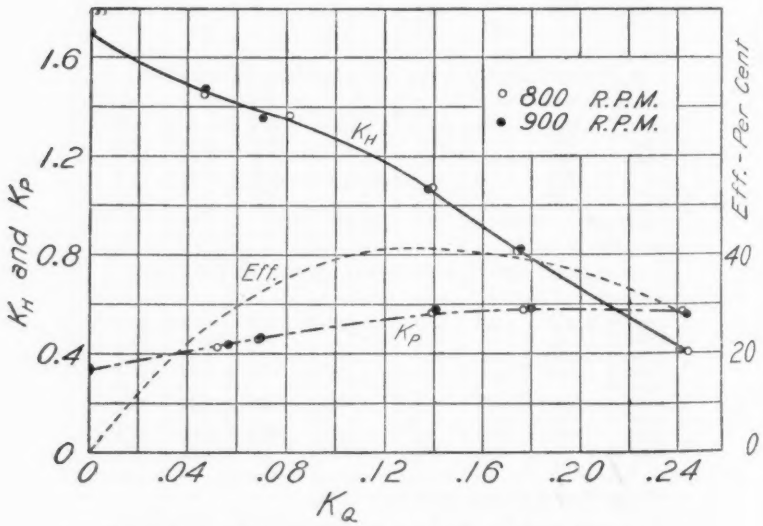

FIGURE 15.—*Characteristics of 8-foot by 3-foot blower fan*
Diameter, 8 feet; pitch, 3 feet; pitch/diameter ratio—0.375.

gressively flatter (figs. 29 and 31), and the useful values of the coefficient of volume and of head progressively increase up to a pitch/diameter

ratio of 0.938.[2] Hence, with the higher ratios larger values of the coefficients are available, and the diameter and the speed of rotation

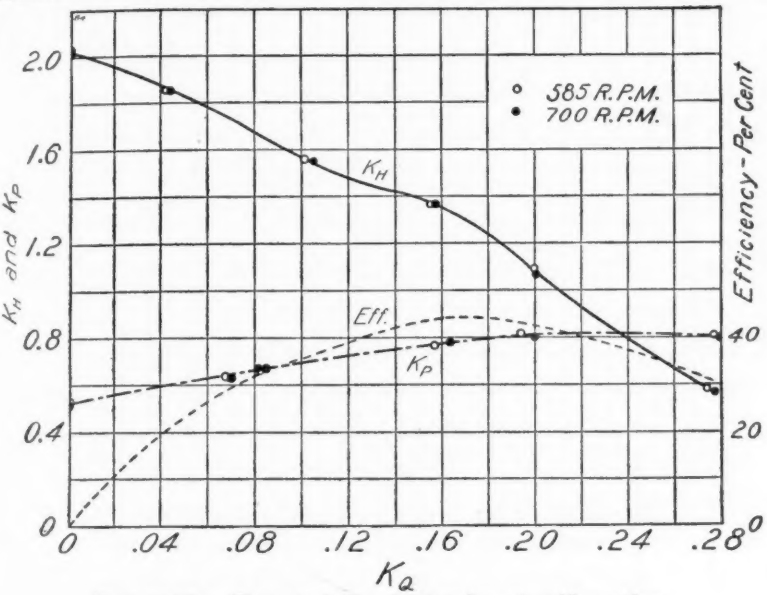

FIGURE 16.—*Characteristics of 8-foot by 4-foot blower fan*
Diameter, 8 feet; pitch, 4 feet; pitch/diameter ratio—0.500.

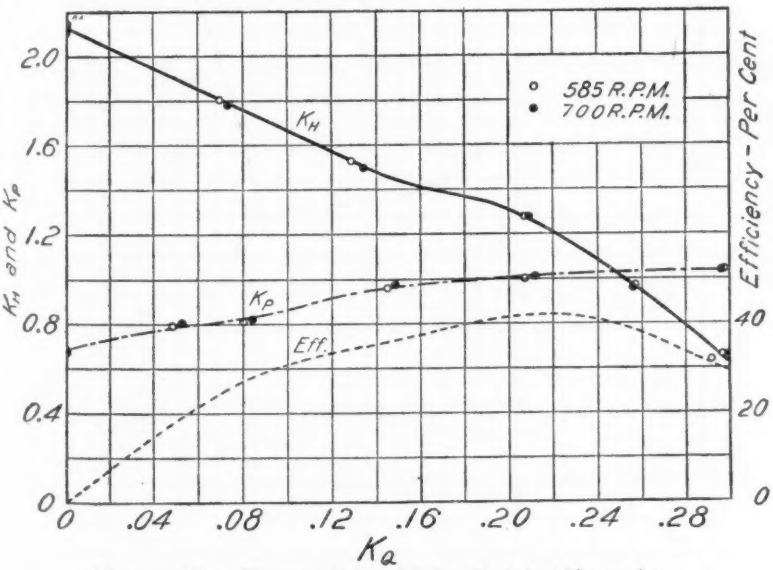

FIGURE 17.—*Characteristics of 8-foot by 5-foot blower fan*
Diameter, 8 feet; pitch, 5 feet; pitch/diameter ratio—0.625.

may be varied, so as to suit given conditions, over a limited range without serious loss in efficiency. The maximum efficiency varies slowly

[2] The coefficients for the fan of pitch/diameter ratio 0.750 are somewhat out of line, probably because the blade widths are smaller than those of the neighboring fans, and the actual pitch is less than the nominal pitch.

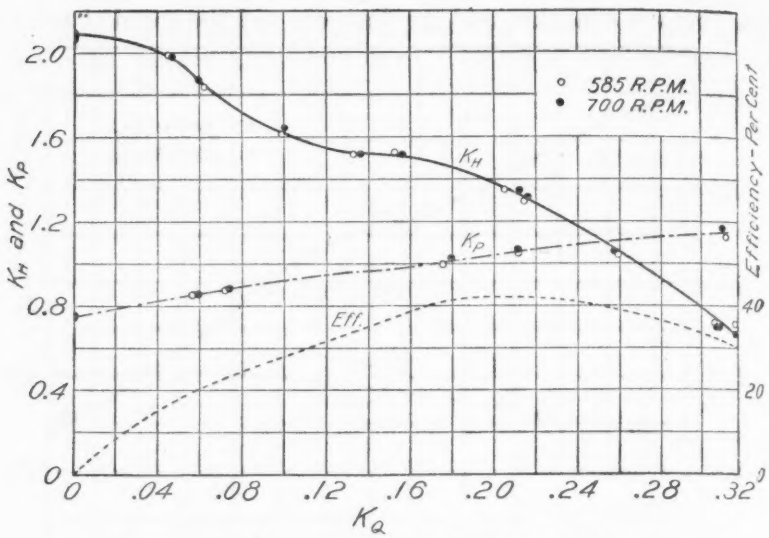

FIGURE 18.—*Characteristics of 8-foot by 6-foot blower fan*

Diameter, 8 feet; pitch, 6 feet; pitch/diameter ratio—0.750.

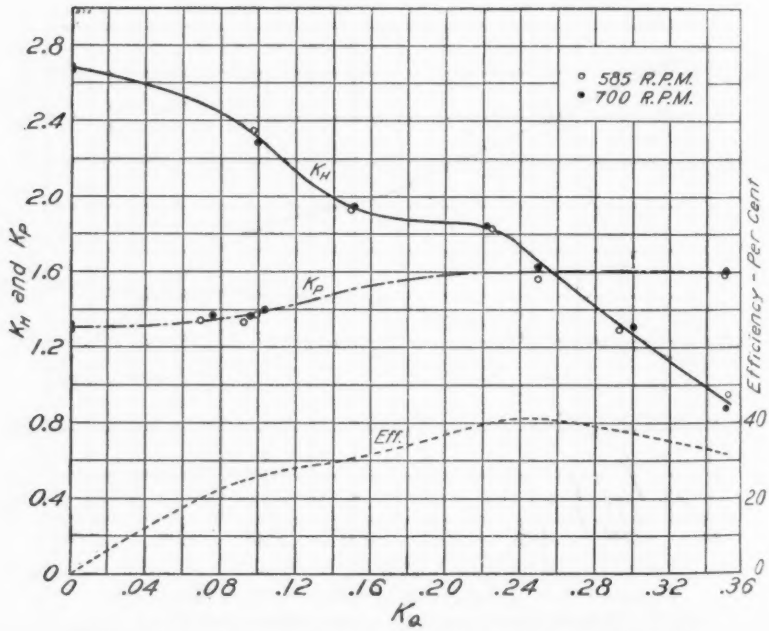

FIGURE 19.—*Characteristics of 8-foot by 7-foot 6-inch blower fan*

Diameter, 8 feet; pitch, 7 feet 6 inches; pitch/diameter ratio—0.938.

with the pitch/diameter ratio, passing through a maximum near the ratio 0.500, and at ratio 1.063 reaching the lowest value observed in this work. In general, ratios less than 0.3 or greater than 1.0 should not be used.

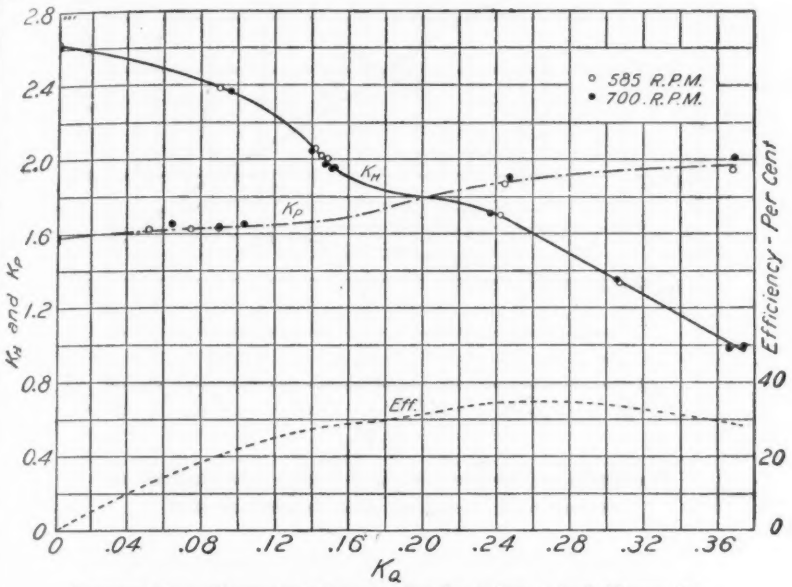

FIGURE 20.—*Characteristics of 8-foot by 8-foot 6-inch blower fan*

Diameter, 8 feet; pitch, 8 feet 6 inches; pitch/diameter ratio—1.063.

In each case, the efficiency of the fan when used for blowing slightly exceeds that when used for exhausting.

To illustrate the method of using the characteristic curves, we may consider some practical problems. It is desired to deliver 34,200

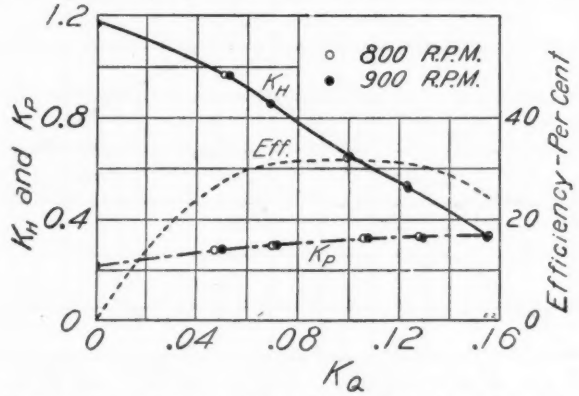

FIGURE 21.—*Characteristics of 8-foot by 2-foot exhaust fan*

Diameter, 8 feet; pitch, 2 feet; pitch/diameter ratio—0.250.

cu. ft./min. against a total pressure of one-half inch of water, using a 2-blade propeller fan 7 feet in diameter and rotating at 700 r. p. m. as a blower. Can this be done; and if so, what will be the pitch of the fan and the power required?

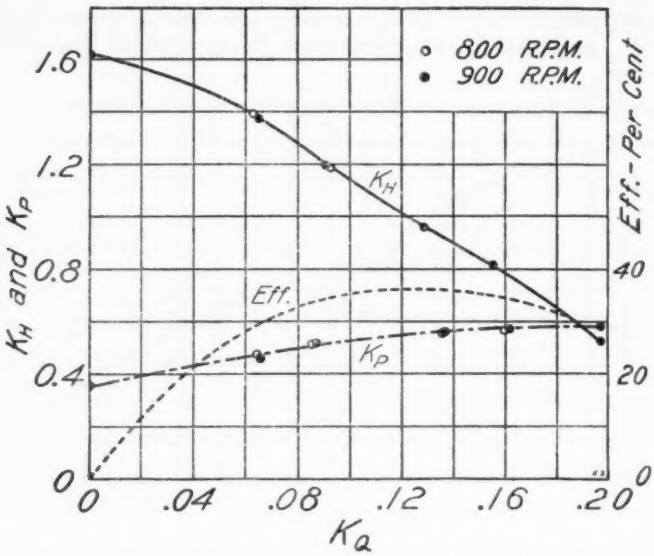

FIGURE 22.—*Characteristics of 8-foot by 3-foot exhaust fan*
Diameter, 8 feet; pitch, 3 feet; pitch/diameter ratio—0.375.

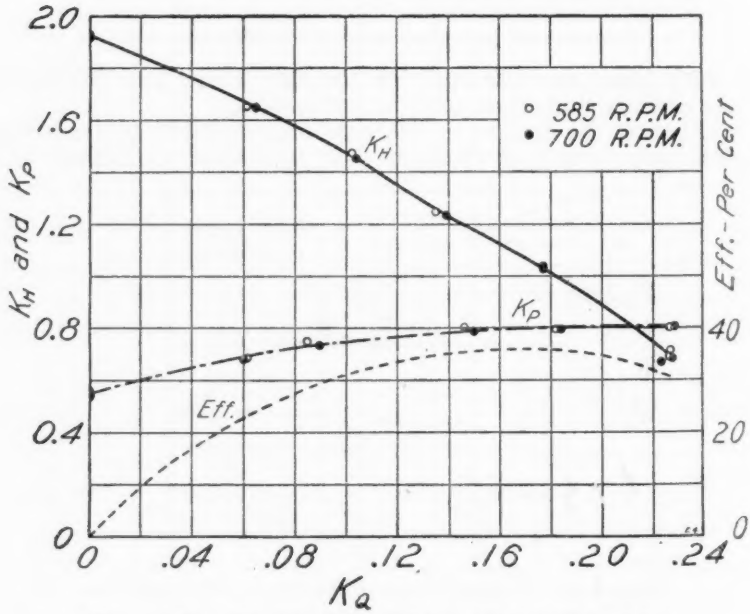

FIGURE 23.—*Characteristics of 8-foot by 4-foot exhaust fan*
Diameter, 8 feet; pitch, 4 feet; pitch/diameter ratio—0.500.

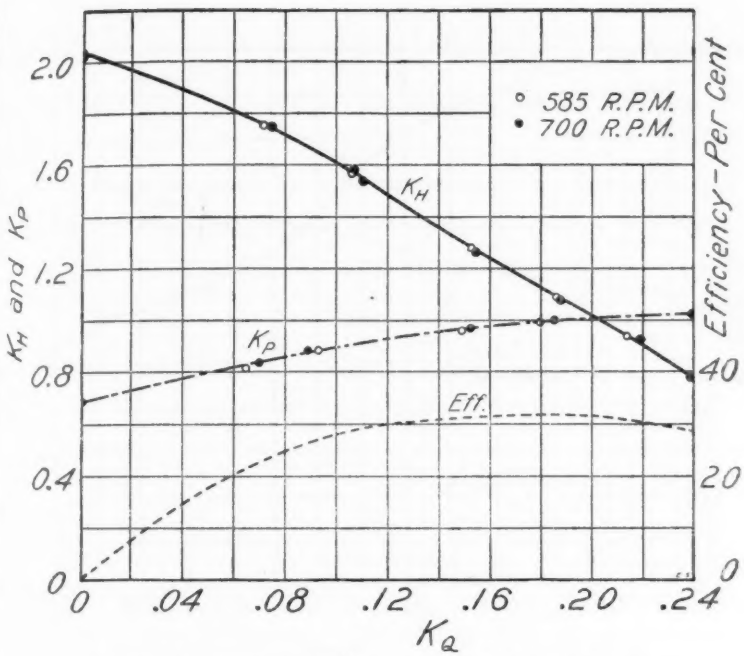

FIGURE 24.—*Characteristics of 8-foot by 5-foot exhaust fan*
Diameter, 8 feet; pitch, 5 feet; pitch/diameter ratio—0.625.

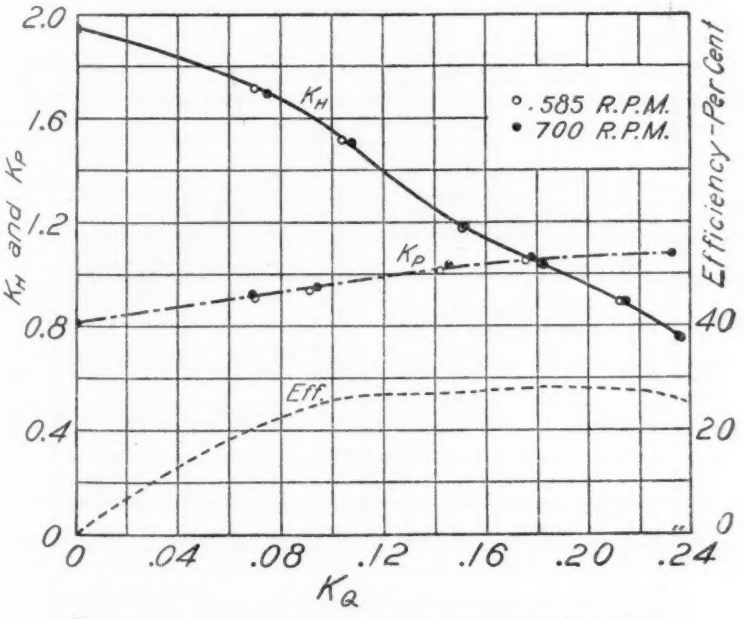

FIGURE 25.—*Characteristics of 8-foot by 6-foot exhaust fan*
Diameter, 8 feet; pitch, 6 feet; pitch/diameter ratio—0.750.

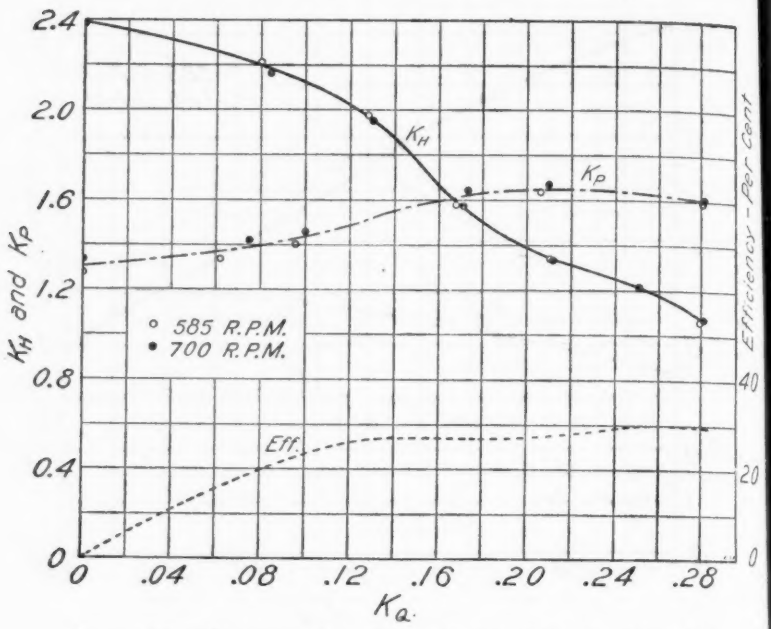

FIGURE 26.—*Characteristics of 8-foot by 7-foot 6-inch exhaust fan*

Diameter, 8 feet; pitch, 7 feet 6 inches; pitch/diameter ratio—0.938.

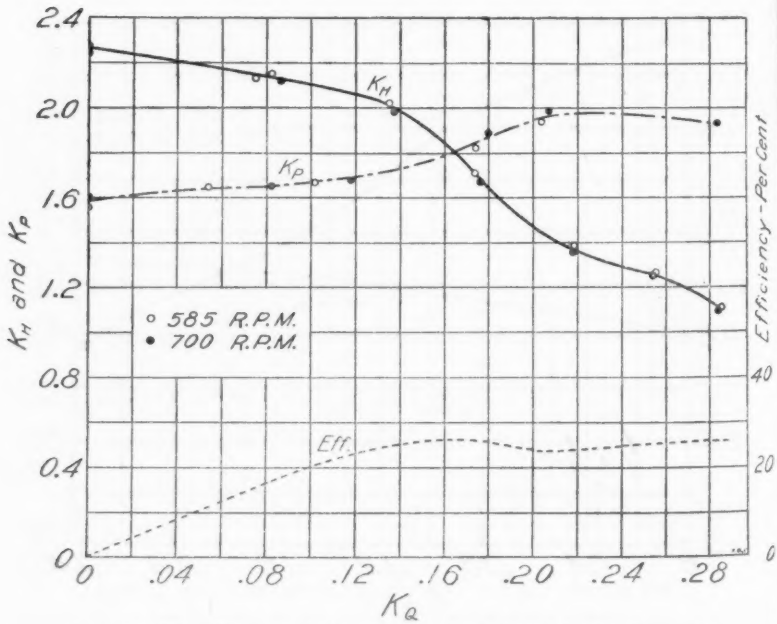

FIGURE 27.—*Characteristics of 8-foot by 8-foot 6-inch exhaust fan*

Diameter, 8 feet; pitch, 8 feet 6 inches; pitch/diameter ratio—1.063.

We find at once that the required $K_Q = \frac{34{,}200}{700 \times 7^3} = 0.1424$ and the required $K_H = \frac{10^8 \times 0.5}{700^2 \times 7^2} = 2.082$. An examination of Figures 19 and

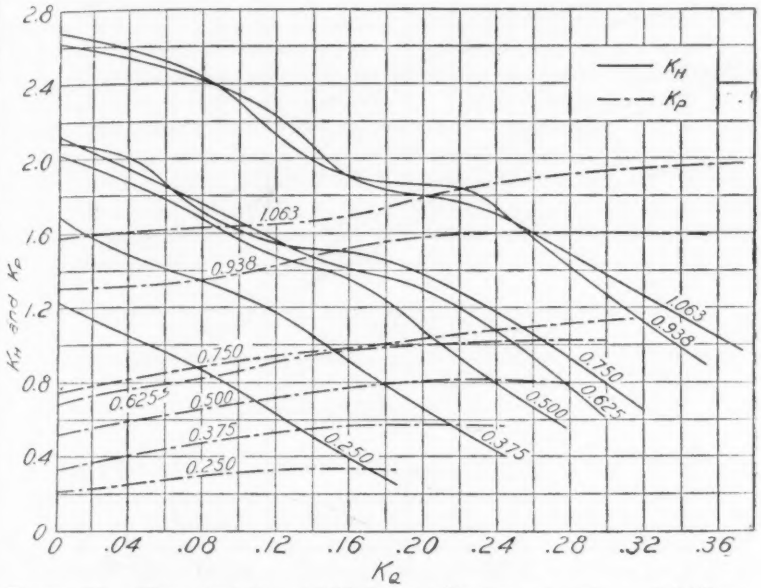

FIGURE 28.—*Characteristics of 2-blade propeller fans of various pitch/diameter ratios*

Blowing condition.

20 shows that this point is above all of the characteristic curves and, therefore, that the desired performance can not be obtained. The nearest point on the characteristic curve for the propeller of

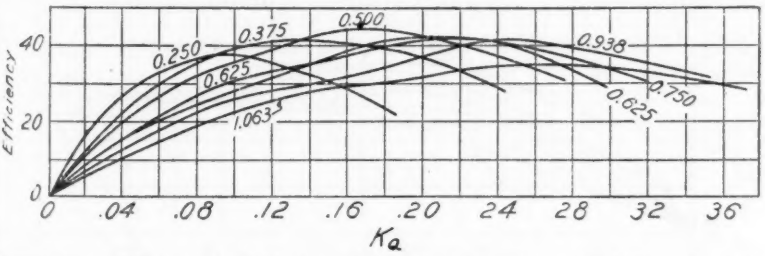

FIGURE 29.—*Efficiency of 2-blade propeller fans of various pitch/diameter ratios*

Blowing condition.

pitch/diameter ratio 0.938 (fig. 19) which has the same value of $\frac{H}{Q^2}$; that is, the same duct resistance, is $K_H = 2.000$, $K_Q = 0.1395$,[3] corresponding

[3] These values are found by trial and error. From the definitions of K_H and K_Q, $\frac{H}{Q^2} = \frac{10^{-8}}{D^4} \frac{K_H}{K_Q^2}$. But $\frac{H}{Q^2}$ for the desired condition is $\frac{0.5}{34{,}200^2}$ and D is 7 feet. By trial we look for values of K_H and K_Q on the curve such that $\frac{K_H}{K_Q^2}$ is equal to $\frac{10^8 \times 0.5 \times 7^4}{34{,}200^2} = 103$. We find the values given.

to a reduction of the volume to 33,500 cu. ft./min. The value of K_P is 1.47 and, hence, the power required is $1.47 \times 10^{-12} \times 700^3 \times 7^5 = 8.48$ h. p. The pitch is of course $0.938 \times 7 = 6.56$ feet.

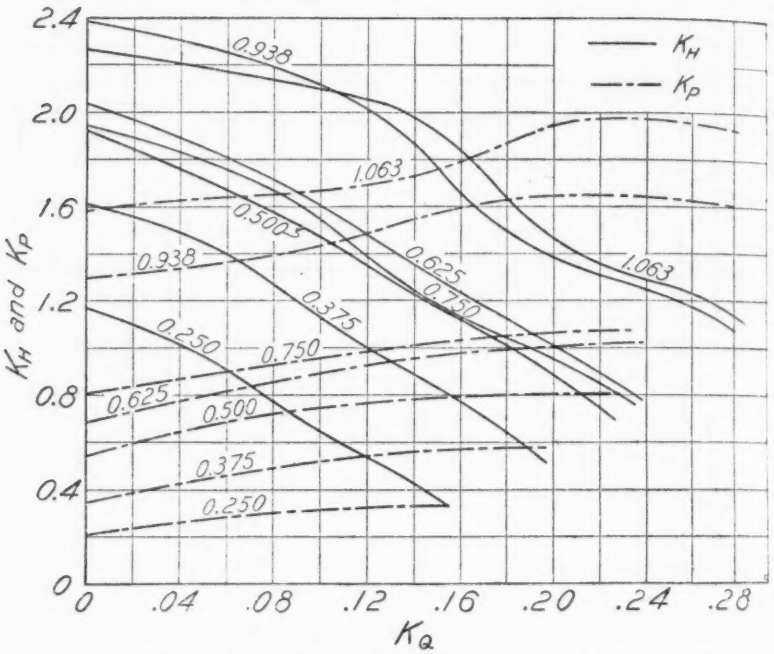

FIGURE 30.—*Characteristics of 2-blade propeller fans of various pitch/diameter ratios*
Exhausting condition.

To secure the desired performance it is necessary to change the diameter or speed of rotation. Suppose we consider a fan of pitch/diameter ratio 0.625 under conditions of maximum efficiency for

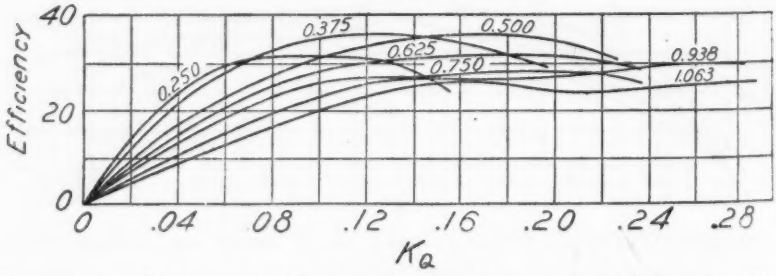

FIGURE 31.—*Efficiency of 2-blade propeller fans of various pitch/diameter ratios*
Exhausting condition.

which $K_H = 1.2$, $K_Q = 0.22$. Hence, by equations (2)

$$D^4 = \frac{1.2 \times 34{,}200^2}{10^8 \times 0.22^2 \times 0.5} = 580$$

whence

$$D = 4.907 \text{ feet.}$$

and

$$N=\frac{34,200}{0.22\times 4.907^3}=1,314 \text{ r. p. m.}$$

The pitch is $4.907\times 0.625=3.066$ feet. From Figure 17 the power coefficient is 1.02 for $K_Q=0.22$, and, hence, the required power is $1.02\times 10^{-12}\times 1,314^3\times 4.91^5=6.61$ h. p. The desired performance is obtained and the power is only 78 per cent of that required for the first fan, which gave a lower performance. The importance of a proper selection of diameter and speed of rotation is evident.

In many cases this fan would be objectionable on account of the high speed of rotation. To reduce the speed of rotation we would use a fan of higher pitch/diameter ratio, say 0.938, but choose the diameter and speed so as to lie near the condition of maximum efficiency (fig. 19) where $K_H=1.75$, $K_Q=0.24$. Hence

$$D^4=\frac{1.75\times 34,200^2}{10^8\times 0.24^2\times 0.5}$$

$$N=\frac{34,200}{0.24D^3}$$

from which $D=5.16$ feet, pitch $=4.84$ feet, $N=1,035$ r. p. m., power $=6.51$ h. p.

It might be desirable to reduce the speed somewhat more by a sacrifice of efficiency. For example, a convenient motor speed is 900 r. p. m. We would then have the problem of selecting D such that $10^8\frac{0.5}{900^2\,D^2}=K_H$ and $\frac{34,200}{900\,D^3}=K_Q$ are points on the characteristic curve of Figure 19. By trial and error, assuming $D=5.3$, 5.4, 5.5, 5.6, 5.7, 5.8, 5.9, 6.0 feet successively, we find $D=5.78$ feet gives $K_H=1.85$, $K_Q=0.197$, $K_P=1.58$ as the solution. The pitch is therefore 5.42 feet and the power required is 7.43 h. p. The additional 0.92 h. p. is the price paid for the reduction of the speed to 900 r. p. m.

In theory, any condition of head and volume may be met efficiently by the use of 2-blade propeller fans; for example, suppose that it is required to select a 2-blade propeller fan to deliver 75,000 cu. ft./min. against a total pressure of 10 inches of water. Again using the fan of pitch/diameter ratio 0.938 for which at maximum efficiency $K_H=1.75$, $K_Q=0.24$, $K_P=1.6$, we have

$$D^4=\frac{1.75\times 75,000^2}{10^8\times 0.24^2\times 10}$$

$$N=\frac{75,000}{0.24D^3}$$

from which we find readily that a fan of diameter 3.61 feet, pitch 3.39 feet, rotating at 6,640 r. p. m., absorbing 287 h. p., meets the requirements. In practice, the high rotational speed makes the use of a propeller fan impracticable, except, perhaps, under unusual

circumstances, because of the problems of motive power at the desired speed, noise, and strength to resist centrifugal force.

The limits of the practical use of propeller fans may be fixed in the following manner: We may decide that the tip speed should not exceed 25,000 feet per minute (an illustrative figure only, since in most cases lower values are desirable). The maximum value of K_H for good efficiency is of the order of 2.0. Hence, the maximum value of the head under the restriction on the tip speed is $2.0 \times 10^{-8} \times \left(\frac{25{,}000}{\pi}\right)^2$ $= 1.26$ inches of water. In round figures, 2-blade propeller fans are not suitable for pressures much greater than 1 inch of water. The propeller fan is adapted to move large volumes of air against relatively small pressures.

This limitation may be overcome by the use of more than two blades or by the use of a number of fans in tandem. Test data are not available on the performance obtained with these arrangements. The reason for the limitation is apparent. The blades which force the air against the pressure occupy only a small part of the duct area and the air leaks back between the blades. Only by moving the blades very rapidly, indeed, can large pressures be maintained.

VIII. ACCURACY OF RESULTS

Table 4 illustrates the degree of uniformity of the velocity over the measuring cross section, by giving for various conditions the mean percentage deviation of the 40 readings from the mean. It will be noted that the maximum deviation for the blower-fan arrangement is about 17 per cent. Such large deviations would seem to be a fruitful source of error, but when check runs were made it was possible to repeat the results within about 2 per cent. Table 2 (*g*) and Figure 18 show a large number of check observations. In this case, the obstructing netting was changed in amount or was readjusted between tests. Consequently, the resistance offered by it in the nominally identical series may differ significantly, depending, as it does in part, upon the amount of overlapping and of accumulated dirt. Hence, these check observations actually correspond to different points upon the characteristic curve. Tables 2 (*g*), and 3 (*c*), (*d*), and (*g*) contain several check measurements made successively without changing the netting in any way.

For the exhaust arrangement, conditions are greatly improved. The maximum deviation is only 6 per cent. The improvement is due in part to the faired entrance cone, in part to the fact that the motor and its supports are now downstream and in part to the generally steadier flow in the inlet side of a propeller fan.

It is believed that the values given are correct to within 5 per cent. The relative values for the several fans are probably within 2 per cent. The agreement of the coefficients at two speeds of rotation is an evidence of the general precision.

TABLE 4.—*Mean percentage deviation from average velocity at measuring cross section; various resistance conditions*

BLOWER FAN							
5-foot pitch		6-foot pitch		7.5-foot pitch		8.5-foot pitch	
585 r. p. m.	700 r. p. m.	585 r. p. m.	700 r. p. m.	585 r. p. m.	700 r. p. m.	585 r. p. m.	700 r. p. m.
17.2	15.7	14.7	15.6	14.7	16.6	10.1	16.6
6.5	6.9	7.6	6.9	5.5	7.0	9.3	7.0
6.7	8.4	8.1	9.0	8.8	8.9	5.9	8.9
9.6	7.8	9.1	6.4	9.1	13.0	9.0	13.00
5.7	4.8	4.7	5.3	6.4	5.4	5.9	5.4
EXHAUST FAN							
4.3	3.2	4.6	3.1	3.6	3.1	2.6	3.1
3.3	3.8	3.5	3.6	4.0	3.8	4.1	3.8
4.4	4.0	4.5	4.3	4.3	4.0	4.9	4.4
5.9	5.3	6.6	6.8	4.9	4.7	5.2	4.9
3.6	3.9	3.0	3.1	3.3	3.4	3.0	3.0
4.9	5.5	5.1	5.9	5.4	5.4	5.1	6.0

IX. CONCLUSION

The characteristics of 2-blade propeller fans have been measured under operating conditions approximating those encountered in cooling towers. The results are expressed in the form of head and power coefficients plotted against a volume coefficient in such a manner as to facilitate the estimation of the performance of similar fans of any diameter and speed of rotation. The effect of pitch/diameter ratio on the maximum efficiency obtainable is shown to be small for pitch/diameter ratios between 0.375 and 0.938. The speed of rotation and fan diameter must be carefully chosen to obtain maximum efficiency. Methods of selection are illustrated by numerical examples.

X. ACKNOWLEDGMENT

We wish to acknowledge the assistance of R. H. Heald, B. H. Monish, C. A. Burner, and W. H. Boyd in connection with the measurements.

WASHINGTON, March 21, 1930.